UNIVERSITY OF CALIFORNIA, SAN DIEGO

SAN DIEGO STATE UNIVERSITY

The role of a *SoxB1* gene in the regeneration and function of sensory neurons in the planarian *Schmidtea mediterranea*

A dissertation submitted in partial satisfaction of the

Requirements for the degree Doctor of Philosophy

in

Biology

by

Kelly Gullette Ross

Committee in charge:

University of California, San Diego

Professor Andrew Chisholm
Professor Karl Willert

San Diego State University

Professor Ricardo Zayas, Chair
Professor Sanford Bernstein
Professor Robert Zeller

2017

The Dissertation of Kelly Gullette Ross is approved, and it is acceptable in quality and form for publication on microfilm and electronically:

Chair

University of California, San Diego

San Diego State University

2017

DEDICATION

I dedicate this thesis to my husband Daniel Pontoriero, who not only supported me through this entire process but has also been my greatest cheerleader.

TABLE OF CONTENTS

LIST OF ABBREVIATIONS

abcb1-like	ATP Binding Cassette Subfamily B Member 1-like
Ac-Tub	Acetylated Tubulin
AMP	adenosine monophosphate
Aq	aqueous
ATPA-like	sodium/potassium-transporting ATPase-like
bHLH	basic helix-loop-helix
CNS	central nervous system
dFISH	double fluorescent in situ hybridization
C2D2A-like	Coiled-Coil And C2 Domain Containing 2A-like
CA	Carnoy's
cAMP	cyclic adenosine monophosphate
cav-1	caveolin-1
chat	choline acetyltransferase
ChIP-seq	chromatin immunoprecipitation sequencing
cm	centimeter
CPM	counts per million
D	Day
DAPI	4′,6-diamidino-2-phenylindole
DI	de-ionized
DPA	days post-amputation
dsRNA	double stranded RNA

DTT	Dithiothreitol
ED	epilepsy disorder
EEG	electroencephalogram
eml1	echinoderm microtubule associated protein like-1
F	Feed
FA	Formaldehyde
FDR	false discovery rate
FISH	fluorescent in situ hybridization
foxJ1-4	Forkhead box protein J1-4
FPKM	fragments per kilobase of transcript per million mapped reads
fps	frames per second
GABA	gamma-Aminobutyric acid
GABRA1	$GABA_A$ Receptor Alpha1 Subunit
GABRB1	$GABA_A$ Receptor Beta 1 Subunit
GABRB3	$GABA_A$ Receptor Beta 3 Subunit
GABRD	$GABA_A$ Receptor Delta Subunit
GABRG2	$GABA_A$ Receptor Gamma 2 Subunit
gabrg3L-2	gaba type a receptor gamma 3 subunit-like-2
gapdh	glyceraldehyde 3-phosphate dehydrogenase
gfp	green fluorescent protein
GO	gene ontology
GWAS	genome-wide association studies

H3-PS10	Phospho-Histone H3 (Ser10)
HCl	Hydrochloric Acid
hmcn-1-L	hemicentin-1-like
HMG	high-mobility group
Hmgb1	High Mobility Group Protein B1
HRP	Horseradish Peroxidase
if-b	intermediate filament-beta
IR	infrared
KCNA1	Potassium Voltage-Gated Channel, Shaker-Related Subfamily 1
KCTD7	Potassium Channel Tetramerization Domain-Containing Protein 7
Lef1	Lymphoid Enhancer Binding Factor 1
µl	microliter
MC	Methacarn
MeOH	Methanol
ml	milliliter
mm	millimeter
msh	muscle segment homeobox
NAC	N-Acetyl-L-Cysteine
NP-40	Nonidet P-40 (octyl phenoxypolyethoxylethanol)
OCT4	octamer-binding transcription factor 4
Otd	orthodenticle
PBS	phosphate buffered saline

PBSTx	1X PBS, 0.3% Triton X-100
PC1	principle component 1
PC2	principle component 2
PC-2	pro-hormone convertase 2
PCA	principle component analysis
PCL	Polycystin-L
pkd	polycystic kidney disease
Piwi	P-element induced wimpy testis
ProK	Proteinase K
qPCR	quantitative PCR
RNAi	RNA interference
RNA-seq	RNA sequencing
SCN1A	Sodium Voltage-Gated Channel Alpha Subunit 1
scRNA-seq	single cell RNA sequencing
SDS	Sodium Dodecyl Sulfate
Sox	Sry-related HMG box
Sry	sex-determining region Y
Tcf7	Transcription Factor 7 T Cell Specific
trpc-like	transient receptor potential-canonical channel-like
TSA	Tyramide Signal Amplification
WISH	whole-mount in situ hybridization

LIST OF FIGURES

LIST OF TABLES

LIST OF SUPPLEMENTAL FILES

ross_rnaseq_spreadsheet.xlsx

day 24 down

day 24 up

day 14 down

day 14 up

day 6 down

day 6 up

day 14 down, stays down at 24

ross_cloned_genes.fasta

ross_scrnaseq_spreadsheet.xlsx

day 6 down

day 6 up

day 14 down

day 14 up

day 24 down

day 24 up

ACKNOWLEDGEMENTS

First, I wish to thank my mentor, Dr. Ricardo Zayas, for allowing me the opportunity to join his lab. He provided excellent guidance throughout my years in the lab and the opportunity and challenge to think and work with independence, while always being available for helpful discussions, critical feedback, suggestions, more ideas than anybody could possibly execute, and constant encouragement to keep moving forward.

I am thankful for all of the past and current members of the Zayas lab for helpful comments on my applications and manuscripts and for contributing to the critical thinking that contributed to every project in which I've participated. Additionally, these projects would not have been possible without help from many hands. Over the years, I've been fortunate to have help at the bench from many talented technicians, graduate students, and undergraduate students.

I would like to thank my committee members for their support and ideas throughout the development of Chapter 4. Their feedback helped me get over some hurdles during the design of this project. I would especially like to thank Dr. Karl Willert for the experience I gained working in his lab. I obtained a wealth of knowledge and skills that have aided in all of my other scientific endeavors, and I am confident they will continue to do so in the future.

I am thankful for San Diego State University, especially all of the faculty and staff of the Biology Department for help throughout the years in navigating the Masters Program, the Doctoral Program, and helping me find the tools and reagents

needed to complete my work. I would also like to thank the ARCS Foundation of San Diego for funding. It has been an honor to be associated with the foundation.

Finally, I thank my family and my family of friends. This would not have been possible without your constant support, encouragement, and your providing the occasional diversion following experimental failures. I'm looking forward to your continued presence as I embark on my next adventures!

Chapter 1, in full, is a reprint of the material as it appears in Wiley Interdisciplinary Reviews – Developmental Biology 2017. Kelly G. Ross, Ko W. Currie, Bret J. Pearson, and Ricardo M. Zayas. The dissertation author was the primary author of this manuscript.

Chapter 2, in full, is a reprint of the material as it appears in Biomed Central – Developmental Biology 2015. Kelly G. Ross, Kerilyn C. Omuro, Matthew R. Taylor, Roma K. Munday, Amy Hubert, Ryan S. King, and Ricardo M. Zayas. The dissertation author was the primary investigator and author of this manuscript.

Chapter 3, in full, has been submitted and accepted for publication of the material. David J. Forsthoefel, Kelly G. Ross, Phillip A. Newmark, and Ricardo M. Zayas. The dissertation author was the co-primary investigator and author of this manuscript and contributed equally with David J. Forsthoefel.

Chapter 4, in full, is in preparation for submission. Kelly G. Ross, Alyssa M. Molinaro, Celeste Romero, Brian Dockter, Katrina L. Cable, Karla Gonzalez, Siqi Zhang, Priscila Rodriguez, Eva-Maria Collins, and Ricardo M. Zayas, 2017. The dissertation author was the primary investigator and author of this paper.

VITA

EDUCATION

Doctor of Philosophy in Biology – June 2017
University of California San Diego and San Diego State University
Joint Doctoral Program in Biology – Cell and Molecular Biology

Bachelor of Science, Microbiology - December 2005
Pennsylvania State University

RESEARCH EXPERIENCE

Doctoral Research, Department of Biology, San Diego State University, Sep. 2010-Present
Research Advisor: Dr. Ricardo Zayas

Research Associate, ViaCyte, Inc. (formerly Novocell, Inc.), Jan. 2008-Dec. 2010
Supervisor: Mark M. Moorman

Research Associate, FACS Core Lab, Veterans Medical Research Foundation, Oct. 2006-Dec. 2007
Supervisor: Mary Frances Keller

Bench Scientist, Safety Assessment Department, GlaxoSmithKline, Nov. 2005-Oct. 2006
Supervisor: Laura M. Storck

Co-Operative Education Student at GlaxoSmithKline through The Pennsylvania State University, Jun. 2004-Nov. 2005
Supervisor: Laura M. Storck

TEACHING AND MENTORING EXPERIENCE

Training of Undergraduate Scholars, San Diego State University (Fall 2013-Present)
- Guided independent projects and provided mentorship to eight undergraduate students.

Instructor and Program Director, Science Exploration for Teens: Regeneration, San Diego County Library, Bonita-Sunnyside Branch (July 2015)
- Taught students (ages 12-16) principles of regeneration biology and led STEM-inspired crafts.

Instructor and Program Director, Science is Fun!: DNA, San Diego County Library, Bonita-Sunnyside Branch (August 2015)
- Taught students (ages 8-13) basics about DNA and genetics including performing a DNA experiment and STEM-inspired crafts.

Training of Southwestern College Summer Interns, San Diego State University (June 2015-September 2015)
- Trained two students in molecular biology laboratory techniques.

Laboratory manager, Zayas Laboratory, San Diego State University (January 2015-July 2015)
- Managed laboratory while the lab's Principle Investigator was abroad on sabbatical.

Teaching Assistant, Biology 366L: Biochemistry, Cell and Molecular Biology Lab I, San Diego State University **(**Spring 2014**)**

Guest lecturer/Discussion Leader, Biology 589: Stem Cell and Regenerative Biology, San Diego State University **(**Fall 2011 and Fall 2015)
- Led multiple discussions on current stem cell topics as a substitute for the instructor.

Training of PhD Rotation Student, San Diego State University (Fall 2011)
- Guided a project characterizing whole-mount immunostaining in various species of planarians.

PUBLICATIONS

Ross KG, Cable KL, Omuro KC, Rodriquez PR, Zhong L, Collins EM, Willert K, and Zayas RM. 2016. A SoxB1 gene is required for regeneration and normal function of sensory neurons in planarians. *In preparation.*

Ross KG, Currie KW, Pearson BJ, and Zayas RM. 2017. Nervous system development and regeneration in freshwater planarians. *WIREs Dev Biol 6(3).*

Forsthoefel DJ*, **Ross KG***, Newmark PA, Zayas RM. 2016. Fixation, processing, and immunofluorescent labeling of whole mount planarians. In *Methods for planarian research: Methods in Molecular Biology. In press.* (*First two authors contributed equally.)

Allen JM, **Ross KG**, and Zayas RM. 2016. Regeneration in invertebrates: model systems. In eLS. John Wiley and Sons, Ltd. Chichester. DOI: 10.1002/9780470015902.a0001095.pub2

Ross KG, Omuro KC, Taylor MR, Munday RK, Hubert A, King RS, and Zayas RM. 2015. Novel monoclonal antibodies to study tissue regeneration in planarians. *BMC Dev Biol 15(1):2.* (Designated as 'highly accessed' by the journal.)

Hubert A, Henderson JM, Cowles MW, **Ross KG**, Hagen M, Anderson C, Szeterlak CJ, and Zayas RM. 2015. A functional genomics screen identifies an Importin-alpha

homolog as a regulator of stem cell function and tissue patterning during planarian regeneration. *BMC Genomics 16:769.*

Hubert AH, Henderson JM, **Ross KG**, Cowles MW, and Zayas RM. 2012. Epigenetic regulation of planarian stem cells by the SET1/MLL family of histone methyltransferases. *Epigenetics 8(1):79-91.*

Schulz, T, Young H, Agulnick A, Babin J, Baetge E, Bang A, Bhoumik A, Cepa I, Cesario R, Haakmeester C, Kadoya K, Kelly J, Kerr J, Marinson L, McLean A, Moorman M, Payne J, Richardson M, **Ross K**, Sherrer E, Song Xuehong, Wilson A, Brandon E, Green C, Kroon E, Kelly O, D'Amour K, and Robins A. 2012. A scalable system for production of functional pancreatic progenitors from human embryonic stem cells. *PLoS One* 7(5):e37004.

Kelly OG, Chan MY, Martinson LA Kadoya K, Ostertag TM, **Ross KG**, Richardson M, Carpenter MK, D'Amour KA, Kroon E, Moorman M, Baetge EE, and Bang AG. 2011. Cell-surface markers for the isolation of pancreatic cell types derived from human embryonic stem cells. *Nat Biotechnol* 29(8):750-756.

SCIENTIFIC PRESENTATIONS

Ross KG, Cable KL, Omuro KC, Quintanilla CG, Collins EMS, and Zayas RM. (Sep 2015). *SoxB1b* expression is essential for neuronal regeneration and function in planarians. 3rd North American Planarian Meeting, Chicago, Illinois. Oral Presentation.

Ross KG, Cable KL, Omuro KC, Quintanilla CG, and Zayas RM. (June 2015). *SoxB1b* expression is essential for neuronal regeneration and function in planarians. Tissue Repair and Regeneration Gordon Research Conference, New London, New Hampshire. Poster.

Ross KG, Cable KL, Omuro KC, Quintanilla CG, and Zayas RM. (Sep 2014). A *SoxB1* homolog is required for nervous system regeneration and function in the planarian *Schmidtea mediterranea*. EMBO Conference on the Molecular and Cellular Basis of Regeneration and Tissue Repair, Sant Feliu de Guixols, Spain. Poster.

Ross KG, Cable KL, Omuro KC, Quintanilla CG, and Zayas RM. (Jul 2014). A *SoxB1* gene is required for nervous system regeneration and function in the planarian *Schmidtea mediterranea*. Abstract No. 83. Annual Society for Developmental Biology Meeting, Seattle, WA. Poster.

Ross KG, Cable KL, Omuro KC, and Zayas RM. (March 2014). SoxB1b is required for nervous system regeneration and function in the planarian *Schmidtea mediterranea*.

San Diego State University Student Research Symposium, San Diego, CA. Oral Presentation.

Forshoefel D, **Ross KG**. (May 2013). Technical workshop on antibody generation for planarian research. 2nd North American Planarian Meeting, Kansas City, Missouri. Co-led presentation and discussion.

Ross KG, Omuro K, Huggins IJ, Willert K, and Zayas RM. (May 2013). The role of Sox genes in planarian and human stem cells. North American Planarian Meeting, Kansas City, Missouri. Poster.

Ross KG, Taylor M, Munday RK, Hubert A, and Zayas RM. (Jul 2012). Novel antibodies to track cell differentiation in planarians. Abstract No. 187. Annual Society for Developmental Biology Meeting, Montreal, Canada. Poster.

Ross KG, Taylor M, Hubert A, and Zayas RM. (Mar 2012). The combination of novel antibodies and bromodeoxyuridine to track neurogenesis in planarians**.** San Diego State University Student Research Symposium, San Diego, CA. Poster.

Ross KG, Taylor M, Munday RK, Hubert A, and Zayas RM. (Dec 2011). Novel antibodies to track neurogenesis in planarians. Abstract No. 2889. American Society for Cell Biology Annual Meeting, Denver, CO. Poster.

AWARDS AND FELLOWSHIPS

Achievement Awards for College Scientists Fellowship, San Diego Chapter, Aug. 2015-present.

Anita Roberts Memorial Fund Travel Fellowship, Tissue Repair and Regeneration Gordon Research Conference, May 2015.

European Molecular Biology Organization Travel Fellowship, EMBO Conference on the Molecular and Cellular Basis of Regeneration and Tissue Repair, Jun. 2014.

Provost's Award for Outstanding Poster Presentation, San Diego State University, Student Research Symposium, Mar. 2012.

Instructionally Related Activities Travel Funding Award, College of Sciences, San Diego State University, Nov. 2011.

PROFESSIONAL SOCIETY MEMBERSHIPS

The American Society for Cell Biology, 2011 – Present
Society for Developmental Biology, 2012 – Present

ABSTRACT OF THE DISSERATION

The role of a *SoxB1* gene in the regeneration and function of sensory neurons in the planarian *Schmidtea mediterranea*

By

Kelly Gullette Ross

Doctor of Philosophy in Biology

University of California, San Diego 2017

San Diego State University 2017

Professor Ricardo Zayas, Chair

Sox genes regulate multiple aspects of neurogenesis, including ectoderm and neuroectoderm specification, maintenance of neural stem cells, and sensory neuron specification and maintenance. Homozygous knockout of the *SoxB1* transcription factor gene *Sox1* causes epileptic seizures in mice. However, the genes regulated by *Sox1* in the adult nervous system or the roles that its abnormal function plays in disease are largely unknown. Planarian flatworms are excellent models for studying the roles of transcription factors in adult neurogenesis; these animals regenerate a

molecularly complex central and peripheral nervous system following injury or amputation from a large population of adult stem cells. Thus, we wanted to use planarians as a model system to study *SoxB1* function during regenerative neurogenesis in planarians. In order to do this, my dissertation work had two broad goals: 1) the further development of methods to assess the effects of perturbations to neurogenesis in planarian flatworms and 2) to assess the roles *soxB1* genes play in planarian neurogenesis. In the first chapter, I describe the current state-of-knowledge of planarian neurogenesis. In the second and third chapters, I demonstrate the strides we have taken to produce more antibodies and methods to use antibodies to label multiple planarian cell types and tissues. And finally, in Chapter 4, I present our work surveying *soxB1* function in planarian neurogenesis. Through this work, we found that inhibition of *soxB1-2* caused a seizure-like movement phenotype. By using single cell RNA sequencing data (scRNA-seq), we were able to identify an ectodermal progenitor in planarians that is marked by *soxB1-2* expression. Functional and expression analysis of 86 downstream genes of *soxB1-2* revealed 17 genes with loss-of-function phenotypes that recapitulated aspects of the *soxB1-2(RNAi)* phenotype. 16 of these genes have confirmed expression in neurons and by coupling expression and function of a subset of these genes, we have identified at the molecular level a rheosensory (water flow sensory) population in planarians. While some downstream genes are implicated in genetic causes of epilepsy disorders (EDs) in humans, additional genes represent novel candidates, in particular, genes encoding components of calcium signaling linked to

primary cilia function, which represents a new field in epilepsy research. Thus, these studies will aid in establishing planarians as a genetic model in which to study the molecular basis of seizure disorders in humans.

INTRODUCTION OF THE DISSERATION

SOXB1 PROTEINS: ROLES IN ECTODERMAL, NEUROECTODERMAL AND SENSORY NEURON SPECIFICATION

During embryonic development, animals must generate all of the different cell types in the organism, including the nervous system. SOXB proteins play broad roles in the developing embryo, from maintaining pluripotency in embryonic stem cells, to specification of the ectoderm and the neuroectoderm, and in development of the nervous system (Figure I.1). *Sox* genes predate multicellularity and there are over 20 different *Sox* genes in vertebrates that are involved in many different functions [1, 2]. The first identified member of the *Sox* gene family was *Sry* (*sex-determining region Y*) [3, 4]. This gene is found only in mammals where it determines male sex. All subsequently identified *Sox* genes share approximately 50% or higher amino acid sequence similarity within the high-mobility group (HMG) box domain found within the *Sry* gene [1, 5]. The HMG domain of SOX proteins is a DNA-binding domain that binds to the minor groove of DNA causing bending, which assists in its function as transcriptional activator or repressor by causing further recruitment of transcriptional machinery components or DNA-modifying complexes [6, 7]. Within the SOX gene family, subfamilies are designated based on sequence similarity and generally share 70% or higher amino acid similarity (Figure I.2). These subfamilies likely arose from multiple rounds of duplication events throughout evolution [5, 6].

SoxB subgroup genes contain a group B homology domain next to the HMG domain [8]. This group is further divided into *SoxB1* and *SoxB2* subgroups based on additional sequence similarity of their HMG domains, which contain highly

conserved residues at key positions [9, 10]. The split between *SoxB1* and *SoxB2* genes is thought to have occurred before the emergence of metazoans [10]. While the entire *Sox* gene family performs crucial roles during development, *SoxB1* genes represent a subfamily whose roles in development start at the very beginning of embryogenesis, in maintaining the pluripotency of stem cells.

The *SoxB1* gene, *Sox2,* is expressed in embryonic stem cells and is required for the establishment of these cells, maintaining their pluripotency, and allowing for their self-renewal [11]. Additionally, *Sox2* represents one of the transcription factors that can re-establish an embryonic stem cell-like pluripotency from terminally differentiated cells when used in combination with a handful of other transcription factors [12]. These feats are accomplished through transcriptional activation of a variety of stem cell-specific genes [13-15].

One of the first steps to accomplishing the task of cellular diversification is the formation of the three germ layers during gastrulation: the outer layer (ectoderm), inner layer (endoderm), and middle layer (mesoderm). The majority of neurons in the adult will arise from the ectoderm. Therefore, understanding the molecular signals that specify the ectoderm is the first step in understanding how neurons are born. *SoxB* gene expression becomes increasingly confined to the ectoderm during gastrulation [11, 16, 17]. In the sea urchin, *Strongylocentrotus purpuratus,* SOXB1 antagonizes β-catenin-mediated Wnt signaling in animal pole cells to promote ectodermal cell fate [18]. Overexpression of *SoxB1* during gastrulation in the sea urchin leads to the formation of ectodermal spheres [19].

Additionally, SOXB1 promotes the transcription of SpAN in the non-vegetal domain in sea urchin [20]. SpAN encodes a tolloid-like metalloprotease that is likely critical for cell movements during gastrulation, thus making the expression of SOXB1 crucial for this process [19]. Finally, the *SoxB1* gene, *Sox3,* promotes ectodermal fate in frog embryos by repressing *nr5,* a gene related to Nodal [21]. Altogether, demonstrating a conserved role for *SoxB1* genes in formation and specification of the ectoderm.

Following formation of the ectoderm, *SoxB1* gene expression is further restricted to the neuroectoderm and neural precursor cells [11, 16, 22-24]. All three members of the mammalian *SoxB1* gene subgroup are expressed in the neuroepithelium and are implicated in specifying neuoroepithelial cell fate [25-27]. Forced expression of either *Sox1* or *Sox2* in embryonic stem cells directs differentiation into the neuroectodermal lineage [28]. *Sox1, -2, and -3* keep neuroepithelial progenitor cells in an undifferentiated stem-like state by counteracting proneural basic helix-loop-helix (bHLH) proteins, which force neuronal differentiation [25]; increased expression of bHLH proteins and SoxB2 proteins force further differentiation of neural precursor cells at the expense of *SoxB1* gene expression, promoting terminal differentiation of neurons [25, 29]. Thus, SoxB1 proteins help to maintain the multipotency and self-renewal capabilities of the neural progenitor population. This function likely continues in adult neurogenesis, because neural progenitor cells in the adult brain express *SoxB1* genes as well [24, 30].

Later during development, when organogenesis is taking place, *SoxB1* genes are redeployed for the specification and maintenance of sensory neurons. For example, *SoxB1* is expressed in the ciliated sensory epithelium in cuttlefish [31] and a *SoxB1* gene is implicated in determination of sensory epidermal cells in amphioxus [32]. Additionally, in human embryonic stem cell derived neural crest models, *Sox2* has been found to play a necessary role in the acquisition of neural fates in sensory ganglia [33]. *Sox2* is also expressed in early sensory cell precursors and is required for their proliferation and specification [34]. *SoxB1* genes directly activate expression of *∂*-crystallin expression in the embryonic eye lens [35]. Ectopic expression of the *SoxB1* gene *Sox3* leads to ectopic sensory placode formation in medaka fish [36]. And finally, *SoxB* genes are expressed in the ectodermal cells that contribute to photoreceptive sensory cells in sponges and ctenophores [37-39], highlighting the roles of these genes in sensory organ development and likely a very ancient role in the differentiation of sensory cells.

Given the versatility and importance of *SoxB1* genes during neurogenesis, it is not surprising that dysfunction of these genes during development can lead to a neuronal disorder like epilepsy. In fact, *Sox1* knockout mice have increased seizures and a decreased life span [40]. SOX1-deficient mice exhibit abnormal excitability in the olfactory cortex correlating with a deficit of postsynaptic target neurons within the olfactory cortex, including GABAergic projection neurons, which are part of the action potential inhibition machinery of the central nervous system (CNS) [40, 41]. SOX1, like SOX2 remains expressed in the adult brain during adult neurogenesis,

suggesting continued roles in adult neurogenesis, including a role in activation of the bHLH gene function that overcomes *SoxB1* gene function to promote terminal differentiation of telencephalic precursors [42, 43]. However, continued expression of SOX1 in post-mitotic telencephalic precursors is necessary for proper migration of these cells to the ventral striatum [44]. Thus, we know there exist links between *SoxB1* function, formation of neuronal architecture, and a necessity for continued expression of *SoxB1* genes in the adult brain, but exactly how this system works during adult neurogenesis, is currently poorly understood.

The planarian flatworm represents an excellent model system in which to study the effects of *SoxB1* gene loss in adult neurogenesis due to their amazing ability to regenerate all adult tissues and cell types from an abundant population of adult pluripotent stem cells [45, 46]. However, there is a need for the development of additional tools to study changes to adult neurogenesis resulting from functional genetic studies. Thus, Chapters 2 and 3 of this dissertation represent work to create additional antibody reagents and methods to label planarian tissues for regeneration and neurogenesis studies. In Chapter 4, I explore the function of *SoxB1* genes in planarian adult neurogenesis and find that loss-of-function of one *SoxB1* gene, *Smed-soxB1-2,* leads to a seizure-like behavioral phenotype. Some genes downstream of *soxB1-2* are related to epilepsy-associated genes in humans. Therefore, the remainder of this introduction will focus on the need for more antibodies to study planarian stem-cell based regeneration and the genetic basis of

epilepsy in humans, which will lead into Chapter 1, which represents an in-depth review of the current state of knowledge on planarian neurogenesis.

A NEED FOR IMPROVED METHODS TO ASCERTAIN PERTERBATIONS TO NEUROGENSIS IN PLANARIANS

The precise events that occur during regeneration of neurons in the adult nervous system are poorly understood and thus require further elucidation. *Schmidtea mediterranea*, a planarian species for which several molecular tools have been developed, is a useful model organism for nervous system regeneration studies due to their ability to regenerate their entire body following injury or amputation [47-50]. This ability is conferred by a population of adult stem cells that exist throughout the adult worm and constitute approximately 20-30% of the total cell count in the intact animal [49, 51, 52]. Planarian stem cells proliferate and migrate to sites of injury where they contribute to the regeneration blastema to reconstitute missing cell types and structures [51, 53, 54].

Previous findings suggest the basic genetic programming for development of the planarian brain is highly conserved with that of the vertebrate brain [55]. Like the human nervous system, the planarian brain contains serotonergic, dopaminergic, GABAergic, and octopaminergic neurons [56]. In addition to nervous system similarities, the functional analysis of two *msh/msx*-related transcription factor genes in planarian regeneration has demonstrated that this family of genes, key to the control of cell differentiation during embryogenesis in vertebrates, is

necessary for proper regenerative events in planarians [57]. All together, these findings strongly support the suitability of planarians as a model system for CNS regeneration.

Initial structural analyses of the planarian nervous system are recorded in works dating back to the late 19th century [58]. The advent of electron microscopy in the 20th century allowed for more detailed observations of the intricate structure of the planarian nervous system, such as the spongy texture of the cephalic ganglia woven with muscles and processes from secretory cells, regularly-spaced ganglionic knots traversing the ventral nerve cords, and the delicate architecture of subepidermal, submuscular, and gastrodermal plexuses [50, 59-63]. In recent years, the implementation of modern molecular tools such as whole-mount *in situ* hybridization (WISH), genomic sequencing, and the ability to inhibit gene expression using RNAi have provided useful information regarding gene expression and function in the planarian CNS. Observations based on mRNA expression in the planarian, *Dugesia japonica*, have shown that 4 distinct molecular domains exist in the cephalic ganglia based on expression of homologues of *Otd/Otx* family genes [64]. Expression of a gene homologous to PC-2 (pro-hormone convertase 2, found in other animals to be specifically expressed in neurons secreting neuropeptides) observed by WISH provides a well-defined image of the positioning and connection of the cephalic ganglia to the ventral nerve cords, a connection occurring on the most ventral inside region of the cephalic ganglia [65].

The visualization of mRNA expression patterns, however, does not allow for a complete understanding of CNS structure and connectivity; visualization of proteins that extend along the length of axonal and dendritic projections allows for visualization of connections in nervous system circuits. It is therefore of interest to use antibodies for visualization of neuronal proteins in this model system. First, an antibody against a *D. japonica* homolog of synaptotagmin allowed staining of neuronal axons [54]. Tracking the expression of this protein during regeneration showed that neural proteins are upregulated in the brain primordium that begins developing while the ventral nerve cords remain truncated, outside the blastema, disputing a conflicting theory that the cephalic ganglia form as an extension from the established ventral nerve cords [66, 67]. Second, an extensive screen of commercially available antibodies that were generated against other organisms identified four antibodies that label cells within the CNS of *S. mediterranea* and *D. dorotocephala*. One of these antibodies, α+β tubulin, also recognizes ciliated epithelium, while others are classified as having weak staining or appear to stain neurons within the CNS without specificity to any particular subset of neurons [68]. Furthermore, Cebrià *et al.* identified five antibodies (anti-Synapsin, anti-Serotonin, anti-Allatostatin, anti-GYRFamide, and anti-NeuropeptideF), as specifically cross-reacting with neurons in the CNS of *S. mediterranea*, allowing for characterization of structures that was previously hindered by staining methods using markers such as α-Tubulin and Phosphotyrosine that are not specific to neurons [47, 48, 50]. Finally,

antibodies have been generated for *D. japonica* to stain specific neurotransmitter neuronal populations, such as serotonergic and dopaminergic neurons [69, 70].

In addition to antibodies that recognize proteins, a protocol has been developed for the visualization of neoblasts (stem cells) in *S. mediterranea* by using a monoclonal antibody against 5-bromodeoxyuridine (a reagent used for its ability to incorporate into the DNA of mitotically active cells) [71]. However, due to the complexity of the planarian nervous system, the number of antibodies that have been generated for use in planarians or that cross-react with specific neurons in planarians is not comprehensive, and this list is further limited with respect to *S. mediterranea.* Thus, one of our goals was to produce monoclonal antibodies that can be used to label neurons and other tissues in planarians (see Chapter 2), including an antibody that labels neuronal projections in the peripheral nervous system. This work, along with another recent publication [72], represents the newest sets of reagents available for surveying changes in planarian tissue regeneration following RNAi experiments. While testing these antibodies, we explored extensive variations to antibody labeling protocols and how these alterations affected the labeling efficiency of multiple tissue-types in the planarian. We summarized this methodology in a methods chapter aimed at providing an extensive guide to using antibodies for immunohistochemical labeling of planarian tissues (see Chapter 3). Using improved methods to assay perturbations in planarian neurogenesis following gene inhibition allowed us to observe changes following *SoxB1-2* RNAi and how *SoxB1-2* inhibition led to an epilepsy-like phenotype in planarians.

THE GENETIC BASIS OF EPILEPSY

Epilepsy disorders (EDs) are defined as neurological disorders consisting of recurrent epileptic seizures [73]. These seizures are characterized by abnormal electrical activity in the CNS [74]. An estimated 3.5-6.5 per 1000 children [75] and 10.8 per 1000 elderly people [76] suffer from EDs and approximately 47% of all epilepsies are thought to have a genetic basis with approximately 1% of these cases having a monogenic inheritance [77], therefore, the genetic basis of epilepsy involves complex inheritance patterns [74, 78]. Although idiopathic epilepsies are generally polygenic, understanding the genes associated with monogenic epilepsies can provide a basic understanding of the neuronal processes that dysfunction in this disease.

The most common genetic mutations associated with epilepsy are in cation channel genes, with the most prevalent mutations in *SCN1A*, which codes for the Sodium Voltage-Gated Channel Alpha Subunit 1 protein and always exhibits dominant inheritance patterns associated with the disease [77] [79, 80]. Sodium channels are necessary for initiating and propagating action potentials in neurons [80], thus resulting in alterations to the excitability of various neuronal populations which leads to electrical imbalance and abnormal function in the CNS.

Mutations in potassium channel genes are also highly associated with EDs. Mutations in these genes likely lead to action potential alterations in numerous ways. For instance, genes that comprise the Potassium Channel Voltage-Gated KQT-like Potassium Channel result in epilepsies by disturbing the production of the M

current in neurons, which is responsible for stabilizing neuronal excitability [81-83]. On the other hand, mutations in the gene *Potassium Voltage-Gated Channel, Shaker-Related Subfamily, Member 1* (*KCNA1*) result in epilepsy due to this gene's contribution to repolarization and shaping of action potentials at presynaptic nerve terminals [84]. Alternatively, mutations in *Potassium Channel Tetramerization Domain-Containing Protein 7* (*KCTD7*) result in alterations of action potential by dysfunction of the potassium channels voltage gating function [85]. Once again, demonstrating that dysfunctions in action potential lead to the abnormal neuronal excitability associated with EDs. Similarly, mutations to Ca^{2+} channels are associated with alterations to action potentials, which result in EDs.

Mutations in GABA receptor genes are highly associated with EDs, in particular, mutations in genes of the ionotropic $GABA_A$ receptor family (*GABRA1, GABRB3, GABRD,* and *GABRG2*) [79]. Reduced $GABA_A$ receptor function results in a decrease of GABA-mediated neuronal inhibition leading to neuronal hyperexcitability [86]. Additional mutations to genes responsible for the function of excitatory and inhibitory neurotransmitters have also been identified [77, 79, 87]. Altogether, these represent alterations to overall neuronal excitability.

A gene family that is not currently associated with epilepsies based on genome-wide association studies (GWAS) data in humans, is the polycystic kidney disease gene family (*pkd* genes). These genes encode for Polycystin proteins, which are expressed on the primary cilia of multiple cell types, including renal epithelial cells, where they promote Ca^{2+} influx following fluid-flow mechanosensation [88]. A

link between Polycystin-L function in the primary cilia of neurons and epilepsy was recently discovered by Yao and colleagues [89]. They demonstrated a role for Polycystin-L at the primary cilia in neurons, where it interacts with Beta-2 adrenergic receptors, likely resulting in the observed decrease in cyclic AMP production (which is known to inhibit neuronal excitability) [90, 91]. These results represent an exciting new field in epilepsy research, which may provide a physiological explanation for the phenotypes observed in Chapter 4. However, to understand how planarians might be used as a model for epilepsy research, it is necessary to understand the planarian nervous system and the conservation of neurogenesis between planarians and vertebrates. Therefore, the first chapter of this dissertation presents a comprehensive review of the planarian nervous system and our current knowledge of planarian neurogenesis.

FIGURES

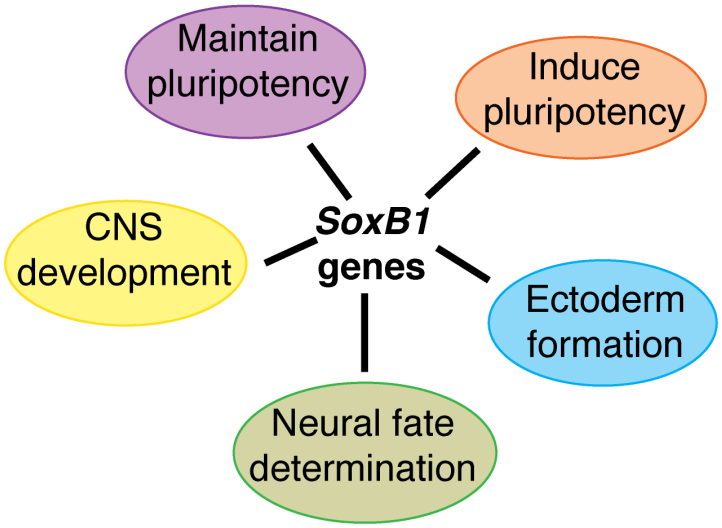

Figure I.1: Multiple functions of *SoxB1* genes. Figure adapted from [6].

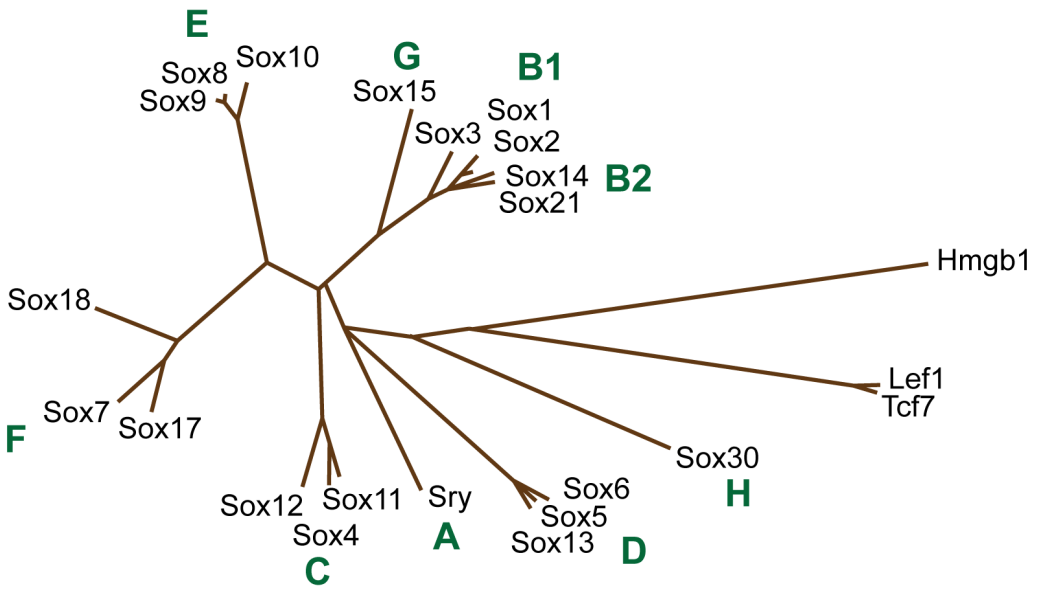

Figure I.2: Phylogeny of the *Sox* gene subgroups in mice. This unrooted neighbor-joining tree made using the HMG domain sequences of SOX proteins from *M. musculus* demonstrates how variation within the HMG domain led to grouping of the genes into subfamilies, which are designated by green letters. The outgroups presented are the HMG domains of Lef1, Tcf7, and Hmgb1 (Lymphoid Enhancer Binding Factor 1, Transcription Factor 7 T Cell Specific, and High Mobility Group Protein B1, all proteins within the HMG superfamily). Figure adapted from [92].

REFERENCES

1. Bowles J, Schepers G, Koopman P: **Phylogeny of the SOX family of developmental transcription factors based on sequence and structural indicators**. *Dev Biol* 2000, **227**(2):239-255.

2. Lefebvre V, Dumitriu B, Penzo-Mendez A, Han Y, Pallavi B: **Control of cell fate and differentiation by Sry-related high-mobility-group box (Sox) transcription factors**. *The international journal of biochemistry & cell biology* 2007, **39**(12):2195-2214.

3. Gubbay J, Collignon J, Koopman P, Capel B, Economou A, Munsterberg A, Vivian N, Goodfellow P, Lovell-Badge R: **A gene mapping to the sex-determining region of the mouse Y chromosome is a member of a novel family of embryonically expressed genes**. *Nature* 1990, **346**(6281):245-250.

4. Sinclair AH, Berta P, Palmer MS, Hawkins JR, Griffiths BL, Smith MJ, Foster JW, Frischauf AM, Lovell-Badge R, Goodfellow PN: **A gene from the human sex-determining region encodes a protein with homology to a conserved DNA-binding motif**. *Nature* 1990, **346**(6281):240-244.

5. Wegner M: **From head to toes: the multiple facets of Sox proteins**. *Nucleic Acids Res* 1999, **27**(6):1409-1420.

6. Guth SIE, Wegner M: **Having it both ways: Sox protein function between conservation and innovation**. *Cell Mol Life Sci* 2008, **65**(19):3000-3018.

7. Scaffidi P, Bianchi ME: **Spatially precise DNA bending is an essential activity of the sox2 transcription factor**. *J Biol Chem* 2001, **276**(50):47296-47302.

8. Uchikawa M, Kamachi Y, Kondoh H: **Two distinct subgroups of Group B Sox genes for transcriptional activators and repressors: their expression during embryonic organogenesis of the chicken**. *Mechanisms of development* 1999, **84**(1-2):103-120.

9. Malas S, Duthie S, Deloukas P, Episkopou V: **The isolation and high-resolution chromosomal mapping of human SOX14 and SOX21; two members of the SOX gene family related to SOX1, SOX2, and SOX3**. *Mammalian genome : official journal of the International Mammalian Genome Society* 1999, **10**(9):934-937.

10. Zhong L, Wang D, Gan X, Yang T, He S: **Parallel expansions of Sox transcription factor group B predating the diversifications of the arthropods and jawed vertebrates**. *PLoS One* 2011, **6**(1):e16570.

11. Avilion AA, Nicolis SK, Pevny LH, Perez L, Vivian N, Lovell-Badge R: **Multipotent cell lineages in early mouse development depend on SOX2 function**. *Genes & development* 2003, **17**(1):126-140.

12. Takahashi K, Yamanaka S: **Induction of pluripotent stem cells from mouse embryonic and adult fibroblast cultures by defined factors**. *Cell* 2006, **126**(4):663-676.

13. Boyer LA, Lee TI, Cole MF, Johnstone SE, Levine SS, Zucker JP, Guenther MG, Kumar RM, Murray HL, Jenner RG *et al*: **Core transcriptional regulatory circuitry in human embryonic stem cells**. *Cell* 2005, **122**(6):947-956.

14. Chen X, Xu H, Yuan P, Fang F, Huss M, Vega VB, Wong E, Orlov YL, Zhang W, Jiang J *et al*: **Integration of external signaling pathways with the core transcriptional network in embryonic stem cells**. *Cell* 2008, **133**(6):1106-1117.

15. Marson A, Levine SS, Cole MF, Frampton GM, Brambrink T, Johnstone S, Guenther MG, Johnston WK, Wernig M, Newman J *et al*: **Connecting microRNA genes to the core transcriptional regulatory circuitry of embryonic stem cells**. *Cell* 2008, **134**(3):521-533.

16. Kishi M, Mizuseki K, Sasai N, Yamazaki H, Shiota K, Nakanishi S, Sasai Y: **Requirement of Sox2-mediated signaling for differentiation of early Xenopus neuroectoderm**. *Development* 2000, **127**(4):791-800.

17. Wood HB, Episkopou V: **Comparative expression of the mouse Sox1, Sox2 and Sox3 genes from pre-gastrulation to early somite stages**. *Mechanisms of development* 1999, **86**(1-2):197-201.

18. Angerer LM, Newman LA, Angerer RC: **SoxB1 downregulation in vegetal lineages of sea urchin embryos is achieved by both transcriptional repression and selective protein turnover**. *Development* 2005, **132**(5):999-1008.

19. Kenny AP, Oleksyn DW, Newman LA, Angerer RC, Angerer LM: **Tight regulation of SpSoxB factors is required for patterning and morphogenesis in sea urchin embryos**. *Dev Biol* 2003, **261**(2):412-425.

20. Kenny AP, Kozlowski D, Oleksyn DW, Angerer LM, Angerer RC: **SpSoxB1, a maternally encoded transcription factor asymmetrically distributed among early sea urchin blastomeres**. *Development* 1999, **126**(23):5473-5483.

21. Zhang C, Basta T, Jensen ED, Klymkowsky MW: **The beta-catenin/VegT-regulated early zygotic gene Xnr5 is a direct target of SOX3 regulation**. *Development* 2003, **130**(23):5609-5624.

22. Cremazy F, Berta P, Girard F: **Sox neuro, a new Drosophila Sox gene expressed in the developing central nervous system**. *Mechanisms of development* 2000, **93**(1-2):215-219.

23. Collignon J, Sockanathan S, Hacker A, Cohen-Tannoudji M, Norris D, Rastan S, Stevanovic M, Goodfellow PN, Lovell-Badge R: **A comparison of the properties of Sox-3 with Sry and two related genes, Sox-1 and Sox-2**. *Development* 1996, **122**(2):509-520.

24. Ferri AL, Cavallaro M, Braida D, Di Cristofano A, Canta A, Vezzani A, Ottolenghi S, Pandolfi PP, Sala M, DeBiasi S *et al*: **Sox2 deficiency causes neurodegeneration and impaired neurogenesis in the adult mouse brain**. *Development* 2004, **131**(15):3805-3819.

25. Bylund M, Andersson E, Novitch BG, Muhr J: **Vertebrate neurogenesis is counteracted by Sox1-3 activity**. *Nature neuroscience* 2003, **6**(11):1162-1168.

26. Graham V, Khudyakov J, Ellis P, Pevny L: **SOX2 functions to maintain neural progenitor identity**. *Neuron* 2003, **39**(5):749-765.

27. Pevny LH, Lovell-Badge R: **Sox genes find their feet**. *Curr Opin Genet Dev* 1997, **7**(3):338-344.

28. Zhao S, Nichols J, Smith AG, Li M: **SoxB transcription factors specify neuroectodermal lineage choice in ES cells**. *Molecular and cellular neurosciences* 2004, **27**(3):332-342.

29. Sandberg M, Kallstrom M, Muhr J: **Sox21 promotes the progression of vertebrate neurogenesis**. *Nature neuroscience* 2005, **8**(8):995-1001.

30. Favaro R, Valotta M, Ferri AL, Latorre E, Mariani J, Giachino C, Lancini C, Tosetti V, Ottolenghi S, Taylor V *et al*: **Hippocampal development and neural stem cell maintenance require Sox2-dependent regulation of Shh**. *Nature neuroscience* 2009, **12**(10):1248-1256.

31. Focareta L, Cole AG: **Analyses of Sox-B and Sox-E Family Genes in the Cephalopod Sepia officinalis: Revealing the Conserved and the Unusual**. *PLoS One* 2016, **11**(6):e0157821.

32. Meulemans D, Bronner-Fraser M: **The amphioxus SoxB family: implications for the evolution of vertebrate placodes**. *International journal of biological sciences* 2007, **3**(6):356-364.

33. Cimadamore F, Fishwick K, Giusto E, Gnedeva K, Cattarossi G, Miller A, Pluchino S, Brill LM, Bronner-Fraser M, Terskikh AV: **Human ESC-derived neural crest model reveals a key role for SOX2 in sensory neurogenesis**. *Cell stem cell* 2011, **8**(5):538-551.

34. Fritzsch B, Beisel KW, Hansen LA: **The molecular basis of neurosensory cell formation in ear development: a blueprint for hair cell and sensory neuron regeneration?** *BioEssays : news and reviews in molecular, cellular and developmental biology* 2006, **28**(12):1181-1193.

35. Kamachi Y, Uchikawa M, Collignon J, Lovell-Badge R, Kondoh H: **Involvement of Sox1, 2 and 3 in the early and subsequent molecular events of lens induction**. *Development* 1998, **125**(13):2521-2532.

36. Koster RW, Kuhnlein RP, Wittbrodt J: **Ectopic Sox3 activity elicits sensory placode formation**. *Mechanisms of development* 2000, **95**(1-2):175-187.

37. Fortunato S, Adamski M, Bergum B, Guder C, Jordal S, Leininger S, Zwafink C, Rapp HT, Adamska M: **Genome-wide analysis of the sox family in the calcareous sponge Sycon ciliatum: multiple genes with unique expression patterns**. *Evodevo* 2012, **3**(1):14.

38. Jager M, Queinnec E, Chiori R, Le Guyader H, Manuel M: **Insights into the early evolution of SOX genes from expression analyses in a ctenophore**. *Journal of experimental zoology Part B, Molecular and developmental evolution* 2008, **310**(8):650-667.

39. Schnitzler CE, Simmons DK, Pang K, Martindale MQ, Baxevanis AD: **Expression of multiple Sox genes through embryonic development in the ctenophore Mnemiopsis leidyi is spatially restricted to zones of cell proliferation**. *Evodevo* 2014, **5**:15.

40. Malas S, Postlethwaite M, Ekonomou A, Whalley B, Nishiguchi S, Wood H, Meldrum B, Constanti A, Episkopou V: **Sox1-deficient mice suffer from epilepsy associated with abnormal ventral forebrain development and olfactory cortex hyperexcitability**. *Neuroscience* 2003, **119**(2):421-432.

41. Koos T, Tepper JM: **Inhibitory control of neostriatal projection neurons by GABAergic interneurons**. *Nature neuroscience* 1999, **2**(5):467-472.

42. Venere M, Han YG, Bell R, Song JS, Alvarez-Buylla A, Blelloch R: **Sox1 marks an activated neural stem/progenitor cell in the hippocampus**. *Development* 2012, **139**(21):3938-3949.

43. Kan L, Jalali A, Zhao LR, Zhou X, McGuire T, Kazanis I, Episkopou V, Bassuk AG, Kessler JA: **Dual function of Sox1 in telencephalic progenitor cells**. *Dev Biol* 2007, **310**(1):85-98.

44. Ekonomou A, Kazanis I, Malas S, Wood H, Alifragis P, Denaxa M, Karagogeos D, Constanti A, Lovell-Badge R, Episkopou V: **Neuronal migration and ventral subtype identity in the telencephalon depend on SOX1**. *PLoS Biol* 2005, **3**(6):e186.

45. Rink JC: **Stem cell systems and regeneration in planaria**. *Dev Genes Evol* 2013, **223**(1-2):67-84.

46. Baguñà J: **The planarian neoblast: the rambling history of its origin and some current black boxes**. *The International journal of developmental biology* 2012, **56**(1-3):19-37.

47. Agata K, Saito Y, Nakajima E: **Unifying principles of regeneration I: Epimorphosis versus morphallaxis**. *Dev Growth Differ* 2007, **49**(2):73-78.

48. Agata K, Umesono Y: **Brain regeneration from pluripotent stem cells in planarian**. *Philos Trans R Soc Lond B Biol Sci* 2008, **363**(1500):2071-2078.

49. Baguñà J, Saló E, Auladell C: **Regeneration and pattern formation in planarians. III. that neoblasts are totipotent stem cells and the cells**. *Development* 1989, **107**(1):77-86.

50. Cebrià F: **Regenerating the central nervous system: how easy for planarians!** *Dev Genes Evol* 2007, **217**(11-12):733-748.

51. Baguñà J: **Mitosis in the intact and regenerating planarian Dugesia mediterranea n.sp. II. Mitotic studies during regeneration, and a possible mechanism of blastema formation**. *J Exp Zool* 1976, **195**:53-64.

52. Baguñà J, Romero R: **Quantitative analysis of cell types during growth, degrowth and regeneration in the planarians Dugesia mediterranea and Dugesia tigrina**. *Hydrobiologia* 1981, **84**(1):181-194.

53. Reddien PW, Sánchez Alvarado A: **Fundamentals of planarian regeneration**. *Annu Rev Cell Dev Biol* 2004, **20**:725-757.

54. Agata K, Watanabe K: **Molecular and cellular aspects of planarian regeneration**. *Semin Cell Dev Biol* 1999, **10**(4):377-383.

55. Umesono Y, Agata K: **Evolution and regeneration of the planarian central nervous system**. *Dev Growth Differ* 2009, **51**(3):185-195.

56. Takeda H, Nishimura K, Agata K: **Planarians maintain a constant ratio of different cell types during changes in body size by using the stem cell system**. *Zoolog Sci* 2009, **26**(12):805-813.

57. Mannini L, Deri P, Picchi J, Batistoni R: **Expression of a retinal homeobox (Rx) gene during planarian regeneration**. *Int J Dev Biol* 2008, **52**(8):1113-1117.

58. Baguñà J, Ballester R: **The nervous system in planarians: Peripheral and gastrodermal plexuses, pharynx innervation, and the relationship between central nervous system structure and the acoelomate organization**. *Journal of Morphology* 1978, **155**(2):237-252.

59. Best JB, Morita M, Noel J: **Fine sturcture and function of planarian goblet cells**. *J Ultrastruct Res* 1968, **24**(5):385-397.

60. MacRae EK: **The fine structure of sensory receptor processes in the auricular epithelium of the planarian, Dugesia tigrina**. *Z Zellforsch Mikrosk Anat* 1967, **82**(4):479-494.

61. Oosaki T, Ishii S: **Observations on the ultrastructure of nerve cells in the brain of the planarian, Dugesia gonocephala**. *Z Zellforsch Mikrosk Anat* 1965, **66**(6):782-793.

62. Ishii S: **Electron microscopic observations on the Planarian tissues II. The intestine**. *Fukushima J Med Sci* 1965, **12**(1):67-87.

63. Macrae EK: **Observations on the Fine Structure of Photoreceptor Cells in the Planarian Dugesia Tigrina**. *J Ultrastruct Res* 1964, **10**:334-349.

64. Umesono Y, Watanabe K, Agata K: **A planarian orthopedia homolog is specifically expressed in the branch region of both the mature and regenerating brain**. *Dev Growth Differ* 1997, **39**(6):723-727.

65. Agata K, Soejima Y, Kato K, Kobayashi C, Umesono Y, Watanabe K: **Structure of the planarian central nervous system (CNS) revealed by neuronal cell markers**. *Zoolog Sci* 1998, **15**(3):433-440.

66. Cebrià F, Kudome T, Nakazawa M, Mineta K, Ikeo K, Gojobori T, Agata K: **The expression of neural-specific genes reveals the structural and molecular complexity of the planarian central nervous system**. *Mechanisms of development* 2002, **116**(1-2):199-204.

67. Cebrià F, Nakazawa M, Mineta K, Ikeo K, Gojobori T, Agata K: **Dissecting planarian central nervous system regeneration by the expression of neural-specific genes**. *Dev Growth Differ* 2002, **44**(2):135-146.

68. Robb SM, Sánchez Alvarado A: **Identification of immunological reagents for use in the study of freshwater planarians by means of whole-mount immunofluorescence and confocal microscopy**. *Genesis* 2002, **32**(4):293-298.

69. Nishimura K, Kitamura Y, Inoue T, Umesono Y, Yoshimoto K, Takeuchi K, Taniguchi T, Agata K: **Identification and distribution of tryptophan hydroxylase (TPH)-positive neurons in the planarian Dugesia japonica**. *Neurosci Res* 2007, **59**(1):101-106.

70. Nishimura K, Kitamura Y, Inoue T, Umesono Y, Sano S, Yoshimoto K, Inden M, Takata K, Taniguchi T, Shimohama S *et al*: **Reconstruction of dopaminergic neural network and locomotion function in planarian regenerates**. *Dev Neurobiol* 2007, **67**(8):1059-1078.

71. Newmark PA, Sánchez Alvarado A: **Bromodeoxyuridine specifically labels the regenerative stem cells of planarians**. *Dev Biol* 2000, **220**(2):142-153.

72. Forsthoefel DJ, Waters FA, Newmark PA: **Generation of cell type-specific monoclonal antibodies for the planarian and optimization of sample processing for immunolabeling**. *BMC Dev Biol* 2014, **14**:45.

73. **Guidelines for epidemiologic studies on epilepsy. Commission on Epidemiology and Prognosis, International League Against Epilepsy**. *Epilepsia* 1993, **34**(4):592-596.

74. Steinlein OK: **Genetic mechanisms that underlie epilepsy**. *Nat Rev Neurosci* 2004, **5**(5):400-408.

75. Lo-Castro A, Curatolo P: **Epilepsy associated with autism and attention deficit hyperactivity disorder: is there a genetic link?** *Brain & development* 2014, **36**(3):185-193.

76. Faught E, Richman J, Martin R, Funkhouser E, Foushee R, Kratt P, Kim Y, Clements K, Cohen N, Adoboe D *et al*: **Incidence and prevalence of epilepsy among older U.S. Medicare beneficiaries**. *Neurology* 2012, **78**(7):448-453.

77. Nicita F, De Liso P, Danti FR, Papetti L, Ursitti F, Castronovo A, Allemand F, Gennaro E, Zara F, Striano P *et al*: **The genetics of monogenic idiopathic epilepsies and epileptic encephalopathies**. *Seizure* 2012, **21**(1):3-11.

78. Michelucci R, Pasini E, Riguzzi P, Volpi L, Dazzo E, Nobile C: **Genetics of epilepsy and relevance to current practice**. *Current neurology and neuroscience reports* 2012, **12**(4):445-455.

79. Deng H, Xiu X, Song Z: **The molecular biology of genetic-based epilepsies**. *Molecular neurobiology* 2014, **49**(1):352-367.

80. Meisler MH, O'Brien JE, Sharkey LM: **Sodium channel gene family: epilepsy mutations, gene interactions and modifier effects**. *The Journal of physiology* 2010, **588**(Pt 11):1841-1848.

81. Wang HS, Pan Z, Shi W, Brown BS, Wymore RS, Cohen IS, Dixon JE, McKinnon D: **KCNQ2 and KCNQ3 potassium channel subunits: molecular correlates of the M-channel**. *Science* 1998, **282**(5395):1890-1893.

82. Brown DA, Adams PR: **Muscarinic suppression of a novel voltage-sensitive K+ current in a vertebrate neurone**. *Nature* 1980, **283**(5748):673-676.

83. Marrion NV: **Control of M-current**. *Annual review of physiology* 1997, **59**:483-504.

84. Browne DL, Gancher ST, Nutt JG, Brunt ER, Smith EA, Kramer P, Litt M: **Episodic ataxia/myokymia syndrome is associated with point mutations in the human potassium channel gene, KCNA1**. *Nature genetics* 1994, **8**(2):136-140.

85. Van Bogaert P, Azizieh R, Desir J, Aeby A, De Meirleir L, Laes JF, Christiaens F, Abramowicz MJ: **Mutation of a potassium channel-related gene in progressive myoclonic epilepsy**. *Annals of neurology* 2007, **61**(6):579-586.

86. Maljevic S, Krampfl K, Cobilanschi J, Tilgen N, Beyer S, Weber YG, Schlesinger F, Ursu D, Melzer W, Cossette P *et al*: **A mutation in the GABA(A) receptor alpha(1)-subunit is associated with absence epilepsy**. *Annals of neurology* 2006, **59**(6):983-987.

87. Ran X, Li J, Shao Q, Chen H, Lin Z, Sun ZS, Wu J: **EpilepsyGene: a genetic resource for genes and mutations related to epilepsy**. *Nucleic Acids Res* 2015, **43**(Database issue):D893-899.

88. Nauli SM, Alenghat FJ, Luo Y, Williams E, Vassilev P, Li X, Elia AE, Lu W, Brown EM, Quinn SJ *et al*: **Polycystins 1 and 2 mediate mechanosensation in the primary cilium of kidney cells**. *Nature genetics* 2003, **33**(2):129-137.

89. Yao G, Luo C, Harvey M, Wu M, Schreiber TH, Du Y, Basora N, Su X, Contreras D, Zhou J: **Disruption of polycystin-L causes hippocampal and thalamocortical hyperexcitability**. *Human molecular genetics* 2016, **25**(3):448-458.

90. Gross RA, Ferrendelli JA: **Effects of reserpine, propranolol, and aminophylline on seizure activity and CNS cyclic nucleotides**. *Annals of neurology* 1979, **6**(4):296-301.

91. Bloom FE: **The role of cyclic nucleotides in central synaptic function**. *Reviews of physiology, biochemistry and pharmacology* 1975, **74**:1-103.

92. Kamachi Y, Kondoh H: **Sox proteins: regulators of cell fate specification and differentiation**. *Development* 2013, **140**(20):4129-4144.

CHAPTER 1:

Nervous system development and regeneration in freshwater planarians

Advanced Review

Nervous system development and regeneration in freshwater planarians

Kelly G. Ross,[1] Ko W. Currie,[2,3,4] Bret J. Pearson[2,3,4] and Ricardo M. Zayas[1]*

Planarians have a long history in the fields of developmental and regenerative biology. These animals have also sparked interest in neuroscience due to their neuroanatomy, spectrum of simple behaviors, and especially, their almost unparalleled ability to generate new neurons after any type of injury. Research in adult planarians has revealed that neuronal subtypes homologous to those found in vertebrates are generated from stem cells throughout their lives. This feat is recapitulated after head amputation, wherein animals are capable of regenerating whole brains and regaining complete neural function. In this review, we summarize early studies on the anatomy and function of the planarian nervous system and discuss our present knowledge of the molecular mechanisms governing neurogenesis in planarians. Modern studies demonstrate that the transcriptional programs underlying neuronal specification are conserved in these remarkable organisms. Thus, planarians are outstanding models to investigate questions about how stem cells can replace neurons *in vivo*.

How to cite this article:
WIREs Dev Biol 2017, 6:e266. doi: 10.1002/wdev.266

INTRODUCTION

The nervous system is one of the most complex and fascinating organ systems in metazoans. Neural networks regulate many aspects of animal physiology and control behavior. Thus, understanding how nervous systems develop, function, and are remodeled throughout life is both a fascinating and challenging topic. Decoding how particular neuronal cell types are specified during development and patterned and wired into a nervous system is a complicated task in any animal model. To help inform the cellular and molecular mechanisms underlying neural development, many scientists utilize invertebrate models, such as nematodes and flies, in which powerful genetic tools have allowed for dissection of conserved mechanisms underlying neuronal development. Another invertebrate nervous system that interests neurobiologists is that of the freshwater planarian, a free-living member of the phylum Platyhelminthes.[1] In contrast to nematodes or flies, these animals are famous for their remarkable ability to regenerate all of their tissues, including the central nervous system (CNS), from a population of adult pluripotent stem cells.[2,3] In addition to this regenerative ability, planarians were historically popular amongst neurobiologists because they were thought to be one of the most primitive organisms to possess anterior cephalization ('brains') and were ostensibly represented as an ancestor of the human brain.[4,5] Contemporary data and evolutionary logic contradict this earlier claim about planarians: with the exception of placozoans and sponges (the latter are thought to use putative neuronal-like cells),[6,7] almost every member of the animal kingdom possesses a nervous system.[8] However, the morphological and molecular diversity of neurons, how they are specified from progenitor

*Correspondence to: rzayas@mail.sdsu.edu

[1]Department of Biology, San Diego State University, San Diego, CA, USA

[2]Program in Developmental and Stem Cell Biology, The Hospital for Sick Children, Toronto, Canada

[3]Department of Molecular Genetics, University of Toronto, Toronto, Canada

[4]Ontario Institute for Cancer Research, Toronto, Canada

Conflict of interest: The authors have declared no conflicts of interest for this article.

cells, and how they are connected together to make a functional nervous system varies substantially between animal clades.[6] It is widely accepted that the ancestor of all bilaterally symmetric animals (the 'urbilaterian') already had a centralized brain that distinguished itself from the prebilaterian nerve-nets found in animals such as cnidarians.[9] In fact, in all bilaterians, neurons are organized into central ganglia and peripheral sensory organs.[6] Planarians are members of the spiralian superphylum that includes annelids, molluscs, and brachiopods.[7] Elements shared by the nervous systems within this superphylum are likely ancestral, including several thousand brain neurons, glial cells, a visual system, ventral nerve cords, and a nerve-net-like peripheral nervous system distributed throughout the body.[8] However, other attributes of the planarian nervous system might be clade specific and derived rather than ancestral. In either case, the phylogenetic position of planarians, their unlimited capacity for neurogenesis, and their experimental accessibility make these animals excellent models to investigate outstanding questions in adult neurogenesis.

The majority of planarian neural regeneration and development studies have been performed across three model species: *Dugesia japonica*, *Schmidtea mediterranea*, and *Schmidtea polychroa*. These species show extensive conservation in the anatomy and gene expression patterns within the nervous system and have been used interchangeably.[10] This review provides an overview of classic literature, describing the intriguing anatomy of the planarian nervous system and their tractable behaviors, as well as an in-depth survey of our current knowledge of the molecular mechanisms underlying regeneration and development of the CNS.

ANATOMY OF THE PLANARIAN NERVOUS SYSTEM

The shape of the planarian head and brain varies across species (e.g., see Refs 11 and 12), but the nervous system morphology retains characteristics that are common to planarians. The CNS is comprised of a pair of cephalic ganglia (brain), photoreceptors (eyes), and ventral nerve cords that run along the length of the animal and are connected by transverse commissures (Figure 1(a) and (b)). The brain and ventral nerve cords can be readily distinguished by their anatomical location and morphology using histological and antibody staining techniques[13–16] (Figure 1). The nerve cords are the most ventral neural structures in the animal and appear to terminate beneath the ventral side of the brain,[17] where they form synaptic connections mainly to the ventromedial region of the brain.[18] The eyes are dorsal to the brain and are generally organized as clusters of approximately 25 photoreceptor neurons that send rhabdomeric photosensory projections into the adjacent pigment cup formed by a monolayer of pigment cells.[19] Photoreceptor axons (labeled with anti-β-Arrestin in Figure 1(c))[20] project to the brain ipsilaterally or cross the midline (forming an optic chiasm) and send contralateral projections to unidentified synaptic partners in the brain.[18,21,22] Neuronal cell bodies in the brain and ventral nerve cords are organized in an outer layer (cortex) that form synaptic connections in the inner neuropil.[23] The neuropil can be visualized using antibodies against abundant neural proteins like Prohormone Convertase-2 (PC-2), Synapsin (Figure 1(d)) or Synaptotagmin,[18,24,25] which reveal that the spongiform appearance is due to densely packed neuronal processes and synapses.[14,26,27] The two lobes of the brain are connected by an anterior commissure (Figure 1(b) and (d)) and possess branches that extend to the head margins[11]; some of the branches extend projections to the auricles where they are hypothesized to participate in chemosensation.[18,28]

The peripheral nervous system (PNS; Figure 1 (e)–(h)) is composed of subepidermal, submuscular, and gastrodermal nerve plexuses.[13,14,16,29] The subepidermal plexus is located in between the epidermis and the muscle wall[14,29] (Figure 1(e) and (g)) and forms a sparse mesh, likely because the cell bodies of the neurons originate in a more proximal region of the body. Thin processes from the subepidermal plexus extend between epidermal cells (Figure 1(f)) and are thought to function in sensory processes. Beneath the muscle wall, a thicker and denser nerve network, the submuscular plexus (Figure 1(e) and (h)), is formed by bundles of nerve fibers that extend in multiple directions from points of intersection.[14] The pharynx contains inner and outer ring-like nerve plexuses (Figure 1(e)) that can be easily observed by staining with antibodies that label components of synapses (Figure 1(d)). The anatomy of the gastrodermal plexus is less understood, but it has been described as a thin net of single nerve fibers that surrounds the intestine.[14] Finally, there are numerous nerve fibers crossing through the parenchyma and other networks of nerves or extensive nervous system innervation can be observed in the reproductive structures of sexually reproducing planarians (reviewed in Refs 14 and 30). Recent studies using gene and antibody markers have begun to fill in details on the anatomy of the planarian PNS.[25,29,31]

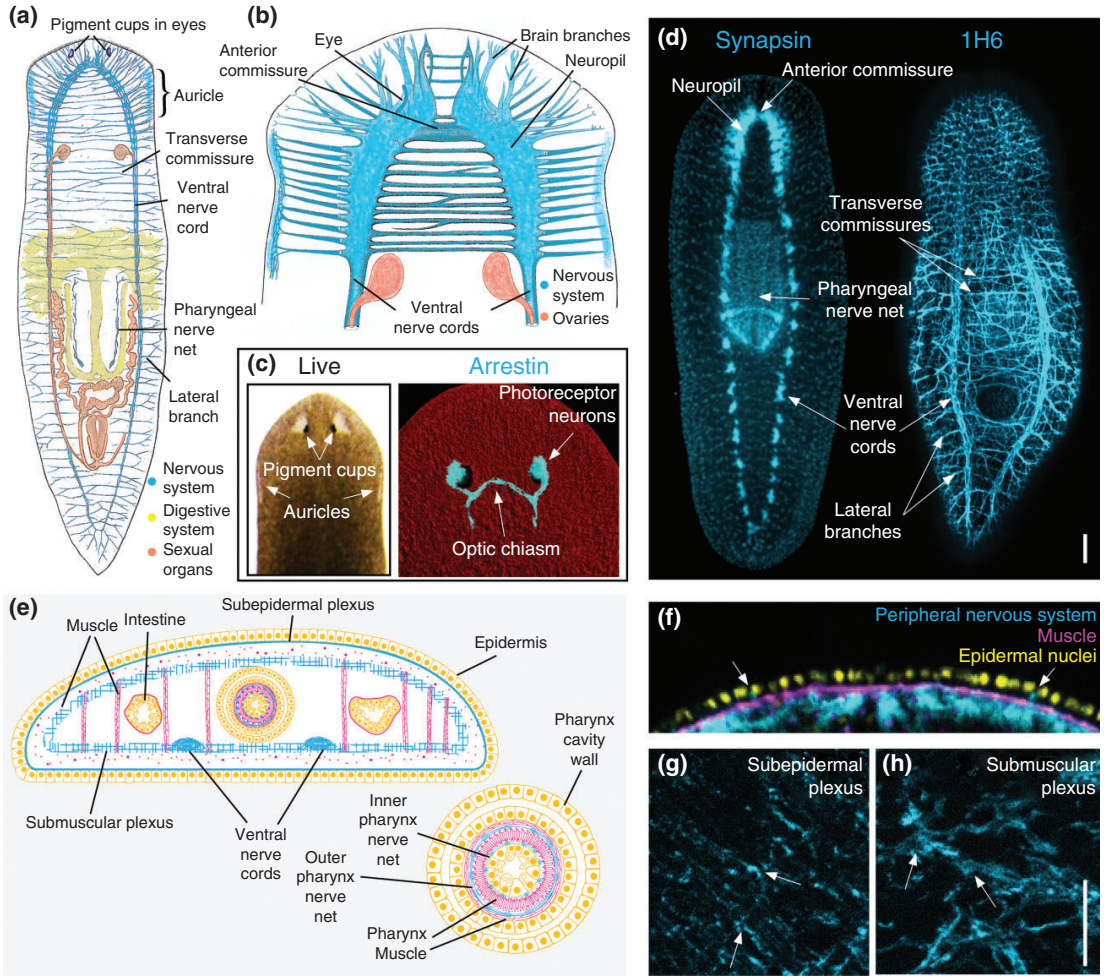

FIGURE 1 | Overview of the anatomy of the planarian nervous system. All images are from *Schmidtea mediterranea* unless otherwise specified. (a) Illustration of the nervous system in *Schmidtea polychroa*. (Adapted from Ref 181) Neural tissues are colored blue, reproductive organs in orange, and the digestive system in yellow. (b) Brain branches extend laterally from the brain of *S. polychroa* as depicted by Micoletzky. (Adapted from Ref 12) Ovaries are colored orange. Regions of interest are labeled on the image. (c) Eye spots on a live planarian head (located on the dorsal surface) consist of pigment cups; photoreceptor neurons are located internally to an area devoid of pigment. Anti-Arrestin antibody labels the photoreceptor neurons and their axons, which reveals the optic chiasm. The sensory neuron-dense auricles are devoid of pigment and are located at the lateral edges of the head. (d) Anti-Synapsin antibody labels the synapses of planarian neurons, highlighting the anterior commissure and neuropil of the brain, the ventral nerve cords and their transverse commissures and lateral branches, and the pharyngeal nerve net. 1H6 antibody labels the peripheral nervous system, including axons extending through the ventral nerve cords. Scale bar = 200 μm. (e) Cartoon depicting the anatomy of neural structures observed in a transverse cross section through the mid-body of a planarian. Neural regions of interest are labeled on the image. (f) The subepidermal plexus (blue; stained with 1H6 antibody) sends projections in between epidermal cells (arrows, epidermal nuclei labeled with DAPI and pseudocolored yellow). The submuscular plexus is located beneath the body wall muscle (muscle labeled with 6G10 mAb and pseudocolored magenta). (g) Examples of neural projections observed in the subepidermal and submuscular plexuses (examples denoted with arrows, labeled with 1H6 mAb). Scale bar = 20 μm. ((f) and (g) were reprinted with permission from Ref 29. Copyright 2015 BMC)

In contrast, innervation of reproductive structures in sexually reproducing planarians is an area ripe for investigation.

In addition to broad characterization of CNS and PNS organization, distinct nerve cell types have been described by histochemistry, including unipolar

and bipolar neurons, neurosecretory cells, and glial cells.[13,15,27,30,32–35] The anterior portion of the head is also characterized by lateral regions referred to as the auricles (Figure 1(a)–(c)), which are thought to possess ciliated sensory neurons that can be distinguished with anti-Acetylated-Tubulin antibody labeling. The auricles are also thought to contain chemosensory neurons[28]; when these structures are amputated the animals are unable to detect food.[36–39] Similar chemosensory function has also been ascribed to the tip of the pharynx.[16,40–42]

Taken together, histochemical studies have built a solid description of the gross anatomy of the planarian nervous system. Yet, it is the reintroduction of these organisms in the modern molecular era, especially the application of whole-mount *in situ* hybridization,[43–45] the ability to perform RNAi knockdown of genes expressed in neurons,[46,47] and transcriptomic projects,[48,49] that has expanded our knowledge of the properties of the planarian nervous system.

MOLECULAR AND FUNCTIONAL HETEROGENEITY OF THE NERVOUS SYSTEM

High-throughput expression and functional screens have established an abundance of molecularly and functionally distinct neural populations in planarians[50–57] (Tables 1 and 2). For example, planarians possess dopaminergic,[58] serotonergic,[59] GABAergic,[60] cholinergic,[61] and octopaminergic[62] neuronal populations (neurotransmitters are shown in Figure 2(a)–(d)). They also display compartmentalization within the brain that can be defined by expression of conserved genes.[43,54] The medial/ventral region of the brain expresses *otxA*,[54] *arx*[63] and *pitx*,[64,65] whereas the outer cortex of the brain expresses *otxB*[54] and the lateral branches express *otp*,[43] *g-protein coupled receptor* (*gpas*),[17] and *cyclic nucleotide-gated channel-1*[56] (see examples of gene expression compartmentalization in Figure 2(e)). Lastly, putative sensory cells located at the dorsolateral region of the branches express distinct genes like *Smed-cintillo*.[66] The synapse dense brain neuropil contains glial cell bodies with elaborate processes. Planarian glia can be visualized by expression of a neurofilament gene (*Smed-if-1*) and a gene sharing similarity with a protocadherin family gene (*Smed-calamari*). These cells lack expression of neural markers *Smed-synapsin*, *-synaptotagmin*, and *-chat*, indicating that they are non-neuronal,[56,57] and are marked by *Smed-glutamine synthetase* (*gs*) and *Smed-excitatory amino acid transporter-2/glt-1* (*eaat2*), which are homologous to genes expressed in vertebrate astrocytes.[67,68] Labeling of these cells with anti-IF-1 antibody demonstrates that the glial cell processes surround areas of high synaptic density.[57]

The expression pattern of genes marking distinct neuropeptidergic populations[69–71] exemplifies the molecular heterogeneity and complexity of the planarian nervous system (Figure 2(f)). There are dozens of neuropeptide genes, encoding at least 140 neuropeptides in *S. mediterranea*[69] and at least 21 neuropeptide-coding genes have been described in *D. japonica*.[71] These genes are expressed in distinct and often very limited populations of neurons spanning diverse spatial patterns across the planarian body. Unique functions are now being attributed to some of these neuropeptide genes. In *D. japonica*, at least five neuropeptide genes are implicated in pharynx extension.[71] Additionally, signaling involving *Smed-npy-8*$^{+}$ neuroendocrine cells and cells expressing the GPCR *Smed-npyr-1* (Figure 2(g)) regulate germline development in the sexual strain of *S. mediterranea*.[69,70]

The most tractable example of neuronal heterogeneity is that of the photoreceptor neurons, a small population of cells that are relatively easy to label post-fixation. Planarian visual neurons share many common features with cerebral eyes. An elegant study performed RNA-seq on eyes isolated from live planarians; these experiments identified approximately 600 genes enriched in planarian photoreceptors,[72] including many conserved eye markers such as TRP channels,[72] R-Opsin,[47] and β-Arrestin orthologs.[22] Interestingly, multiple genes expressed in the photoreceptor neurons are spatially segregated. Anterior photoreceptors express *Smed-SoxB1-1* (*Smed-SoxB*), *Smed-Smad6/7-2*, and the neuropeptide gene *Smed-eye53-1*, whereas the posterior photoreceptor neurons express *Smed-zfp-2* and the neuropeptide genes *Smed-eye53-2* and *Smed-mpl-2*.[69,72,73] *Smed-mpl-2* is also expressed in a ventral photoreceptor neuron population that lacks *eye53-2*, suggesting further heterogeneity along the Dorsal–Ventral (DV) axis of the photoreceptor neurons.[69] A thorough comparison of the functional differences between these different populations has not been explored, but a dye-tracing study showed preferential projection of anterior photoreceptor neurons to the contralateral side of the brain, indicating potential differences in function.[18]

Classically, the function of neurons can be studied and defined by recording their electrical properties in combination with stimulation, but in planarians, this technique has only been successfully applied to the photoreceptor neurons.[74–77]

TABLE 1 | Commonly Used Whole-Mount In Situ Hybridization and Antibody Markers for the Planarian Nervous System

Type of Marker	Gene/Antibody Target	Labeled Cells	References
Broadly Expressed Neuronal Genes	*Dj-prohormone convertase 2* (*pc-2*)	Neuronal cell bodies	22
	Dj-choline acetyltransferase (*chat*)	Cholinergic neurons	61
Pan-Neural	Anti-SYNORF (Synapsin)	Neuronal axon tracts	25
	Dj-Synaptotagmin	Neuronal axon tracts	24 and 152
Glia	*Smed-intermediate filament-1* (*if-1*)	Glial cell bodies	56 and 57
	Anti-Smed-IF-1	Glial cell bodies and their processes	57
Visual System	Anti-Dj-Arrestin (VC-1)	Photoreceptor neurons and visual axon tracts	20 and 22
	Smed-tyrosinase	Pigment cup cells	115
	Smed-ovo	Photoreceptor neurons, pigment cup cells, and eye progenitor cells	72
Neuronal Subpopulations	*Dj-glutamic acid decarboxylase* (*gad*)	GABAergic neurons	60
	Dj-tyrosine hydroxylase (*th*)	Dopaminergic neurons	58
	Dj-tyramine-beta hydroxylase (*tbh*)	Octopaminergic neurons	62
	Dj-tryptophan hydroxylase (*tph*)	Serotonergic neurons	59
	Anti-5-HT	Serotonergic neurons and axon tracts	25
	Dj-G-beta	Lateral brain branches	152
	Anti-Neuropeptide F	Diffuse neurons (most often associated with ventral nerve cords)	25
	Anti-GYRFamide	Most neurons in cephalic ganglia and ventral nerve cords	25
	Smed-cintillo	Lateral chemosensory neurons (putative)	66
	Dj-g-protein alpha subunit (*gpas*)	Lateral brain branches	17
	Dj-otxA	Medial brain region	54
	Dj-otxB	Lateral brain region	54
	Dj-otp	Lateral sensory brain branches	43
	Smed-cyclic nucleotide gated (*CNG*) *channel-1*	Lateral sensory brain branches	56
	Neuropeptide genes	Multiple neuropeptidergic populations	69

Some markers nearly label the entire central nervous system, whereas others specifically label the visual system or other discrete neuronal subpopulations. *In situ* hybridization mRNA probes are italicized.

Consequently, the field has relied on RNAi technology to assess the function of neuronal populations. Candidate-based functional assays show that many genes responsible for neural programs in vertebrates have similar roles in planarians (Table 2). These animals have stereotypical behaviors such as a response to water flow (rheotaxis), preference for smooth surfaces and other thigmotactic responses, movement away from light (negative phototaxis), movement toward food (chemotaxis), and movement toward cooler areas (thermotaxis),[40,78] with which consequences of genetic perturbations can be assayed.[21,79–81] Planarians ordinarily move by gliding, which is powered by ventral motile cilia[82] that beat with metachronal synchrony.[83] The worms are also capable of muscle-driven movements like inching[61] and scrunching,[84] providing more testable modalities. The combination of molecular functional experiments with behavioral and movement analyses led to the determinations that serotonergic neurons coordinate cilia-driven gliding[64,65] and thermotaxis,[85] whereas autonomous muscle-driven movements are attenuated with loss-of-function of either dopaminergic[58] or cholinergic neurons,[61] highlighting roles for these neurotransmitters similar to those found in other animals, including mammals. Additionally, GABAergic neuronal function is implicated in phototaxis behavior.[60] An overall loss of brain function results in diminished behavioral outputs (e.g., phototaxis and thermotaxis),[79,81,85] which demonstrates the brain's

TABLE 2 | Abnormal Behavioral Phenotypes Observed after RNAi Knockdown and the Neuronal Cell Population(s) Affected

Gene Name	Behavioral Phenotype	Cell Type Affected	References
Smed-ovo	Loss of negative phototaxis	Photoreceptor neurons and eye pigment cells	72 and 125
Dj-eye53, *1020HH*	Loss of negative phototaxis	Photoreceptor neurons and cells in the brain	17 and 21
Dj-gad	Loss of negative phototaxis	GABAergic neurons	60
Smed-netR (*dcc*), *Smed-netrin2*	Decreased negative phototaxis	Photoreceptor neurons	149
Smed-pitx, *Smed-lhx1/5-1*	Loss of gliding locomotion	Serotonergic neurons	64 and 65
Dj-tph	Loss of thermotaxis (when expression in the head is lost)	Serotonergic neurons	85
Dj-TRPMa	Loss of thermotaxis	$TRPMa^{+}$ sensory neurons	85
Multiple neuropeptide genes	Loss of ability to extend pharynx	Multiple neuropeptidergic populations	71
Smed-dynaminA-1	Uncoordinated locomotion	All neurons	155
six-1, *eya* (multiple species)	Loss of negative phototaxis	Photoreceptor neurons and eye pigment cells	124, 126, and 127
Smed-pc-2	Loss of coordinated movement and paralysis	All neuropeptidergic neurons	51 and 156
Dj-chat	Reduced drug-induced muscle contractions	Cholinergic neurons	61
Dj-th	Attenuation of drug-induced muscle contractions	Dopaminergic neurons	58
Smed-β-tubulin	Loss of coordinated movement and paralysis	All neurons	51
Smed-ActivinR-1	Flattened body posture and movement defects	Unknown	51 and 95
Smed-inr-1	Locomotion defects	Unknown	103
Smed-RNA-binding protein homolog (*HE.1.08H*)	Locomotion, flipping response, and eating defects	Unknown; enriched in neurons	51 and 88
Smed-Na^{+}/K^{+} ATPase transporter (*HE.4.01H*)	Locomotion, vibration response, flipping, and light response defects	Unknown; enriched in neurons	51 and 88
Smed-secretory granule neuroendocrine protein (*HE.4.05F*)	Locomotion, vibration response, flipping, and light response defects	Unknown; enriched in neurons	51 and 88
Smed-SoxB2-2	Reduced vibration response	Unknown	56
Smed-fli-1	Loss of chemotaxis	Chemosensory branches in the cephalic ganglia	56
Smed-Elongation factor Tu (*NBE.1.05B*)	Locomotion defects	Unknown; enriched in neurons	51 and 88

role in decision-making processes in response to environmental cues.

The function of many genes that are expressed in neural populations is still unknown and there are many cell types that remain poorly understood. For instance, the control of autonomous muscle movement by cholinergic neurons[61] suggests that a motor neuron population exists in planarians. Although projections from cholinergic neurons[61] have been found in close proximity to the unique muscle cells that make up the planarian body wall musculature,[86] the motor neuron population and how it innervates the musculature remains uncharacterized. Thus, on-going work is improving the resolution of what we know about the organization and specific identity of the many types of neurons in the planarian nervous system. It is this molecular complexity that has drawn even more excitement to investigate how these animals construct the nervous system in the totipotent zygote and then retain an

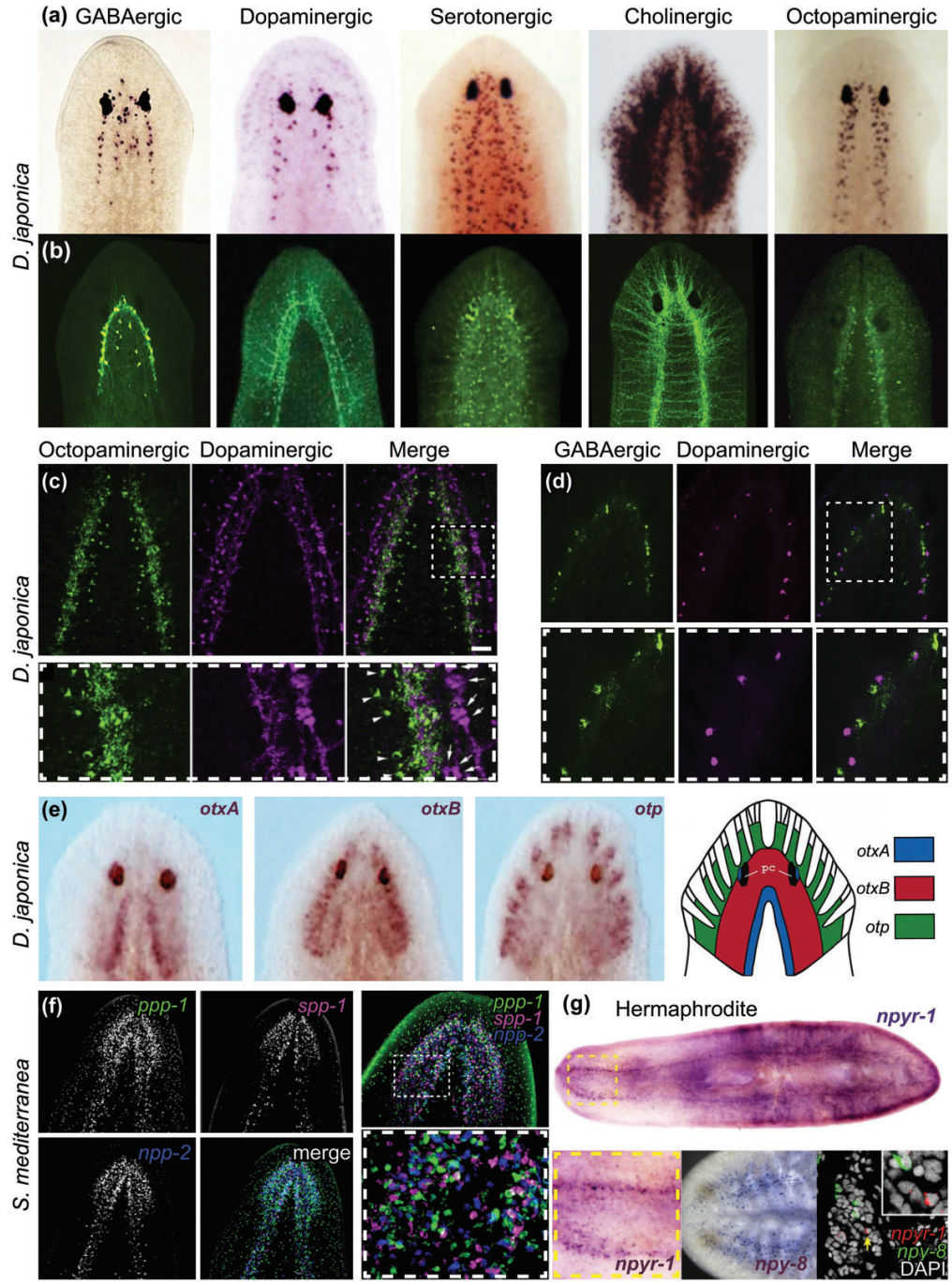

FIGURE 2 | Legend on next page.

unprecedented capacity to regenerate, in a matter of days, the molecularly complex nervous system of the post-embryonic worm.

MOLECULAR MECHANISMS UNDERLYING NERVOUS SYSTEM REGENERATION

Planarians are capable of repairing the CNS following any injury, but it is whole-brain regeneration following head amputation that provides the most striking and unparalleled paradigm to study *de novo* replacement of a CNS organ in an adult bilaterian. Owing to their fast regeneration capacity and the abundance of genomic resources, *S. mediterranea* and *D. japonica* have been the most popular species for regeneration studies.[1] Following decapitation, these worms restore a fully functioning nervous system in 1 week[17,21] (Figure 3). Through the extensive use of whole-mount immunohistochemistry and *in situ* hybridization experiments, major events of brain regeneration have been broken down into a series of steps.[17,31,43,51,54] The first clusters of neurons in the anterior blastema appear within 24–48 h.[17,43,54,56] This nascent brain is distinguishable from the truncated ventral nerve cords in the pre-existing tissue located beneath the blastema, and within 36 h, these newly specified cells begin to express mRNAs restricted to distinct regions of the brain.[43,54,56] In 2–3 days following amputation, new neural connections are formed that are characterized by the reappearance of the anterior commissure between the two halves of the brain, the formation of the optic chiasm, and connection between the new brain and the pre-existing nerve cords.[43,54] Brain morphology is restored between 3 and 5 days post-decapitation, as inferred by the appearance of the dense neuropil and restoration of simple behaviors. After 7 days of regeneration, the new brain resembles the uninjured (intact) brain and is coincident with full functional recovery.[21,51,85]

Recent work has begun to uncover signals and genetic programs that coordinate head regeneration. Following decapitation, several signaling cues, including established polarity factors and other yet unidentified molecules, induce regeneration of the head and brain at the anterior wound site. Subsequently, differentiation programs become activated that direct nearby stem cells to generate neural progenitors that differentiate and integrate with already existing neural tissues to restore full brain function (Figure 3(f)). During regeneration and homeostasis, positional cues also control the size and shape of the newly formed nervous system and maintain allometric proportion with the rest of the organism. In the sections to follow, we survey the evidence supporting discrete steps underlying regeneration and neuronal replacement in planarians.

Kick-Starting Head Regeneration: Restoring Anterior Polarity

Immediately following tissue loss, a wound-response program is activated.[87,88] Of the numerous early wound response genes, only *notum*, the Wnt signaling inhibitor, is differentially expressed at the

FIGURE 2 | The planarian nervous system is comprised of distinct neuronal subtypes. The species used for each image are specified in the corresponding panels. (a) Whole-mount *in situ* hybridization labeling of genes that encode enzymes required for the synthesis of neurotransmitter populations: *Dj-glutamic acid decarboxylase*, GABAergic neurons; *Dj-tyrosine hydroxylase*, dopaminergic neurons; *Dj-tryptophan hydroxylase*, serotonergic neurons; *Dj-choline acetyl transferase*, cholinergic neurons; *Dj-tyramine beta hydroxylase*, octopaminergic neurons. (b) Antibody labeling of the enzymatic proteins found in the same neurotransmitter populations as in (a). ((a) and (b) are reprinted with permission from: GABAergic neurons (Ref 60. Copyright 2008 Elsevier); dopaminergic neurons (Ref 58. Copyright 2007 John Wiley & Sons; Ref 182. Copyright 2011 John Wiley & Sons); serotonergic neurons (Ref 59. Copyright 2007 Elsevier); cholinergic neurons (Ref 61. Copyright 2010 Elsevier); octopaminergic neurons (Ref 62. Copyright 2008 Elsevier)) (c) Double-labeling of octopaminergic and dopaminergic neurons with antibody markers (same markers as specified in (b)) shows that these neuronal populations are unique. Arrowheads and arrows point to octopaminergic and dopaminergic neural cell bodies, respectively. Scale bar = 50 μm. (Reprinted with permission from Ref 62. Copyright 2008 Elsevier) (d) Glutamic Acid Decarboxylase$^+$ (GABAergic neurons) and Tyrosine Hydroxylase$^+$ (dopaminergic neurons) represent distinct and separate populations of neurons in the dorsal region of the brain. (Reprinted with permission from Ref 60. Copyright 2008 Elsevier) (e) The brain contains distinct spatial domains identified by expression of specific genes. Expression of the transcription factors *Dj-otxA, -otxB*, and *-otp* is restricted to the medial region of the brain, the region of the brain below the photoreceptors, and the lateral branches of the brain, respectively. The cartoon depicts the mediolateral expression pattern of all three genes in the planarian brain. (Reprinted with permission from Ref 54. Copyright 1999 Springer) (f) Planarians have many distinct neuropeptidergic populations, including *Smed-ppp-1*$^+$, *-spp-1*$^+$, and *-npp-2*$^+$ neurons, which are detected throughout the body and are abundant in the central nervous system (CNS) of *Schmidtea mediterranea*. (Reprinted with permission from Ref 69. Copyright 2010 PLOS) (g) Neurons expressing *Smed-npy-8* target a distinct population of *Smed-npyr-1*$^+$ cells in the CNS of *S. mediterranea* hermaphrodites. Distinct cell populations can be visualized by labeling animals with probes for specific neuropeptide genes (*Smed-npyr-1*, red; *Smed-npy-8*, green; DAPI, gray). Function of both of these genes is required for sexual maturation and differentiation of the germ cells. (Reprinted with permission from Ref 70. Copyright 2016 PLOS) Anterior is up in all images except for (g) where anterior is to the left.

anterior wound site early (before 12 h post-amputation) and is required for anterior regeneration.[88,89] Thus, Wnt-mediated re-establishment of Anterior–Posterior (A–P) polarity is a key component of the wound-induced regeneration program. Excessive Wnt signaling caused by silencing pathway antagonists *Smed-notum* or *Smed-adenomatous polyposis coli* (*APC*) can completely block head regeneration.[89–91] In contrast, RNAi against the canonical Wnt signal transducer, *Smed-β-catenin-1*, causes global anteriorization of the body plan, with extreme cases exhibiting ectopic brain formation at the lateral margins of the animal.[90–92] Similarly, excessive Hedgehog pathway activity blocks head and brain regeneration following decapitation, in part by regulating the expression of Wnt genes.[93,94] A *follistatin* homolog, *Smed-fst*, is also upregulated after amputation and promotes normal head and brain regeneration by inhibiting the TGF-β family member *Smed-activin*.[95] In addition to these classical signaling pathways, several transcription factors are necessary for establishing anterior identity.[96,97] One key transcription factor is *Smed-prep*, a homeotic transcription factor involved in instructing anterior regeneration in response to polarity cues. Knockdown of *Smed-prep* activity does not inhibit early polarity gene expression in the anterior pole, but does block regeneration of anterior tissues, including the brain.[98,99] Many HOX genes are expressed in restricted domains along the A–P axis,[100] but no phenotypes have yet been observed and it is unknown whether the HOX genes provide spatial information during regeneration. Thus, as in embryonic development, establishment of axial polarity and tissue patterning are upstream of the signaling cues required for activation of cell differentiation programs in regeneration. Notwithstanding, little is known about the downstream signals that induce head formation and regulate neurogenesis in planarians.

Signaling Factors Involved In Brain Induction

Studies have convincingly illustrated that head formation during regeneration is facilitated by creating a head-permissive environment via repression of canonical Wnt signaling at anterior facing wounds. It is reasonable to hypothesize that inductive signals must confer head cell fate identify to neoblasts, but identification of those signals has largely eluded global gene expression profiling approaches. Nevertheless, some potential factors or downstream effectors have been identified from RNAi screens. The epidermal growth factor receptor (EGFR) signaling pathway is crucial for neoblast regulation and cell fate specification.[101–103] *Smed-egfr-3* RNAi inhibits blastema formation and impairs cellular differentiation because of a dysregulation in asymmetric cell division.[101,103] *Smed-egr-4*, a putative downstream target of *Smed-egfr-3*, is primarily expressed in the brain and is required for brain regeneration; when *Smed-egr-4* is knocked down, planarians re-establish anterior polarity, but fail to induce neural specification or form a brain primordium.[104] A neuregulin homolog, *Smed-nrg-7* is also expressed in the brain and regulates stem cell division and specification. The *Smed-nrg-7* RNAi phenotype recapitulates the effect of *Smed-egfr-3* knock down. In addition, biochemical analyses indicate that *Smed-nrg-7* encodes a ligand for *Smed-egfr-3*,[103] further implicating this ligand-receptor pair in neoblast cell fate commitment. A recent RNAi screen has also identified putative signaling molecules CRELD, F-spondin, and LDLRR family genes, all of which encode secreted or transmembrane proteins that could be involved in cell signaling required for brain regeneration.[56]

Other classic signaling pathways have been implicated in the induction of stem cell differentiation. Fibroblast Growth Factor (FGF) receptors (FGFRs) are expressed in neoblasts[105] and perturbation of the FGFR-like gene *nou-darake* (*ndk*; Japanese for 'brains everywhere') leads to ectopic neurogenesis.[106] However, no FGF-like molecules/ligands have been identified to date, nor is it clear if FGF signaling functions as an inductive signal (the role of *ndk* in patterning is discussed below). One pathway that plays a role in neoblast neural fate commitment is the Hedgehog-signaling pathway. In addition to its many known morphogenetic roles in animal development, Hedgehog molecules often act as mitogenic signals in nervous system development.[107] *Smed-hedgehog* (*hh*) is required for regulation of glial gene expression in planarians, a common feature of Hedgehog signaling in other model organisms.[57,108,109] The mature nervous system is the major source of *Dj/Smed-hh* expression, and Hedgehog signaling levels have been shown to positively influence global proliferation dynamics in the planarian body.[93,94] *Smed-hh* is expressed by cholinergic, GABAergic and octopaminergic neurons in the medial region of the brain,[63] and neoblasts located in between the medial cortex of the brain express the core *hh* signaling transduction genes (*Smed-patched*, *-smoothened*, and *-gli1*).[63] When *hh* expression is reduced, fewer neural progenitor cells are present

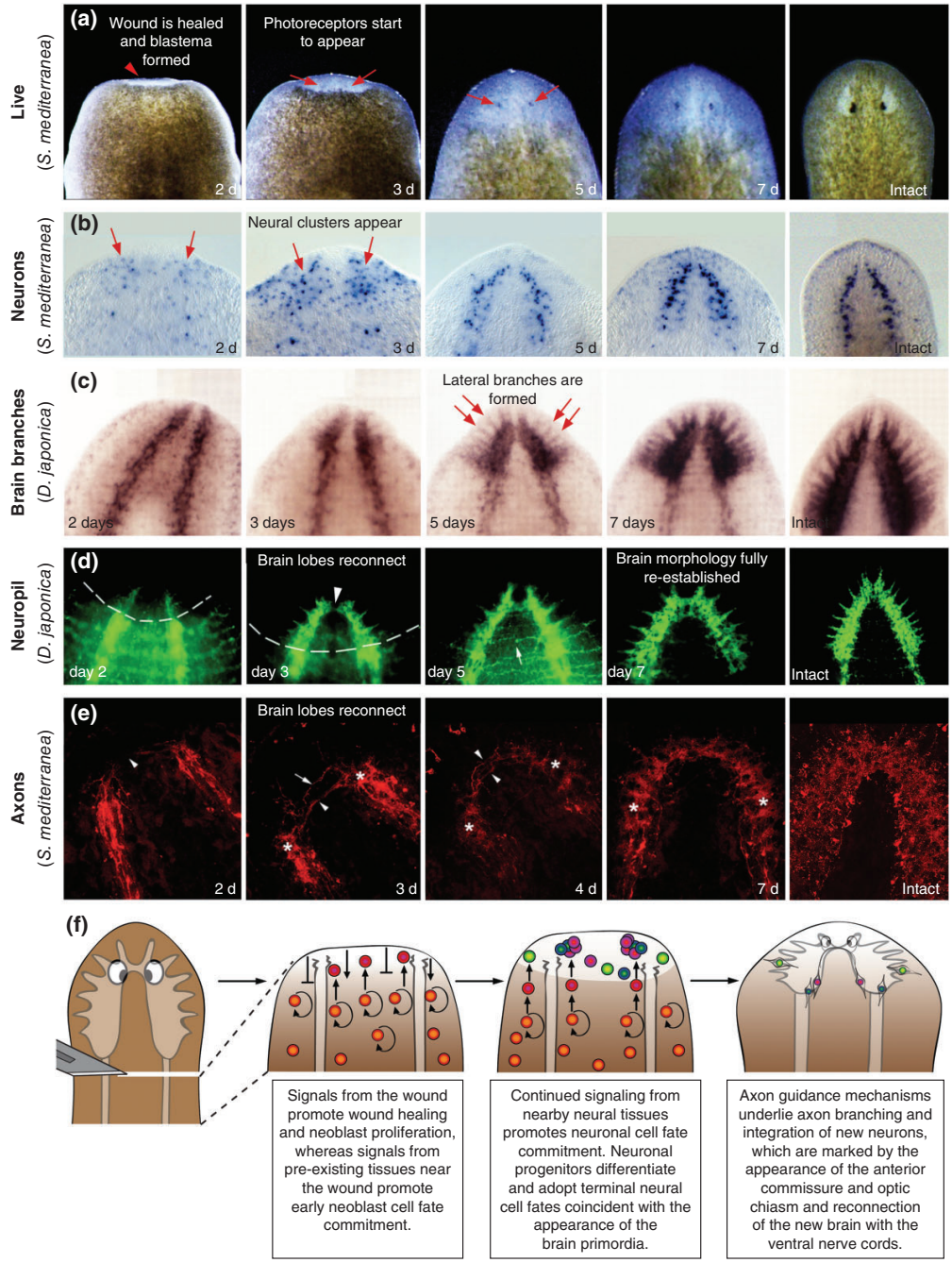

FIGURE 3 | Legend on next page.

between the halves of the brain and fewer cholinergic neurons are generated.[63]

Neuronal Specification: From Neoblasts to Neurons

The most crucial step in neurogenesis is the activation of transcriptional regulatory networks that promote generation of specific neurons from the stem cell population. The last decade has provided insights into transcription factors necessary for planarian neurogenesis. Evidence of early neoblast cell fate commitment comes from studies demonstrating that subsets of stem cells express lineage-specific transcription factors. *In situ* hybridization to the pan-neoblast marker *Smed-piwi-1*, combined with pulse-chase experiments using thymidine analogs (that are exclusively incorporated in proliferating stem cells and remain in their post-mitotic progeny),[110] have revealed some of these cycling neoblasts that are fated (or 'specialized'[111]) to specific lineages.[72,87,111–118] Individual RNAi knockdowns of some genes expressed in lineage-committed neoblasts profoundly affect neurogenesis. For example, *Smed-coe* is required for the differentiation of multiple subsets of neurons (e.g., *Smed-cpp-1*$^+$ neurons; Figure 4), and the bHLH family members *Smed-sim* and *Smed-hesl-3* are required for brain regeneration.[56,112,119] *Smed-hb-2*, *-mitfl-2*, *-da*, *-castor*, *-pax3/7*, and *-klf* (*Smed-klf* is required for regeneration of *Smed-cintillo*$^+$ sensory neurons; Figure 4) represent additional examples of transcription factor genes that have been previously implicated in neural development that are also expressed in lineage-committed neoblasts.[111] The *adipocyte lipid-binding protein* gene, *Smed-ap2* is required for the production of *Smed-trpA*$^+$ brain neurons during regeneration (Figure 4); along with other lineage-restricted neoblast populations, *Smed-ap2*$^+$*/piwi-1*$^+$ neoblasts are expressed near the tissues that require their expression for regeneration (in this case, the brain).[87] In some cases, neural transcription factor genes have been shown to function as terminal selector genes in planarians (i.e., they are necessary for both the initial specification and the maintenance of neuronal identity for the entire life of the cell).[120] In particular, *Smed-lhx1/5-1* and *Smed-pitx* are indispensable for the maintenance and function of serotonergic neurons[64,65] (Figure 4).

One gene that is upregulated following amputation and is expressed within a subset of neoblasts near the wound site[87] is the Runx family transcription factor, *Smed-runt-1*.[56,121] *Smed-runt-1* is necessary for the expression of downstream transcription factors that are involved in the differentiation of neural tissues.[87] As a result, *Smed-runt-1* RNAi animals have reduced levels of some neural progeny genes,[56] lack particular subsets of mature neurons, and fail to regenerate the eyes normally.[56,87] In vertebrates, the expression of the *SoxB2* gene *Sox21* is important for the progression of neurogenesis.[122] A recent functional screen found that the *SoxB2* gene, *Smed-SoxB2-2*, that is expressed in some stem cells and their progeny,[123] is likely playing an important role in neurogenesis during regeneration. *SoxB2-2* RNAi animals regenerate a smaller brain and have a reduction in the expression of neural progenitor genes.[56] It should be noted that the best-understood example of neuronal regeneration at the cellular level is that of the photosensitive neurons, which involve the

FIGURE 3 | Planarian brain regeneration visualized by staining animals with specific gene or protein markers. Species used for each experiment are indicated to the left of the images. (a) Live regenerating *Schmidtea mediterranea*. In the live images, the blastema is easily distinguishable at 2 days post head amputation (2d, arrowhead). As the blastema grows, eyespots are visible by 3 days post-amputation (3d) and become well developed as regeneration continues (arrows in 3d and 5d). (b) Brain regeneration visualized by the appearance of neuronal cell bodies marked by expression of *Smed-th*, which labels serotonergic neurons. The appearance of the brain primordia is observed as small clusters of cells beginning at day 2 of regeneration. These clusters are more defined as more neurons differentiate at day 3 of regeneration (arrows in 2d and 3d images). (c) Regeneration of the brain branches visualized by *in situ* hybridization to *Dj-517HH* (a gene encoding a receptor protein tyrosine phosphatase). Branches extend laterally from the regenerating brain by 5 days post-amputation (arrows in 5 days image), increase in length, and appear denser as regeneration proceeds. (d) Regeneration of the brain neuropil labeled with anti-Dj-Synaptotagmin antibody. In this regeneration time series, reconnection of the brain lobes is observed by day 3 of regeneration (arrowhead in day 3 image); the transverse commissures of the nerve cords appear ventrally in relationship to the cephalic ganglia (denoted with arrow in day 5 image) and the fully re-established brain morphology is apparent by day 7 of regeneration. (e) Re-establishment of neural network during brain regeneration visualized by labeling a subset of axonal projections with anti-Neuropeptide F. At 2 days post-amputation, the brain lobes are not yet connected at the anterior commissure (arrowhead in 2d image). By 3 days post-amputation, the brain lobes begin to reconnect at the anterior commissure (arrowheads in 3d and 4d images) and the transverse commissures of the ventral nerve cords are also re-established (arrow in 3d image). Anterior is to the top in all images. (Reprinted with permission from: *Smed-th* and NPF (Ref 31. Copyright 2012 UBC Press); *Dj-517HH* (Ref 183. Copyright 2011 Company of Biologists, which was reprinted from Ref 17. Copyright 2002 John Wiley & Sons); DjSYT (Ref 17. Copyright 2002 John Wiley & Sons)). (f) Schematic depicting some of the major events involved in whole-brain regeneration.

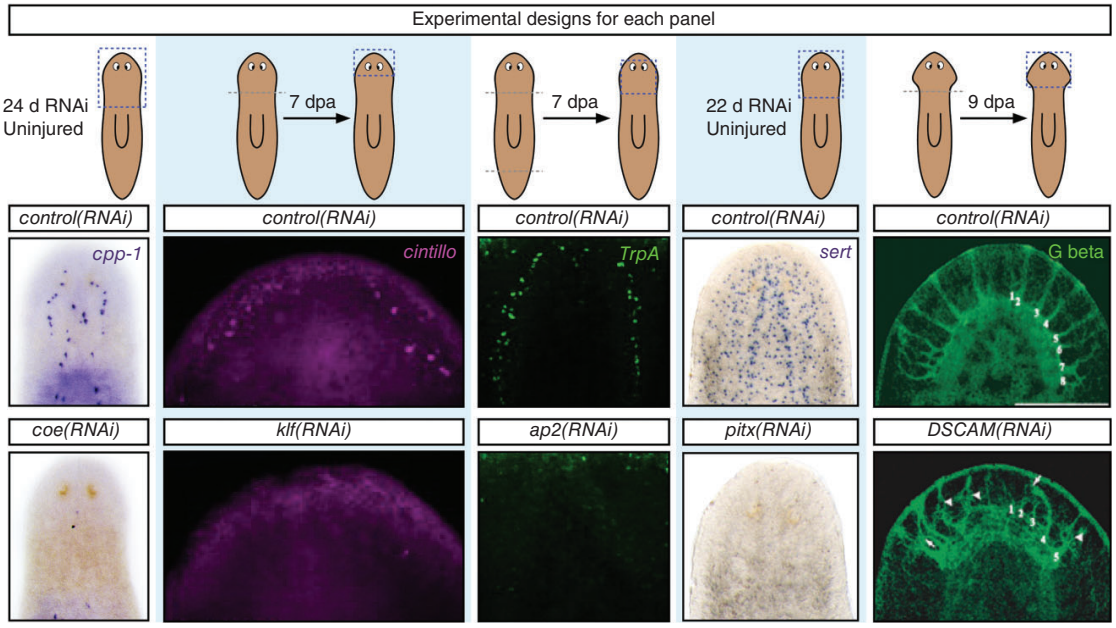

FIGURE 4 | Inhibition of genes expressed in neuronal progenitors or involved in nervous system patterning causes defects in nervous system regeneration. All images are from *Schmidtea mediterranea* unless otherwise specified. Illustrations of the experimental design are displayed above the corresponding panels. Where specified, images show uninjured worms following the specified period of RNAi exposure or of worms treated with RNAi, amputated (amputation site denoted by gray dashed lines) and allowed to regenerate for the specified time period. The blue dashed boxes in the cartoons indicate the region of the animals shown in the figures below. *Smed-coe* knockdown results in loss of *Smed-cpp-1*$^{+}$ neuropeptidergic cells in the head. *Smed-krüppel-like factor (klf)* RNAi causes a loss of *Smed-cintillo*$^{+}$ putative sensory neuron gene expression (magenta) in the anterior of the head. *Smed-ap2* RNAi results in loss of *Smed-transient receptor potential A* (*TrpA*$^{+}$, green) neurons in the brain. *Smed-pitx* RNAi knock down results in loss of *Smed-serotonin transporter* (*sert*$^{+}$, serotonergic neurons) in the regenerated planarian. And, *Dj-DSCAM* RNAi causes fasciculation impairments in the regenerated brain branches (labeled with anti-G-beta in *Dugesia japonica*; green). (Reprinted with permissions from: *coe(RNAi)* (Ref 112. Copyright 2013 Company of Biologists); *klf(RNAi)* (Ref 111. Copyright 2014 Elsevier); *ap2(RNAi)* (Ref 87. Copyright 2012 CLHL); *pitx(RNAi)* (Ref 64. Copyright 2013 Company of Biologists); *DSCAM(RNAi)* (Ref 153. Copyright 2006 John Wiley & Sons))

function of conserved transcription factors *eyes absent*, *sine oculis*, *ovo* and *six-1/2*.[72,124–127]

Given that dozens of different neuronal cell types have been identified, much remains to be learned about the mechanisms regulating neurogenesis in planarians. Application of single cell sequencing technology has expanded our ability to identify neoblast subclasses and to begin resolving stem cell lineages.[128] It is well established that all cell types in planarians arise from a pluripotent stem cell population (coined clonogenic Neoblasts or cNeoblasts[129]). Recent single cell sequencing analysis of neoblasts from the head region of planarians combined with *in silico* analysis that can predict the lineage trajectory of single cells have helped to further characterize the neural neoblast population.[113] This analysis captured the progression from the least restricted neoblast population (possibly cNeoblasts), to neoblasts expressing neuronal cell fate determinants, and finally to a population that is highly enriched for neural genes but still found within the mitotically active neoblast population. This cell population, called 'nu' Neoblasts (νNeoblasts),[113] is characterized by very low expression of *Smed-piwi-1*, high expression of *Smed-piwi-2* (expressed in neoblasts and also in the brain), and detectable expression of PIWI-1 protein (which perdures into post-mitotic progenitor populations[130]). This gene expression profile strongly indicates that νNeoblasts represent a population of neuronal progenitors[113,130,131] (Figure 5). Furthermore, many of the genes highly expressed in νNeoblasts appear to be expressed in mature neural populations as well, including homologs of some classic neuronal progenitor markers like *Smed-elav-2* and *-musashi-1* (*msi-1*) (Figure 5; *msi-1* is also referred to as *Dj-mlgB*[132]). νNeoblasts also show a peak of expression of the bHLH transcription factor *achaete-scute* homolog, *Smed-ascl-2*, at a point of

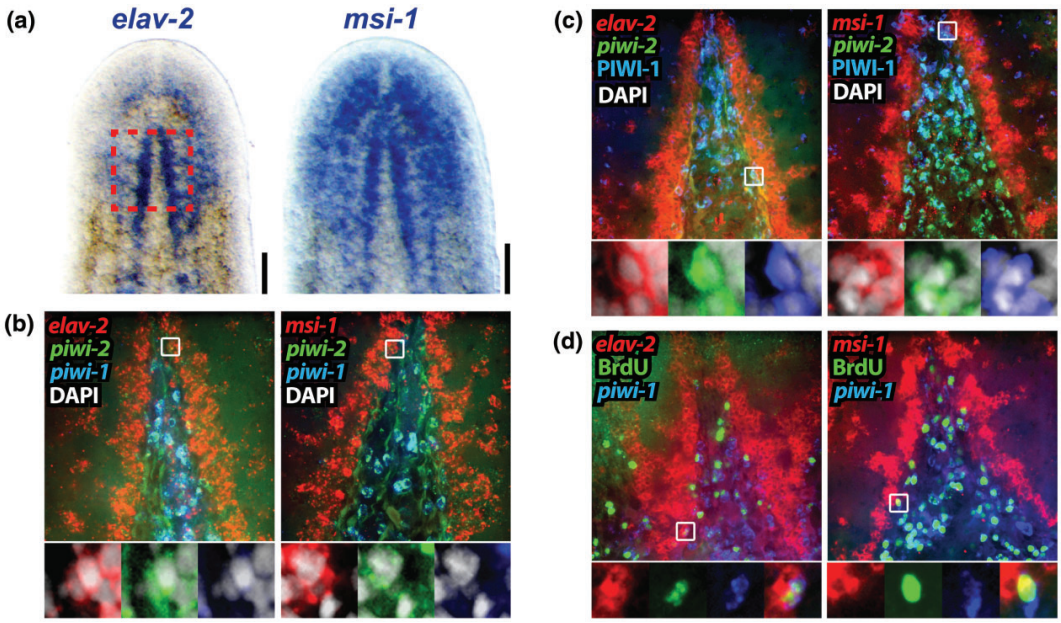

FIGURE 5 | Single cell analysis identifies conserved markers of neuronal progenitors in *Schmidtea mediterranea*. Homologs of conserved neural stem cell genes *Smed-embryonic lethal abnormal vision-2* and *Smed-musashi-1* (*elav-2* and *msi-1*, respectively) were identified in the νNeoblast population. (a) Expression of *elav-2* and *msi-1* visualized in differentiated regions of the central nervous system. Boxed region in *elav-2* image indicates region of images in (b–d). (b–d) *elav-2*$^+$ and *msi-1*$^+$ νNeoblasts (gene expression shown in red) co-express *Smed-piwi-2* transcript (green), but very little *Smed-piwi-1* (blue, a marker for neoblasts, in (b)). νNeoblasts, however, retain high expression of Smed-PIWI-1 protein (blue, a hallmark of progenitor cells, in (c)). νNeoblasts are BrdU$^+$ (green, following a 4 h chase, in (d)), indicating mitotic activity. (Reprinted with permission from Ref 113. Copyright 2016 BMC)

transition from less restricted neoblasts to the νNeoblast population. *Smed-ascl-2* RNAi experiments have yet to yield a distinguishable phenotype,[112] but its expression during neuronal specification is consistent with its role in nervous system development of other organisms.[133] It remains to be determined whether any of these neural-restricted neoblast populations (or any lineage-restricted neoblasts in planarians) are capable of self-renewal or are merely a state of expression during the transition from pluripotent neoblasts to terminally differentiated neurons.

Neurogenesis is not only restricted to tissue repair or replacement events, but also normal cell attrition. DNA analog pulse-chase experiments combined with *in situ* hybridization to neuronal genes have enabled researchers to definitively demonstrate that the adult planarian continues to produce mature neurons, even in the absence of any injury stimuli.[116,134] It also appears that planarians can respond to minor perturbations of neuronal composition. For example, following loss of dopaminergic neurons after exposure to the neurotoxin 6-hydroxydopamine, the intact planarian brain is able to sense the missing population of neurons and replace them within 2 weeks.[135] Planarians also undergo neurogenesis during brain re-sizing and re-scaling events based on nutritional availability.[66,136] During starvation or growth, each of their organ systems, including the brain, will re-adjust their size and shape to maintain relative proportions to the rest of the body by adding or subtracting cells from the existing organ.[66,137] During growth, the adult planarian must modulate neurogenesis to increase overall neuronal production and ensure that the ratio and patterning of all unique neural cell types is maintained in the re-scaled brain.[136–138] In all of these regenerative scenarios, as in developmental processes, tight regulatory mechanisms are vital to control neural production. Accordingly, there is a great deal of interest in the discovery of the specific biological signals that communicate with planarian stem cells to control levels of neurogenesis.

Regulation of Brain Size and Pattern

Following brain regeneration and during neuronal homeostasis, the animals are able to maintain the

correct ratio of neurons in proportion to the planarian body and organ patterning. It is not clear yet what cell signaling or cell–cell interactions regulate neuronal number and location, but some clues come from studies on how planarians specify a body plan. The earliest discovered phenotype that affects CNS scaling occurs after silencing *Dj/Smed-ndk*; *ndk* RNAi results in a dramatic posterior expansion of brain tissue.[99,106,112] *ndk* is expressed in anterior neural tissues and is theorized to sequester a diffusible brain tissue determinant (possibly an FGF-like protein). *ndk* loss-of-function and posterior expansion of head CNS tissues correlates with a nearly doubled increase in *Smed-coe*$^{+}$ and *-sim*$^{+}$ neural progenitors in the area directly posterior to the brain[112] (Figure 6). Thus, neoblasts appear to respond to a diffusible ligand that is repressed by *ndk* activity, but much remains to be learned about the signaling cascade underlying FGFR-like signaling in planarians.

A Wnt signaling feedback loop, composed of *Smed-wnt11-6* (also referred to as *wntA* and *wnt4a*) and the Wnt antagonist *Smed-notum*, regulates brain size along the A–P axis.[136] Loss of the posteriorly expressed *wnt11-6* (Figure 7), or the Wnt receptor, *Smed-fzd5/8-4*, results in posterior brain expansion during regeneration or body re-scaling; by contrast, silencing of *Smed-notum* causes the re-scaled brain to be shortened along the A–P axis[136,139–141] (Figure 7). Many of these patterning genes appear to act synergistically because combinatorial knockdowns of *Smed-wnt11-6*, *-ndk*, and *-fzd5/8-4* result in more severe phenotypes than single knockdowns.[140] Whereas the *Smed-wnt11-6/notum* feedback loop regulates growth past the posterior brain boundary, the lateral boundaries of the brain are demarcated by *Smed-wnt5* expression, which functions to suppress lateral expansion of the brain.[139,142]

Neuronal cell fate is also affected by the role of the Bone Morphogenic Protein (BMP) pathway in patterning the DV boundary.[143–145] *Smed-bmp4* (*Dj-bmp*) represses ventral cell specification in dorsal locations; consequently, knockdown of *Smed-bmp4* or any of its downstream signaling components (e.g., *Smed-smad1* and *-smad4*) results in ventralized animals and causes ectopic brain tissues to grow in the dorsal region of the worm.[143–145] Knockdown of a combination of the BMP antagonist *Smed-noggin* genes leads to a dorsalized worm because their expression maintains the ventral domain.[146] Altogether, these genes are part of a complement of factors that provide cues for positional identity and are thus necessary for restoration following injury and the homeostatic maintenance of the brain in the adult planarian.

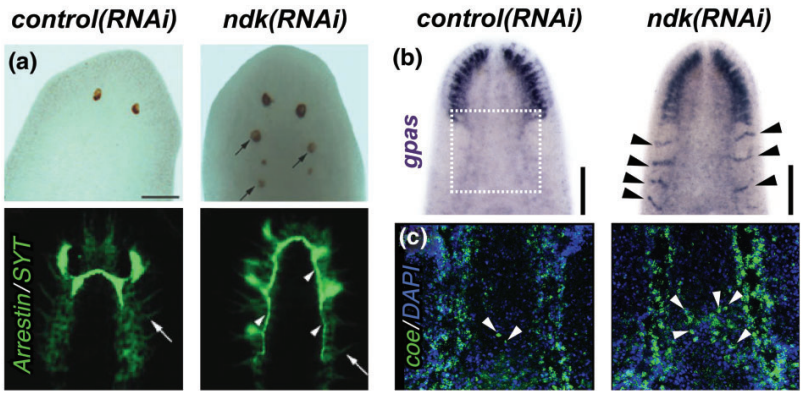

FIGURE 6 | Abnormal fibroblast growth factor receptor (FGFR)-like signaling leads to ectopic neurogenesis. (a) Following knockdown of *Dj-nou-darake* (*ndk*, a fibroblast growth factor receptor-like gene) and head regeneration 16 days after amputation, ectopic eyespots (arrows in bleached image) are observed in locations posterior to the original photoreceptors of *Dugesia japonica*. The formation of these eyespots corresponds with ectopic photoreceptor neurons (labeled with anti-Arrestin in green) that project to more posterior positions (arrowheads) along with the regeneration of brain tissue in posterior positions revealed by anti-Synaptotagmin labeling (green, highlighted with arrows). Scale bar = 400 μm. (Reprinted with permission from Ref 106. Copyright 2002 Macmillan Publishers Ltd) (b) Knockdown of *Smed-ndk* causes expansion of brain tissues in non-regenerating animals. The brain branch marker *Smed-g-protein alpha subunit* (*gpas*, arrowheads) is ectopically expressed in regions posterior to the brain after 2 weeks of RNAi in *Schmidtea mediterranea*. Scale bars = 100 μm. White box indicates the location of images in (c). (Reprinted with permission from Ref 112. Copyright 2013 Company of Biologists) (c) Posterior expansion of neural tissues corresponds with an increase in neural progenitors. More *Smed-coe*$^{+}$ neural progenitors (blue, arrowheads) are observed in the area anterior to the pharynx and between the brain lobes following 14 days of *Smed-ndk* RNAi knockdown in *S. mediterranea*. (Reprinted with permission from Ref 112. Copyright 2013 Company of Biologists)

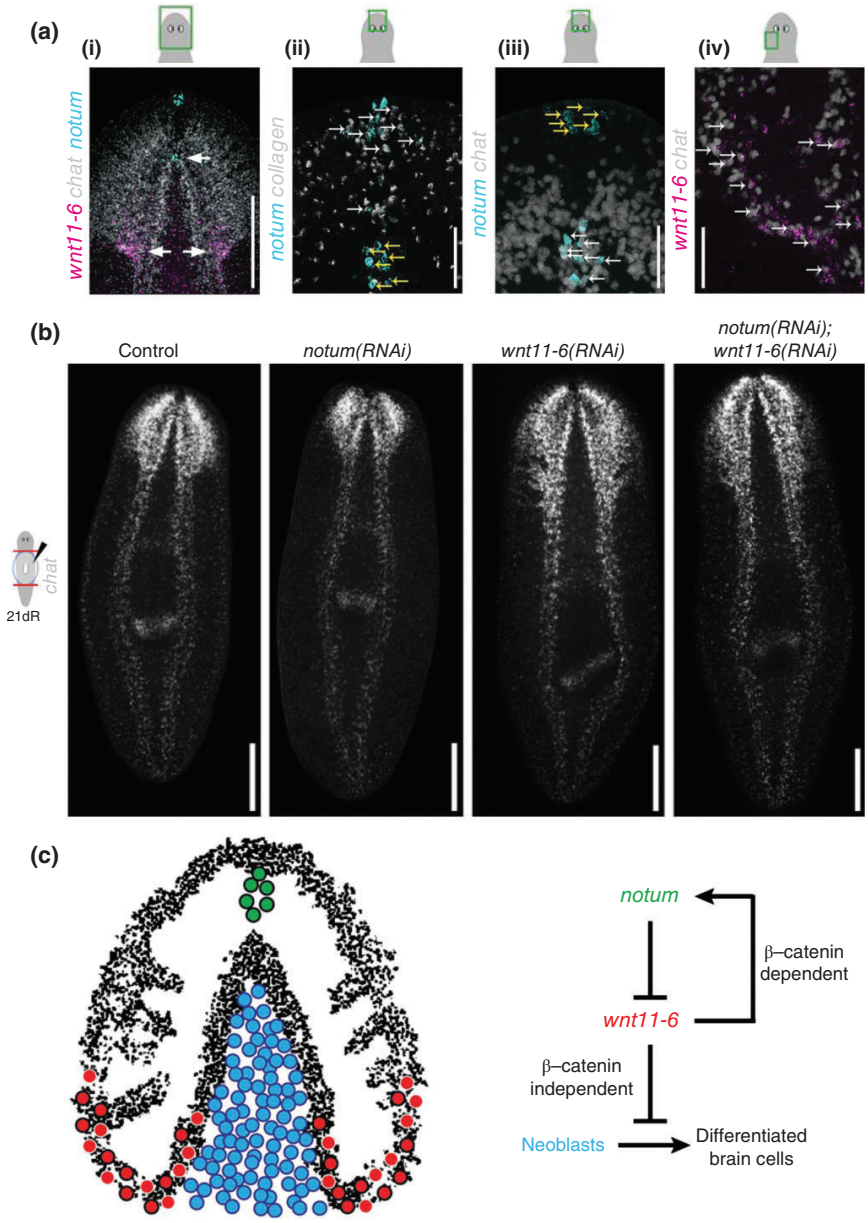

FIGURE 7 | Conserved polarity determinants regulate scaling of the planarian brain. (a) *Smed-notum* (blue) and *Smed-wnt11-6* (magenta) are expressed in neurons on the opposite anterior and posterior poles of the brain (indicated with arrows in i). *Smed-notum* (blue) is expressed in muscle cells at the anterior pole (co-expressed with *Smed-collagen*, gray, white arrows in ii, yellow arrows in iii) and in the brain anterior commissure (yellow arrows in ii, white arrows in iii, co-expressed with *Smed-chat*, gray), whereas *Smed-wnt11-6* (magenta) is expressed at the posterior end of each brain lobe (in *Smed-chat*$^{+}$ cells, gray, arrows in iv). The green boxes in the cartoons indicate the region of the animal shown in the corresponding figures. (b) *Smed-notum* inhibits *Smed-wnt11-6* to control brain size during regeneration. At 21 days post-amputation, trunks regenerate a smaller brain in *Smed-notum(RNAi)* animals, and larger brains in *Smed-wnt11-6(RNAi)* and *Smed-notum;wnt11-6(RNAi)* animals compared to controls. Amputation schematic is illustrated in the cartoon. (c) Illustration depicting the regulation of brain size by *notum* and *wnt11-6*. (All images are in *Schmidtea mediterranea* and are reprinted with permission from Ref 136. Copyright 2015 Company of Biologists)

Recovering Function: Re-Establishing Connections in the CNS

Remarkably, following just about any type of injury, the animals integrate new and old tissues seamlessly and regain normal function. This capacity requires cues for pathfinding of the axonal projections and reconnection into the synaptic machinery. Once more, conserved developmental mechanisms are redeployed in the context of tissue regeneration. For example, Netrins and Slits, which are well known for their roles in axon guidance,[147] are necessary for reconnecting old and new neural tissues in regenerating worms and for maintaining neural architecture in uninjured planarians.[148–151] *Smed-netrin2* or the Netrin receptor gene *Smed-netR* (ortholog of *Dj-dcc*[151]) knockdowns lead to a severely disorganized network of axonal projections and ectopic brain growth along the mediolateral axis.[149] Similarly, loss of *Smed-netrin2* or *-netR* function by RNAi results in loss of the connection of the photoreceptive neurons to the brain and an impairment to negative phototaxis behavior.[149] This pathfinding function likely lies in cooperative signaling between the photoreceptor neurons expressing the receptors *Dj-unc5A* and *Dj-dcc*,[151] and the brain.[17]

In planarian regenerates, *Smed-slit* knockdown leads to a dramatic collapse at the midline of neural and non-neural tissues (e.g., 'cyclopia,' intestinal branch fusion, and mispatterning of the nerve cords). The *Smed-slit* RNAi midline collapse phenotype occurs during tissue homeostasis as well, but does not seem to affect all neurons: following head regeneration, the lateral branches of the brain differentiate and project to the periphery normally.[148] However, knockdown of homologs of the putative Slit receptors, *Smed-roboA* and *-roboB*, do not to cause this phenotype.[148,150] Instead, RNAi against *Smed-roboA* causes loss of the anterior commissure of the brain and combinatorial RNAi of *DjRoboA* with either *DjnetB* (ortholog of *Smed-netrin2*) or the Netrin receptor *Dj-unc5A* show either a failure of the photoreceptor axons to cross the midline at a low penetrance or axon bundle fasciculation errors[150,151] This could indicate that this function of Slit is Robo independent or that there are yet unidentified Slit receptors. Clathrin-mediated endocytosis has also been shown as a requirement for circuit formation of neurons and loss of function causes morphological defects, atrophy, and death of neurons in the planarian brain.[152] The cell adhesion molecules Dj-CAM and Dj-DSCAM are expressed in the mature CNS, are differentially expressed during regeneration and have roles in axon formation, neuronal cell migration, axon outgrowth, fasciculation, and projection[153]; their inhibition leads to a disorganized neuropil and reduced lateral branches, as well as fasciculation impairments (Figure 4).

The transcription factors *Smed-arrowhead* and *Smed-coe* are also involved in restoration of the nervous system circuitry. Following *Smed-arrowhead* RNAi, the halves of the brain fail to reconnect at the anterior commissure and display defects in patterning of the photoreceptor axons. When *Smed-coe* expression is inhibited in regenerates, the anterior brain commissure also fails to reconnect and there is a significant reduction in axonal projections in the brain.[112,119] This might be a later requirement for maintaining the function and form of neurons that is independent of the role of *Smed-coe* in neural determination and differentiation, but corroborates a conservation of function in axon guidance found in other organisms.[154]

As discussed earlier, perturbation of neurotransmitter systems can profoundly affect planarian behavior or locomotion (Table 2). Many of the genes that affect behavior have been linked to morphological defects of the nervous system. However, for genes like *Dj-eye53* and *-1020HH*, loss-of-function results in morphologically normal brains and visual axon projections, but the worms exhibit a loss of phototactic behavior.[21] This suggests that the photoreceptor neurons or the transduction of their signals in the brain is not functioning correctly. Inhibition of genes involved in synaptic transmission[79,152,155] or neuropeptide processing also have profound effects on nervous system function.[51,156] Knockdown of *Smed-pc2* impairs mobility[51,156] and disruption of dopaminergic signaling leads to severe locomotion defects.[58] Nevertheless, understanding the molecular basis of planarian behaviors by combining molecular function with automated tracking of behavioral outputs is only just gaining traction (reviewed in Ref 157). Thus, the door is wide open for further dissection of the complex mechanisms involved in reconstruction of neural tissues, the recovery of function, and the retention of simple learned behaviors (reviewed in Ref 158) using the planarian model.

NERVOUS SYSTEM DEVELOPMENT

Embryogenesis in Planarians: A Tough Shell to Crack

Compared to our knowledge of adult planarian biology, our understanding of planarian embryonic development is limited. This gap is not due to a lack of interest, but rather to the biology of these

organisms during embryogenesis (discussed in Ref 159). Because sexually reproducing planarians are non-selfing, obligate hermaphrodites, oocyte fertilization occurs internally, and one or more fertilized eggs are enclosed in an opaque egg capsule that prevents live visualization of embryonic development. Furthermore, the eggs are ectolecithal (yolk cells are produced by yolk glands and deposited in the egg capsule), which has hampered the ability to culture and manipulate the embryos *in vitro*. Despite these obstacles, some classic work (reviewed in Refs 159 and 160) and a handful of noteworthy studies in the planarian *S. polychroa*[161–169] have contributed to our understanding of how embryogenesis proceeds within freshwater flatworms.

Planarian development diverges from the traditional spiralian cleavage pattern observed in other members of the Lophotrochozoan superphylum,[159] and has been divided into eight stages that take approximately 15 days from egg laying to hatching in *S. polychroa* (Figure 8). Stages 1–4 (first 5 days of development) are characterized by the zygote undergoing cleavages in which the resulting blastomeres lose their contacts and disperse within the maternally derived yolk syncytium. Some of these blastomeres are thought to differentiate into putative transient structures that include an epidermis and an embryonic pharynx for ingestion of the nutrient-providing yolk cells.[163] Within these early-stage embryos, a primordial nervous system is generated that exhibits expression of conserved genes required for neurogenesis in other developmental model organisms.[167] The primordial nervous system is speculated to be required for modulation of feeding behaviors essential for the early embryo to digest yolk cells,[161] and is likely similar to the function of serotonergic neurons described in the pond snail embryo.[170,171] Through the next phase of development (Stages 5 and 6; days 10–15 of development), planarian blastomeres continue to proliferate as the embryonic body plan begins to develop definitive axial polarity.[164] This time period also marks the emergence of the definitive CNS. Finally, during Stages 7 and 8 (days 10–15 development), the embryo acquires a body plan that resembles that of the adult organism, including a CNS with all of its basic components.[159,167]

Early embryonic neurogenesis programs in most bilateria can be broken into four prototypical stages: induction of the neurogenic ectoderm, patterning the size and shape of this neuroectoderm, proliferation of neural precursor cells, and finally migration of differentiating neural progenitors.[6] Neurogenic tissues in the planarian embryo do not appear to originate from a prototypical ectodermal layer. Instead, the definitive embryonic CNS appears to be generated by neural progenitor cells within the mesenchyme that are themselves derived from the blastomeres of the early embryo.[163,167] Yet, planarian homologs of the SoxB family of transcription factors, which are fundamental for the induction and maintenance of the neurogenic ectoderm in most animals,[172] are expressed in blastomeres in Stage 4 embryos as well as in differentiated neurons in late stage embryos.[167] Similarly, several planarian homologs of the proneural bHLH transcription factors [e.g., *Spol-achaete-scute*, *-neuroD*, *-beta3* (*Smed-e22/23* in Ref 112), and *-olig*] that promote differentiation of neural progenitor cells in the developing CNS, are expressed within the definitive CNS of planarian embryos,[167] and the differentiating photoreceptor cells express *Spol-eyes absent*, *-sine oculis*, and *-ovo*.[72,165] The function of these genes has yet to be experimentally assessed in embryos, but their expression patterns suggest their roles in development are conserved. Therefore, despite the evolutionary distance of planarians to other models, nervous system development appears molecularly similar to mechanisms described for more 'traditional' neural development.

The Potential Role of Planarian Neoblasts in Development: Regeneration in the Embryo

An outstanding question in planarian development is the embryonic origin of the pluripotent neoblast population. Le Moigne's classic experiments addressed this question by performing amputations of *Polycelis nigra* embryos.[173] He found that cells with neoblast-like morphology were present in Stage 4 embryos, and that embryos were capable of surviving decapitation around Stage 5, when the definitive embryo begins to form the structures found in the adult worm.[173,174] Furthermore, irradiation of Stage 4 embryos did not prevent development and hatching, but these animals could no longer regenerate,[173] perhaps indicating different roles of the neoblasts in development versus regeneration. However, it is possible that lineage-committed neoblasts survive and differentiate, allowing the animals to complete development of a smaller worm.[3] Molecular studies of germ cell-expressed genes *vasa-like* and *tudor* (*Spol-vlgA* and *-tud-1*) support that the expression pattern of these genes in neoblast-like cells is similar in late stage embryos and the neoblasts of post-embryonic planarians.[168,169] Further analysis of the expression of pan-neoblast marker genes like the RNA-interacting protein coding genes *piwi-1*[175] and

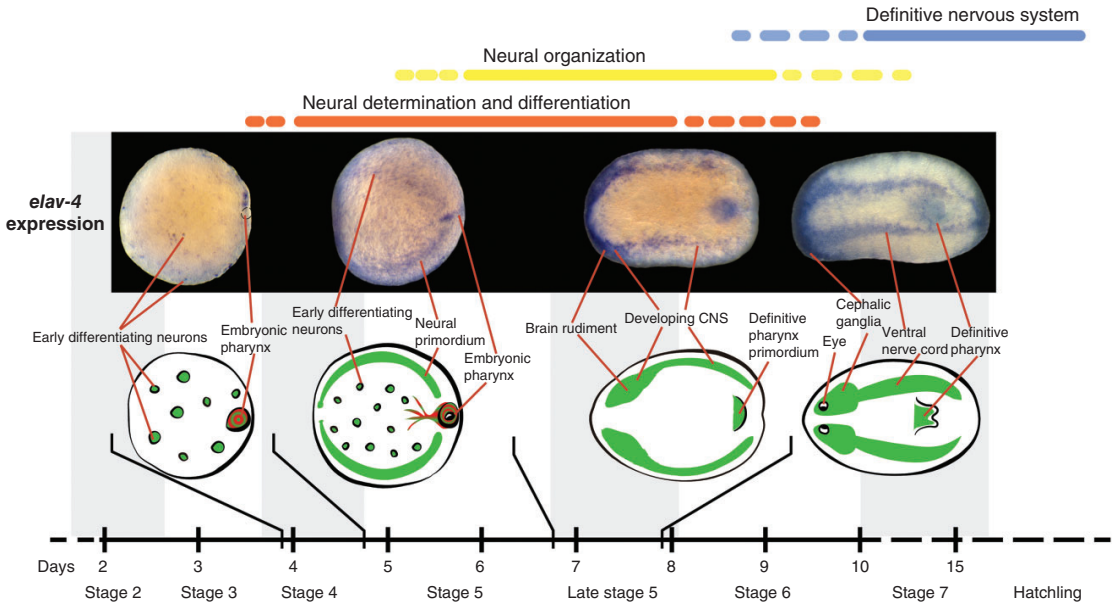

FIGURE 8 | Development of the nervous system in planarians. Neurogenesis can be visualized by *in situ* hybridization to *Spol-elav-4* in the developing *Schmidtea polychroa* embryo. Around Stage 4, early differentiating neurons can be detected. Early in Stage 5, these neurons form a neural primordium and, in late Stage 5, the developing brain rudiment and nerve net of the definitive pharynx primordium are readily detected. By Stage 7 (just prior to hatching), a defined brain, ventral nerve cords, and the nerve net of the definitive pharynx are visible. (Modified and reprinted with permission from Ref 167. Copyright 2015 Elsevier)

bruli[130] will be useful to investigate the origin and developmental contribution of pluripotent neoblasts in planarians. It is an intriguing possibility that the neoblast population plays a role in embryonic organogenesis, including neurogenesis in the developing planarian nervous system. If this is indeed the case, understanding how neurons originate from neoblasts in adult planarians will provide mechanistic insights into the embryonic development of the nervous system in these organisms.

CONCLUSION

Planarians have sparked the imagination of naturalists for over 100 years.[1] Modern advances in molecular and genomic technology over the past two decades have aided an expanding community of scientists to further cultivate the planarian as a model organism.[176,177] In the field of neurobiology and specifically neurogenesis, planarians offer outstanding opportunities to investigate developmental mechanisms underlying neuronal repair and function. Our knowledge of how neuronal subtypes are specified in the embryo or during regeneration is currently superficial. The photoreceptor and serotonergic neurons are amongst the best-understood cell lineages in planarians,[64,65,72,115,126,127] but these represent only a minor subset of the neural populations in the adult planarian. Thus, how any neurons are signaled to acquire their fates in space and time is not well understood. In the coming years, combining single cell trancriptomics with computational approaches will continue to help uncover and resolve the transcriptional programs that underlie cell lineage trajectories. A major obstacle in the field that limits our ability to study cell lineages is the current inability to perform transient or transgenic gene expression manipulations in planarians. The capacity to label individual cells and trace their lineages will be crucial to resolve how diverse neuronal subtypes (or any other differentiated cells) are generated *in vivo*. Transgenic techniques would also facilitate gain- or loss-of-function experiments in specific tissues or cell types to distinguish the function of genes within individual cell populations; for example, it would be possible to further examine the roles of Wnt signaling in global A–P patterning versus controlling brain shape and size.

Additionally, we do not have a clear understanding of how injured neurons and axons regenerate and integrate into the pre-existing neural circuits.

Genetically marking individual neurons or further application of vital dye cell labeling would facilitate visualization of nerve repair and further examination of the signaling pathways involved in axon guidance, as well as analyzing the role of the differentiated nervous system in providing cues to regenerating axons. During head regeneration, some of the positional cues are likely coming from the muscle tissue.[178] However, the mature nervous system also expresses genes necessary for proper nervous system regeneration. For instance, *ndk*,[106] *Smed-egr-4*,[104] and *Smed-nrg-7*,[103] are expressed in the nervous system. It is likely that gene expression in existing neural tissues assists in driving the regenerative process by providing additional positional information, and later by providing guidance cues to integrate newly formed or damaged neurons into the existing circuitry. Thus, many fundamental questions about the cellular and molecular basis of planarian regenerative neurobiology await exploration.

Current data indicates that regenerative processes in the adult worm recapitulate embryonic development and utilize the same genetic programs. A clear-cut example of this is in the development of the photoreceptor neurons, wherein the cell types found in the eye appear to share a common precursor and require the same transcription factors in planarian embryogenesis and regeneration.[72,165] However, in the context of planarian embryonic development, not much is known about the differentiation of neural cells and the formation of the embryonic brain. The fact that transcription factors found in lineage-committed neural progenitors in the adult are found in neural progenitor cells in the developing embryo provides evidence of shared regulatory networks,[56,111,112,167] further indicating that regeneration studies will inform how the nervous system is assembled in the developing planarian. In many other bilaterians, neural progenitors are derived from the neuroectoderm via asymmetric cell divisions. There is no clear evidence planarians form a neuroectoderm that is comparable to other organisms during development or regeneration. Instead, these animals appear to produce neurons from pluripotent neoblasts in the mesenchyme. In planarian embryogenesis, neural progenitors appear to be patterned stochastically (reviewed in Ref 6). In studies of adult planarians, a common pattern has emerged where progenitor cells are found near the tissues that they will ultimately become.[29,72,112,115,117,179] This suggests that local inductive signals, such as EGF or Hh, are directing the differentiation of the neoblasts, including regulation of asymmetric cell divisions in neuronal regeneration.[103] However, the cell–cell interactions or attributes that define the niches of the stem cell population remain unknown.

Many of the typical neurogenesis regulators in other organisms are conserved in planarian neurogenesis. For example, SoxB family members that are expressed in the ectoderm during gastrulation and provide neurogenic potential are also observed in progenitors and neural populations in the planarian.[72,111,167] Upstream of neurogenic genes are conserved factors like BMP family members and Wnt genes. These genes have been shown to control the size and shape of the planarian brain and eyes and regulate neurogenic factors that have been detected during planarian neural regeneration and in νNeoblasts[112,113,136,180] (such as *achaete-scute*), suggesting a high degree of conservation of neurogenesis regulatory programs deployed during embryogenesis in a multitude of organisms with programs in both the embryonic and adult planarian. Considering the diversity of neuronal cell types faithfully regenerated over a short time span in planarians, future on-going studies are poised to provide broad insights into sequential genetic programs required to produce neurons from pluripotent stem cells, which will advance regenerative biology and medicine.

NOTE

While this manuscript was in press, Davies *et al.* (*eLife* 2017, 6:e21052) reported that throughout embryogenesis in *Schmidtea mediterranea*, *piwi-1*$^+$ cells give rise to all temporary and definitive structures. Their data support the idea that the neoblasts, which arise from *piwi-1*$^+$ blastomeres at the onset of organogenesis, contribute to the development of all major organ systems during planarian development.

ACKNOWLEDGMENTS

We thank Dr. Francesc Cebrià, Alyssa Molinaro, and Dr. Francisco Monjo for contributions indicated in the figure legends, and John 'Jack' Allen and Dr. Nicholas Strand for helpful comments on the review. K.G.R. was supported by the San Diego Chapter of the ARCS Foundation, K.W.C. by a Natural Sciences and Engineering Research Council of Canada (NSERC) grant RGPIN-2016-06354, B.J.P. by an Ontario Institute for Cancer Research (OICR) grant IA-026, and R.M.Z. by NSF CAREER IOS-1350302.

FURTHER READINGS

Schmidtea mediterranea Genome Database (SmedGD): http://smedgd.stowers.org/

PlanMine, an integrated resource of data and tools to mine planarian biology: http://planmine.mpi-cbg.de/planmine/begin.do

Pearson lab website: http://pearsonlab.ca/

Zayas lab website: http://www.bio.sdsu.edu/faculty/zayas/index.html

REFERENCES

1. Elliott SA, Sánchez Alvarado A. The history and enduring contributions of planarians to the study of animal regeneration. *WIREs Dev Biol* 2013, 2:301–326.
2. Rink JC. Stem cell systems and regeneration in planaria. *Dev Genes Evol* 2013, 223:67–84.
3. Baguñà J. The planarian neoblast: the rambling history of its origin and some current black boxes. *Int J Dev Biol* 2012, 56:19–37.
4. Sarnat HB, Netsky MG. The brain of the planarian as the ancestor of the human brain. *Can J Neurol Sci* 1985, 12:296–302.
5. Sarnat HB, Netsky MG. When does a ganglion become a brain? Evolutionary origin of the central nervous system. *Semin Pediatr Neurol* 2002, 9:240–253.
6. Hartenstein V, Stollewerk A. The evolution of early neurogenesis. *Dev Cell* 2015, 32:390–407.
7. Dunn CW, Giribet G, Edgecombe GD, Hejnol A. Animal phylogeny and its evolutionary implications. *Annu Rev Ecol Evol Syst* 2014, 45:371–395.
8. Holland LZ, Carvalho JE, Escriva H, Laudet V, Schubert M, Shimeld SM, Yu JK. Evolution of bilaterian central nervous systems: a single origin? *Evodevo* 2013, 4:27.
9. Arendt D, Tosches MA, Marlow H. From nerve net to nerve ring, nerve cord and brain—evolution of the nervous system. *Nat Rev Neurosci* 2016, 17:61–72.
10. Nishimura O, Hirao Y, Tarui H, Agata K. Comparative transcriptome analysis between planarian *Dugesia japonica* and other platyhelminth species. *BMC Genomics* 2012, 13:289.
11. von Graff L, ed. Vermes. Ic*:* Turbellaria, vol. 4. Leipzig: C. F. Winter'sche Verlangshandlung; 1912–1917.
12. Micoletzky H. Zur kenntnis des Nerven-und Excretionssystems einiger süßwassertricladen nebst andern beiträgen zur Anatomie von planaria alpina. *Z wiss Zool* 1907, 87:382–434.
13. Bullock TH, Horridge GA. *Structure and Function in the Nervous Systems of Invertebrates*. San Francisco, CA: W. H. Freeman; 1965.
14. Baguñà J, Ballester R. The nervous system in planarians: peripheral and gastrodermal plexuses, pharynx innervation, and the relationship between central nervous system structure and the acoelomate organization. *J Morphol* 1978, 155:237–252.
15. Lentz TL. The nervous system of planaria. In: *Primitive Nervous Systems*. New Haven, CT: Yale University Press; 1968, 69–102.
16. Hyman LH. *The Invertebrates: Platyhelminthes and Rhynchocoela. The Acoelomate Bilateria*, vol. II. New York: McGraw Hill; 1951.
17. Cebrià F, Nakazawa M, Mineta K, Ikeo K, Gojobori T, Agata K. Dissecting planarian central nervous system regeneration by the expression of neural-specific genes. *Dev Growth Differ* 2002, 44:135–146.
18. Okamoto K, Takeuchi K, Agata K. Neural projections in planarian brain revealed by fluorescent dye tracing. *Zoolog Sci* 2005, 22:535–546.
19. Carpenter KS, Morita M, Best JB. Ultrastructure of the photoreceptor of the planarian *Dugesia dorotocephala*. I. Normal eye. *Cell Tissue Res* 1974, 148:143–158.
20. Sakai F, Agata K, Orii H, Watanabe K. Organization and regeneration ability of spontaneous supernumerary eyes in planarians—eye regeneration field and pathway selection by optic nerves. *Zoolog Sci* 2000, 17:375–381.
21. Inoue T, Kumamoto H, Okamoto K, Umesono Y, Sakai M, Sánchez Alvarado A, Agata K. Morphological and functional recovery of the planarian photosensing system during head regeneration. *Zoolog Sci* 2004, 21:275–283.
22. Agata K, Soejima Y, Kato K, Kobayashi C, Umesono Y, Watanabe K. Structure of the planarian central nervous system (CNS) revealed by neuronal cell markers. *Zoolog Sci* 1998, 15:433–440.
23. Best JB, Noel J. Complex synaptic configurations in planarian brain. *Science* 1969, 164:1070–1071.
24. Tazaki A, Gaudieri S, Ikeo K, Gojobori T, Watanabe K, Agata K. Neural network in planarian revealed by an antibody against planarian synaptotagmin homologue. *Biochem Biophys Res Commun* 1999, 260:426–432.
25. Cebrià F. Organization of the nervous system in the model planarian *Schmidtea mediterranea*: an immunocytochemical study. *Neurosci Res* 2008, 61:375–384.

26. Morita M, Best JB. Electron microscopic studies on Planaria. II. Fine structure of the neurosecretory system in the planarian *Dugesia dorotocephala*. *J Ultrastruct Res* 1965, 13:396–408.

27. Morita M, Best JB. Electron microscopic studies of Planaria. 3. Some observations on the fine structure of planarian nervous tissue. *J Exp Zool* 1966, 161:391–411.

28. Pigon A, Morita M, Best JB. Cephalic mechanism for social control of fissioning in planarians. II. Localization and identification of the receptors by electron micrographic and ablation studies. *J Neurobiol* 1974, 5:443–462.

29. Ross KG, Omuro KC, Taylor MR, Munday RK, Hubert A, King RS, Zayas RM. Novel monoclonal antibodies to study tissue regeneration in planarians. *BMC Dev Biol* 2015, 15:2.

30. Reuter M, Gustafsson MKS. The flatworm nervous system: pattern and phylogeny. In: Breidbach O, Kutsch W, eds. *The Nervous Systems of Invertebrates: An Evolutionary and Comparative Approach: With a Coda Written by T.H. Bullock*. Basel: Birkhäuser; 1995, 25–59.

31. Fraguas S, Barberán S, Ibarra B, Stoger L, Cebrià F. Regeneration of neuronal cell types in *Schmidtea mediterranea*: an immunohistochemical and expression study. *Int J Dev Biol* 2012, 56:143–153.

32. Lentz TL. Fine structure of nerve cells in a planarian. *J Morphol* 1967, 121:323–337.

33. Oosaki T, Ishii S. Observations on the ultrastructure of nerve cells in the brain of the planarian, *Dugesia gonocephala*. *Z Zellforsch Mikrosk Anat* 1965, 66:782–793.

34. Trawicki W, Czubaj A, Moraczewski J. The brain ultrastructure of *Dendrocoelum lacteum* (O.F. Muller). *Prog Zool* 1988, 36:195–200.

35. Golubev A. Glia and neuroglia relationships in the central nervous system of the Turbellaria (electron microscopic data). *Fortschr Zool* 1988, 36:31–37.

36. Fraenkel A, Gunn DL. *The Orientation of Animals*. New York, NY: Dover; 1961.

37. Koehler O. Beiträge zur Sinnesphysiologie der Süßwasserplanarien. *Z vergl Physiol* 1932, 16:606–756.

38. MacRae EK. The fine structure of sensory receptor processes in the auricular epithelium of the planarian, *Dugesia tigrina*. *Z Zellforsch Mikrosk Anat* 1967, 82:479–494.

39. Farnesi RM, Tei S. *Dugesia lugubris* s.l. auricles: research into the ultrastructure and on the functional efficiency. *Riv Biol* 1980, 73:65–77.

40. Pearl R. The movements and reactions of fresh-water planarians: a study in animal behavior. *Q J Microsc Sci* 1903, 46:509–714.

41. Köhler O. Sinnesphysiologie der Süsserwasserplanarien. *Z vergl Physiol* 1932, 16:606–756.

42. Müller HG. Untersuchungen über spezifische Organe niederer Sinne bei rhabdocoelen Turbellarien. *Z vergl Physiol* 1936, 23:253–292.

43. Umesono Y, Watanabe K, Agata K. A planarian orthopedia homolog is specifically expressed in the branch region of both the mature and regenerating brain. *Dev Growth Differ* 1997, 39:723–727.

44. Pearson BJ, Eisenhoffer GT, Gurley KA, Rink JC, Miller DE, Sanchez Alvarado A. Formaldehyde-based whole-mount *in situ* hybridization method for planarians. *Dev Dyn* 2009, 238:443–450.

45. King RS, Newmark PA. *In situ* hybridization protocol for enhanced detection of gene expression in the planarian *Schmidtea mediterranea*. *BMC Dev Biol* 2013, 13:8.

46. Newmark PA, Reddien PW, Cebria F, Sánchez Alvarado A. Ingestion of bacterially expressed double-stranded RNA inhibits gene expression in planarians. *Proc Natl Acad Sci USA* 2003, 100(suppl 1): 11861–11865.

47. Sánchez Alvarado A, Newmark PA. Double-stranded RNA specifically disrupts gene expression during planarian regeneration. *Proc Natl Acad Sci USA* 1999, 96:5049–5054.

48. Brandl H, Moon H, Vila-Farre M, Liu SY, Henry I, Rink JC. PlanMine—a mineable resource of planarian biology and biodiversity. *Nucleic Acids Res* 2016, 44: D764–D773.

49. Robb SM, Gotting K, Ross E, Sanchez Alvarado A. SmedGD 2.0: the *Schmidtea mediterranea* genome database. *Genesis* 2015, 53:535–546.

50. Mineta K, Nakazawa M, Cebrià F, Ikeo K, Agata K, Gojobori T. Origin and evolutionary process of the CNS elucidated by comparative genomics analysis of planarian ESTs. *Proc Natl Acad Sci USA* 2003, 100:7666–7671.

51. Reddien PW, Bermange AL, Murfitt KJ, Jennings JR, Sánchez Alvarado A. Identification of genes needed for regeneration, stem cell function, and tissue homeostasis by systematic gene perturbation in planaria. *Dev Cell* 2005, 8:635–649.

52. Cebrià F, Kudome T, Nakazawa M, Mineta K, Ikeo K, Gojobori T, Agata K. The expression of neural-specific genes reveals the structural and molecular complexity of the planarian central nervous system. *Mech Dev* 2002, 116:199–204.

53. Nakazawa M, Cebria F, Mineta K, Ikeo K, Agata K, Gojobori T. Search for the evolutionary origin of a brain: planarian brain characterized by microarray. *Mol Biol Evol* 2003, 20:784–791.

54. Umesono Y, Watanabe K, Agata K. Distinct structural domains in the planarian brain defined by the

expression of evolutionarily conserved homeobox genes. *Dev Genes Evol* 1999, 209:31–39.

55. Hubert A, Henderson JM, Cowles MW, Ross KG, Hagen M, Anderson C, Szeterlak CJ, Zayas RM. A functional genomics screen identifies an importin-alpha homolog as a regulator of stem cell function and tissue patterning during planarian regeneration. *BMC Genomics* 2015, 16:769.
56. Roberts-Galbraith RH, Brubacher JL, Newmark PA. A functional genomics screen in planarians reveals regulators of whole-brain regeneration. *Elife* 2016, 5: e17002.
57. Wang IE, Lapan SW, Scimone ML, Clandinin TR, Reddien PW. Hedgehog signaling regulates gene expression in planarian glia. *Elife* 2016, 5:e16996.
58. Nishimura K, Kitamura Y, Inoue T, Umesono Y, Sano S, Yoshimoto K, Inden M, Takata K, Taniguchi T, Shimohama S, et al. Reconstruction of dopaminergic neural network and locomotion function in planarian regenerates. *Dev Neurobiol* 2007, 67:1059–1078.
59. Nishimura K, Kitamura Y, Inoue T, Umesono Y, Yoshimoto K, Takeuchi K, Taniguchi T, Agata K. Identification and distribution of tryptophan hydroxylase (TPH)-positive neurons in the planarian *Dugesia japonica*. *Neurosci Res* 2007, 59:101–106.
60. Nishimura K, Kitamura Y, Umesono Y, Takeuchi K, Takata K, Taniguchi T, Agata K. Identification of glutamic acid decarboxylase gene and distribution of GABAergic nervous system in the planarian *Dugesia japonica*. *Neuroscience* 2008, 153:1103–1114.
61. Nishimura K, Kitamura Y, Taniguchi T, Agata K. Analysis of motor function modulated by cholinergic neurons in planarian *Dugesia japonica*. *Neuroscience* 2010, 168:18–30.
62. Nishimura K, Kitamura Y, Inoue T, Umesono Y, Yoshimoto K, Taniguchi T, Agata K. Characterization of tyramine beta-hydroxylase in planarian *Dugesia japonica*: cloning and expression. *Neurochem Int* 2008, 53:184–192.
63. Currie KW, Molinaro AM, Pearson BJ. Neuronal sources of hedgehog modulate neurogenesis in the adult planarian brain. *Elife* 2016, 5:e19735.
64. Currie KW, Pearson BJ. Transcription factors lhx1/5-1 and pitx are required for the maintenance and regeneration of serotonergic neurons in planarians. *Development* 2013, 140:3577–3588.
65. Marz M, Seebeck F, Bartscherer K. A pitx transcription factor controls the establishment and maintenance of the serotonergic lineage in planarians. *Development* 2013, 140:4499–4509.
66. Oviedo NJ, Newmark PA, Sánchez Alvarado A. Allometric scaling and proportion regulation in the freshwater planarian *Schmidtea mediterranea*. *Dev Dyn* 2003, 226:326–333.
67. Lehmann C, Bette S, Engele J. High extracellular glutamate modulates expression of glutamate transporters and glutamine synthetase in cultured astrocytes. *Brain Res* 2009, 1297:1–8.
68. Liang J, Takeuchi H, Doi Y, Kawanokuchi J, Sonobe Y, Jin S, Yawata I, Li H, Yasuoka S, Mizuno T, et al. Excitatory amino acid transporter expression by astrocytes is neuroprotective against microglial excitotoxicity. *Brain Res* 2008, 1210:11–19.
69. Collins JJ 3rd, Hou X, Romanova EV, Lambrus BG, Miller CM, Saberi A, Sweedler JV, Newmark PA. Genome-wide analyses reveal a role for peptide hormones in planarian germline development. *PLoS Biol* 2010, 8:e1000509.
70. Saberi A, Jamal A, Beets I, Schoofs L, Newmark PA. GPCRs direct germline development and somatic gonad function in planarians. *PLoS Biol* 2016, 14: e1002457.
71. Shimoyama S, Inoue T, Kashima M, Agata K. Multiple neuropeptide-coding genes involved in planarian pharynx extension. *Zoolog Sci* 2016, 33:311–319.
72. Lapan SW, Reddien PW. Transcriptome analysis of the planarian eye identifies ovo as a specific regulator of eye regeneration. *Cell Rep* 2012, 2:294–307.
73. Gonzalez-Sastre A, Molina MD, Salo E. Inhibitory Smads and bone morphogenetic protein (BMP) modulate anterior photoreceptor cell number during planarian eye regeneration. *Int J Dev Biol* 2012, 56:155–163.
74. Azuma K, Okazaki Y, Asai K, Iwasaki N. Electrical responses and K+ activity changes to light in the ocellus of the planarian *Dugesia japonica*. *Comp Biochem Physiol A Physiol* 1994, 109:593–599.
75. Azuma K. Light-induced extracellular changes of calcium and sodium concentrations in the planarian ocellus. *Comp Biochem Physiol A Mol Integr Physiol* 1998, 119:321–325.
76. Behrens ME. The electrical response of planarian photoreceptor. *Comp Biochem Physiol* 1962, 5:129–138.
77. Brown HM, Ogden TE. The electrical response of the planarian ocellus. *J Gen Physiol* 1968, 51:237–253.
78. Weimer BR. Thigmotactic reactions of the fresh water turbellarian, *Phagocata gracilis*, Leidy. *Trans Am Microsc Soc* 1918, 37:111–124.
79. Takano T, Pulvers JN, Inoue T, Tarui H, Sakamoto H, Agata K, Umesono Y. Regeneration-dependent conditional gene knockdown (Readyknock) in planarian: demonstration of requirement for Djsnap-25 expression in the brain for negative phototactic behavior. *Dev Growth Differ* 2007, 49:383–394.
80. Hagstrom D, Cochet-Escartin O, Zhang S, Khuu C, Collins EM. Freshwater planarians as an alternative animal model for neurotoxicology. *Toxicol Sci* 2015, 147:270–285.

81. Inoue T, Hoshino H, Yamashita T, Shimoyama S, Agata K. Planarian shows decision-making behavior in response to multiple stimuli by integrative brain function. *Zoolog Lett* 2015, 1:7.

82. Stringer CE. The means of locomotion in planarians. *Proc Natl Acad Sci USA* 1917, 3:691–692.

83. Rompolas P, Patel-King RS, King SM. An outer arm Dynein conformational switch is required for metachronal synchrony of motile cilia in planaria. *Mol Biol Cell* 2010, 21:3669–3679.

84. Cochet-Escartin O, Mickolajczyk KJ, Collins EM. Scrunching: a novel escape gait in planarians. *Phys Biol* 2015, 12:056010.

85. Inoue T, Yamashita T, Agata K. Thermosensory signaling by TRPM is processed by brain serotonergic neurons to produce planarian thermotaxis. *J Neurosci* 2014, 34:15701–15714.

86. Cebrià F. Planarian body-wall muscle: regeneration and function beyond a simple skeletal support. *Front Cell Dev Biol* 2016, 4:8.

87. Wenemoser D, Lapan SW, Wilkinson AW, Bell GW, Reddien PW. A molecular wound response program associated with regeneration initiation in planarians. *Genes Dev* 2012, 26:988–1002.

88. Wurtzel O, Cote LE, Poirier A, Satija R, Regev A, Reddien PW. A generic and cell-type-specific wound response precedes regeneration in planarians. *Dev Cell* 2015, 35:632–645.

89. Petersen CP, Reddien PW. Polarized notum activation at wounds inhibits Wnt function to promote planarian head regeneration. *Science* 2011, 332:852–855.

90. Gurley KA, Rink JC, Sánchez Alvarado A. Beta-catenin defines head versus tail identity during planarian regeneration and homeostasis. *Science* 2008, 319:323–327.

91. Petersen CP, Reddien PW. Smed-betacatenin-1 is required for anteroposterior blastema polarity in planarian regeneration. *Science* 2008, 319:327–330.

92. Iglesias M, Gomez-Skarmeta JL, Saló E, Adell T. Silencing of Smed-betacatenin1 generates radial-like hypercephalized planarians. *Development* 2008, 135:1215–1221.

93. Rink JC, Gurley KA, Elliott SA, Sánchez Alvarado A. Planarian Hh signaling regulates regeneration polarity and links Hh pathway evolution to cilia. *Science* 2009, 326:1406–1410.

94. Yazawa S, Umesono Y, Hayashi T, Tarui H, Agata K. Planarian hedgehog/patched establishes anterior-posterior polarity by regulating Wnt signaling. *Proc Natl Acad Sci USA* 2009, 106:22329–22334.

95. Roberts-Galbraith RH, Newmark PA. Follistatin antagonizes activin signaling and acts with notum to direct planarian head regeneration. *Proc Natl Acad Sci USA* 2013, 110:1363–1368.

96. Scimone ML, Lapan SW, Reddien PW. A forkhead transcription factor is wound-induced at the planarian midline and required for anterior pole regeneration. *PLoS Genet* 2014, 10:e1003999.

97. Vogg MC, Owlarn S, Perez Rico YA, Xie J, Suzuki Y, Gentile L, Wu W, Bartscherer K. Stem cell-dependent formation of a functional anterior regeneration pole in planarians requires Zic and Forkhead transcription factors. *Dev Biol* 2014, 390:136–148.

98. Evans DJ, Owlarn S, Tejada Romero B, Chen C, Aboobaker AA. Combining classical and molecular approaches elaborates on the complexity of mechanisms underpinning anterior regeneration. *PLoS One* 2011, 6:e27927.

99. Felix DA, Aboobaker AA. The TALE class homeobox gene Smed-prep defines the anterior compartment for head regeneration. *PLoS Genet* 2010, 6:e1000915.

100. Currie KW, Brown DD, Zhu S, Xu C, Voisin V, Bader GD, Pearson BJ. HOX gene complement and expression in the planarian *Schmidtea mediterranea*. *Evodevo* 2016, 7:7.

101. Fraguas S, Barberan S, Cebria F. EGFR signaling regulates cell proliferation, differentiation and morphogenesis during planarian regeneration and homeostasis. *Dev Biol* 2011, 354:87–101.

102. Barberán S, Martín-Durán JM, Cebrià F. Evolution of the EGFR pathway in Metazoa and its diversification in the planarian *Schmidtea mediterranea*. *Sci Rep* 2016, 6:28071.

103. Lei K, Thi-Kim Vu H, Mohan RD, McKinney SA, Seidel CW, Alexander R, Gotting K, Workman JL, Sanchez Alvarado A. Egf signaling directs neoblast repopulation by regulating asymmetric cell division in planarians. *Dev Cell* 2016, 38:413–429.

104. Fraguas S, Barberán S, Iglesias M, Rodríguez-Esteban G, Cebrià F. egr-4, a target of EGFR signaling, is required for the formation of the brain primordia and head regeneration in planarians. *Development* 2014, 141:1835–1847.

105. Wagner DE, Ho JJ, Reddien PW. Genetic regulators of a pluripotent adult stem cell system in planarians identified by RNAi and clonal analysis. *Cell Stem Cell* 2012, 10:299–311.

106. Cebrià F, Kobayashi C, Umesono Y, Nakazawa M, Mineta K, Ikeo K, Gojobori T, Itoh M, Taira M, Sánchez Alvarado A, et al. FGFR-related gene nou-darake restricts brain tissues to the head region of planarians. *Nature* 2002, 419:620–624.

107. Fuccillo M, Joyner AL, Fishell G. Morphogen to mitogen: the multiple roles of hedgehog signalling in vertebrate neural development. *Nat Rev Neurosci* 2006, 7:772–783.

108. Watson JD, Wheeler SR, Stagg SB, Crews ST. Drosophila hedgehog signaling and engrailed-runt mutual repression direct midline glia to alternative

ensheathing and non-ensheathing fates. *Development* 2011, 138:1285–1295.

109. Sirko S, Behrendt G, Johansson PA, Tripathi P, Costa M, Bek S, Heinrich C, Tiedt S, Colak D, Dichgans M, et al. Reactive glia in the injured brain acquire stem cell properties in response to sonic hedgehog. [corrected]. *Cell Stem Cell* 2013, 12:426–439.
110. Newmark PA, Sánchez Alvarado A. Bromodeoxyuridine specifically labels the regenerative stem cells of planarians. *Dev Biol* 2000, 220:142–153.
111. Scimone ML, Kravarik KM, Lapan SW, Reddien PW. Neoblast specialization in regeneration of the planarian *Schmidtea mediterranea*. *Stem Cell Rep* 2014, 3:339–352.
112. Cowles MW, Brown DD, Nisperos SV, Stanley BN, Pearson BJ, Zayas RM. Genome-wide analysis of the bHLH gene family in planarians identifies factors required for adult neurogenesis and neuronal regeneration. *Development* 2013, 140:4691–4702.
113. Molinaro AM, Pearson BJ. In silico lineage tracing through single cell transcriptomics identifies a neural stem cell population in planarians. *Genome Biol* 2016, 17:87.
114. Scimone ML, Srivastava M, Bell GW, Reddien PW. A regulatory program for excretory system regeneration in planarians. *Development* 2011, 138:4387–4398.
115. Lapan SW, Reddien PW. dlx and sp6-9 control optic cup regeneration in a prototypic eye. *PLoS Genet* 2011, 7:e1002226.
116. van Wolfswinkel JC, Wagner DE, Reddien PW. Single-cell analysis reveals functionally distinct classes within the planarian stem cell compartment. *Cell Stem Cell* 2014, 15:326–339.
117. Adler CE, Seidel CW, McKinney SA, Sánchez Alvarado A. Selective amputation of the pharynx identifies a FoxA-dependent regeneration program in planaria. *Elife* 2014, 3:e02238.
118. Thi-Kim Vu H, Rink JC, McKinney SA, McClain M, Lakshmanaperumal N, Alexander R, Sanchez Alvarado A. Stem cells and fluid flow drive cyst formation in an invertebrate excretory organ. *Elife* 2015, 4:e07405.
119. Cowles MW, Omuro KC, Stanley BN, Quintanilla CG, Zayas RM. COE loss-of-function analysis reveals a genetic program underlying maintenance and regeneration of the nervous system in planarians. *PLoS Genet* 2014, 10:e1004746.
120. Hobert O. Terminal selectors of neuronal identity. *Curr Top Dev Biol* 2016, 116:455–475.
121. Sandmann T, Vogg MC, Owlarn S, Boutros M, Bartscherer K. The head-regeneration transcriptome of the planarian *Schmidtea mediterranea*. *Genome Biol* 2011, 12:R76.
122. Sandberg M, Kallstrom M, Muhr J. Sox21 promotes the progression of vertebrate neurogenesis. *Nat Neurosci* 2005, 8:995–1001.
123. Labbé RM, Irimia M, Currie KW, Lin A, Zhu SJ, Brown DDR, Ross EJ, Voisin V, Bader GD, Blencowe BJ, et al. A comparative transcriptomic analysis reveals conserved features of stem cell pluripotency in planarians and mammals. *Stem Cells* 2012, 30:1734–1745.
124. Mannini L, Rossi L, Deri P, Gremigni V, Salvetti A, Saló E, Batistoni R. Djeyes absent (Djeya) controls prototypic planarian eye regeneration by cooperating with the transcription factor Djsix-1. *Dev Biol* 2004, 269:346–359.
125. Cross SD, Johnson AA, Gilles BJ, Bachman LA, Inoue T, Agata K, Marmorstein LY, Marmorstein AD. Control of maintenance and regeneration of planarian eyes by ovo. *Invest Ophthalmol Vis Sci* 2015, 56:7604–7610.
126. Pineda D, Gonzalez J, Callaerts P, Ikeo K, Gehring WJ, Saló E. Searching for the prototypic eye genetic network: sine oculis is essential for eye regeneration in planarians. *Proc Natl Acad Sci USA* 2000, 97:4525–4529.
127. Saló E, Pineda D, Marsal M, Gonzalez J, Gremigni V, Batistoni R. Genetic network of the eye in Platyhelminthes: expression and functional analysis of some players during planarian regeneration. *Gene* 2002, 287:67–74.
128. Zhu SJ, Pearson BJ. (Neo)blast from the past: new insights into planarian stem cell lineages. *Curr Opin Genet Dev* 2016, 40:74–80.
129. Wagner DE, Wang IE, Reddien PW. Clonogenic neoblasts are pluripotent adult stem cells that underlie planarian regeneration. *Science* 2011, 332:811–816.
130. Guo T, Peters AH, Newmark PA. A Bruno-like gene is required for stem cell maintenance in planarians. *Dev Cell* 2006, 11:159–169.
131. Reddien PW, Oviedo NJ, Jennings JR, Jenkin JC, Sánchez Alvarado A. SMEDWI-2 is a PIWI-like protein that regulates planarian stem cells. *Science* 2005, 310:1327–1330.
132. Higuchi S, Hayashi T, Tarui H, Nishimura O, Nishimura K, Shibata N, Sakamoto H, Agata K. Expression and functional analysis of musashi-like genes in planarian CNS regeneration. *Mech Dev* 2008, 125:631–645.
133. Kageyama R, Ohtsuka T, Hatakeyama J, Ohsawa R. Roles of bHLH genes in neural stem cell differentiation. *Exp Cell Res* 2005, 306:343–348.
134. Zhu SJ, Hallows SE, Currie KW, Xu C, Pearson BJ. A mex3 homolog is required for differentiation during planarian stem cell lineage development. *Elife* 2015, 4:e07025.

135. Nishimura K, Inoue T, Yoshimoto K, Taniguchi T, Kitamura Y, Agata K. Regeneration of dopaminergic neurons after 6-hydroxydopamine-induced lesion in planarian brain. *J Neurochem* 2011, 119:1217–1231.

136. Hill EM, Petersen CP. Wnt/notum spatial feedback inhibition controls neoblast differentiation to regulate reversible growth of the planarian brain. *Development* 2015, 142:4217–4229.

137. Baguñà J, Romero R. Quantitative analysis of cell types during growth, degrowth and regeneration in the planarians *Dugesia mediterranea* and *Dugesia tigrina*. *Hydrobiologia* 1981, 84:181–194.

138. Takeda H, Nishimura K, Agata K. Planarians maintain a constant ratio of different cell types during changes in body size by using the stem cell system. *Zoolog Sci* 2009, 26:805–813.

139. Adell T, Saló E, Boutros M, Bartscherer K. Smed-Evi/Wntless is required for beta-catenin-dependent and -independent processes during planarian regeneration. *Development* 2009, 136:905–910.

140. Scimone ML, Cote LE, Rogers T, Reddien PW. Two FGFRL-Wnt circuits organize the planarian anteroposterior axis. *Elife* 2016, 5:e12845.

141. Kobayashi C, Saito Y, Ogawa K, Agata K. Wnt signaling is required for antero-posterior patterning of the planarian brain. *Dev Biol* 2007, 306:714–724.

142. Gurley KA, Elliott SA, Simakov O, Schmidt HA, Holstein TW, Sánchez Alvarado A. Expression of secreted Wnt pathway components reveals unexpected complexity of the planarian amputation response. *Dev Biol* 2010, 347:24–39.

143. Molina MD, Saló E, Cebrià F. The BMP pathway is essential for re-specification and maintenance of the dorsoventral axis in regenerating and intact planarians. *Dev Biol* 2007, 311:79–94.

144. Orii H, Watanabe K. Bone morphogenetic protein is required for dorso-ventral patterning in the planarian *Dugesia japonica*. *Dev Growth Differ* 2007, 49:345–349.

145. Reddien PW, Bermange AL, Kicza AM, Sánchez Alvarado A. BMP signaling regulates the dorsal planarian midline and is needed for asymmetric regeneration. *Development* 2007, 134:4043–4051.

146. Molina MD, Saló E, Cebrià F. Organizing the DV axis during planarian regeneration. *Commun Integr Biol* 2011, 4:498–500.

147. Killeen MT, Sybingco SS. Netrin, Slit and Wnt receptors allow axons to choose the axis of migration. *Dev Biol* 2008, 323:143–151.

148. Cebrià F, Guo T, Jopek J, Newmark PA. Regeneration and maintenance of the planarian midline is regulated by a slit orthologue. *Dev Biol* 2007, 307:394–406.

149. Cebrià F, Newmark PA. Planarian homologs of netrin and netrin receptor are required for proper regeneration of the central nervous system and the maintenance of nervous system architecture. *Development* 2005, 132:3691–3703.

150. Cebrià F, Newmark PA. Morphogenesis defects are associated with abnormal nervous system regeneration following roboA RNAi in planarians. *Development* 2007, 134:833–837.

151. Yamamoto H, Agata K. Optic chiasm formation in planarian I: cooperative netrin- and robo-mediated signals are required for the early stage of optic chiasm formation. *Dev Growth Differ* 2011, 53:300–311.

152. Inoue T, Hayashi T, Takechi K, Agata K. Clathrin-mediated endocytic signals are required for the regeneration of, as well as homeostasis in, the planarian CNS. *Development* 2007, 134:1679–1689.

153. Fusaoka E, Inoue T, Mineta K, Agata K, Takeuchi K. Structure and function of primitive immunoglobulin superfamily neural cell adhesion molecules: a lesson from studies on planarian. *Genes Cells* 2006, 11:541–555.

154. Prasad BC, Ye B, Zackhary R, Schrader K, Seydoux G, Reed RR. unc-3, a gene required for axonal guidance in *Caenorhabditis elegans*, encodes a member of the O/E family of transcription factors. *Development* 1998, 125:1561–1568.

155. Talbot JA, Currie KW, Pearson BJ, Collins EM. Smed-dynA-1 is a planarian nervous system specific dynamin 1 homolog required for normal locomotion. *Biol Open* 2014, 3:627–634.

156. Nogi T, Zhang D, Chan JD, Marchant JS. A novel biological activity of praziquantel requiring voltage-operated Ca2+ channel beta subunits: subversion of flatworm regenerative polarity. *PLoS Negl Trop Dis* 2009, 3:e464.

157. Hagstrom D, Cochet-Escartin O, Collins EM. Planarian brain regeneration as a model system for developmental neurotoxicology. *Regeneration (Oxf)* 2016, 3:65–77.

158. Neuhof M, Levin M, Rechavi O. Vertically- and horizontally-transmitted memories – the fading boundaries between regeneration and inheritance in planaria. *Biol Open* 2016, 5:1177–1188.

159. Martín-Durán JM, Monjo F, Romero R. Planarian embryology in the era of comparative developmental biology. *Int J Dev Biol* 2012, 56:39–48.

160. Baguñà J, Boyer BC. Descriptive and experimental embryology of the Turbellaria: present knowledge, open questions and future trends. In: Marthy H-J, ed. *Experimental Embryology in Aquatic Plants and Animals*. New York: Plenum Press; 1990, 95–128.

161. Cardona A, Hartenstein V, Romero R. Early embryogenesis of planaria: a cryptic larva feeding on maternal resources. *Dev Genes Evol* 2006, 216:667–681.

162. Cardona A, Fernández J, Solana J, Romero R. An *in situ* hybridization protocol for planarian embryos:

monitoring myosin heavy chain gene expression. *Dev Genes Evol* 2005, 215:482–488.

163. Cardona A, Hartenstein V, Romero R. The embryonic development of the triclad *Schmidtea polychroa*. *Dev Genes Evol* 2005, 215:109–131.
164. Martín-Durán JM, Amaya E, Romero R. Germ layer specification and axial patterning in the embryonic development of the freshwater planarian *Schmidtea polychroa*. *Dev Biol* 2010, 340:145–158.
165. Martín-Durán JM, Monjo F, Romero R. Morphological and molecular development of the eyes during embryogenesis of the freshwater planarian *Schmidtea polychroa*. *Dev Genes Evol* 2012, 222:45–54.
166. Martín-Durán JM, Romero R. Evolutionary implications of morphogenesis and molecular patterning of the blind gut in the planarian *Schmidtea polychroa*. *Dev Biol* 2011, 352:164–176.
167. Monjo F, Romero R. Embryonic development of the nervous system in the planarian *Schmidtea polychroa*. *Dev Biol* 2015, 397:305–319.
168. Solana J, Romero R. SpolvlgA is a DDX3/PL10-related DEAD-box RNA helicase expressed in blastomeres and embryonic cells in planarian embryonic development. *Int J Biol Sci* 2009, 5:64–73.
169. Solana J, Lasko P, Romero R. Spoltud-1 is a chromatoid body component required for planarian long-term stem cell self-renewal. *Dev Biol* 2009, 328:410–421.
170. Kuang S, Doran SA, Wilson RJ, Goss GG, Goldberg JI. Serotonergic sensory-motor neurons mediate a behavioral response to hypoxia in pond snail embryos. *J Neurobiol* 2002, 52:73–83.
171. Diefenbach TJ, Koss R, Goldberg JI. Early development of an identified serotonergic neuron in *Helisoma trivolvis* embryos: serotonin expression, de-expression, and uptake. *J Neurobiol* 1998, 34:361–376.
172. Pevny L, Placzek M. SOX genes and neural progenitor identity. *Curr Opin Neurobiol* 2005, 15:7–13.
173. Le Moigne A. Etude du développement embryonnaire et recherches sur les cellules de régénération chez l'embryon de la Planaire *Polycelis nigra* (Turbellarié, Triclade). *J Embryol Exp Morphol* 1966, 15:39–60.
174. Le Moigne A. Mise en évidence d'un pouvoir de régénération chez l'embryon de *Polycelis nigra* (Turbellarié-Triclade). *Bull Soc Zool France* 1965, 90:355–361.
175. Eisenhoffer GT, Kang H, Sánchez Alvarado A. Molecular analysis of stem cells and their descendants during cell turnover and regeneration in the planarian *Schmidtea mediterranea*. *Cell Stem Cell* 2008, 3:327–339.
176. Newmark PA, Sánchez Alvarado A. Not your father's planarian: a classic model enters the era of functional genomics. *Nat Rev Genet* 2002, 3:210–219.
177. Sánchez Alvarado A. Planarian regeneration: its end is its beginning. *Cell* 2006, 124:241–245.
178. Witchley JN, Mayer M, Wagner DE, Owen JH, Reddien PW. Muscle cells provide instructions for planarian regeneration. *Cell Rep* 2013, 4:633–641.
179. Forsthoefel DJ, Park AE, Newmark PA. Stem cell-based growth, regeneration, and remodeling of the planarian intestine. *Dev Biol* 2011, 356:445–459.
180. Kao D, Felix D, Aboobaker A. The planarian regeneration transcriptome reveals a shared but temporally shifted regulatory program between opposing head and tail scenarios. *BMC Genomics* 2013, 14:797.
181. Iijima I. Untersuchungen über den Bau un die Entwicklungsgeschichte der Süswasser-Dendrocoelen (Tricladen). *Z Wiss Zool XL Bd* 1884, 40:359–464.
182. Umesono Y, Tasaki J, Nishimura K, Inoue T, Agata K. Regeneration in an evolutionarily primitive brain—the planarian *Dugesia japonica* model. *Eur J Neurosci* 2011, 34:863–869.
183. Gentile L, Cebrià F, Bartscherer K. The planarian flatworm: an *in vivo* model for stem cell biology and nervous system regeneration. *Dis Model Mech* 2011, 4:12–19.

Chapter 1, in full, is a reprint of the material as it appears in Wiley Interdisciplinary Reviews – Developmental Biology 2017. Kelly G. Ross, Ko W. Currie, Bret J. Pearson, and Ricardo M. Zayas. The dissertation author was the primary author of this manuscript.

CHAPTER 2:

Novel monoclonal antibodies to study tissue regeneration in planarians

BMC
Developmental Biology

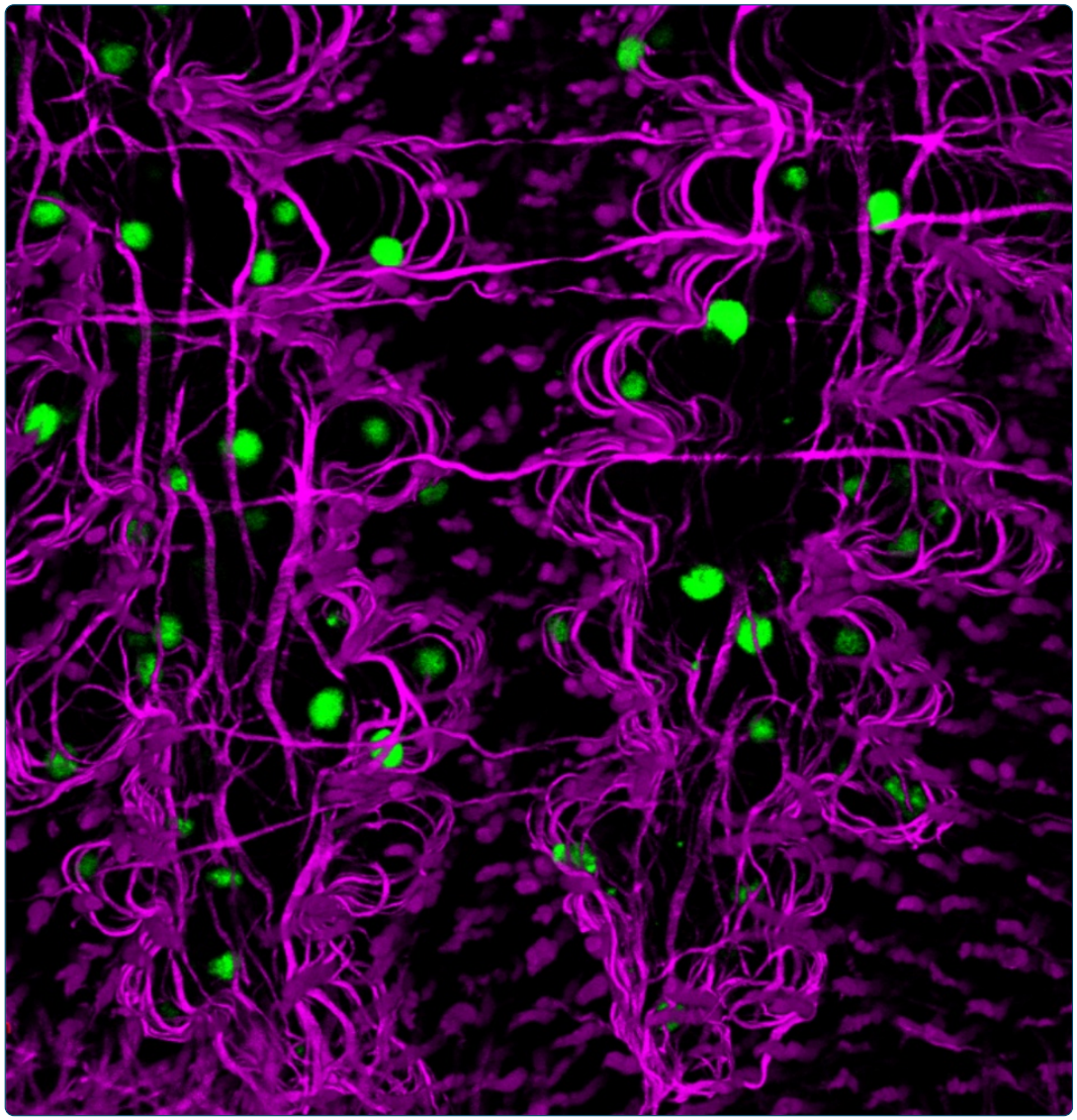

Novel monoclonal antibodies to study tissue regeneration in planarians

Ross *et al.*

BioMed Central

Ross *et al. BMC Developmental Biology* (2015) 15:2
DOI 10.1186/s12861-014-0050-9

Ross et al. BMC Developmental Biology (2015) 15:2
DOI 10.1186/s12861-014-0050-9

BMC Developmental Biology

METHODOLOGY ARTICLE Open Access

Novel monoclonal antibodies to study tissue regeneration in planarians

Kelly G Ross[1], Kerilyn C Omuro[1], Matthew R Taylor[1], Roma K Munday[1], Amy Hubert[1,3], Ryan S King[2,4] and Ricardo M Zayas[1*]

Abstract

Background: Planarians are an attractive model organism for studying stem cell-based regeneration due to their ability to replace all of their tissues from a population of adult stem cells. The molecular toolkit for planarian studies currently includes the ability to study gene function using RNA interference (RNAi) and observe gene expression via *in situ* hybridizations. However, there are few antibodies available to visualize protein expression, which would greatly enhance analysis of RNAi experiments as well as allow further characterization of planarian cell populations using immunocytochemistry and other immunological techniques. Thus, additional, easy-to-use, and widely available monoclonal antibodies would be advantageous to study regeneration in planarians.

Results: We have created seven monoclonal antibodies by inoculating mice with formaldehyde-fixed cells isolated from dissociated 3-day regeneration blastemas. These monoclonal antibodies can be used to label muscle fibers, axonal projections in the central and peripheral nervous systems, two populations of intestinal cells, ciliated cells, a subset of neoblast progeny, and discrete cells within the central nervous system as well as the regeneration blastema. We have tested these antibodies using eight variations of a formaldehyde-based fixation protocol and determined reliable protocols for immunolabeling whole planarians with each antibody. We found that labeling efficiency for each antibody varies greatly depending on the addition or removal of tissue processing steps that are used for *in situ* hybridization or immunolabeling techniques. Our experiments show that a subset of the antibodies can be used alongside markers commonly used in planarian research, including anti-SYNAPSIN and anti-SMEDWI, or following whole-mount *in situ* hybridization experiments.

Conclusions: The monoclonal antibodies described in this paper will be a valuable resource for planarian research. These antibodies have the potential to be used to better understand planarian biology and to characterize phenotypes following RNAi experiments. In addition, we present alterations to fixation protocols and demonstrate how these changes can increase the labeling efficiencies of antibodies used to stain whole planarians.

Keywords: Planaria, Regeneration, *Schmidtea mediterranea*, Monoclonal antibodies, Immunostaining, Immunohistochemistry

Background

Planarians, free-living flatworms with an extraordinary ability to regenerate, are regarded as an excellent model system for regenerative studies. These animals possess the ability to regenerate an entire organism from small body fragments from a population of adult stem cells (neoblasts) [1-3]. Recently, single neoblast transplantation experiments demonstrated that a subset of these cells (clonogenic neoblasts) are truly pluripotent and can differentiate into any planarian cell type or tissue lost by amputation, injury, or normal physiological turnover [4].

Planarians have several distinct major organ systems (illustrated in Figure 1A). They possess a centralized nervous system (CNS), consisting of bi-lobed cephalic ganglia, a brain-like structure located at the anterior end of the animal, connected to two longitudinal ventral nerve cords (VNC) that project posteriorly along the length of the worm [5-7]. The majority of planarians' light detection is achieved by their photoreceptors, which are rich in photosensitive pigment cells and

* Correspondence: rzayas@mail.sdsu.edu
[1]Department of Biology, San Diego State University, San Diego, CA 92182, USA
Full list of author information is available at the end of the article

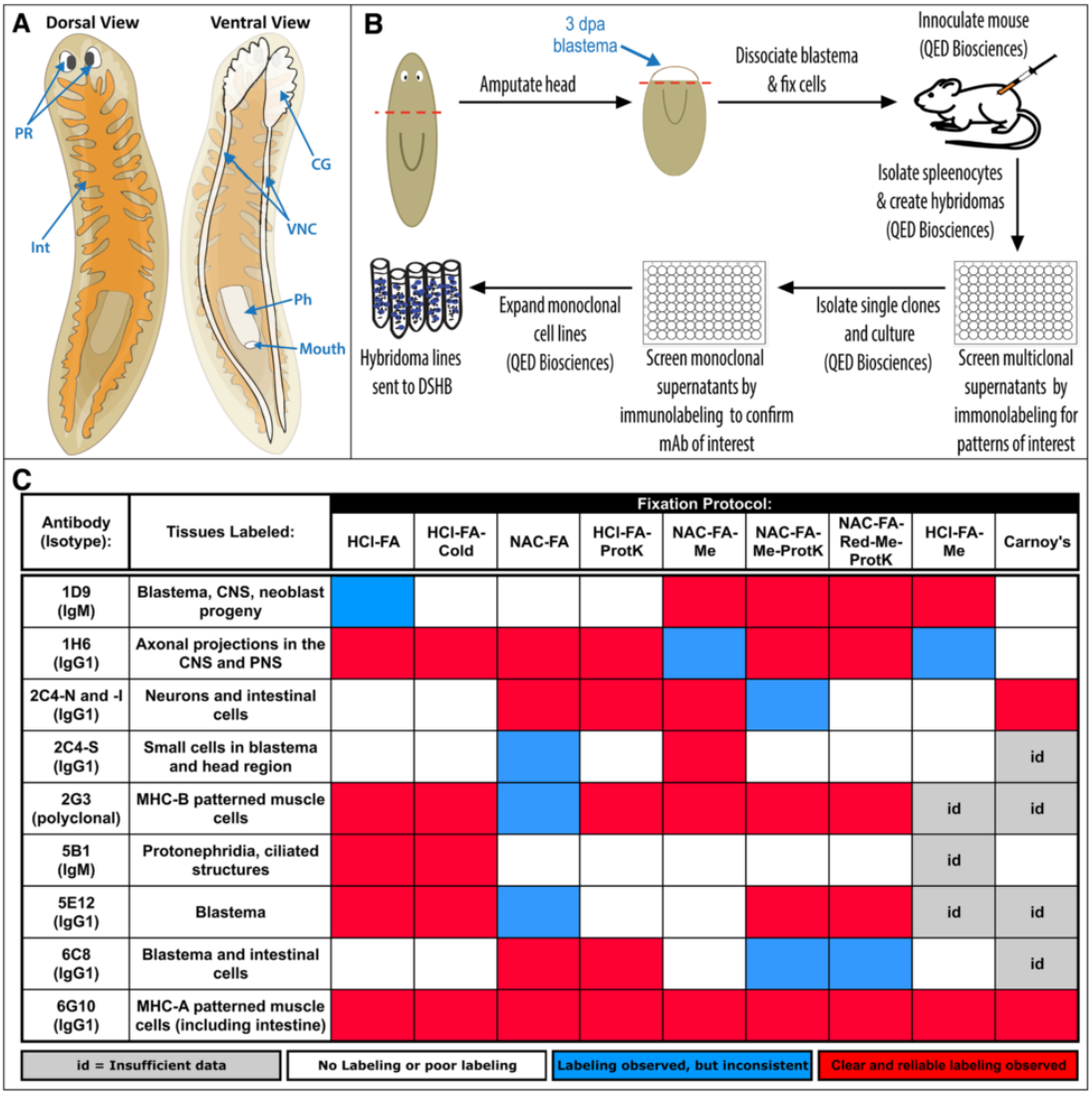

Figure 1 Overview of the basic anatomy of asexual *Schmidtea mediterranea* recognized by the monoclonal antibodies generated in this study and tissue fixation protocols tested. (A) Cartoon of the basic anatomy of asexual *S. mediterranea* with arrows highlighting some of the major organs labeled with the monoclonal antibodies generated in this study. PR, photoreceptors; Int, intestine; CG, cephalic ganglia; VNC, ventral nerve cords; Ph, pharynx. **(B)** Summary of the creation of the monoclonal antibodies used in the subsequent experiments. dpa: days post amputation. **(C)** A heat map summarizing the labeling efficiency for each antibody following eight variations of a formaldehyde-based fixation protocol or Carnoy's fixation. For each fixation and antibody, at least 2 experiments were performed with ≥ 4 worms, which were scored independently by 2 or more individuals. The fixation protocols are named according to the reagents used for each processing step. HCl, hydrochloric acid; FA, formaldehyde; ProtK, Proteinase-K; NAC, N-Acetyl Cysteine; Me, methanol; Red, reduction solution.

photoreceptor neurons that are located on the anterior dorsal surface of the head [8]. Planarians possess a blind digestive system (also referred to as the gastrovascular system) that consists of a pharynx, through which they ingest food and defecate, connected to three primary intestinal branches that distribute nutrients [9-12]. They excrete soluble waste and maintain osmoregularity with their protonephridial systems, tubular structures that extend to the exterior of the animals and are analogous to the vertebrate kidney [13-15]. Thus, we can use planarians to study how defined organ systems are regenerated from adult stem cells.

There have been many great advances in the past decade in identifying and optimizing tools to study the molecular basis of planarian regeneration. Gene expression can be inhibited using RNA interference (RNAi), which allows the study of gene function [16]. Genomic sequencing of *Schmidtea mediterranea* and the availability of multiple transcriptomes combined with custom microarrays or mRNA sequencing have facilitated identification of genes involved in the regeneration of planarian organ systems (recently reviewed in [17]). Whole-mount *in situ* hybridization protocols have been developed and optimized for the visualization of gene expression in planarians [16,18,19]; this information can be coupled with functional analyses to determine the role specific genes play in tissue regeneration. Further, fluorescent lectins have been utilized to label several cell types in planarians, including secretory cells and the reproductive organs of hermaphroditic strains [20,21]. However, there is a dearth of cell-type and tissue-specific antibodies to examine the effects of experimental manipulation in planarians. Available antibodies known to label tissues in *S. mediterranea* include a handful of antibodies created against well-conserved antigens in other species, such as anti-Phospho-Tyrosine (used in planarian studies to label the gut and central nervous system) [22,23], anti-Tubulin, which recognizes ciliated epithelium and neurons [24], and anti-Acetylated Tubulin can be used to visualize ciliated structures, including protonephridia [16,25]. Cebrià *et al.* [6] identified five antibodies (anti-SYNAPSIN, anti-5HT, anti-allatostatin, anti-GYRFamide, and anti-neuropeptide F) that cross-react with neurons in the CNS of *S. mediterranea* [6]. A small selection of monoclonal and polyclonal antibodies have been created against *S. mediterranea* antigens such as anti-SMEDWI, which labels planarian stem cells and their progeny [23]. TMUS-13, originally generated against *Dugesia tigrina* [26], has since been used to label the musculature in *S. mediterranea* [16], and monoclonal antibodies that recognize plasma membrane proteins on subsets of cells within X-ray sensitive and insensitive populations have also been created [27].

Additional antibodies will be useful to further characterize the cellular diversity found within planarian tissues, to track differentiation of planarian cell types, and to expand our understanding of the distribution and dynamics of tissue repair and replacement following wounding events. Discovery of cell surface markers would allow for sorting of specific cell populations, enabling the analysis of gene expression profiles for defined cell populations like the transcriptional profiles available for the heterogeneous irradiation sensitive populations, X1 (highly enriched for cycling neoblasts) and X2 (enriched for progenitor cells) [28,29]. Finally, it would be advantageous to have additional markers available for analyzing regeneration phenotypes following RNAi experiments.

Here, we report on the generation of monoclonal antibodies that recognize tissues in *S. mediterranea*. These antibodies were created by inoculating mice with formaldehyde-fixed cells derived from 3-day head blastemas. We tested the utility of these reagents for immunocytochemistry using multiple fixation protocols on intact and regenerating planarians and determined the optimal conditions for each antibody in asexual *S. mediterranea*. We describe this new set of markers and their staining patterns in muscle, neural structures, ciliated structures (including protonephridia), intestinal cells, and stem cell progeny. These antibodies are currently available to the community through the Developmental Studies Hybridoma Bank (DSHB).

Results and discussion

To generate monoclonal antibodies (mAbs) that label planarian neoblast progeny and differentiated cell populations, we isolated cells from regeneration blastemas. Planarians were amputated pre-pharyngeally, and trunk fragments were allowed to initiate regeneration of a new head. At 3 days post-amputation (dpa), regeneration blastemas were isolated by transverse cutting, dissociated into single cells, fixed with formaldehyde, and used to inoculate mice to create hybridoma lines (see Methods and Figure 1B). We tested supernatants from 576 hybridoma lines by immunostaining intact and regenerating planarians; 236 supernatants were positive for staining in 3 dpa regeneration blastemas, discrete cell populations, or tissues in formaldehyde-fixed planarians. We selected 126 hybridomas for expansion and retesting. The majority (80%) of these 126 hybridomas were positive for immunostaining in 3 dpa blastemas. Based on the staining patterns, signal and background intensities, 42 lines were chosen for additional expansion and re-screened in planarians, using eight different fixation protocols (Figure 1C; Additional file 1). When retested, 33 of 42 were positive, and 17 were selected for hybridoma sub-cloning. Seven monoclonal hybridoma cell-lines and one polyclonal antibody were successfully generated (Table 1). Below, we describe the labeling patterns of these antibodies.

Smed-6G10 and -2G3 label planarian musculature

Planarians have a subepidermal muscle wall that consists of four layers of muscle fibers: circular, longitudinal, diagonal, and a final layer of longitudinal fibers located between two nerve plexuses [10,30,31]. Additionally, there are abundant fibers traversing the parenchyma along the dorsoventral axis, muscle fibers surrounding the intestine, pharynx, and the mouth, and some transverse muscle fibers associated with the intestine [10,32,33].

Table 1 Summary of monoclonal antibodies generated from selected hybridoma cell lines

Parental hybridoma	Clone at DSHB	Isotype	Dilution factor	Concentration of DSHB supernatant tested (μg/ml)	Tissues labeled
1D9	E11	IgM kappa	500	34	Blastema, brain primordia, neoblast progeny
1H6	E9	IgG1 kappa	1000	54	Axonal projections in CNS and PNS
2C4	C2	IgG1 kappa	1000	26	Blastema, neurons, intestinal cells, anterior cells
2G3 (polyclonal)	N/A	N/A	Undiluted	N/A	Muscle fibers
5B1	E6	IgM kappa	1000	18	Protonephria, ciliated structures
5E12	E3	IgG1 kappa	1000	35	Blastema
6C8	A2	IgG1 kappa	1000	26	Blastema, intestinal cells
6G10	2C7	IgG1 kappa	1000	59	Muscle fibers

Smed-6G10 (6G10) and polyclonal antibody Smed-2G3 (2G3) labeled an extensive network of muscle fibers in the planarian body (shown in the planarian head region in Figure 2A). In the muscle wall, we observed strong 6G10 and 2G3 labeling in circular and diagonal muscle fibers (Figure 2B, arrows and closed arrowheads, respectively), and strong 2G3 labeling in longitudinal fibers (Figure 2B, open arrowheads). Interestingly, 6G10 weakly labeled some longitudinal fibers (bottom insets in Figure 2B), whereas a subset of circular fibers marked by 6G10 were weakly labeled with 2G3 (top insets in Figure 2B). In addition, 6G10 labeled the layer of enteric muscles that surrounds the intestine (Figure 2C, arrow) and the transverse fibers near the intestine (Figure 2C, closed arrowhead). By contrast, 2G3 staining was not detected in this muscle population, but was detected in the dorsoventral fibers of the parenchyma (open arrowhead, Figure 2C). This difference was striking in the mouth region where 6G10 marked the pharyngeal muscles; 2G3 labeled circular fibers surrounding the periphery of the mouth but did not label the pharynx (Figure 2D).

The planarian musculature is composed of myocytes that lack striations but match neither the smooth nor striated muscle types. Planarian muscle fibers differ in their composition of myosin heavy chain proteins (MHC-A and -B) [32,34]. The 6G10 and 2G3 staining patterns were similar to those of MHC-A and -B containing muscle fibers, respectively [32,34]. It has been shown that MHC-A containing muscle fibers are found in the pharynx, enteric muscles, and the circular and diagonal muscle wall fibers in *Dugesia japonica*, similar to what we observed in *S. mediterranea* labeled with 6G10 (Figure 2B-D). By contrast, MHC-B containing muscle fibers are located in body-wall muscles and dorsoventral fibers, but not in enteric muscle fibers [32], which correlates with 2G3 labeling. Similar to MHC-A and -B proteins, our data suggest 6G10 and 2G3 recognize differentially expressed proteins in muscle.

Smed-1H6 marks axonal projections in the nervous system

Smed-1H6 (1H6) labeled the axonal projections in subsets of cells in both the central and peripheral nervous systems. In the CNS, 1H6 labeled the ventral nerve cords (VNCs) (Figure 3A, closed arrowheads), which are known to extend anteriorly through the head region, beneath the cephalic ganglia [35]. $1H6^{+}$ projections were observed in the anterior tip of the VNCs (Figure 3A and 3B, arrows). 1H6 also labeled the transverse axon branches between the VNCs and the lateral axon branches extending from the VNCs (Figure 3A, open arrowheads). We observed 1H6 labeling in the lateral branches of the cephalic ganglia (Figure 3B, arrowhead); these axon projections are known to extend to the sides of the head where they penetrate the epidermis in sensory neuron-rich areas [36,37]. To confirm 1H6 labeling in these branches, we processed planarians for 1H6 immunolabeling and *in situ* hybridization to *G protein α-subunit* (*gpas*), which marks distal lateral branch neurons [7]. We found that 1H6 strongly co-labeled with *gpas* (arrowheads in Figure 3C), suggesting that 1H6 binds an antigen found in the axonal projections of sensory neurons.

Our initial observations were that 1H6 did not label the neuropil region of the cephalic ganglia; thus, we co-stained 1H6-labeled planarians with the pan-neural antibody anti-SYNAPSIN [6]. We found that while 1H6 labeling corresponded with SYNAPSIN expression along many neural projections throughout the nervous system (Figure 3D; arrows in Figure 3E) 1H6 labeling was absent in the SYNAPSIN-dense neuropil of the cephalic ganglia (Figure 3F, arrowheads).

Axons labeled with 1H6 partially overlapped with neural projections that were positive for anti-Collapsin Response Mediator Protein 2 (anti-CRMP2) throughout the body (examples in the head region are highlighted with arrowheads in Figure 3G). CRMP2 is a cytosolic phosphoprotein found across the metazoans with high expression during neural development and retained expression in mature neurons, and is implicated in neurite

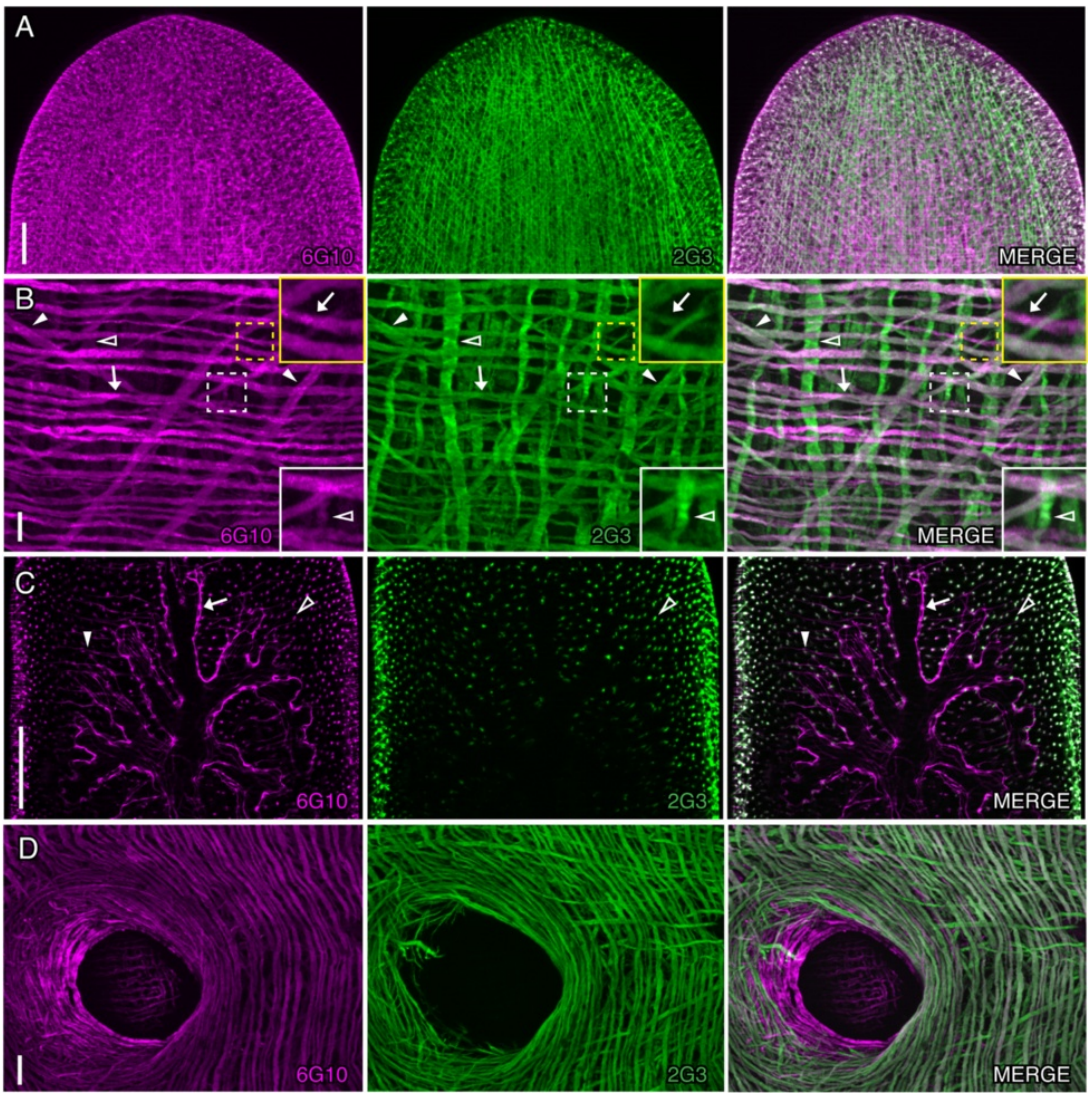

Figure 2 Smed-6G10 and -2G3 label different populations of muscle fibers. (A-D) Whole-mount immunostaining of intact planarians with 6G10 (magenta) and 2G3 (green). **(A)** 6G10 and 2G3 staining in the head region of the animal showing partial co-labeling. **(B)** 6G10 predominantly labels the circular and diagonal fibers, whereas 2G3 strongly labels circular, longitudinal, and diagonal fibers in the body wall musculature. Arrows indicate circular fibers. Closed arrowheads mark diagonal fibers. Open arrowheads highlight an example of a longitudinal fiber weakly labeled with 6G10. Insets show zoomed in regions marked by dashed white and yellow boxes. **(C)** Image of the anterior intestinal branches showing that 6G10 labels the intestinal musculature and transverse muscle fibers (marked by arrows and closed arrowheads, respectively). Open arrowhead highlights a transverse fiber in the parenchyma, which is co-labeled by 6G10 and 2G3. **(D)** 6G10 labels the circular muscle fibers of the body wall, mouth, and the pharynx; 2G3 labels circular, longitudinal, and diagonal fibers and the exterior portion of the mouth. Images are maximum intensity projections of optical sections. Anterior of the animal is to the top in **A**-**C**, and to the left in **D**. Scale bars: **(A, D)** 100 μm; **(B, D)** 10 μm.

outgrowth, synaptic assembly, calcium channel regulation, and neurotransmitter release [38]. We found that a commercially available antibody designed against human CRMP2 marked neurons throughout the planarian CNS and peripheral nervous system (PNS, both cell bodies and projections) and recently reported that CRMP2^{+} neurons co-label with the neural markers β-TUBULIN and *choline acetyltransferase* (*ChAT*) [39]. Additionally,

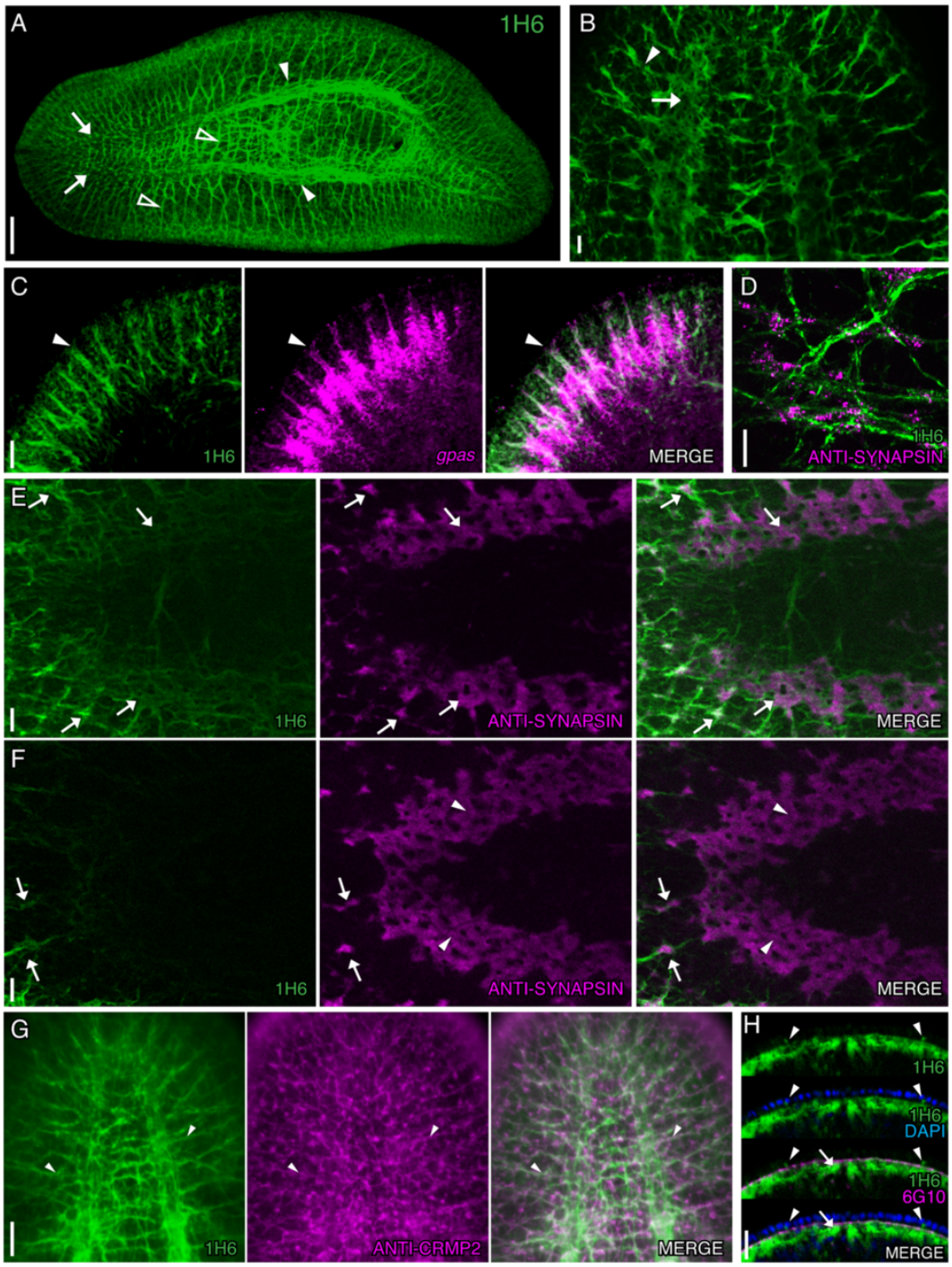

Figure 3 (See legend on next page.)

(See figure on previous page.)
Figure 3 Smed-1H6 labels CNS and PNS axonal projections. (A-F) Whole-mount view of intact planarians immunostained with 1H6 (green) in conjunction with other antibodies or FISH to genes indicated in the panels. **(A)** 1H6 labels neural structures in the intact planarian. Arrows mark the anterior end of the ventral nerve cords (VNCs); closed arrowheads mark the VNCs near the pharynx. Open arrowheads highlight transverse and lateral axon branches. **(B)** Higher magnification image of 1H6 staining in the head region shows labeling in the anterior end of the VNCs (arrow) and in lateral branches (arrowhead). **(C)** 1H6 labels *gpas*$^+$ (magenta) brain branches in the head. Arrowheads denote one of the co-labeled branches. **(D-F)** Planarians double-labeled with1H6 and anti-SYNAPSIN (magenta). **(D)** High magnification shows that 1H6 labels neuronal projections in close association with SYNAPSIN$^+$ synapses. **(E)** Co-labeling in the anterior region of the VNCs. **(F)** 1H6 staining is absent in the neuropil of the cephalic ganglia. Arrows point to examples of 1H6 and anti-SYNAPSIN co-labeling, whereas arrowheads (in **F**) mark the SYNAPSIN$^+$ neuropil of the cephalic ganglia. **(G)** 1H6 labels many CRMP2$^+$ (magenta) neurons in the intact planarian (shown in the head region, highlighted with arrowheads). **(H)** 1H6, 6G10 (magenta), and DAPI (blue, epidermal nuclei) labeling at the anterior tip of the worm demonstrates that 1H6 labels axon projections within the submuscular plexus. Arrowheads mark 1H6$^+$ axons extending between epithelial cells. Images are maximum intensity projections of optical sections, except in **A**. Anterior is to the left in **A**, **E**, and **F** and to the top in **B**-**D** and **G**-**H**. Images were taken to the right side of the pharynx (facing the ventral side of the animal) in **D** and to the left side of the cephalic ganglia in **C**. Scale bars: **(A)** 200 μm; **(B-G)** 20 μm; **(H)** 50 μm.

we observed that some 1H6$^+$ cells were positive for *prohormone convertase 2* (*pc2*; arrowheads in Additional file 2: Figure S1); *pc2*, which encodes a protease that is essential for processing neuropeptide precursor proteins to their mature forms, is found in a subset of cells throughout the planarian nervous system [5,40].

Planarians are enveloped with a monolayer of ciliated epithelium, beneath which lies a thin (0.1-0.2 μm) nerve net, referred to as the subepidermal nerve plexus [10,41]. The fibers in this plexus extend through the basement membrane of the epidermal layer, forming intra-epithelial fibers [41]. Proximal to the subepidermal plexus lies the muscle wall, followed by a submuscular nerve net (submuscular nerve plexus) [41]. These plexuses are part of the peripheral nervous system in planarians [41]. To determine if these plexuses contained 1H6$^+$ projections, we co-stained 1H6-labeled planarians with 6G10 and DAPI to label the contractile muscle layer and visualize the epithelial nuclei, respectively. 1H6$^+$ fibers were seen in the submuscular plexus (Figure 3H, arrows) and in projections extending between epithelial cells (arrowheads in Figure 3H). To resolve labeling in the subepidermal plexus, we observed 1H6-labeled planarians from the ventral surface through the submuscular plexus at 0.44 μm intervals. We noted projections extending between and past the epithelial nuclei (Additional file 3: Figure S2, 0.44 μm to 4.40 μm) and sparse mesh-like fibers as the epithelial nuclei disappeared from the field-of-view (4.84 μm and 5.28 μm in Additional file 3: Figure S2) indicating labeling of the subepidermal plexus. 1H6$^+$ fibers projected through the muscle layers, etching a pattern in the negative impressions of the muscle fibers: circular, longitudinal, diagonal, and finally the last layer of longitudinal fibers of the muscle wall (seen from 5.28 μm to 9.68 μm in Additional file 3: Figure S2). The thicker, more clearly defined meshwork of the submuscular plexus was detected below the final muscle layer (shown from 10.12 μm through 11.88 μm in Additional file 3: Figure S2). It will be interesting to identify the epitope recognized by 1H6 to resolve if it labels a subpopulation of neurons in the central and peripheral nervous systems or a specific cellular compartment found in most neurons.

Smed-2C4 is expressed in discrete cells in the regeneration blastema and a subset of neurons and intestinal cells

We observed multiple distinct cell morphologies (which we refer to as cell types hereafter) throughout the planarian body that labeled with Smed-2C4 (2C4) (Figure 4A). The first cell type (2C4-S cells) had cytoplasmic 2C4 labeling and small cell bodies approximately 4.4 μm in diameter (N = 123 cells measured from 10 worms). We observed that 2C4-S cells were weakly labeled with 2C4 near the epidermis throughout the intact worm (Figure 4A, closed arrowhead; Additional file 4: Figure S3A, arrows) but strongly labeled within the regeneration blastema (Figure 4B and C). To explore whether these cells were secretory, we performed co-labeling experiments with the lectin wheat germ agglutinin (WGA), which labels a subset of secretory cells [20] and found that 2C4-S cells were not WGA$^+$ (Additional file 4: Figure S3A). In order to determine when the protein recognized by 2C4 is expressed during regeneration, we amputated animals anterior and posterior to the pharynx to analyze the presence of 2C4-S cells during 7 days post-amputation. 2C4$^+$ cells were detected in both the anterior and posterior blastemas at all the timepoints we examined (Figure 4B-C).

The second cell type labeled by 2C4 consisted of ventrally located oblong cells (2C4-N cells) of approximately 10.7 μm in diameter (N = 58 cells measured from 9 worms through the longest path of the cell body) (Figure 4A, open arrowhead; Figure 4D, arrows). These cells have bipolar projections and resemble the large multipolar neurons observed in flatworms using silver nitrate staining and Lucifer Yellow dye [42,43]. The projections from these cells extend both laterally and longitudinally (arrowheads in Figure 4D). We found that 2C4-N cells were located on the ventral side of the planarian, excluding the head region (Figure 4A, open arrowhead). Similar to 2C4-S cells, these cells did not co-label with WGA (Additional file 4: Figure S3B.) Based on

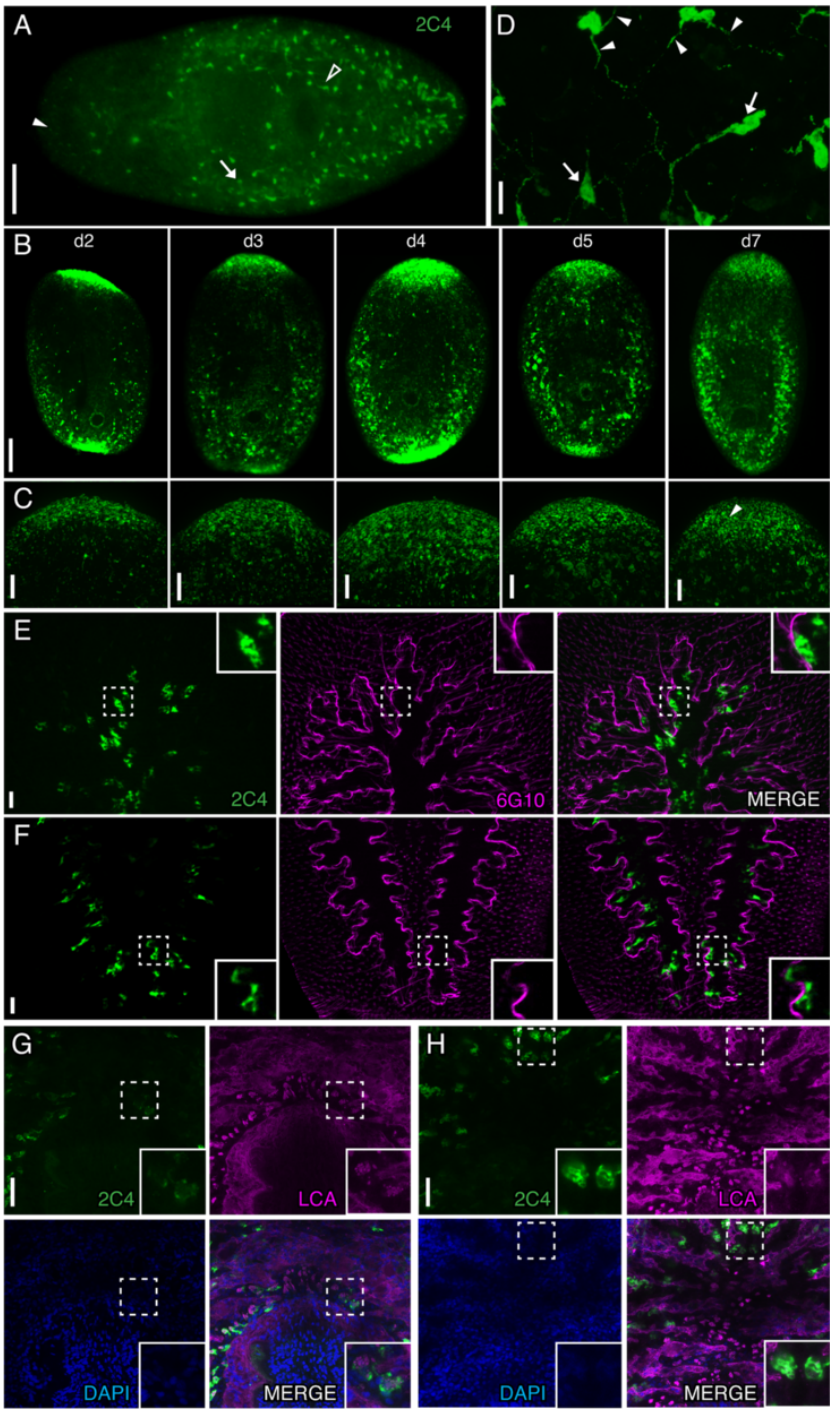

Figure 4 (See legend on next page.)

(See figure on previous page.)
Figure 4 Smed-2C4 labels multiple cells with distinct morphologies and anatomical locations. (A-F) Whole-mount staining of intact planarians or regenerating planarians with 2C4 (green) and with either 6G10 (magenta) in panels **E** and **F** or *Lens culinaris* agglutinin lectin (LCA, magenta) in panels **G** and **H**. **(A)** 2C4 labels multiple distinct cell types in the intact worm. Closed arrowhead indicates an example of a 2C4-S cell. Open arrowhead highlights a 2C4-N cell. Arrow indicates a large round 2C4-I cell. **(B, C)** 2C4 labels the anterior and posterior blastema during regeneration in 2, 3, 4, 5, and 7 dpa trunk regenerates. Higher magnification images of the anterior blastemas are shown in **C**. Arrowhead highlights an example of the 2C4-S cells seen throughout regeneration. **(D)** Magnified image of 2C4-N cells. Arrows denote the large cell bodies and arrowheads indicate their projections. **(E, F)** 2C4-I cells are located within the anterior (shown in **E**) and posterior (shown in **F**) intestinal branches (delineated by labeling of the intestinal wall musculature with 6G10). **(G, H)** 2C4 is expressed in a subset of goblet cells marked with LCA. Strongly labeled LCA^+ cells immediately anterior to the pharynx were weakly labeled with 2C4 (shown in **G**). In contrast, strongly labeled 2C4 cells in anterior secondary branches were weakly labeled with LCA (shown in **H**). Dashed boxes in **E**-**G** indicate the areas shown in the inset images. Images are maximum intensity projections of optical sections except for **A** and **B**. Anterior is to the left in **A** and to the top in **B**-**G**. Image **D** was acquired adjacent to the pharynx. Scale bars: **(A, B)** 200 μm; **(C, E-H)** 50 μm; **(D)** 20 μm.

morphology and their large size, we hypothesize that 2C4-N cells are likely neurosecretory cells. Future experiments should test if 2C4 co-labels cells expressing neuropeptide genes in planarians [40].

The third cell type observed with 2C4 labeling was a large 18.4 μm in diameter (N = 83 cells measured from 10 animals) round cell with large cytoplasm that appeared to be located in or near the intestine (2C4-I cell, arrows in Figure 4A; insets in Figures 4E-F). To determine the relative location of these cells, we co-labeled 2C4-stained planarians with 6G10 to visualize the enteric muscles, which serve as a boundary between the intestinal epithelium and the mesenchyme (as described in [11]). We found that 2C4-I cells were located within the anterior and posterior branches of the intestine (Figure 4E- F). We further explored the identity of these cells by performing co-labeling experiments with the lectin *Lens culinaris* agglutinin (LCA), which labels goblet cells [20]. We found that a subset of 2C4-I cells were indeed LCA^+ goblet cells (Figure 4G). Strikingly, we found that 2C4-I^+ cells in the secondary and tertiary intestinal branches had fainter LCA expression (Figure 4H, inset), whereas the goblet cells with strongest LCA expression anterior to the pharynx were weakly positive for 2C4 (Figure 4G, inset). Because 2C4 labels large neuronal cells surrounding the pharynx and cells within the intestine, the protein that 2C4 recognizes may be highly expressed in cells involved in secretion; however, this question will only be definitively answered upon identification of the 2C4 epitope.

We found that 2C4 labeling was highly dependent on the fixation protocol used (Figure 1C). Whereas 2C4-I and -N cells could be seen with a multitude of fixation protocols, labeling of 2C4-S cells within the blastema was absent or very difficult to detect in fixations using HCl for the initial kill step or with inclusion of Proteinase K treatment.

Smed-5B1 marks ciliated cells

Staining planarians with Smed-5B1 (5B1) revealed a pattern strikingly similar to those observed with anti-Acetylated Tubulin and *in situ* hybridizations against protonephridial markers (arrowheads in Figure 5A) [14,15]. The planarian protonephridial system, analogous to the metanephridial systems found in vertebrates [44], maintains osmoregularity and excretes waste. Protonephridia in planaria consist of fenestrated, ciliated flame cells, which connect to tubules that are ciliated proximal to the flame cells and are non-ciliated distal to the flame cells [14,15]. Protonephridia are located along the majority of the length of the planarian body. Anti-Acetylated Tubulin labels the flame cells and ciliated tubules of protonephridia as well as all other ciliated structures in planarians [25]. Therefore, we tested if 5B1 would co-label with anti-Acetylated Tubulin. We found that 5B1 labeled the tubules of the protonephridia, exterior to the cilia, in a pattern consistent with labeling of the ciliated tubule cells' cytoplasm or membrane (arrows in Figure 5B and C). Labeling was also observed surrounding Acetylated Tubulin labeling at the flame bulb, which is also highly ciliated (arrowheads in Figure 5C). This observation led us to explore whether 5B1 was associated with other ciliated cell types. Planarians have a high abundance of ciliated cells in the epithelium on their ventral surface and in a discrete stripe running along the dorsal anteroposterior axis; these structures are positive for Acetylated Tubulin [24,45,46]. We detected 5B1 labeling within the dorsal ciliated stripe and the ventral ciliated epithelial cell surface (dorsal staining shown as a representative example in Figure 5D).

Smed-1D9 labels the nucleus of a subset of progenitors and cells in close proximity to the central nervous system

Smed-1D9 (1D9) marked cells throughout the mesenchyme and surrounding the cephalic ganglia (Figure 6A, arrows) and VNCs (Figure 6A, arrowheads). Counterstaining with DAPI revealed that 1D9 labeled cell nuclei (Figure 6B, inset). The labeling pattern in the mesenchyme was reminiscent of staining for neoblasts [47] and their early progeny [48]. During our initial screenings, we noted that 1D9 strongly labeled the regeneration blastema; thus, we examined the pattern of 1D9 expression during regeneration. We found that 1D9

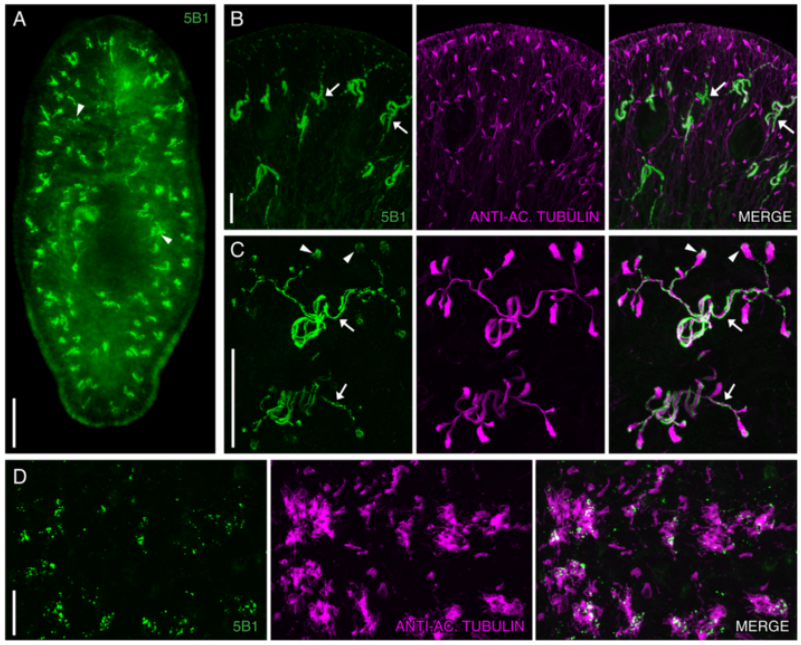

Figure 5 Smed-5B1 labels ciliated cells. (A-C) Whole-mount view of intact planarians immunostained with 5B1 (green), and co-labeled with anti-Acetylated Tubulin (magenta) and DAPI (blue) in panel **B** and anti-Acetylated Tubulin (magenta) in **C**. **(A)** 5B1 labels protonephridial tubules. Arrowheads indicate examples of protonephridia. **(B)** Image of the head region showing that 5B1 labels the protonephridial tubules that are positive for Acetylated Tubulin. Arrows show examples of protonephridia tubules. **(C)** A higher magnification image of protonephridia. Arrows point to examples of 5B1-labeled tubules. Arrowheads show examples of 5B1 labeling in flame cells. **(D)** 5B1is shown to label in immediate proximity to anti-Acetylated Tubulin in the dorsal ciliated stripe. Images are maximum intensity projections of optical sections except for in **A**. The anterior of the animal is to the top in **A** and **B** and to the left in **D**. Scale bars: **(A)** 200 μm; **(B, C)** 50 μm; **(D)** 20 μm.

labeled the blastema at 2 dpa through one week of regeneration in a pattern reminiscent of the nascent cephalic ganglia (arrowheads in Figure 6C and 6D), although we do not think the staining is exclusively in neurons. Co-labeling with additional markers will be necessary to confirm which cell types label with 1D9 during regeneration.

The neoblast and progenitor-like labeling pattern and the presence of $1D9^+$ cells in the regeneration blastema led us to explore the possibility that 1D9 labels either neoblasts or progenitors. To test this, we performed co-labeling experiments with 1D9 and anti-SMEDWI, which labels both neoblasts and their progeny [23]. We first examined the region near the cephalic ganglia in the intact worm and detected many co-labeled cells (inset in Figure 6E). Next, we inspected the animals for co-labeling in the mesenchyme, immediately posterior to the pharynx, which is rich in neoblasts. Intriguingly, we observed that fewer $SMEDWI^+$ cells co-labeled with 1D9 in this region and also noticed that the levels of 1D9 expression were lower when compared with double-labeled cells proximal to the cephalic ganglia (Figure 6F, N = 6 animals). Further experimentation and quantitative analysis will be required to resolve the differential expression of 1D9 throughout the animal. The expression of genes known to play roles in neural differentiation has been observed in both differentiated cells and their progenitors [49-51]. Therefore, we hypothesize that 1D9 recognizes a protein present in progenitors and cells associated with the nervous system.

Smed-6C8 is expressed in cells within the planarian intestine and the regeneration blastema

Smed-6C8 (6C8) labeled cells in a punctate pattern throughout the planarian body that resembled the shape of the intestinal branches (Figure 7A). Therefore, we performed co-labeling experiments with 6G10 to visualize the enteric musculature and determine if 6C8 marks intestinal cells. These experiments showed that $6C8^+$ cells were generally located on the luminal side of the enteric muscle wall in both the anterior and posterior of the animal (Figures 7B and C). However, some $6C8^+$ cells were detected outside, but still associated with the enteric muscular boundary (arrowheads in Figures 7B and C; Additional file 5: Figure S4).

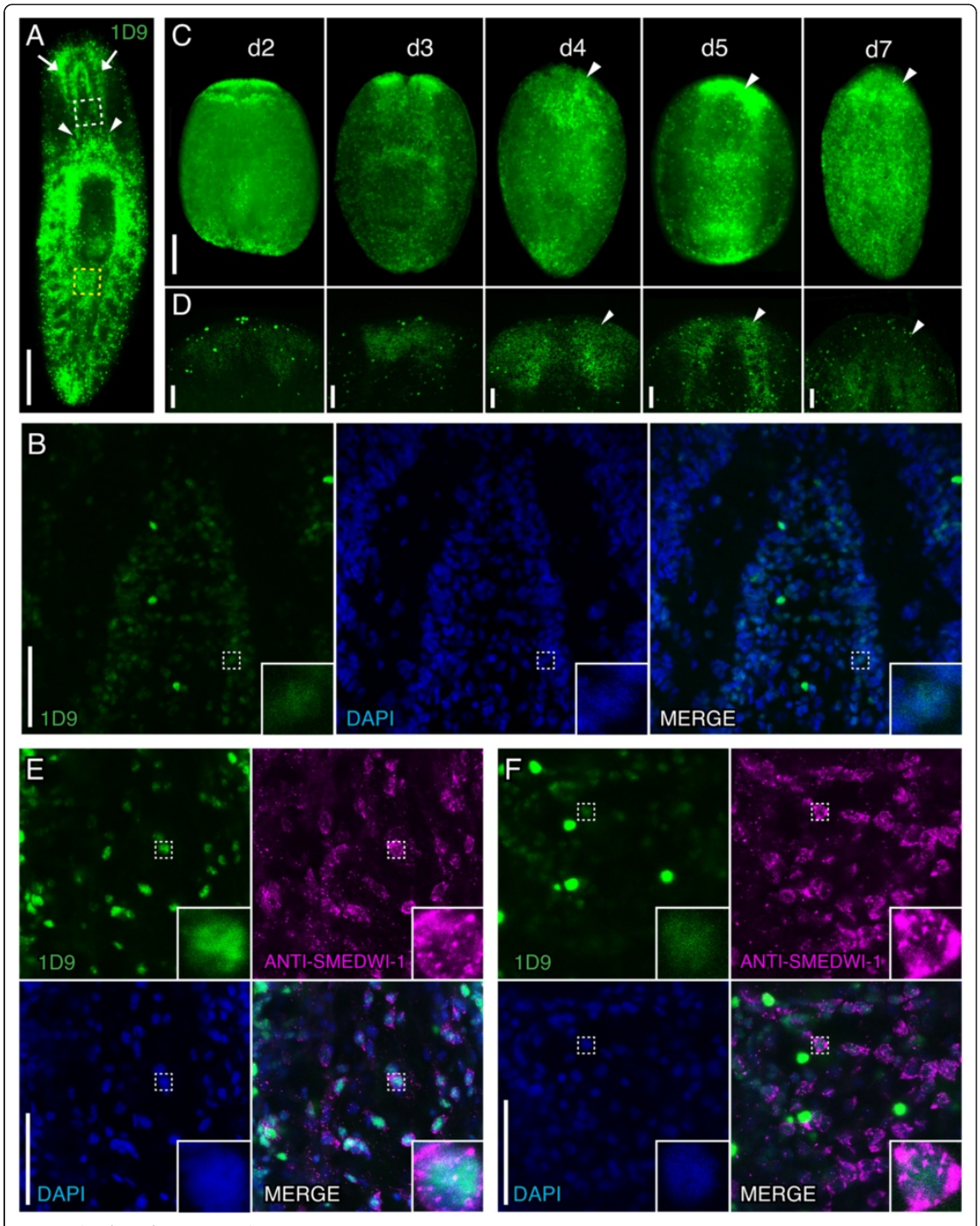

Figure 6 (See legend on next page.)

(See figure on previous page.)
Figure 6 Smed-1D9 labels the CNS and neoblast progeny. (A-D) Whole-mount view of intact planarians or regenerating planarians immunostained with 1D9 (green), and counterstained with DAPI (blue) in **B** and stained with anti-SMEDWI (magenta) in **E**-**F**. **(A)** 1D9 staining in the intact planarian reveals labeling surrounding the cephalic ganglia (arrows) and ventral nerve cords (arrowheads), and in the mesenchyme. Dashed boxes indicate the regions shown in **E** (white), and **F** (yellow). **(B)** Higher magnification image of the cephalic ganglia demonstrates that 1D9 labels the nucleus (counterstained with DAPI). **(C, D)** 1D9 labels the anterior and posterior blastema during regeneration in 2, 3, 4, 5, and 7 dpa trunk regenerates. The morphology of the nascent cephalic ganglia is apparent by 4 dpa (indicated by arrowheads). **(D)** View of the anterior regeneration blastema. **(E)** Image of the area proximal to the posterior end of the cephalic ganglia in an intact planarian shows a large population of $1D9^+$ cells co-labeled with anti-SMEDWI. **(F)** Image of the area immediately posterior to the pharynx showing the presence of $1D9^+$ cells co-labeled with anti-SMEDWI. Dashed boxes indicate the area shown in the insets. Images are maximum intensity projections of optical sections except for **A** and **C**. Anterior is to the top in all images. Scale bars: **(A)** 200 μm; **(B, D-F)** 50 μm; **(C)** 100 μm.

We counterstained samples with DAPI and found that 6C8 labeling was located in the nucleus of cells (Figure 7D, inset). Because 2C4 also labeled an intestinal cell population, we examined if the 2C4 and 6C8 epitopes were expressed in the same cells or in different cell populations. When we performed co-labeling experiments, we noted that 2C4 and 6C8 marked distinct intestinal cell populations (Additional file 6: Figure S5A). Furthermore, 6C8 was not expressed in LCA^+ goblet cells (Additional file 6: Figure S5B).

Intestinal cells are derived from neoblasts that divide outside of the intestine [11]. Our experiments showed 6C8 labels a cell population adjacent and within the intestinal musculature boundary. Thus, we hypothesized that 6C8 labels cells that are specified to become intestinal cells in the mesenchyme and are in the process of incorporating into the intestinal epithelium. To evaluate this possibility further, we examined 6C8 expression during regeneration. We amputated planarians anterior and posterior to the pharynx and observed 6C8 labeling between 2 and 7 days of regeneration (Figure 7E and 7F). 6C8-labeled cells were difficult to detect or completely absent in 2 dpa regenerates in the blastema and throughout the worm (Figure 7E). In contrast, we readily detected strong expression of 6C8 near the anterior and posterior regeneration blastemas from 3 to 7 dpa (Figure 7E, arrowheads; Figure 7F, insets); we also noted cells with 6C8 expression in a cytoplasmic punctate pattern (insets in Figure 7F). Interestingly, beginning at 4 dpa we observed 6C8 labeling outside of the blastema in a pattern resembling the intestinal branches (arrows in Figure 7E). Extensive remodeling of the intestine is required to restore proper intestinal morphology following amputation [11]. The presence of $6C8^+$ cells within the intestinal musculature boundary and their location during regeneration suggests to us that these cells represent differentiating intestinal cells. This possibility should be tested further with BrdU pulse/chase experiments to determine if $6C8^+$ cells co-label with BrdU within the enteric muscle boundary [11].

Smed-5E12 is strongly expressed in cells in the regeneration blastema

Smed-5E12 (5E12) was not readily detected in intact planarians. We observed a punctate expression pattern in some animals, but this was inconsistent (i.e., the pattern was completely absent from some of the samples). Therefore, it was difficult to discern 5E12 labeling in defined cell types or tissues (Figure 8A). By contrast, when we amputated planarians, fixed, and immunolabeled them at 3 dpa, we observed strong 5E12 labeling in anterior and posterior regeneration blastemas (Figure 8B). To determine the expression of this antibody during the course of regeneration we fixed and stained regenerating trunk fragments at 2–7 dpa and observed 5E12 labeling in the blastema at all the time points tested (Figure 8B, arrowheads). It was interesting to note that expression was seen in a population of cells proximal to the blastema in regenerating animals (highlighted posterior to the 3 dpa anterior regeneration blastema in Figure 8B and C, arrows), suggesting that 5E12 labels a progenitor population. Thus, 5E12 can serve as a marker of the blastema following injury or amputation. It will be interesting to determine if 5E12 can mark the formation of ectopic structures such as generation of supernumerary heads that follow RNAi knockdown of *β-catenin-1* in intact animals [52-54]. In addition, the fixation protocol for this antibody may require further optimization to stain or preserve the epitope in non-injured animals, and additional co-labeling experiments will be needed to investigate the identity of the $5E12^+$ blastema cells.

Visualization of the *slit* RNAi midline collapse phenotype with the newly generated mAbs

As a proof of concept, we revisited the knockdown of *Smed-slit* [55] to test the utility of our new mAbs in characterizing regeneration defects present following RNAi. *Smed-slit* (*slit*) encodes a conserved axon-guidance glycoprotein that has a repellent role at the midline and is necessary for patterning of the major organ systems in

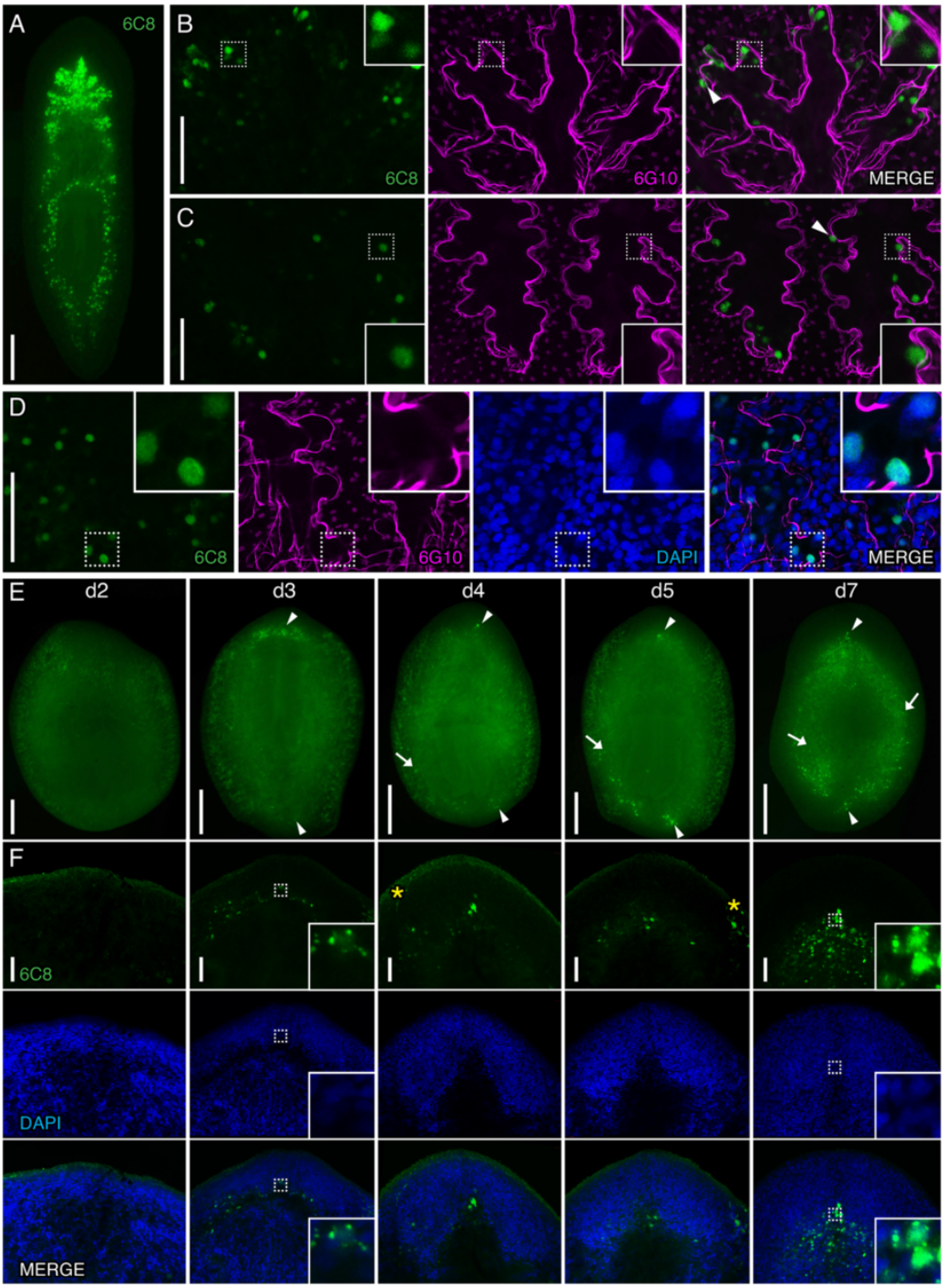

Figure 7 (See legend on next page.)

(See figure on previous page.)
Figure 7 Smed-6C8 labels intestinal cells and cells near the regeneration blastema. (A-C) Whole-mount view of intact or regenerating planarians immunostained with 6C8 (green) and co-labeled with 6G10 (magenta) in panels **B**-**D** and/or counterstained with DAPI (blue) in **D** and **F**. **(A)** 6C8-labeled cells near or within the intestine. **(B, C)** 6C8 cells are located within the anterior (shown in **B**) and posterior (shown in **C**) intestinal branches or in contact with the enteric musculature wall, which is delineated with 6G10 labeling. Examples of cells observed outside the enteric muscle boundary are highlighted with arrowheads. **(D)** 6C8 labels cell nuclei (observed within the boundary of the enteric musculature). **(E, F)** $6C8^+$ cells appear near the anterior and posterior regeneration blastemas at 3 dpa and are detected in the blastema at all later timepoints assayed (examples highlighted with arrowheads). By 5 dpa, examples of $6C8^+$ cells were detected far from the blastemas (arrows). Higher magnification image of the anterior blastema shown in **F**. Yellow asterisks indicate non-specific labeling of secretory cells. Dashed boxes indicate the area of the high magnification image shown in the insets. Images are maximum intensity projections except for **A** and **E**. Anterior of is to the top in all images. Scale bars: **(A, E)** 200 μm; **(B-D, F)** 50 μm.

planarians with respect to distance from the midline [55]. Loss of *slit* by RNAi causes planarians to regenerate mis-patterned VNCs and fused primary intestinal branches in the posterior of the animal [55]. We knocked down *slit,* amputated the animals along the sagittal plane, and labeled regenerates with 6G10 and 1H6 to visualize the intestinal muscle boundary and the VNCs, respectively. We observed widely spaced axonal tracks in the VNCs posterior to the pharynx in all *slit(RNAi)* animals (Figure 9A, arrows) giving the appearance of either the formation of multiple VNCs or a diversion of a subset of VNC axonal tracks from the midline. The VNCs were collapsed at the midline in the posterior of all *slit(RNAi)* animals (Figure 9A, arrowheads), whereas the nerve cords regenerated normally in the control animals. We also observed that the primary intestinal branches in the posterior regions of *slit(RNAi)* animals appeared to be connected (Figure 9B, arrows), unlike those in *gfp*

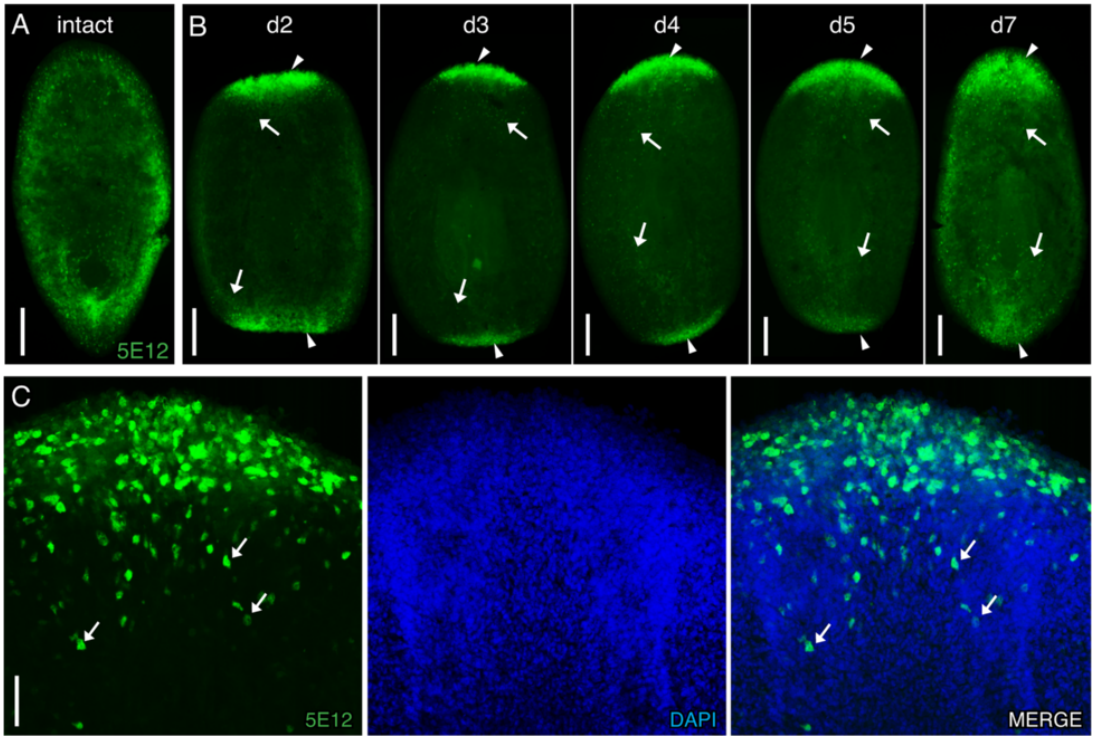

Figure 8 Smed-5E12 labels the regeneration blastema. Whole-mount images of intact or regenerating planarians immunostained with 5E12 (green) and counterstained with DAPI (blue) in panel **B**. **(A)** 5E12-labeled cells detected throughout the body of an intact animal. **(B)** 5E12 labels the anterior and posterior blastemas in regenerating trunk fragments stained over the course of 7 days post-amputation (marked by arrowheads), and cells proximal to the regeneration blastemas or throughout the body (marked by arrows at 2–7 dpa). **(C)** Higher magnification image of $5E12^+$ cells within a 3 dpa regeneration blastema and posterior to the blastema (arrows). Images in **C** are maximum intensity projections of optical sections. Anterior is up in all images. Scale bars: **(A, B)** 200 μm; **(C)** 50 μm.

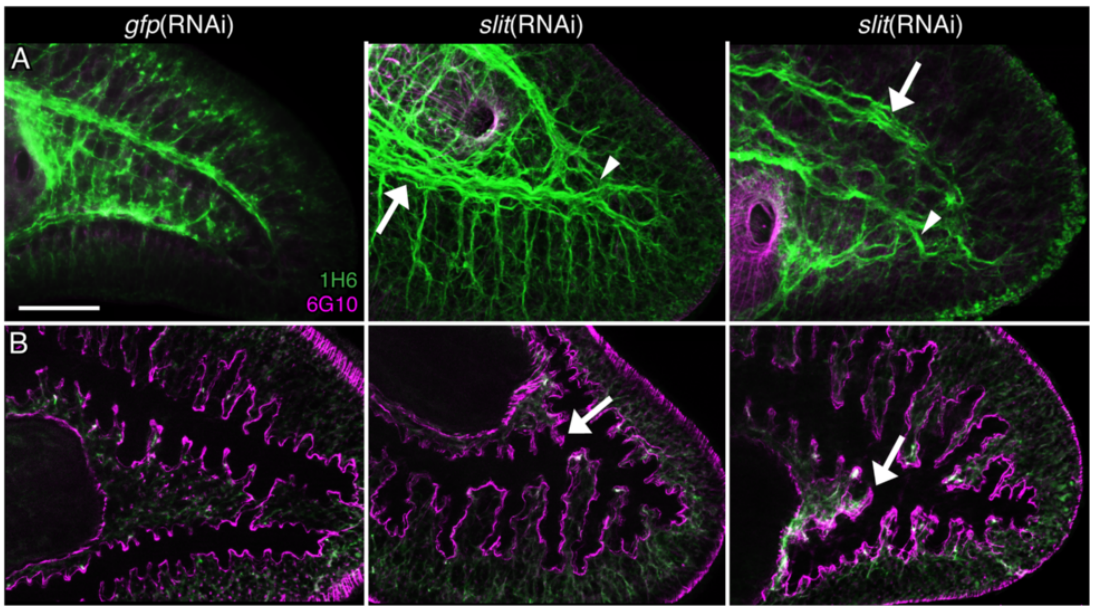

Figure 9 Smed-1H6 and -6G10 co-labeling reveal the complexity of the midline collapse phenotype following slit RNAi. (A-B) Whole-mount view of a planarian bisected sagittally and immunostained 15 dpa with 1H6 (green) and 6G10 (magenta). **(A)** Image of the ventral nerve cords (VNCs) shows *slit(RNAi)* worms with intersecting VNCs (arrowheads, 3/5 *slit(RNAi)*, 0/5 *gfp(RNAi)* animals), as well as *slit(RNAi)* worms with widely spaced VNC tracks (arrows, (5/5 *slit(RNAi)*, 0/5 *gfp(RNAi)* animals). **(B)** Image of the enteric muscles delineating the intestine illustrates fusion of the intestinal branches posterior to the pharynx in *slit(RNAi)* animals (arrows, 5/5 *slit(RNAi)* animals, 1/5 *gfp(RNAi)* animals). Images are maximum intensity projections of optical sections. Anterior is to the left in all images. Scale bar: 200 μm.

(RNAi) animals, which regenerated two posterior primary gut branches. Thus, use of these new mAbs allowed robust visualization of morphological defects present after RNAi.

Conclusions

We have produced new monoclonal antibodies that can be used to study tissue regeneration, structure, and function in planarians. With the exception of polyclonal Smed-2G3, these antibodies were deposited to the Developmental Studies Hybridoma Bank. We have demonstrated that these antibodies label diverse tissues in planarians and can be useful for examining phenotypes following RNAi. In addition, we determined that the labeling efficiency of antibodies used for whole-mount staining of planarians greatly depends on the fixation protocols. Many of the mAbs that we generated did not display any discernable staining pattern when treated with subsets of the reagents used in the eight formaldehyde fixation protocols we tested (Figure 1C). The observation that most of the antibodies do not work well with Carnoy's fixative is likely due to the fact that these antibodies were generated against cells fixed with formaldehyde. Further optimization of these protocols could prove helpful for future experiments that warrant co-labeling with currently incompatible antibodies.

Future studies will examine the epitopes detected by these mAbs, which could potentially increase their usefulness as markers for phenotypic analysis or other applications. It will be interesting to determine if these antibodies label other species of planarians and the hermaphroditic strain of *S. mediterranea.* As an initial test, we performed labeling experiments with three of these antibodies (1H6, 2C4, 6G10) in hermaphrodites. As expected, we found that these mAbs produced the same staining patterns observed in the asexual strain, but with limited penetrance throughout the body and increased background signal (data not shown). Additional modifications to the fixation protocols will be necessary to use the mAbs with larger animals as in previous studies [21,40,56]. In conclusion, these antibodies should help to expand the molecular toolkit available for studies using planarians.

Methods

All experiments involving mice were performed at QED Bioscience Inc. (San Diego, CA) in strict accordance with the policies and guidelines of the Public Health Service Policy on Humane Care and Use of Laboratory

Animals and the Institutional Animal Care and Use Committee (IACUC) of QED Bioscience Inc. (San Diego, CA). Immunizations were performed in accordance with QED Bioscience's IACUC-approved protocol (SOP #22).

Planarian culture

Asexual *Schmidtea mediterranea* (CIW4) were maintained in ultrapure water containing either Instant Ocean (Spectrum brands) at 0.21 g/l, 0.83 mM $MgSO_4$, 0.9 mM $CaCl_2$, 0.04 mM $KHCO_3$, and 0.9 mM $NaHCO_3$, or Montjuïc salts as previously described [22]. Unless otherwise noted, planarians 3–5 mm in length that were starved for at least 5 days were used for all experiments.

Dissociation of cells for immunization

Three days prior to the initial amputation, animals were fed to increase cell proliferation [57]. Animals were amputated anterior to the pharynx, and fragments containing the tail were allowed to regenerate for approximately 3 days and then washed in Calcium Magnesium Free media (CMF) [58], followed by a second wash in CMF with 30 μg/ml trypsin inhibitor (CMF+TI [T9253, Sigma]) prior to amputation immediately posterior to the blastema. The blastemas were collected and incubated in CMF+TI at 4°C for 10 minutes. After removing the CMF+TI, blastemas were diced and transferred into a tube with CMF plus 2 U/ml trypsin (T0303, Sigma) and incubated, while rocking, at 4°C for 1–3 hours (triturated every 30–45 minutes with a transfer pipette). Once the tissues neared complete dissociation, the samples were triturated with a 1000 ml micropipette tip. The cell suspension was spun down at 300 × g at 4°C for 5 minutes, and the pellet was re-suspended in CMF and passed through a 50 μm mesh filter. The cell suspension was centrifuged as above and re-suspended in 4% formaldehyde (FA) for 10 minutes at room temperature, after which the cells were centrifuged at 300 × g for 5 minutes and re-suspended in Phosphate Buffered Saline (PBS). Cell counts were performed on a Petroff-Hausser counter to determine cell density.

Mouse immunizations

Five Balb/c mice were injected a total of 5 times over the course of 7 weeks. The initial immunization and first boost contained a mixture of 5×10^5 fixed cells suspended in 250 μl mixed with 250 μl of a propriety adjuvant (QED Bioscience). All subsequent boost injections contained 5×10^5 cells in PBS. Following all injections, one mouse was selected and its spleen was harvested. Blood sera were collected and tested for cross-reactivity to planarian epitopes after each booster administration using FA-fixed planarians. For these tests, planarians were killed in 2% HCl in PBS for 3 minutes followed by a 4 hour incubation at 4°C in 4% FA in PBSTx (PBS + 0.3% Triton X-100) and bleached overnight in a 6% H_2O_2 solution in PBS. Prior to overnight incubation in blood sera, the worms were blocked for 4 hours in PBSTB (PBSTx + 1% Bovine Serum Albumin [Jackson ImmunoResearch Laboratories]). After extensive washing with PBSTx, worms were blocked again for 1 hour in PBSTB and incubated in Alexa Fluor 488 goat-anti-mouse IgG (1:400 in PBSTB, [A11029, Life Technologies]) overnight at 4°C and then washed again with PBSTx the next day.

Hybridoma screen and antibody production

At QED Bioscience Inc. (San Diego, CA), spleenocytes from the immunized mice were fused with myeloma cells, Species F0 or P3X63Ag8U.1. The resulting hybridomas were expanded and screened to generate a library of polyclonal parental hybridomas. From these parental lines, further expansion and screening allowed generation of monoclonal hybridoma lines producing antibody. Cells were cultured in high glucose-DMEM with sodium pyruvate, supplemented with 2% L-glutamine, 10% FBS and 1% penicillin-streptomycin. For selected monoclonal lines, additional purification of the antibody was carried out. *In vitro* production was performed for the following antibodies: 1D9, 1H6, 2C4, 5E12, and 6G10. The 1D9 and 2C4 antibodies were affinity purified. After the initial testing, the monoclonal cell lines were submitted to the DSHB.

Immunostaining

For all images shown, we performed labeling experiments with at least three worms and visualized similar staining patterns using an optimal fixation protocol for each antibody (see Additional file 1 and summary in Figure 1C) unless variations were made for co-labeling experiments (described below). Fixations for whole-mount immunostaining were optimized using eight modifications to a formaldehyde fixation protocol developed for *in situ* hybridizations [19]. Briefly, animals were killed in either cold 2% HCl or 5% N-acetyl cysteine in PBS for 5 minutes. Animals were then fixed for either 15 minutes at room temperature or 6 hours at 4°C in 4% FA in PBSTx. To enhance possible presentation of epitopes, some protocols added a reducing step (50 mM DTT, 1% NP-40, 0.5% SDS for 5 to 10 minutes at 37°C). Animals were bleached overnight in 6% H_2O_2 diluted either in PBSTx (aqueous) or methanol (anhydrous after stepping through 50% methanol) under direct light. The next morning, if bleaching was performed in methanol, animals were re-introduced into PBSTx through a 50% methanol intermediate and washed with PBSTx. Some protocols included a Proteinase K treatment (2 μg/ml Proteinase K, 0.1% SDS in PBSTx for 10 minutes at room temperature) followed by a post-

fix step in 4% FA for 10 minutes at room temperature. Animals were washed twice with PBSTx before blocking for 4 hours at room temperature in PBSTB. Hybridoma supernatant was either added directly to the samples or diluted in PBSTB and incubated overnight at 4°C. The following day, animals were washed extensively with PBSTx, then blocked in PBSTB for 1 hour before an overnight incubation at 4°C in either goat-anti-mouse IgG+IgM-horse radish peroxidase (HRP) (1:1000 [Life Technologies]) or goat-anti-mouse IgG-HRP (1:1000 [Life Technologies]) in PBSTB. The following day, animals were washed extensively and then incubated in FITC-tyramide (1:1000 in PBSTI [PBSTx + 10 mM imidazole]) for 30 minutes and developed in FITC-tyramide in PBSTI containing 0.015% H_2O_2 for 5 minutes. Alternatively, animals were developed as previously described [18], with the following modifications: animals were incubated for 5 minutes at room temperature in 0.1 M borate buffer, pH 8.5, with 0.1% Tween-20 and then for 10 minutes at room temperature in 0.1 M borate buffer, pH 8.5, with 0.1% Tween-20, 0.003% H_2O_2, 2% dextran sulfate, 1:250 FITC-tyramide. An additional 0.003% H_2O_2 was added and incubated for 10 minutes at room temperature. Animals were then washed extensively with PBSTx. Where indicated in the Results section, worms were counterstained with DAPI (0.05 μg/ml) by including it with the secondary antibody incubation step or subsequent overnight incubation at 4°C.

Double-immunostaining experiments

Immunostaining was carried out as described above, except for the following modifications. To double label planarians with 1H6 and 6G10, the antibodies were detected using either Zenon Alexa Fluor 488, 568, or Zenon HRP IgG1 Labeling Kits (Z-25002, Z-25006, Z-25054, Life Technologies). The ratios of the antibody, kit component A, and kit component B used were 2:1:1; samples were incubated according to manufacturer's instructions. Labeled antibodies were then diluted to 1:250 in PBSTB. Double-labeling with 2C4 and 6C8 was performed as described above for 2C4; then TSA signaling was quenched with 10 μg/ml Proteinase K in PBSTx with 0.1% SDS for 10 minutes at room temperature. Animals were post-fixed in 4% FA for 10 minutes at room temperature, followed by another quenching step performed in 1% H_2O_2 (diluted in PBSTx) for 1 hour at room temperature. Following quenching, worms were rinsed and 6C8 labeling proceeded as described above.

Another modified fix was used to label planarians with anti-Acetylated Tubulin (1:1000 [clone 6-11B-1, Sigma]). Incubation times were shortened to 3 minutes in HCl for the initial kill and 2 hours at 4°C for the FA fixation. Animals were bleached and stained as described above for 5B1 antibody. After development, animals were quenched in Proteinase K and washed, blocked, and incubated in anti-Acetylated Tubulin (1:1000 [Sigma]) overnight at 4°C. The following day, worms were washed extensively and incubated overnight at 4°C in goat-anti-mouse AlexaFluor 568 (1:400 in PBSTB, [A11031, Life Technologies]) followed by additional washes.

For co-labelings with anti-SYNAPSIN (1:400 3C10, DSHB), fixations and bleaching were aqueous and had no Proteinase K treatment. SYNAPSIN labeling was always performed first using goat-anti-mouse AlexaFluor488 secondary antibodies. Following anti-SYNAPSIN labeling, samples were quenched with the Proteinase K and post-fix (as described above) before washing, blocking, and proceeding with immunostainings using the monoclonal antibodies.

Two anti-rabbit primary antibodies were used: anti-CRMP2 (1:50 [9393, Cell Signaling]) and anti-SMEDWI-1 (1:1000 [a kind gift from P. Reddien]); both were visualized with the goat-anti-rabbit Alexa Fluor 568 secondary antibodies. These were combined with the anti-mouse monoclonal primaries during the initial incubation. The secondary antibodies were also combined for incubation; development proceeded as described above.

Co-labeling experiments with Fluorescein labeled wheat germ agglutinin (WGA) or Rhodamine labeled *Lens culinaris* agglutinin (LCA) (Vector Labs) [20] were performed on intact planarians killed in N-acetyl cysteine and fixed in FA (as described in Additional file 1) with the following change: for LCA co-labeling, worms were incubated with either 6C8 or 2C4 at 1:100 dilution and subsequently labeled with goat anti-mouse AF488 at 1:500. Following secondary labeling, the worms were re-blocked for 1 hour in PBSTx with 0.6% BSA and 0.45% fish gelatin (PBSTB+FG) and incubated with WGA ([1 μg/ml [FL-1021, Vector Laboratories, Inc.]) or LCA (5 μg/ml [RL-1042, Vector Laboratories, Inc.]) and diluted in PBSTB+FG overnight at 4°C.

Fluorescent *in situ* hybridization

Riboprobes were synthesized as previously described [19]. Animals were processed using a protocol developed for *in situ* hybridization [18]. Some modifications were made to the protocol: MABTw (Maleic Acid Buffer + 0.1% Tween-20) was used instead of TNTx for washes, and peroxidase inactivation for double-labeling was performed with 1% H_2O_2 in PBSTx for 1 hour instead of azide solution. After peroxidase-inactivation, animals were washed in PBSTx extensively, blocked in PBSTB for 1 hour at room temperature, and then incubated in the antibody overnight. Immunostaining proceeded as described above.

Imaging

Single channel whole animal images were acquired with an Axiocam MRm camera mounted on a Zeiss SteREO Lumar.V12 stereomicroscope equipped with a NeoLumar S 1.5X objective running AxioVision v4.8. Higher magnification images and the whole animal image in Figure 3B were obtained on either a Zeiss Axio Observer.Z1 inverted microscope using an ApoTome for optical sectioning running AxioVision v4.8 or on a Carl Zeiss LSM710 confocal microscope running ZEN 2011 or 2012. Objectives used on the Axio Observer.Z1 were: 40 × 1.3 NA oil immersion objective, 20 × 0.8 NA objective, and 10 × 0.3 NA objective. Objectives used on the LSM710 were: 40 × 1.2 NA water immersion objective, 20 × 0.8 NA objective, or 10 × 0.3 NA objective. Images were processed in Adobe Photoshop CS4, CS6, or ImageJ 1.47f to normalize levels, color, and brightness. 3D reconstruction images were performed using ZEN 2012 software with a Z-stack containing 48 sections at 1 μm intervals.

Cell size measurements

For cell size measurements of 2C4-labeled cells, maximum intensity projections of 20–36 × 0.54 μm slices were collected for analysis in ImageJ. The thickest diameter across the cell body was measured. A minimum of 58 cells was counted from 9 animals for each cell type analyzed.

RNA interference

Animals were fed bacterially-expressed *gfp* or *Smed-slit* [55] double stranded RNA, as previously described [52], 8 times over a 2.5 week period. One day following the final RNAi feeding, animals were bisected along the sagittal plane and allowed to regenerate for 15 days before fixation.

Additional files

Additional file 1: Detailed fixation and staining protocols. This word document contains step-by-step instructions for the fixation/immunostaining protocols for use in the laboratory.

Additional file 2: Figure S1. Smed-1H6 labels neurons found in close association with *pc2*$^+$ cell bodies (magenta). Whole-mount view of intact planarians labeled with 1H6 and processed for *in situ* hybridization to *pc2* (magenta) and counterstained with DAPI (blue). Examples of co-labeled cells are highlighted with arrowheads. Image taken to the right side of the pharynx, facing the ventral side of the worm. Anterior is to the top of the image. Images are maximum intensity projections of optical sections. Scale bar: 20 μm.

Additional file 3: Figure S2. Smed-1H6 labels the subepidermal and submuscular plexuses. Single optical sections taken in the head region of intact planarians labeled with 1H6 (green) and counterstained with DAPI (blue) at 0.44 μm intervals starting on the ventral side of the animal. Depth of each optical section is displayed on each image. Dashed boxes indicate the regions of the inset images, which highlight the mesh-like pattern of 1H6 labeling at the subepidermal plexus in the 4.84-5.28 μm images and 1H6 labeling in the submuscular plexus at 11.00 μm. Anterior is to the left of the images. Scale bar: 20 μm.

Additional file 4: Figure S3. Smed-2C4$^+$ cells are not WGA$^+$. Whole-mount view of intact planarians labeled with 2C4 (green) and wheat germ agglutinin (WGA, magenta) shows 2C4$^+$ cells do not stain with WGA. (A) Image showing 2C4-S cells denoted by arrows. (B) Image of 2C4-N cells, which also lack WGA signal. Images were taken to the right side of the pharynx, facing the ventral side of the worm. Anterior is to the left. Images are maximum intensity projections. Scale bars: 50 μm.

Additional file 5: Figure S4. Images of 6C8-labeled cells in close association with enteric muscular fibers. (A-B) 3-dimensional reconstruction of a Z-stack acquired from planarian enteric musculature labeled with 6G10 (magenta) and 6C8 (green) highlights the 6C8$^+$ cell located outside of the enteric musculature shown in Figure 7C. Dashed boxes indicate the regions of the inset images. (A) View of 6C8-labeled cells from different angles of rotation around the X-axis (numbers in top right corner indicate the degree angle of rotation from the Y-axis). Arrows denote some examples of 6C8$^+$ cells that are clearly on the luminal side of the enteric muscle boundary. (B) Images from angles of rotation around the Y-axis (numbers indicate the degree angle of rotation from the X-axis. Anterior of the animal is to the top in all images. Scale bars: 50 μm.

Additional file 6: Figure S5. Smed-6C8$^+$ cells are not 2C4 or LCA$^+$. (A-B) Whole-mount view of intact planarians labeled with 6C8 (magenta in A, green in B), co-labeled with 2C4 (green) in A, or *Lens culinaris* agglutinin lectin (LCA, magenta) and counterstained with DAPI (blue) in B. (A) Co-staining of 6C8 and 2C4 in the primary anterior branch of the intestine demonstrates that these two antibodies label cell populations that are distinct or at different developmental stages. (B) Co-staining with LCA indicates that 6C8 does not label goblet cells in the intestine (shown in a posterior intestinal branch). The images are maximum intensity projections of optical sections acquired through the tissues described. Anterior is to the top in all images. Scale bars: 50 μm.

Abbreviations

CMF: Calcium magnesium free media; CMF+TI: Calcium magnesium free media plus trypsin inhibitor; CNS: Central nervous system; DMEM: Dulbecco's modified Eagle's medium; dpa: Days post-amputation; DSHB: Developmental Studies Hybridoma Bank; DTT: Dithiothreitol; FA: Formaldehyde; FBS: Fetal bovine serum; FISH: Fluorescent *in situ* hybridization; *gpas*: G protein α-subunit; HRP: Horseradish peroxidase; LCA: *Lens culinaris* agglutinin; mAb: Monoclonal antibody; MHC: Myosin heavy chain; NP-40: Nonidet P-40; PBS: Phosphate buffered saline; PBSTB: Phosphate buffered saline plus Triton X-100 and BSA; PBSTB+FG: Phosphate buffered saline plus Triton X-100, BSA, and fish gelatin; PBSTx: Phosphate buffered saline + Triton-X 100; *pc-2*: *Prohormone convertase 2*; PNS: Peripheral nervous system; RNAi: RNA interference; SDS: Sodium dodecyl sulfate; T: Trypsin; TI: Trypsin inhibitor; VNC: Ventral nerve cords; WGA: Wheat germ agglutinin.

Competing interests

The authors declare that they have no competing interests.

Authors' contributions

RMZ conceived the project. KGR, KCO, MRT, RKM, AH, RSK, and RMZ designed and performed experiments, and analyzed data. KGR and RMZ interpreted results and wrote the manuscript. All authors read and approved the final manuscript.

Acknowledgements

We thank Ionit Iberkleid and Joi Weeks for helpful comments on the manuscript; David Forsthoefel for helpful discussions about this project and sharing unpublished results; Zayas laboratory members for insights and discussions on this work; Eileen Skaletsky and Mary Sumner from QED Bioscience, Inc., for advice and antibody production services; Peter Reddien for his kind gift of the anti-SMEDWI antibody; and Phil Newmark in whose laboratory Ryan King performed experiments with Smed-5B1. We thank Karla Daniels and Brian Berger for their assistance with the submission of hybridoma lines to the DSHB; for the final tests described here, the monoclonal antibody supernatants were obtained from the DSHB, created by the NICHD and maintained at The University of Iowa, Department of Biology, Iowa City, IA 52242. This work was supported by California Institute for Regenerative Medicine Grant RN2-00940-1 to RMZ.

Author details
[1]Department of Biology, San Diego State University, San Diego, CA 92182, USA. [2]Howard Hughes Medical Institute, Department of Cell and Developmental Biology, University of Illinois at Urbana-Champaign, 601 S. Goodwin Ave., Urbana, IL 61801, USA. [3]Present address: Department of Biological Sciences, Southern Illinois University Edwardsville, Edwardsville, IL 62026, USA. [4]Present address: Department of Biology, St. Norbert College, De Pere, WI 54115, USA.

Received: 10 August 2014 Accepted: 22 December 2014
Published online: 21 January 2015

References

1. Baguñà J, Saló E, Auladell C. Regeneration and pattern formation in planarians. III. Evidence that neoblasts are totipotent stem cells and the source of blastema cells. Development. 1989;107(1):77–86.
2. Baguñà J. Mitosis in the intact and regenerating planarian Dugesia mediterranea n.sp. II. Mitotic studies during regeneration, and a possible mechanism of blastema formation. J Exp Zool. 1976;195:53–64.
3. Baguñà J, Romero R. Quantitative analysis of cell types during growth, degrowth and regeneration in the planarians Dugesia mediterranea and Dugesia tigrina. Hydrobiologia. 1981;84(1):181–94.
4. Wagner DE, Wang IE, Reddien PW. Clonogenic neoblasts are pluripotent adult stem cells that underlie planarian regeneration. Science. 2011;332(6031):811–6.
5. Agata K, Soejima Y, Kato K, Kobayashi C, Umesono Y, Watanabe K. Structure of the planarian central nervous system (CNS) revealed by neuronal cell markers. Zoolog Sci. 1998;15(3):433–40.
6. Cebrià F. Organization of the nervous system in the model planarian Schmidtea mediterranea: an immunocytochemical study. Neurosci Res. 2008;61(4):375–84.
7. Cebrià F, Kudome T, Nakazawa M, Mineta K, Ikeo K, Gojobori T, et al. The expression of neural-specific genes reveals the structural and molecular complexity of the planarian central nervous system. Mech Dev. 2002;116(1–2):199–204.
8. Saló E, Pineda D, Marsal M, Gonzalez J, Gremigni V, Batistoni R. Genetic network of the eye in Platyhelminthes: expression and functional analysis of some players during planarian regeneration. Gene. 2002;287(1–2):67–74.
9. Brøndsted HV. Planarian Regeneration. 1969.
10. Hyman LH. The Invertebrates, Vol II: Platyhelminthes and Rhynchocoela. New York: Mcgraw-Hill Book Company, Inc; 1951.
11. Forsthoefel DJ, Park AE, Newmark PA. Stem cell-based growth, regeneration, and remodeling of the planarian intestine. Dev Biol. 2011;356(2):445–59.
12. Forsthoefel DJ, James NP, Escobar DJ, Stary JM, Vieira AP, Waters FA, et al. An RNAi screen reveals intestinal regulators of branching morphogenesis, differentiation, and stem cell proliferation in planarians. Dev Cell. 2012;23(4):691–704.
13. Ruppert EE, Smith PR. The functional organization of filtration nephridia. Biol Rev. 1988;63(2):231–58.
14. Rink JC, Vu HT, Sánchez Alvarado A. The maintenance and regeneration of the planarian excretory system are regulated by EGFR signaling. Development. 2011;138(17):3769–80.
15. Scimone ML, Srivastava M, Bell GW, Reddien PW. A regulatory program for excretory system regeneration in planarians. Development. 2011;138(20):4387–98.
16. Sánchez Alvarado A, Newmark PA. Double-stranded RNA specifically disrupts gene expression during planarian regeneration. Proc Natl Acad Sci U S A. 1999;96(9):5049–54.
17. Elliott SA, Sánchez Alvarado A. The history and enduring contributions of planarians to the study of animal regeneration. Wiley Interdiscip Rev Dev Biol. 2013;2(3):301–26.
18. King RS, Newmark PA. In situ hybridization protocol for enhanced detection of gene expression in the planarian Schmidtea mediterranea. BMC Dev Biol. 2013;13:8.
19. Pearson BJ, Eisenhoffer GT, Gurley KA, Rink JC, Miller DE, Sánchez Alvarado A. Formaldehyde-based whole-mount in situ hybridization method for planarians. Dev Dyn. 2009;238(2):443–50.
20. Zayas RM, Cebria F, Guo T, Feng J, Newmark PA. The use of lectins as markers for differentiated secretory cells in planarians. Dev Dyn. 2010;239(11):2888–97.
21. Chong T, Stary JM, Wang Y, Newmark PA. Molecular markers to characterize the hermaphroditic reproductive system of the planarian Schmidtea mediterranea. BMC Dev Biol. 2011;11:69.
22. Cebrià F, Newmark PA. Planarian homologs of netrin and netrin receptor are required for proper regeneration of the central nervous system and the maintenance of nervous system architecture. Development. 2005;132(16):3691–703.
23. Guo T, Peters AH, Newmark PA. A Bruno-like gene is required for stem cell maintenance in planarians. Dev Cell. 2006;11(2):159–69.
24. Robb SM, Sánchez Alvarado A. Identification of immunological reagents for use in the study of freshwater planarians by means of whole-mount immunofluorescence and confocal microscopy. Genesis. 2002;32(4):293–8.
25. Glazer AM, Wilkinson AW, Backer CB, Lapan SW, Gutzman JH, Cheeseman IM, et al. The Zn finger protein Iguana impacts Hedgehog signaling by promoting ciliogenesis. Dev Biol. 2010;337(1):148–56.
26. Bueno D, Baguñà J, Romero R. Cell-, tissue-, and position-specific monoclonal antibodies against the planarian Dugesia (Girardia) tigrina. Histochem Cell Biol. 1997;107(2):139–49.
27. Moritz S, Stöckle F, Ortmeier C, Schmitz H, Rodríguez-Esteban G, Key G, et al. Heterogeneity of planarian stem cells in the S/G2/M phase. Int J Dev Biol. 2012;56(1–3):117–25.
28. Labbé RM, Irimia M, Currie KW, Lin A, Zhu SJ, Brown DD, et al. A comparative transcriptomic analysis reveals conserved features of stem cell pluripotency in planarians and mammals. Stem Cells. 2012;30(8):1734–45.
29. Önal P, Grün D, Adamidi C, Rybak A, Solana J, Mastrobuoni G, et al. Gene expression of pluripotency determinants is conserved between mammalian and planarian stem cells. EMBO J. 2012;31(12):2755–69.
30. Rieger RM, Tyler S, Smith JPI, Riger G. Platyhelminthes: Turbellaria. Pp. 7–140. In: Harrison FW, Bogitsh BJ, editors. Microscopic Anatomy of Invertebrates. Vol. 3. New York, NY: Wiley-Liss; 1991a. p. 347
31. Cebrià F, Vispo M, Newmark P, Bueno D, Romero R. Myocyte differentiation and body wall muscle regeneration in the planarian Girardia tigrina. Dev Genes Evol. 1997;207(5):306–16.
32. Orii H, Ito H, Watanabe K. Anatomy of the planarian Dugesia japonica I. The muscular system revealed by antisera against myosin heavy chains. Zoolog Sci. 2002;19(10):1123–31.
33. Romero R, Fibla J, Bueno D, Sumoy L, Soriano M, Baguñà J. Monoclonal antibodies as markers of specific cell types and regional antigens in the freshwater planarian Dugesia (G.) tigrina. Hydrobiologia. 1991;227(1):73–9.
34. Kobayashi C, Kobayashi S, Orii H, Watanabe K, Agata K. Identification of two distinct muscles in the Planarian Dugesia japonica by their expression of Myosin heavy chain genes. Zoolog Sci. 1998;15(6):861–9.
35. Cebrià F. Regenerating the central nervous system: how easy for planarians! Dev Genes Evol. 2007;217(11–12):733–48.
36. Okamoto K, Takeuchi K, Agata K. Neural projections in planarian brain revealed by fluorescent dye tracing. Zoolog Sci. 2005;22(5):535–46.
37. Pigon A, Morita M, Best JB. Cephalic mechanism for social control of fissioning in planarians. II. Localization and identification of the receptors by electron micrographic and ablation studies. J Neurobiol. 1974;5(5):443–62.
38. Khanna R, Wilson SM, Brittain JM, Weimer J, Sultana R, Butterfield A, et al. Opening Pandora's jar: a primer on the putative roles of CRMP2 in a panoply of neurodegenerative, sensory and motor neuron, and central disorders. Future Neurol. 2012;7(6):749–71.
39. Cowles MW, Omuro KC, Stanley BN, Quintanilla CG, Zayas RM. COE loss-of-function analysis reveals a genetic program underlying maintenance and regeneration of the nervous system in planarians. PLoS Genet. 2014;10(10):e1004746.
40. Collins 3rd JJ, Hou X, Romanova EV, Lambrus BG, Miller CM, Saberi A, et al. Genome-wide analyses reveal a role for peptide hormones in planarian germline development. PLoS Biol. 2010;8(10):e1000509.
41. Baguñà J, Ballester R. The nervous system in planarians: peripheral and gastrodermal plexuses, pharynx innervation, and the relationship between central nervous system structure and the acoelomate organization. J Morphol. 1978;155(2):237–52.
42. Hanström B. Über den feineren bau des nervensystems der tricladen turbellarien auf grund von untersuchungen an *Bdelloura candida*. Acta Zool. 1926;7(1):101–15.
43. Keenan CL, Coss R, Koopowitz H. Cytoarchitecture of primitive brains: Golgi studies in flatworms. J Comp Neurol. 1981;195(4):697–716.
44. Bartolomaeus T, Ax P. Protonephridia and metanephridia - their relation within the bilateria. Zeitschrift Fur Zoologische Systematik Und Evolutionsforschung. 1992;30(1):21–45.

45. MacRae EK. The fine structure of sensory receptor processes in the auricular epithelium of the planarian, Dugesia tigrina. Z Zellforsch Mikrosk Anat. 1967;82(4):479–94.
46. Hyman LH: The invertebrates, Vol. II. Platyhelminths and rhyncocoela. New York: McGraw-Hill; 1951
47. Reddien PW, Oviedo NJ, Jennings JR, Jenkin JC, Sánchez Alvarado A. SMEDWI-2 is a PIWI-like protein that regulates planarian stem cells. Science. 2005;310(5752):1327–30.
48. Eisenhoffer GT, Kang H, Sánchez Alvarado A. Molecular analysis of stem cells and their descendants during cell turnover and regeneration in the planarian Schmidtea mediterranea. Cell Stem Cell. 2008;3(3):327–39.
49. Lapan SW, Reddien PW. Transcriptome analysis of the planarian eye identifies ovo as a specific regulator of eye regeneration. Cell Rep. 2012;2(2):294–307.
50. Cowles MW, Brown DD, Nisperos SV, Stanley BN, Pearson BJ, Zayas RM. Genome-wide analysis of the bHLH gene family in planarians identifies factors required for adult neurogenesis and neuronal regeneration. Development. 2013;140(23):4691–702.
51. Adler CE, Seidel CW, McKinney SA, Sánchez Alvarado A. Selective amputation of the pharynx identifies a FoxA-dependent regeneration program in planaria. Elife. 2014;3:e02238.
52. Gurley KA, Rink JC, Sánchez Alvarado A. Beta-catenin defines head versus tail identity during planarian regeneration and homeostasis. Science. 2008;319(5861):323–7.
53. Petersen CP, Reddien PW. Smed-betacatenin-1 is required for anteroposterior blastema polarity in planarian regeneration. Science. 2008;319(5861):327–30.
54. Iglesias M, Gomez-Skarmeta JL, Saló E, Adell T. Silencing of Smed-betacatenin1 generates radial-like hypercephalized planarians. Development. 2008;135(7):1215–21.
55. Cebrià F, Guo T, Jopek J, Newmark PA. Regeneration and maintenance of the planarian midline is regulated by a slit orthologue. Dev Biol. 2007;307(2):394–406.
56. Wang Y, Stary JM, Wilhelm JE, Newmark PA. A functional genomic screen in planarians identifies novel regulators of germ cell development. Genes Dev. 2010;24(18):2081–92.
57. Kang H, Sánchez Alvarado A. Flow cytometry methods for the study of cell-cycle parameters of planarian stem cells. Dev Dyn. 2009;238(5):1111–7.
58. Romero BT, Evans DJ, Aboobaker AA. FACS analysis of the planarian stem cell compartment as a tool to understand regenerative mechanisms. Methods Mol Biol. 2012;916:167–79.

Chapter 2, in full, is a reprint of the material as it appears in Biomed Central – Developmental Biology 2015. Kelly G. Ross, Kerilyn C. Omuro, Matthew R. Taylor, Roma K. Munday, Amy Hubert, Ryan S. King, and Ricardo M. Zayas. The dissertation author was the primary investigator and author of this manuscript.

CHAPTER 3:

Fixation, processing, and immunofluorescent labeling of whole mount planarians

ABSTRACT

Efforts to elucidate mechanisms of regeneration in the planarian *Schmidtea mediterranea* have included the application of immunocytochemical methods to detect specific molecules and label cells and tissues *in situ*. Here we describe methods for immunofluorescent labeling of whole mount planarians. We outline protocols for fixation and steps for processing animals prior to immunolabeling, incorporating commonly utilized reagents for mucus removal, pigment bleaching, tissue permeabilization, and antigen retrieval. Because processing steps can mask or degrade antigens, we also recommend protocol parameters that can be tested simultaneously to optimize sample preparation for novel antibodies.

INTRODUCTION

Investigation of the cellular and molecular mechanisms underlying planarian regeneration has been advanced by the application of immunohistochemical techniques to detect proteins, post-translational modifications, and other antigens *in situ*. These efforts have included the development of antibodies that recognize specific proteins [1-5], the identification of commercially and publicly available reagents that cross-react with planarian epitopes [6-10], and larger-scale screens to generate novel monoclonal antibody collections that label a variety of cell types [11-13].

Adaptation of immunocytochemical techniques to planarians has required identification of suitable tissue processing steps to prepare specimens for immunolabeling. Many of the processing steps were initially developed to enable specific, low-background immunodetection of modified nucleic acids in whole mount planarians [9,14-17] and subsequently adapted for detection of proteins [6,7,18-20]. These efforts have included the implementation of various fixatives [11,13,14,21,22], as well as chemical treatments to compensate for idiosyncracies of planarian tissue such as removal of mucous secretions prior to fixation, bleaching to remove pigmentation and enable visualization of internal structures, and methods for tissue permeabilization and antigen retrieval [14-16,23]. Effective sample preparation requires achieving a balance between fixation and permeabilization of tissues to allow antibody access, while simultaneously preserving antigenicity and epitope localization. Therefore, development of novel, planarian-specific antibodies,

or evaluation of cross-reactivity of existing antibodies from commercial suppliers or other sources, has entailed efforts to test reagents on samples processed using several tissue preparation procedures (summarized in Figure 3.1).

Our laboratories have conducted independent monoclonal antibody screens to raise cell-type-specific markers in uninjured and regenerating planarians. In the course of these projects, we found that, as in other organisms [24-26], achieving optimal staining necessitated experimenting with multiple tissue processing variables (Figure 3.2). Mucus removal, fixative choice, permeabilization methods, and even bleaching in aqueous instead of organic solutions can influence immunolabeling with unique antibodies (see examples in Figure 3.2A-C).

In this chapter, we provide step-by-step protocols for fixation and immunofluorescent labeling of whole mount planarians. We highlight the most critical stages and commonly used sample preparation, blocking, labeling, and detection approaches (Figure 3.1), and outline strategies for testing a range of options at each step to optimize processing and labeling for new antibodies.

METHODS

Materials for Fixations and Immunolabeling

1. 8 ml borosilicate glass vials.

2. 20 ml borosilicate glass vials with urea poly seal cone lined screw caps.

3. 1.5 ml polypropylene microcentrifuge tubes.

4. 15 ml polypropylene conical centrifuge tubes.

5. Multiwell polystyrene plates (24, 48, or 96 well).

Mucus Removal/Kill Method 1: Hydrochloric Acid Reagents

1. 2% HCl: 36.5-38% HCl diluted 1:18 into ultrapure water.

Mucus Removal/Kill Method 2: *N*-Acetyl Cysteine Reagents

1. 1X phosphate buffered saline (PBS; 137 mM NaCl, 2.7 mM KCl, 10 mM Na_2HPO_4, 2 mM KH_2PO_4, pH 7.4).

2. 5% *N*-Acetyl-L-Cysteine (NAC) (w/v) dissolved in 1X PBS.

Fixation Method 1 and 2: Formaldehyde Reagents

1. PBSTx: 1X PBS, 0.3% Triton X-100.

2. 4% Formaldehyde Solution: dilute to 4% from commercial 37% stabilized formaldehyde stock in PBSTx.

Fixation Method 3: Methacarn Reagents

1. Methacarn: 6 volumes methanol, 3 volumes chloroform, 1 volume glacial acetic acid.

Fixation Method 4: Carnoy's Fixation Reagents

1. Carnoy's Fixative: 6 volumes ethanol, 3 volumes chloroform, 1 volume glacial acetic acid.

Permeabilization/Reduction Reagents

1. 1 M Dithiothreitol (DTT) Solution: 1 M DTT, 10 mM sodium acetate (pH 5.2). Store aliquots at -20°C.

2. 10% (w/v) Sodium Dodecyl Sulfate (SDS): Weigh out appropriate amount and dissolve in ultrapure water. Careful: SDS is a fine powder and strong irritant when inhaled, thus take appropriate protective measures.

3. Reduction Solution: 50 mM DTT diluted from a 1 M stock, 1% NP-40, and 0.5% SDS diluted from a 10% (w/v) stock in 1X PBS.

Bleaching Methods 1 and 2 (Aqueous or Dehydrated) Reagents

1. 6% H_2O_2-PBSTx: Dilute commercial 30% H_2O_2 stock solution in PBSTx.

2. 6% H_2O_2-MeOH: Dilute commercial 30% H_2O_2 stock solution in methanol.

Proteinase K Treatment Reagents

1. Proteinase K (ProK): Dilute to a 10 mg/ml stock according to the manufacturer's instructions. Store aliquots at -20°C.

2. ProK Solution: 2 µg/ml Proteinase K, 0.1% SDS diluted in PBSTx.

Reagents for Immunolabeling Whole Planarians

1. Blocking Solution A: 1% BSA (IgG-free), diluted in PBSTx.

2. Blocking Solution B: 0.3% BSA (IgG-free), 0.45% Fish Gelatin diluted in PBSTx.

3. 1% (w/v) sodium azide diluted in ultrapure water.

4. HRP-conjugated secondary antibody (e.g., Goat Anti-Mouse IgG+IgM, Horseradish Peroxidase Conjugate).

5. Fluorophore-conjugated secondary antibody.

6. Mounting Media (e.g., 50-80% glycerol in PBS, Vectashield [Vector Laboratories] or similar).

Tyramide Signal Amplification (TSA) Development Reagents

1. Fluorophore-conjugated Tyramide (Fluor-tyramide), (commercially available or prepared as described in [27,28]).

2. TSA Buffer: 10 mM Imidazole, 1:250-1:1000 Fluor-Tyramide, diluted in PBSTx.

3. Mounting Media (e.g., 50-80% glycerol in PBS, Vectashield [Vector Laboratories] or similar).

Dispensing Planarians into Vials for Fixation

1. Transfer animals in planarian salts to appropriate tubes or vials (*see* Note 1).

- 1.5 ml polypropylene microcentrifuge tube: 1-10 animals
- 8 ml glass scintillation vial: 20-50 animals
- 20 ml glass scintillation vial: 50-100 animals

- 15 ml polypropylene conical: 10-100 animals

2. Use the following guide to determine the volume of reagents to use for all steps in the following methods (until the section "Immunolabeling of Whole Planarians"). Use at least 1 ml of fluid per 10 planarians (*see* **Note 1**).

- 1.5 ml polypropylene microcentrifuge tube: 1 ml volume
- 8 ml glass scintillation vial: 2-5 ml volume
- 20 ml glass scintillation vial: 5-10 ml volume
- 15 ml polypropylene conical: 5-10 ml volume

Mucus Removal/Kill Method 1: Hydrochloric Acid

1. Incubate animals on ice 30 seconds – 2 minutes, until movement slows considerably. Quickly remove salt solution (e.g., by decanting or using a plastic Pasteur pipette).

2. Replace planarian salts with pre-chilled, ice-cold 2% HCl.

3. Incubate in 2% HCl for 3 minutes total, alternating between gently inverting by hand for 1 minute and incubating on ice for 1 minute (*see* Note 2).

4. Rinse once with 1X PBS.

5. Proceed immediately to fixation.

Mucus Removal/Kill Method 2: *N*-Acetyl Cysteine

1. Replace planarian salts with 5% NAC solution (*see* Note 3).

2. Incubate 5-10 minutes (*see* Note 4) at room temperature, with gentle rocking.

3. Remove 5% NAC.

4. Proceed immediately to fixation.

Fixation Method 1: Formaldehyde at Room Temperature

1. Add 4% Formaldehyde Solution (*see* Note 5).

2. Incubate 15-20 minutes at room temperature, with gentle rocking.

3. Remove 4% Formaldehyde Solution and rinse 2-3 times with PBSTx.

4. Proceed to reduction step, bleaching, or storage (*see* Note 6).

Fixation Method 2: Formaldehyde at 4°C

1. Add 4% Formaldehyde Solution.

2. Incubate for 6 hours at 4°C, with gentle rocking.

3. Remove fixative and rinse 2-3 times with PBSTx.

4. Proceed to reduction step, bleaching, or storage (*see* Note 6).

Fixation Method 3: Methacarn

1. Add pre-chilled, ice-cold Methacarn and rock gently for 20 minutes at 4°C.

2. Remove Methacarn, add pre-chilled -20°C methanol, and rock gently for 15-30 minutes at 4°C.

3. Rinse animals 2 more times in methanol (room temperature).

4. Proceed to Bleaching Method 2 (recommended), Bleaching Method 1 (optional, *see* Note 7), or storage (*see* Note 8).

Fixation Method 4: Carnoy's

1. Add pre-chilled, ice-cold Carnoy's Fixative and rock gently for 2 hours at 4°C.

2. Remove Carnoy's, add pre-chilled -20°C methanol, and rock gently for 1 hour at 4°C.

3. Rinse animals 2 more times in methanol (room temperature).

4. Proceed to Bleaching Method 2 (recommended), Bleaching Method 1 (optional, *see* Note 7), or storage (*see* Note 8).

(Optional) Permeabilization/Reduction

1. Add Reduction Solution (pre-heated to 37°C) (*see* Note 9).

2. Incubate at 37°C (in water bath) for 5-10 minutes, with gentle inversion every 2-3 minutes.

3. Remove solution and rinse 1-3 times with PBSTx.

4. Proceed immediately to bleaching or storage (*see* Note 6).

Bleaching Method 1: Aqueous in PBSTx

1. Add 6% H_2O_2-PBSTx (*see* Note 10).

2. Place tubes in an open, foil-lined box, 10-15 cm under a fluorescent lamp, for 8-24 hours (*see* Note 11 and Note 12).

3. Remove bleaching solution and rinse 3 times in PBSTx.

4. Proceed immediately to Proteinase K treatment, immunolabeling, or storage (*see* Note 6).

Bleaching Method 2: Dehydrated into MeOH

1. Add 1:1 methanol:PBSTx.

2. Incubate 5 minutes at room temperature, with gentle rocking.

3. Replace solution with methanol and incubate 5 minutes at room temperature, with gentle rocking.

4. Replace with fresh methanol and incubate at -20°C for at least one hour.

5. Replace methanol with 6% H_2O_2-MeOH or store animals at -20°C (*see* Note 8).

6. Place tubes in an open, foil-lined box, 10-15 cm under a fluorescent lamp, for 8-24 hours (*see* Note 11 and Note 12).

7. Remove bleaching solution and rinse 2-3 times in methanol. Animals can be stored at -20°C (*see* Note 8).

8. Replace with 1:1 methanol:PBSTx and incubate for 5-10 minutes at room temperature, with gentle rocking.

9. Replace with PBSTx and incubate for 5-10 minutes at room temperature, with gentle rocking.

10. Rinse 1-2 times with PBSTx.

11. Proceed immediately to Proteinase K treatment, or blocking.

(Optional) Proteinase K Treatment

1. Add ProK Solution (pre-heated to 37° C) (*see* Notes 13 and 14).

2. Incubate at room temperature for 10 minutes, with gentle rocking.

3. Replace ProK Solution with 4% Formaldehyde Solution and incubate for 10 minutes, with gentle rocking.

4. Remove fixative and rinse animals 2-3 times with PBSTx.

5. Proceed to Immunolabeling.

Immunolabeling of Whole Planarians

1. Transfer fixed and processed animals to a 96-, 48-, or 24-well plate, or a 1.5 ml polypropylene microcentrifuge tube (*see* Note 15).

2. Replace PBSTx with Blocking Solution (*see* Note 16), then incubate 4 hours at room temperature with gentle rocking (*see* Note 17).

3. Replace with primary antibody diluted into Blocking Solution (*see* Note 18).

4. Incubate overnight (12-16 hours) at 4°C with gentle rocking.

5. Remove antibody solution (*see* Note 19).

6. Remove antibody and rinse 3 times with PBSTx, then wash 6-8 hours, replacing PBSTx at least 6 times.

7. Re-block for 1 hour at room temperature on rocker in Blocking Solution.

8. Replace with secondary antibody (*see* Note 20 and 21) diluted in Blocking Solution (at a dilution of 1:250-1:1000) plus DAPI at 1 µg/ml (*see* Note 22). Keep plate or tubes wrapped in foil or in a light-protective container from this point forward if using fluorophore-conjugated secondary or DAPI.

9. Incubate overnight (12-16 hours) at 4°C with gentle rocking.

10. Remove antibody. Rinse 3 times with PBSTx, then wash 6-8 hours, replacing PBSTx at least 6 times. If HRP-conjugated secondary antibody was used, proceed to Tyramide Signal Amplification Development.

11. Mount animals in mounting medium for imaging.

Tyramide Signal Amplification Development

1. Pre-incubate in TSA Buffer for 30 minutes at room temperature.

2. Replace with TSA Buffer plus 0.015% H_2O_2 (*see* Note 23), then incubate for 5-10 minutes at room temperature (*see* Note 24).

3. Remove TSA Buffer and rinse animals in PBSTx.

4. Wash 3 times in PBSTx (10 minutes each), then overnight at room temperature or 4°C. Keep plate or tubes wrapped in foil or in a light-protective container.

5. Mount animals in mounting medium for imaging.

Notes: Dispensing Planarians into Vials for Fixation

1. Processing steps for larger animals or different species might require additional testing. For example, *S. mediterranea* hermaphrodites are considerably larger and require higher reagent concentrations and longer incubation times during some processing steps [29]. In addition, it has been reported that species such as *Dendrocoelum lacteum* require adjustments for successful immunolabeling [30]. Animal number per tube will also need to be adjusted for larger animals.

Notes: HCl Mucus Removal/Kill Step

2. Mucus removal may be more effective with a longer, 5 minute HCl treatment on animals larger than 3-5 mm, when more animals are fixed in the same vial, or for some antibodies. Consider optimizing the duration of this step if you notice uneven or poor antibody labeling of the specimens.

Notes: *N*-Acetyl Cysteine Mucus Removal/Kill Step

3. NAC concentrations of up to 7.5% and treatment times up to 10 minutes may be required for larger animals and should be optimized for individual antibodies.

4. NAC-treated, Methacarn-fixed animals may disintegrate during bleaching. NAC treatment can be reduced to 3 minutes and/or H_2O_2 concentration can be reduced to 1%. We have not tested NAC treatment with Carnoy's fixation.

Notes: Formaldehyde-based Fixations

5. We have compared the labeling of multiple antibodies using either PBSTx or PBS (detergent-free) during all steps in formaldehyde-based fixation. Labeling quality was unaffected by the presence of detergent, but may need to be tested for new antibodies. Additionally, animals fixed and washed in PBSTx are less likely to stick together. Further measures that can reduce stickiness include: increasing tube size and fluid volumes, minimizing buffer exchange time to 45 seconds or less, and processing only 3-4 tubes at once to avoid delays during buffer exchanges.

6. For many antibodies, labeling is unaffected by animal storage in PBSTx at 4°C for up to one week. We advise testing of storage effects for new antibodies.

Notes: Methacarn and Carnoy's Fixations

7. Animals must be rehydrated prior to bleaching in PBSTx. Incubate animals in 1:1 methanol:PBSTx for 5 minutes, then 2 times in PBSTx (5 minutes each).

8. Animals can be stored in Methanol at -20°C for up to one month. Further storage could potentially decrease labeling efficiency. Storage effects should be tested for new antibodies.

Notes: Reduction/Permeabilization

9. Carnoy's- or Methacarn-fixed animals should be rehydrated first (*see* **Note 7**). We have no examples of this treatment improving labeling on Methacarn and Carnoy's fixed animals. However, this combination has not been tested extensively and is an option for antibodies that only label alcohol-fixed specimens.

Notes: Bleaching

10. We have compared labeling by multiple antibodies after bleaching in PBSTx or PBS, and found no difference in labeling quality. PBSTx is recommended because animals in PBSTx were less likely to stick together, but PBS may be more appropriate for antibodies with detergent sensitivity. The shelf life of commercial peroxide varies and the effective concentration can decrease over time as H_2O_2 decays. We recommend storing the stock solution at 4°C and replacing it regularly.

11. Bleach times of 12-16 hours are appropriate for asexual planarians 3-5 mm in length and for many antibodies. However, smaller animals may require shorter bleaching times, while larger animals may require longer times. In addition, some antibodies are more sensitive to hydrogen peroxide treatment. Optimal bleaching time should therefore be determined empirically for individual antibody and animal size combinations.

12. Animals may retain a light yellow color, especially after shorter bleaching times. Although rehydration and Proteinase K treatment will further reduce pigment levels, fresh H_2O_2 solution can be added after 8-12 hours to accelerate bleaching if animals retain dark yellow pigment. Effects on immunolabeling should be determined on an antibody-to-antibody basis.

Notes: Proteinase K Treatment

13. We have no examples of this treatment improving labeling on Methacarn and Carnoy's fixed animals, but this step is an option for antibodies that only label alcohol-fixed specimens.

14. ProK concentration (2-20 µg/ml) and/or treatment time (5-20 minutes) may need to be empirically determined for smaller or larger animals, or for regenerates.

Notes: Immunolabeling of Whole Planarians

15. Recommendations for appropriate animal numbers and volumes per well/tube for blocking and labeling. For animals/fragments larger than 3-5 mm, animal numbers should be reduced. Use twice the volumes listed for washing steps.

- 96-well plate: 3-5 animals, 75-100 µl
- 48-well plate: 3-10 animals, 200-400 µl
- 24-well plate: 10-20 animals, 300-600 µl
- 1.5 ml microcentrifuge tube: 10-20 animals, 250-500 µl

16. We have successfully used both Blocking Solution "A" and "B" for antibodies and hybridoma supernatants. Blocking Solution "B" with fish gelatin may be more suitable for antibodies/supernatants with higher background labeling. Optimal blocking solution can be determined empirically for new antibodies.

17. Four hour blocking time is standard. However, blocking can be extended overnight (12-16 hours) to improve signal-to-noise for antibodies with higher non-specific labeling.

18. Optimal dilution should be determined for each lot of antibody. Some examples of antibodies commonly used to label whole planarians and recommended dilutions are listed in Table 3.1.

19. Primary antibodies can be stored at 4° C after adding 2 µl per ml of 10% Sodium Azide (for a final concentration of 0.02%). Sodium Azide inactivates HRP and should not be added to HRP-conjugated secondary antibodies. Diluted, stored

antibodies can often be used multiple times, but storage effects should be determined empirically for each antibody.

20. 1:250 dilution is optimal for HRP-conjugated Anti-mouse IgG+IgM (Jackson) and 1:1000 is optimal for Alexa Fluor 488 Anti-Mouse IgG (Life Technologies).

21. Additional secondary antibodies that we have successfully used to label whole planarians and their recommended dilutions:

- Alexa Fluor 568 Goat Anti-Mouse IgG (Life Technologies), 1:400.
- Alexa Fluor 488 Goat Anti-Rabbit IgG (Life Technologies), 1:1000.
- Alexa Fluor 568 Goat Anti-Rabbit IgG (Life Technologies), 1:1000.
- Goat Anti-Rabbit IgG, Horseradish Peroxidase Conjugate (Life Technologies), 1:250.
- Goat Anti-Mouse IgG, IgM, Horseradish Peroxidase Conjugate (Life Technologies), 1:1000.

22. DAPI incubation can be performed later, after TSA, but will add time to the protocol.

Notes: Tyramide Signal Amplification:

23. To preserve H_2O_2 activity, aliquot and store 30% stock at -20°C.

24. Tyramide-only pre-incubation and/or longer development times may improve labeling in animals over 5 mm in length.

FIGURES

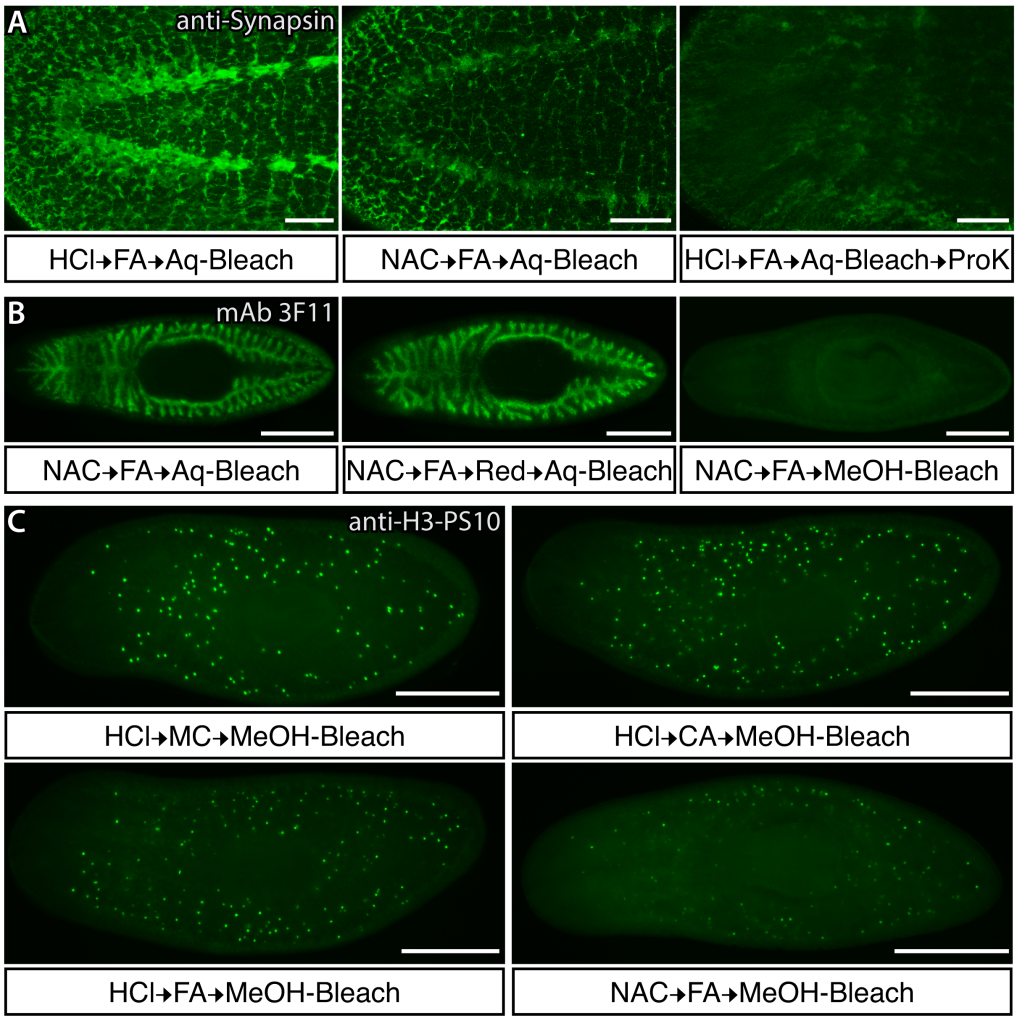

Figure 3.1: Variations in tissue processing protocols affect immunolabeling. Planarians were killed in either hydrochloric acid (HCl) or *N*-Acetyl-L-Cysteine (NAC), fixed with Carnoy's (CA), Formaldehyde (FA) or Methacarn (MC) and bleached in either aqueous (Aq-Bleach) or Methanol (MeOH-Bleach). (**A**) Anti-Synapsin labeling of the cephalic ganglia. Labeling was reduced by mucus removal with NAC and abolished by Proteinase K (ProK) treatment. Aq-Bleach was prepared in PBSTx. (**B**) Planarian intestine labeled with monoclonal antibody 3F11. The addition of a reduction step (Red) post-fixation enhanced labeling, whereas bleaching in methanol inhibited labeling. Aq-Bleach was prepared in PBS. (**C**) Planarians labeled with the mitotic marker anti-H3-PS10. Fixation in either Carnoy's or Methacarn produced the clearest labeling. Signal was reduced in Formaldehyde-fixed animals and further diminished by NAC mucus removal. Anterior is to the left in all panels. Scale bars in A = 100 μm; B-C = 500 μm.

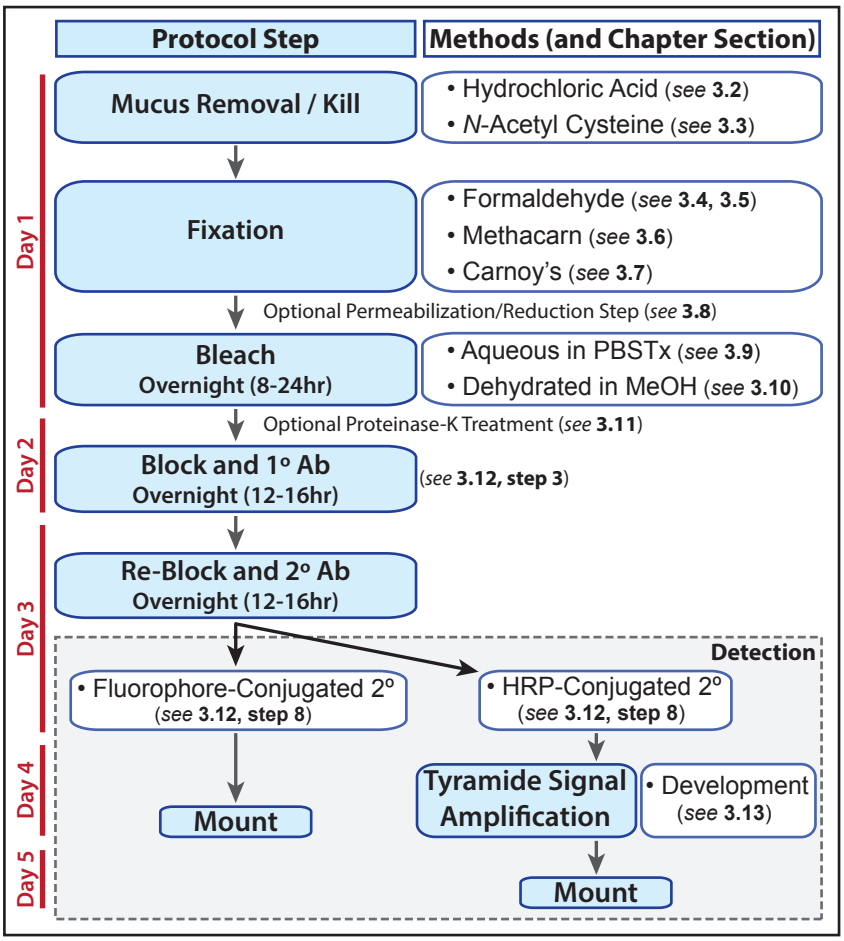

Figure 3.2: Flowchart of steps used to prepare and immunolabel whole mount planarians.

TABLES

Table 3.1: Recommended immunolabeling protocol steps for antibodies commonly used to label whole mount planarians[1].

Antibody, Cat #, Supplier	1° Dilution, 2° Antibody Detection	Recommended Preparations for Whole Mount Labeling			
		Kill Step Method	Fixation Method	Optional Steps	Bleaching Method
Mouse anti-Synapsin, 3C11, DSHB	1:400, Fluor-conjugated	HCl	Formaldehyde	None	Aqueous
		HCl	Carnoy's	None	Aqueous
Mouse anti-β-Tubulin, E7, DSHB	1:500, Fluor-conjugated	HCl	Carnoy's	None	Dehydrated
		NAC	Formaldehyde	ProK	Dehydrated
Mouse anti-Acetylated-Tubulin, T6793, Sigma	1:1000, Fluor-conjugated	HCl	Carnoy's	None	Dehydrated
		HCl	Formaldehyde at 4°C	ProK	Aqueous
Rabbit anti-Histone-H3-PS10, 3377S, Cell Signaling	1:2000, HRP-conjugated	HCl	Carnoy's / Methacarn	None	Dehydrated
Mouse anti-Phospho-Tyrosine, 9411S, Cell Signaling	1:500, Fluor-conjugated	HCl	Carnoy's / Methacarn	None	Dehydrated
		HCl	Formaldehyde at 4°C	None	Aqueous

Notes:

1. The table lists parameters the authors have identified that enable specific and robust labeling with individual antibodies. However, we have not tested all possible combinations of protocol variables and double-labeling with any of them could require additional adjustments. Antibodies from other suppliers can be substituted, but optimal sample preparation and antibody dilution may need to be empirically determined.

REFERENCES

1. Guo T, Peters AH, Newmark PA (2006) **A Bruno-like gene is required for stem cell maintenance in planarians.** Dev Cell **11**(2):159-169. doi:10.1016/j.devcel.2006.06.004.

2. Orii H, Ito H, Watanabe K (2002) **Anatomy of the planarian *Dugesia japonica* I. The muscular system revealed by antisera against myosin heavy chains.** Zoolog Sci **19**(10):1123-1131.

3. Orii H, Sakurai T, Watanabe K (2005) **Distribution of the stem cells (neoblasts) in the planarian *Dugesia japonica*.** Dev Genes Evol **215**(3):143-157. doi:10.1007/s00427-004-0460-y.

4. Nishimura K, Yamamoto H, Kitamura Y, Agata K (2008) **Brain and neural networks. In: Raffa RB, Rawls SM (eds) Planaria: A Model for Drug Action and Abuse.** Landes Bioscience, pp 4-12.

5. Ito H, Saito Y, Watanabe K, Orii H (2001) **Epimorphic regeneration of the distal part of the planarian pharynx.** Dev Genes Evol **211**(1):2-9.

6. Cebrià F (2008) **Organization of the nervous system in the model planarian *Schmidtea mediterranea*: an immunocytochemical study.** Neurosci Res **61**(4):375-384. doi:10.1016/j.neures.2008.04.005.

7. Robb SM, Sánchez Alvarado A (2002) **Identification of immunological reagents for use in the study of freshwater planarians by means of whole-mount immunofluorescence and confocal microscopy.** Genesis **32**(4):293-298.

8. Fraguas S, Barberán S, Ibarra B, Stöger L, Cebrià F (2012) **Regeneration of neuronal cell types in *Schmidtea mediterranea:* an immunohistochemical and expression study.** Int J Dev Biol **56**(1-3):143-153. doi:10.1387/ijdb.113428sf.

9. Newmark PA, Sánchez Alvarado A (2000) **Bromodeoxyuridine specifically labels the regenerative stem cells of planarians.** Dev Biol **220**(2):142-153.

10. Zayas RM, Cebrià F, Guo T, Feng J, Newmark PA (2010) **The use of lectins as markers for differentiated secretory cells in planarians.** Dev Dyn **239**(11):2888-2897. doi:10.1002/dvdy.22427.

11. Bueno D, Baguñà J, Romero R (1997) **Cell-, tissue-, and position-specific monoclonal antibodies against the planarian *Dugesia (Girardia) tigrina*.** Histochem Cell Biol **107**(2):139-149.

12. Moritz S, Stockle F, Ortmeier C, Schmitz H, Rodriguez-Esteban G, Key G, Gentile L (2012) **Heterogeneity of planarian stem cells in the S/G2/M phase.** Int J Dev Biol **56**(1-3):117-125. doi:10.1387/ijdb.113440sm.

13. Romero R, Fibla J, Bueno D, Sumoy L, Soriano MA, Baguna J (1991) **Monoclonal-Antibodies as Markers of Specific Cell-Types and Regional Antigens in the Fresh-Water Planarian *Dugesia (G) Tigrina*.** Hydrobiologia **227**:73-79. doi:Doi 10.1007/Bf00027585.

14. Umesono Y, Watanabe K, Agata K (1997) **A planarian *orthopedia* homolog is specifically expressed in the branch region of both the mature and regenerating brain.** Dev Growth Differ **39**(6):723-727.

15. Pearson BJ, Eisenhoffer GT, Gurley KA, Rink JC, Miller DE, Sánchez Alvarado A (2009) **Formaldehyde-based whole-mount in situ hybridization method for planarians.** Dev Dyn **238**(2):443-450. doi:10.1002/dvdy.21849.

16. Tazaki A, Kato K, Orii H, Agata K, Watanabe K (2002) **The body margin of the planarian *Dugesia japonica*: characterization by the expression of an intermediate filament gene.** Dev Genes Evol **212**(8):365-373. doi:10.1007/s00427-002-0253-0.

17. Pellettieri J, Fitzgerald P, Watanabe S, Mancuso J, Green DR, Sánchez Alvarado A (2010) **Cell death and tissue remodeling in planarian regeneration.** Dev Biol **338**(1):76-85. doi:10.1016/j.ydbio.2009.09.015.

18. Cebrià F, Newmark PA (2005) **Planarian homologs of netrin and netrin receptor are required for proper regeneration of the central nervous system and the maintenance of nervous system architecture.** Development **132**(16):3691-3703.

19. Sánchez Alvarado A, Newmark PA (1999) **Double-stranded RNA specifically disrupts gene expression during planarian regeneration.** Proc Natl Acad Sci U S A **96**(9):5049-5054.

20. Forsthoefel DJ, James NP, Escobar DJ, Stary JM, Vieira AP, Waters FA, Newmark PA (2012) **An RNAi screen reveals intestinal regulators of branching morphogenesis, differentiation, and stem cell proliferation in planarians.** Dev Cell **23**(4):691-704. doi:10.1016/j.devcel.2012.09.008.

21. Willier BH, Hyman LH, Rifenburgh SA (1925) **A histochemical study of intracellular digestion in triclad flatworms.** Journal of Morphology and Physiology **40**(2):299-340. doi:Doi 10.1002/Jmor.1050400205.

22. Kobayashi C, Kobayashi S, Orii H, Watanabe K, Agata K (1998) **Identification of two distinct muscles in the planarian *Dugesia japonica* by their expression of myosin heavy chain genes.** Zoological Science **15**(6):861-869. doi:Doi 10.2108/Zsj.15.861.

23. Bueno D, Espinosa L, Baguñà J, Romero R (1997) **Planarian pharynx regeneration in regenerating tail fragments monitored with cell-specific monoclonal antibodies.** Dev Genes Evol **206**:425-434.

24. Ramos-Vara JA, Beissenherz ME (2000) **Optimization of immunohistochemical methods using two different antigen retrieval methods on formalin-fixed paraffin-embedded tissues: experience with 63 markers.** J Vet Diagn Invest **12**(4):307-311.

25. Stadler C, Skogs M, Brismar H, Uhlen M, Lundberg E (2010) **A single fixation protocol for proteome-wide immunofluorescence localization studies.** J Proteomics **73**(6):1067-1078. doi:10.1016/j.jprot.2009.10.012.

26. Duerr JS (2006) **Immunohistochemistry (June 19, 2006). In: The *C. elegans* Research Community (ed) WormBook.** doi:10.1895/wormbook.1.105.1, http://www.wormbook.org.

27. Hopman AH, Ramaekers FC, Speel EJ (1998) **Rapid synthesis of biotin-, digoxigenin-, trinitrophenyl-, and fluorochrome-labeled tyramides and their application for In situ hybridization using CARD amplification.** J Histochem Cytochem **46**(6):771-777.

28. King RS, Newmark PA (2013) **In situ hybridization protocol for enhanced detection of gene expression in the planarian *Schmidtea mediterranea*.** BMC Dev Biol **13**:8. doi:10.1186/1471-213X-13-8.

29. Wang Y, Stary JM, Wilhelm JE, Newmark PA (2010) **A functional genomic screen in planarians identifies novel regulators of germ cell development.** Genes Dev **24**(18):2081-2092. doi:10.1101/gad.1951010.

30. Liu SY, Selck C, Friedrich B, Lutz R, Vila-Farre M, Dahl A, Brandl H, Lakshmanaperumal N, Henry I, Rink JC (2013) **Reactivating head regrowth in a regeneration-deficient planarian species.** Nature **500**(7460):81-84. doi:10.1038/nature12414.

CHAPTER 4:

A SoxB1 gene is required for regeneration and normal function of sensory neurons in planarians

INTRODUCTION

The post-embryonic mammalian brain represents one of the most complex organs in metazoans and dysfunction of neural subtypes or components of the many signaling pathways can lead to debilitating diseases and disorders. One such group of disorders is epilepsy disorders (EDs), which represents one of the most common chronic neurological disorders in humans by imposing a range of challenges to the daily lives of 65 million people worldwide [1]. People with epilepsy have a 20 times higher rate of sudden death and on average live 10 years fewer than the general population. Individuals with epilepsy also cope with side effects from anti-seizure drug therapies. The direct medical care cost of epilepsy in the United States is $9.6 billion annually [1]. Epilepsy is caused by an array of factors, but all epileptic seizures are characterized by abnormal neural activity that leads to an imbalance of electrical activity in the brain [2].

Studies dating back to the 1930s have contributed to the understanding of inheritance of seizure disorders. Whereas rare Mendelian inherited epilepsy disorders and hundreds of new genetic mutations have been identified, the majority of clinical data suggests complex inheritance patterns and the genetic determinants underlying common epilepsies remain largely unknown (reviewed in [3, 4]). The advent of high-throughput DNA sequencing has led to the steady growth of whole genome data for genome-wide association studies (GWAS) and has helped to identify many additional gene loci implicated in EDs [5]. A recent study has integrated data from thousands of publications to create a list of 499 genes and 331

clinical phenotypes associated with epilepsy disorders in humans [6]. Additionally, at least 100 genes have been implicated in single gene loss causes of epilepsy in rodents [7]. The most commonly identified genetic determinants of epilepsy in humans and animal models are genes associated with ion transport, establishment of cellular localization, gated channel activity, and neurotransmitter receptor activity [4-6]. These cellular components offer potential for the design of future treatments [8]. Current therapies for epilepsy include a multitude of anti-seizure drugs with wide range of side effects [1]. Thus, a better understanding of the molecular pathways involved in epilepsy disorders could lead to the discovery of better targeted drug therapies with less deleterious side effects.

One genetic link to epilepsy disorders may lie within the multifaceted *SoxB1* gene family. *SoxB1* transcription factor gene function (*Sox1-3* in mammals) is implicated in a wide range of developmental processes, including maintenance of pluripotency. For instance, SOX2 interacts with OCT4 to alter the chromatin structure of genes required for maintaining pluripotency in embryonic stem cells, which is likely why SOX2 can be used to induce pluripotency [9]. *SoxB1* genes are important regulators of neural development, especially as key players in the maintenance of neural stem cells, which has mostly been studied during development [10]. Recent evidence suggests that well-conserved developmental genes are reused during adult stem cell-based regeneration [11]. *SoxB1* genes are involved in neural stem cell regulation during both development and in adult neurogenesis. Two of the three *SoxB* genes (*Sox1* and *Sox2*) are enriched in a dataset

for partial epilepsies (GWAS ID #HGVST522). Knockout of *Sox1* in mice leads to epileptic seizures and increased mortality due to a loss of olfactory cortex postsynaptic target neurons in the ventral striatum [12]. *Sox1* must remain expressed in post-mitotic neurons in the ventral telencephalon for the correct specification and migration of neurons in the ventral striatum [13]; however, the molecular targets through which SOX1 acts to specify and maintain the molecular identity of these neurons in the adult CNS remain largely unknown.

SoxB1 genes are also implicated in the development and maintenance of sensory organs. For example, *SoxB1* genes directly activate expression of delta-crystallin expression in the embryonic eye lens [14]and a *SoxB1* gene is implicated in determination of sensory epidermal cells in amphioxus [15]. Additionally, in human embryonic stem cell derived neural crest models, *Sox2* has been found to play a necessary role in the acquisition of neural fates in sensory ganglia [16]. *SoxB* genes in sponges and ctenophores are expressed in ectodermal cells that contribute to sensory cells with photoreceptive functions [17-19]. *Sox2* is also implicated in the proliferation and specification of hair cells in the inner ear. It is expressed in the early sensory cell precursors and is required for later differentiation of these cell types [20]. Ectopic expression of the *SoxB1* gene *Sox3* ectopic leads to ectopic sensory placode formation in medaka fish [21] highlighting the roles of these genes in sensory organ formation and demonstrating an ancient role in sensory neural and epidermal cell fate.

The planarian *Schmidtea mediterranea* is an excellent model animal in which to study transcription factors that contribute to adult neurogenesis and seizure disorders. Planarians have a molecularly complex nervous system, including a central nervous system that consists of bi-lobed cephalic ganglia (brain) connected to two ventral nerve cords and a peripheral nervous system including multiple nerve plexuses (including the subepidermal and submuscular plexuses, which extend processes past the epidermis), that likely function in sensory roles [22-24]. Planarians are able to regenerate all missing tissues, including their nervous system, from a population of adult stem cells (called neoblasts). In addition, transcriptome analyses have revealed that many stem cell genes are highly conserved between planarians and mammals [25, 26]. The ability to inhibit gene function in planarians by dsRNA-mediated genetic interference (RNAi), coupled with their low cost of maintenance, size, and fast regeneration times allow high-throughput screening of genes involved in neural regeneration. Furthermore, planarians can be induced by chemoconvulsants to exhibit seizure-like movements, which can be attenuated by treatment with anti-seizure compounds [27].

Recent studies have reaffirmed the hypothesis that planarian neoblasts are not comprised of a homogeneous, pluripotent, stem cell population, but rather multiple populations of stem cells [11, 28], only a fraction of which are truly pluripotent, and thus able to differentiate into cells of all germ cell layers [28, 29]. Molecular markers, originally thought to distinguish most stem cell progeny [30] have now been determined specific to epidermal lineage [28], leaving many

unanswered questions about the relationship and overlap between cells termed neoblasts versus neoblast progeny and the differentiation potentials of subsets of these cells. Further, it is still unclear whether stem cell progeny in planarians represent any cell lineages that are capable of self-renewal. One *soxB1* gene has been previously studied in *S. mediterranea,* which is expressed in a subset of neoblasts as well as in a subset of photoreceptor neurons [26, 31, 32]. Its expression is required for the formation of an anterior photoreceptive neuron population [31, 32]. An additional *SoxB1* gene has been identified in *Schmidtea polychroa* (*Spol-soxB1-2*) and the timing of its expression during embryonic development in this planarian species suggests functions in neural development similar to roles found in other bilaterians [33].

We found that the ortholog of this gene in *S. mediterranea*, *Smed-soxB1-2* (hereafter referred to as *soxB1-2*), is expressed in the epidermis, a stem cell population that may represent an ectodermal lineage progenitor, and the nervous system, including putative sensory neural populations. Remarkably, *soxB1-2* RNAi-treated animals exhibited seizure-like behaviors upon light exposure; in addition, amputated planarians regenerating new heads and uninjured planarians developed significantly smaller cephalic ganglia and reduced sensory structures. These animals also had defects in the epidermis and in sensory nervous system function. These data suggest that *soxB1-2* controls transcription of genes required for the differentiation of a subset of ectodermal progenitor cells into mature epidermal and neural cell types. In this study, we identified downstream targets of *soxB1-2*,

including many genes closely related to those found within the human 'epileptome' (a resource of 499 genes associated with EDs), multiple polycystic kidney disease genes, and GABA receptor components, all of which were found within putative ciliated sensory cell populations. Loss of *soxB1-2* function or the function of a subset of these downstream genes leads to loss of sensory function, including loss of rheosensation (detection of water flow) and vibration sensation. Recent work has identified links between *pkd* genes, cilia function, and epilepsy [34]. This highlights a potential future role for planarians as a model for epilepsy disorders.

METHODS

Animal Care

Asexual *S. mediterranea* (CIW4) were maintained in 1X Montjuïc salts and cared for as previously described [35]. Animals used for all experiments measured 2-5 mm in length and were starved for 1 week prior to initiation of experiments.

Whole mount *in situ* hybridizations and Immunohistochemistry

Whole animals were processed for whole-mount in situ hybridization as outlined in [36] with fast blue labeling performed as described in [37]. For immunostaining with anti-Synapsin (anti-SYNORF1, 1:400, 3C11, DSHB) or anti-Acetylated Tubulin, animals were prepared with the Carnoy's method as described in [38] with a shortened (2 minutes total) incubation in 2% ice cold hydrochloric acid.

RNA interference

Animals were fed bacterially-expressed dsRNA mixed with liver puree [39] 6 times over 3 weeks for most experiments, unless otherwise specified in the figure. *gfp* dsRNA was used as a control in all feedings. Animals were fixed and processed 7 days following the sixth feed for all experiments unless otherwise specified. For regeneration studies animals were amputated anterior to the pharynx 1 day following the 6th feed and allowed to regenerate 14 days before fixation and processing, unless otherwise specified.

RNA sequencing

RNA was extracted from 3 biological replicate groups of 2 worms of either *soxB1-2(RNAi)* or *gfp(RNAi)* animals at days 6, 14, and 24 following the first dsRNA feeding using Trizol (Life Tech) and purified using Direct-zol RNA miniprep kit (Zymo). The extracted RNA was then treated with DNase using the Turbo DNA-free Kit (Life Technologies) and purified with RNeasy MinElute Cleanup kit (Qiagen). cDNA libraries were generated using either TruSeq RNA Sample Prep Kit v2 and sequenced on a HiSeq 2000 System (Illumina) or for the day 6 and day 14 samples, the cDNA libraries were generated using NEBNext® Ultra™ II DNA Library Prep Kit for Illumina® and also sequenced on a HiSeq 2000 System. Sequences were aligned to an asexual genome assembly v1.1 [40]. The R Bioconductor package was used to identify differentially expressed genes with cutoff values of FDR ≤ 0.1, LogCPM score ≥0.15 and Magnified Fold Change of ≥ 1.4. Changes were represented as linear fold changes over controls. Sequences were aligned to the dd_Smed_v4 and dd_Smed_v6 transcriptomes [41] with cut-offs of e-value ≤ e-100 to first determine inclusion in ciliated neuron class per [42], and secondly for gene annotation information that was determined for the dd_Smed_v6 transcriptome, available at http://planmine.mpi-cbg.de/. Additional Gene Ontology terms were determined by taking the transcript sequences from SmedGD and translating through virtual ribosome (http://www.cbs.dtu.dk/services/VirtualRibosome/) using the longest open reading frame finder, using the settings “none_ORF”, stop at stop codon, and search all 6 possible reading frames. These translated peptide sequences were

loaded into Blast2GO version 3.3 using the blastP to nr function with e-value 1e-3, # blast hits = 20, word size = 3, and HSP cutoff length of 25. And then InterProScan was run and GO terms obtained with annotation GO Weight of 5 and E-Value Filter of 1e-6. Duplicated alignments to the dd_Smed_v4 transcriptome were used as criteria to eliminate duplicate transcripts in the RNA-seq lists, in which case duplicate genes that with smaller Magnified Fold Change values were eliminated from the final list. The venn diagram showing overlapping genes was created using eulerAPE v3 software (http://www.eulerdiagrams.org/eulerAPE/).

qPCR

RNA was extracted as described above for 3 biological replicate groups and cDNA was synthesized using the iScript cDNA Synthesis Kit from BioRad. Quantitative PCR was performed on a CFX Connect Real-Time System (BioRad) using SsoAdvanced SYBR Green Supermix (BioRad) with a two-step cycling protocol and annealing and extension temperatures of 58.5°C. The following primers were used for experiments: *caveolin-1* Forward (GAAGCTAATAGCGGTCTACG), *caveolin-1* Reverse (CTGAAACAGAGGCTGCAC), *soxB1-2* Forward (AACTTTCTTGCAGCCAATGC), *soxB1-2* Reverse (GGGAGAATTGTGGAATGATG), *gapdh* Forward (AGCTCCATTGGCGAAAGTTA), and *gapdh* Reverse (CTTTTGCTGCACCAGTTGAA). Three biological and three technical replicates were used for each experiment. *gapdh* was used as a reference gene to normalize the relative amount of each target gene. The changes in gene expression and standard deviations were performed in CFX Manager Software v3.0.

Gene identification and cloning

Sequences were obtained from either an EST library [43] or cloned using gene specific primers into PJC.53.2 [44] or pPR-T4P [45] using ligation independent cloning techniques as described in [46].

Imaging and statistical analyses

All images comparing control and RNAi worms were taken on the same day, under the same light conditions. Live and whole mount *in situ* hybridization animals were imaged using a Leica DFC450 camera mounted on a Leica M205 stereomicroscope. Immunolabeled animals were imaged on a Zeiss Lumar microscope and fluorescent *in situ* hybridization animals were imaged on a Zeiss LSM710 Confocal microscope using 20X and 40X objectives as described in [38]. For *if-b* co-labeling images, approximately 1 mm sections were performed following labeling using razor blades and sections were mounted with anterior sides touching the slide. ImageJ Software [47] was used to determine brain area normalized to the periphery of the body (6 biological replicates) of both *soxB1-2(RNAi)* and *gfp(RNAi)* animals using anti-Synapsin staining or *chat* labeling by tracing the area of the brain with the freeform tool. The two groups were compared using a Student's t-test and significance was accepted at $P<0.05$.

Vibration sensation experiments

Initial vibration sensation experiments for screening were performed by anchoring the dish to a flat surface manually and manually tapping the sides of the

dish to compare reactions to those of control animals using at least 5 animals per experiment. The quantified vibration sensation experiments were conducted in a standard 100 mm petri dish. The petri dish was immobilized by inserting it in the corresponding lid, which was glued to a cold light LED panel and modified using a silicone paste to snugly hold the petri dish in place. The petri dish was filled with 25ml of Montjuïc salts before 4-8 planarians were added to the dish using a 691 plastic transfer pipet. Control *(gfp)RNAi* and experimental RNAi groups were assayed alternatingly. All conditions were run in triplicate, with a total of N=20 specimen each. To account for potential behavioral differences independent of the stimulus, no stimulus controls were performed for all conditions. The trials consisted of three 8 sec free runs followed by 3 stimuli of 10 taps each. The taps were fully automated using a computer-controlled custom tapping device. Recording was performed at 5 frames per second (fps) using a Basler A641f CCD camera and a custom MATLAB routine. Image analysis was performed in MATLAB to obtain center-of-mass motion and worm length over time. To account for size differences among planarians, the average gliding length for each animal was calculated and applied to further analysis. The behavior of each animal during each tapping series was then quantified as the contraction amplitude, which is the ratio of worm length at the most contraction point to the average gliding length.

Rheosensation experiments

Initial rheosensation experiments for screening were performed by using a P1000 pipette to gently squirt planarian water across the dorsal surface of the

animals to compare reactions to those of control animals using at least 5 animals per experiment. Rheosensation experiments were performed in a custom rectangular imaging arena, 13.4mm width x 60.4mm length x 15mm depth. The arena was illuminated from the side using a white cold light LED panel and imaged from the side. The same MATLAB-controlled camera and lens were used for recording at 5fps as in the vibriosensation experiments. 3ml of Montjuïc salts were added to the arena for an experiment. Colored Montjuïc salts were prepared by adding 7.5 µl blue food color to 1ml Montjuic salts. A planarian was added to the arena using a 691 plastic transfer pipet. Once gliding parallel to the long side of the arena (and the camera), the worm was stimulated by pipetting 15 µl of the blue water onto its back. Care was taken that the pipet tip was immersed in the water before pipetting. The blue color allowed for a visualization of the dye as it hit the specimen. The side-view imaging ensured that the stimulus was solely through the water flow and not through accidentally touching the animal. After each experiment, the specimen was removed and the arena was rinsed with DI water, wiped, and refilled with 3 ml of fresh Montjuïc salts. As in the vibriosensation experiments, control and experimental groups were assayed alternatingly. Image analysis was performed in Image J and MATLAB to obtain worm length over time. To account for size differences among planarians, worm length was normalized by worm's gliding length before being pipet. The behavior in rheosensation assay was then quantified as the contraction amplitude.

Movement imaging experiments

The movement imaging experiments were performed in a standard 100mm petri dish. The petri dish was filled with 25 ml Montjuïc salts before 10-11 planarians were transferred into the petri dish by a 691 plastic transfer pipet. Both control *(gfp)RNAi* and experimental RNAi planarians were run in two plates. The experiments consist of imaging on an IR panel (Advanced Illumination, BL-0404) and a white LED panel (LEDwholesealers, 2101WH). Before the imaging on the IR panel, the dish was put onto the IR panel and allowed to sit for 15 min so the worms could settle down. The imaging of worms on the IR panel was 10 min long, recorded by a MATLAB-controlled Basler A641f CCD camera at 5 fps. After imaging on the IR panel, the dish was put aside and exposed to white LED light (KEDSUM LED desk lamp, 7w) for 40 min. The dish was then put onto the white LED panel and recorded by camera for 10 min at 5 fps. Image analysis was quantified in MATLAB. The spline of each worm was extracted in MATLAB by fitting the spline to facilitate the further calculation of the bending angle. The spline was then split into 9 segments, resulting in 8 consecutive angles. The sum of the absolute value of the 8 consecutive angles was then used to describe the worm's bending property. By tracking the worms throughout the video, the average value of the total bending angle was calculated. Additionally, the center-of-mass of each worm was tracked throughout the video. Worm tracks were sometimes truncated, when worms were across each other or on the edge. Speed was calculated for all tracks at 2s intervals to reduce the

effect of noise. The speed was scaled by the worm's length squared to the worm's area. The mean gliding speed was calculated by averaging the speed data.

Chemotaxis experiments

The chemotaxis experiments were conducted in a standard 100mm petri dish. The dish was filled with 25ml Montjuïc salts before 10-11 planarians were transferred into the petri dish by a 691 plastic transfer pipet. Both control *(gfp) RNAi* and experimental RNAi planarians were run in two plates. The liver mixture was prepared with organic chicken liver diluted by 1x Montjuïc salts at the ratio of 1:2. Each dish was imaged on a white LED panel by the Basler A641f camera at 5fps. The dish was first imaged without any food for 10 min as a control imaging. After the control imaging, 50uL liver mixture was injected into the center of the dish slowly by a pipet (Gilson, 200uL) and the dish then was imaged for 10 min. Image analysis was performed in MATLAB to track worms' movements. A food area (a circle with half of the radius of the dish) was defined for each group manually and applied to both videos with and without food. The amount of time worms spent in the food area during the second half of the videos with and without food, was calculated and compared with each other.

Single cell RNA-sequencing analysis

scRNA-seq data was obtained from NCBI Gene Expression Omnibus (GEO accession GSE79866) [48] and NCBI Sequence Read Archive (SRA:PRJNA276084) [42]. Reads were aligned to the SmedASXL transcriptome assembly under NCBI

BioProject PRJNA215411 using bowtie2 with 15 bp 3' trimming. All cells with detection of *soxB1-2* expression were extracted for analysis. The violin plot was constructed using log2-transformed read counts with the Seurat R package [49]. Heatmaps were produced using log2-transformed read counts [48]. Pseudotime analysis was performed using Waterfall source code available from [50], as described in [48]. Briefly, *soxB1-2*-positive cells were extracted and cell groups were identified by hierarchical clustering based on the top 1000 most variable transcripts across these cells. Principal components analysis was performed, revealing three distinct cell branches extending from a central vertex. Expression of known tissue-specific markers was used to identify one of the branches as neural and another as epithelial, while the third branch could not be identified and was removed from the analysis. Pseudotime values were assigned to each cell, with pseudotime 0 being the vertex, positive values representing progression along an epithelial lineage and negative values representing progression along a neural lineage.

RESULTS

soxB1-2 loss of function causes seizure-like phenotype, reduction in brain size, and loss of mechanosensory function in planarians

We sought to determine if *SoxB1* genes play a role in planarian neural regeneration and function due to their known functions during neurogenesis. *Smed-soxB1-1* is expressed in a subset of planarian neoblasts and loss-of-function results in non-regeneration of a subset of anterior photoreceptors [31, 32]. However, the function of another *soxB1-2* gene in planarians had yet to be explored. We performed RNAi-mediated knockdown experiments on planarians to determine the function of this gene (Figure 4.1A) and found that the animals displayed abnormal behaviors when they were exposed to white light (Figure 4.1B). These behaviors included body movements that were previously described as seizure-like behaviors [27]. In particular, these worms exhibited snake-like twisting movements, bending movements, and corkscrew movements, all resulting in various degrees of bending (Figure 4.1B-C). To verify the phenotype was not due to off target effects, we performed knockdown experiments with two additional non-overlapping constructs and observed consistent behavioral results (data not shown). Interestingly, *soxB1-2(RNAi)* animals did not exhibit these behaviors when kept in the dark or in infrared light (Figure 4.2A). We observed that these animals lost contact of their ventral surface with the dish when exhibiting these behaviors (Figure 4.1A). These movements were detrimental to the forward movement progress of the worms; the speed of their center of body mass was significantly slower than that of the control worms (Figure 4.1D).

soxB1-2 is expressed in the epidermal and neural lineages as well as putative sensory neurons

The robust behavioral phenotype we observed in *soxB1-2(RNAi)* worms led us to hypothesize this gene is expressed in the nervous system. We performed whole-mount in situ hybridization (WISH) to *soxB1-2* with an RNA probe to determine its expression pattern and observed strong labeling in the head periphery (Figure 4.1E, black arrowheads), along the dorsal ciliated stripe (Figure 4.1E, yellow arrows), and in the mouth of the pharynx (Figure 4.1E, black arrow), all areas thought to be anatomical regions rich in sensory neurons [24, 51-55]. We observed punctate labeling throughout the animal and faint epidermis staining, which we also detected when we labeled animals with two other non-overlapping *soxB1-2* riboprobes (Figure 4.2B). To confirm our WISH results, we queried two published single cell RNA-sequencing datasets (scRNA-seq) to determine if there was enrichment of gene expression in specific cell populations [42, 48]. We found the greatest enrichment of expression in the ciliated neuron category (the putative sensory neuron class), a subset of neurons, and cells from the epidermal lineage (Figure 4.1F).

To further explore the identity of the *soxB1-2*$^{+}$ cell types, we performed double fluorescent *in situ* hybridization experiments (dFISH). These experiments revealed *soxB1-2* expression in PIWI-1 protein-expressing cells (a marker of stem cells and their progeny, [56]). These cells were abundant in the dorsal head region of the planarian, near the dorsal ciliated stripe region (Figure 4.3A). Due to this

labeling, we hypothesized that there exists a population of *soxB1-2+* stem cells and neural progenitor cells. To test this, we assayed for co-expression of *soxB1-2* and the stem cell marker, *piwi-1* [57], as well as a marker of the neural progenitor class, *piwi-2* [48]. Although rare, we did observe both of these populations (*piwi-1* co-labeled cells shown anterior to the pharynx, arrows in Figure 4.3B, and *piwi-2* co-labeled cells shown in between the lobes of the brain, arrows in Figure 4.3C).

Given that it has been hypothesized that the dorsal ciliated stripe functions in rheosensation and the expression of *soxB1-2* in this area, we wanted to confirm that the *soxB1-2+* cells in this area were neuronal. We performed dFISH with *soxB1-2* riboprobe and a riboprobe mixture of the pan-neuronal markers *synaptotagmin* and *synapsin.* This experiment revealed extensive co-labeling of *soxB1-2* and the neuronal mix in the area of the dorsal ciliated stripe (arrows in Figure 4.3D). These cells are located beneath the epidermis, therefore, it is likely that the abundant cilia labeling seen at the dorsal ciliated stripe does not originate from the monolayer of epidermis on the dorsal side of the animal, but rather from this population of neurons located deeper within the mesenchymal space.

soxB1-2 loss of function causes reduction in brain size and loss of mechanosensory function in planarians

Due to the expression of *soxB1-2* in the neural lineage, we sought to determine if there were overall morphological changes to the central nervous system following *soxB1-2* loss of function. Therefore, we repeated RNAi experiments on intact and regenerating animals (Figure 4.1G) and found an overall reduction in

the size of the regenerating and homeostatic brain in *soxB1-2(RNAi)* worms (Figures 4.1H-I, Figure 4.2C).

Planarians have multiple ciliated structures. The ventral epidermal cilia are the source of the normal gliding locomotion of planarians [58]. Additionally, cilia are abundant in the protonephria (the filtering organs akin to the vertebrate kidney) and finally, there are multiple ciliated structures that are hypothesized to contain ciliated sensory neurons, including the auricles (found in the peripheral region of the head in *S. mediterranea*) and the dorsal ciliated stripe [24, 51-55]. The movement phenotype that we observed (Figure 4.1B-D), coupled with expression in the epidermal and neural classes, led us to explore whether there were changes to the cilia in the dorsal ciliated stripe, the auricle region, and the ventral cilia. Indeed, we observed a visible loss of anti-Acetylated Tubulin labeling of the cilia [59] at the dorsal ciliated stripe (Figure 4.1J, white arrowheads), an overall reduction of labeling across the dorsal and ventral ciliated surfaces (Figure 4.1J, yellow arrowheads) and a loss in the density and thickness of labeling at the auricle region compared to control animals (Figure 4.1J, white arrows). The dorsal ciliated stripe is hypothesized to function in rheosensation (detection of water flow) [24, 51-55]. Thus, we tested the ability of *soxB1-2(RNAi)* animals to detect water flow across their dorsal surface, which results in a body contraction characterized by shortening of the length of the animal from the anterior to the posterior end in controls. This reaction has also been observed when providing a tapping stimulus [60], which may be due to the water flow movements created by the tapping stimulus or to detection

of vibration caused by the tapping. Due to the severe movement defects of *soxB1-2(RNAi)* worms following our original RNAi feeding scheme, we altered the dsRNA feeding schedule to find a treatment course wherein the worms were still gliding similarly to the control worms (Figure 4.1K). We then developed rheosensation and vibration sensation assays to deliver consistent stimuli across groups (see methods). *soxB1-2(RNAi)* planarians showed significantly reduced responses to vibration and rheosensory inputs compared to controls (Figure 4.1L-M).

Determination of *soxB1-2*-transcriptionally regulated genes by RNA-seq

soxB1 genes constitute a well-conserved transcription factor subfamily (reviewed in [61]), therefore the dysfunction we observed in *soxB1-2(RNAi)* animals likely represented changes in the transcription of genes necessary for neuronal function. Therefore, we wanted to determine the downstream genes responsible for these behaviors. We started by comparing the whole-animal transcriptomes of control animals versus *soxB1-2(RNAi)* animals at 24 days following the first RNAi treatment (Figure 4.4A). This resulted in a list of 2246 differentially expressed genes (1192 downregulated and 1054 upregulated genes, Supplemental file: ross_rnaseq_spreadsheet.xlsx, day 24 down and day 24 up). However, we observed that defects in rheosensation and an initial snake-like phenotype occurred as early as day 14 following the initial RNAi feed (data not shown), thus we surmised that the day 14 list included genes far downstream of *soxB1-2* transcriptional regulation in sensory neurons. In order to perform a functional screen better targeted to genes directly regulated by *soxB1-2* within sensory neurons, we decided to determine

differentially expressed genes at earlier time points. We observed on the day 24 downregulated list (Supplemental file: ross_rnaseq_spreadsheet.xlsx, day 24 down), *caveolin-1* (*cav-1*, transcript ID: GCZZ01029462.1), a gene that has an expression pattern resembling that of *soxB1-2* in the auricle region and dorsal ciliated stripe [37]. We confirmed co-expression of this gene with *soxB1-2* in the ciliated neuron class [42]. Although there was no reported phenotype caused by knockdown of this gene, we figured that it represented a good candidate for *soxB1-2* transcriptional regulation within sensory neurons; therefore, we used the following criteria to determine two additional timepoints at which to perform RNA-seq: 1) a timepoint when expression of both *soxB1-2* and *cav-1* was stably reduced (which we determined by qPCR to be day 6 following the first RNAi feeding, Figure 4.5A-B), and 2) the timepoint when the *soxB1-2* phenotype first appeared (day 14 following the first feeding). These resulting datasets consisted of 630 differentially expressed genes in the day 14 dataset (327 downregulated genes, Supplemental file: ross_rnaseq_spreadsheet.xlsx, day 14 down, and 303 upregulated genes, Supplemental file: ross_rnaseq_spreadsheet.xlsx, day 14 up) and 220 differentially regulated genes in the day 6 dataset (116 downregulated genes, Supplemental file: ross_rnaseq_spreadsheet.xlsx, day 6 down, and 104 upregulated genes, Supplemental file: ross_rnaseq_spreadsheet.xlsx, day 6 up). As expected, there was significant overlap between the downregulated datasets (Figure 4.4B).

We subsequently asked if there was a correlation between the genes regulated by *soxB1-2* in planarians and genes implicated in human EDs. We searched

a comprehensive dataset of genes associated with human EDs [6] for similarity with genes in our datasets by performing blastx (e-value cutoff of e^{-1}) and found many represented genes in our datasets (Supplemental file: ross_rnaseq_spreadsheet.xlsx, all lists). The list that had the highest number of genes related to human epileptome genes was the day 14 down list, with 30% of the 327 down-regulated genes showing similarity to genes within the human epileptome.

Although there are some examples of transcriptional repression by *soxB1* genes [62, 63], *soxB1* genes are generally known to function as transcriptional activators [64-66]. Given this activating role, the sensory loss and movement defects at day 14, and the strong correlation with human epileptome genes, we decided to focus on genes found within the d14 downregulated list. Furthermore, we reduced this list to only include genes that remained downregulated at day 24. This reduced the total number of genes to 205 (Supplemental file: ross_rnaseq_spreadsheet.xlsx, day 14 down, stays down at 24), of which 36% showed similarity to proteins found within the human epileptome. To select genes for a functional screen, we exploited a publicly available dataset of planarian genes enriched in neural or ciliated neural populations [42] by performing blastn of transcripts within the day 14 down dataset to the transcriptome used for this scRNA-seq dataset (cutoff set at e-value of e^{-40}). We found 21 and 19 genes of the 205 genes to be enriched in the neural and ciliated neural classes, respectively. Knowing that this did not represent a completely inclusive dataset (only 7 cells from that scRNA-seq study were attributed to the ciliated neuron cluster), we wanted to search for genes that might represent

functions necessary for neural function. Therefore, we used Blast2GO to obtain a list of functional GO terms and mined our list for the following key GO terms: ion channel activity, cation or calcium ion binding, intermediate filament, ion transport or transmembrane transport, and microtubule-based movement. Overall, this list included a total of 89 genes, including genes selected for inclusion within the neural and ciliated neural scRNA-seq classes. We successfully cloned, determined expression patterns by WISH, and performed functional analysis on 86 of these genes (highlighted genes in Supplemental file: ross_rnaseq_spreadsheet.xlsx, day 14 down, stays down at 24, cDNA fragment sequences of genes used in this study are supplied in Supplemental file: ross_cloned_genes.fasta).

We next wanted to correlate expression of these genes within *soxB1-2*$^{+}$ cells and determine if they were expressed in epidermal or neural lineages. To do this, we mined two available scRNA-seq datasets [42, 48] for any cells that expressed *soxB1-2* (FPKM of ≥ 1), performed hierarchical clustering of these cells to sort them into epidermal and neuronal clusters and confirmed the expression of known epidermal and neural marker genes to confirm the identity of the cells within these clusters (Figure 4.4C-D). We then mined the transcriptomes of these cells for expression of the genes from our datasets (Figure 4.5C). We were able to cluster 28 *soxB1-2*$^{+}$ cells into an epidermal class and 9 *soxB1-2*$^{+}$ cells into a neuronal cell class (Figure 4.4C and 4.4D, respectively). Additionally, we confirmed expression of *rootletin*, a gene encoding a structural protein that is specific to cilia, in 7 out of the 9 *soxB1-2* neurons, confirming that the majority of cells within this class are ciliated neurons

(Figure 4.4D). To further confirm the expression of *soxB1-2* in ciliated neurons, we mapped the expression of all of the genes enriched in the ciliated neuron cluster from [42] to the *soxB1-2*$^{+}$ cells that we determined to be neurons and found overwhelming expression of the majority of these genes in this cell class (Figure 4.6). We then explored the transcriptomes of each of the *soxB1-2*$^{+}$ epidermal and neuronal cells for the expression of all *soxB1-2* differentially regulated genes and examined if they were expressed in the epidermal, neuronal, or both of these cell classes with FPKM > 1 (Supplemental file: ross_scranseq_spreadsheet.xlsx, all lists). These data allowed us to confirm that 63% and 59% of the day 14-downregulated genes were expressed in the *soxB1-2+* epidermal and neural classes, respectively (Supplemental file: ross_scranseq_spreadsheet.xlsx, day 14 down).

soxB1-2 labels a population of ectodermal progenitor cells as well as cells undergoing differentiation through the epidermal and neural lineages

In other major model organisms, *soxB1* genes have roles in ectoderm specification [62, 67, 68]. Given the expression of *soxB1-2* in cells of both the epidermal and neural lineages, we asked whether *soxB1-2* might be expressed in an ectodermal progenitor population in the planarian. Therefore, we performed Waterfall pseudotime analysis to investigate the expression of *soxB1-2* during ectodermal differentiation. We first performed hierarchical clustering of all *soxB1-2*$^{+}$ cells present within scRNA-seq datasets [42, 48] and clustered the cells into 8 different classes (Figure 4.7A). Next, we performed principle component analysis (PCA) on all *soxB1-2*$^{+}$ cells and noticed three distinct lines originating from a

common vertex (Figure 4.7B). To determine the identity of these groups of cells, we marked the expression of known neural markers (Figure 4.7C), the stem cell marker *piwi-1* (Figure 4.7D), and epidermal lineage markers (Figure 4.7E) onto the cells of the PCA plot and identified a neural lineage branch, epidermal lineage branch, and that the cell cluster at the vertex had the highest expression of *piwi-1*. However, the identity of the third branch was still unknown; we explored the expression of lineage markers of the other major tissue groups in the planarian, but we could not predict the cell-type relationship of this third branch (Figure 4.7F). Therefore, we excluded this cluster from further analysis. After removal of cells within the third branch and performing of PCA analysis, two distinct branches were resolved that stemmed from a common vertex (Figure 4.8A). One of these branches appeared to have increasing expression of *soxB1-2* and, after overlaying the expression of known lineage genes onto the PCA plot, we determined an epidermal branch, a neural branch, and highest expression of both the stem cell marker, *piwi-1,* and the neural progenitor (called nuNeoblasts, [48]) marker *piwi-2,* at the vertex, with expression of *piwi-2* maintained in the neural lineage. We subsequently noted that the branch with increasing expression of *soxB1-2* was the neural branch. These expression patterns suggested a trajectory wherein an ectodermal progenitor population diverged down two paths, either neural or epidermal fates. To temporally arrange the cells and assign them pseudotime values, we used Waterfall analysis [48, 50] to flatten the trajectories from the PCA analysis. In the pseudotime plots, we once again visualized the increase in *soxB1-2* expression during differentiation along the

neural lineage (Figure 4.8B). We also explored the timing of expression of neural progenitor markers *ptprd-9* and *ski-1.* These genes had a peak of expression early during the neural differentiation process (Figure 4.8C). As expected, known pan-neural and pan-epidermal markers increased during the differentiation process to neurons or the epidermis, respectively (Figure 4.8D-E). This analysis allowed us to plot the expression of some of the genes from our screen that were downregulated in the *soxB1-2(RNAi)* worms at day 14. As predicted, we saw an increase of expression in genes expressed in *soxB1-2*$^{+}$ neurons during neural differentiation (Figure 4.8F), and an increase in expression during both neural and epidermal differentiation in genes expressed in both the neural and epidermal lineages (Figure 4.8G). Interestingly, the expression of the downstream genes expressed in both neurons and the epidermis resembled that of *soxB1-2*, in that the expression in the neural lineage tended to be relatively higher than expression in the epidermal lineage.

Genes downstream of *soxB1-2* mark the epidermis and sensory neuron populations

We wanted to determine the location of expression of genes downstream of *soxB1-2* transcriptional regulation to visualize the patterns of epidermal and neuronal expression predicted by the scRNA-seq data. We performed WISH on the 86 genes we cloned from our screen list and sorted them based on inclusion in the *soxB1-2*$^{+}$ epidermal, neuronal, or neuronal and epidermal classes (Figures 4.9-4.10). Some genes for which we could not attribute expression to a class based on the

single cell sequencing data, we assigned to a class based on their expression pattern in the animal (see genes with an asterisk in Figures 4.9-4.10, 4.11A-C). We were able to classify 84 of the 86 genes to epidermal or neuronal classes and the classifications based on scRNA-seq data were overwhelmingly confirmed. Some genes were also expressed in other tissues, for instance, some genes (for example *sodium/potassium-transporting ATPase-like, ATPA-like,* Figure 4.11B), were expressed in the protonephridia (the filtering organ akin to the vertebrate kidney, [69-71] as well as the epidermis. We often observed expression in areas thought to be rich in sensory neurons, including expression along the dorsal ciliated stripe, the auricle region of the head, along the body periphery, and in the pharynx (Figure 4.11A). Many genes had a recurring pattern of expression that consisted of labeling in the dorsal ciliated stripe, which terminated at the anterior of the worm in a triangle shape, and labeling of two stripes at the periphery of the body. To further characterize this population, we performed dFISH for a subset of these genes with the dorsal-ventral boundary marker *intermediate filament-b* (*if-b*) and inspected the presumed sensory-neuron gene expression relative to the animal's dorsal-ventral boundary (Figure 4.11D). We found consistent labeling of a population of cells beneath the epidermis on the dorsal side of the worms (the dorsal ciliated stripe, Figure 4.11D, red arrows), as well two distinct peripheral populations, one located dorsally to the *if-b*$^{+}$ boundary that we named the dorsal peripheral stripe (white arrow in Figure 4.11D), and one located ventrally to the *if-b* boundary that we termed the ventral peripheral stripe (yellow arrowhead in Figure 4.11D). To

confirm that these putative sensory neurons were *soxB1-2+,* we performed dFISH for the *soxB1-2* downstream gene, *polycystic kidney disease 1-like-2* (*pkd1L-2*), with *soxB1-2;* we found extensive co-expression of *soxB1-2* within this population (shown in the dorsal ciliated stripe region and highlighted with arrows in Figure 4.11E). To further characterize this putative sensory population, we performed additional co-labeling experiments within the *pkd1L-2* population with other *soxB1-2* downstream genes to determine the extent of co-expression within this population. We observed extensive overlap of expression between *pkd1L-2* and other genes with similar expression patterns. For example, both *sargasso* and *gaba type a receptor gamma 3 subunit-like-2 (gabrg3L-2)* labeled nearly all *pkd1L-2* cells (white arrows in Figure 4.11F, H, I), as well as cells located near these putative sensory neuron rich areas (yellow arrowheads in Figure 4.11F, H, I). Additionally, *gabrg3L-2* was expressed in a *pkd1L-2*^{neg} population located in a more ventral region of the head periphery (yellow arrowheads in Figure 4.11I). *gabrg3L-1* appears to have a nearly complete overlap of expression in the dorsal ciliated stripe area with *pkd1L-2* (Figure 4.11G). Unlike *sargasso, gabrg3L-2,* and *gabrg3L-1*, which extensively co-label *pkd1L-2+* cells, *hemicentin-1-like* (*hmcn-1-L*) is expressed in a mutually exclusive population to *pkd1L-2* (yellow and white arrowheads in Figure 4.11J), despite having a very similar expression pattern to *pkd1L-2* by WISH (Figure 4.11A).

RNAi knockdown of genes downstream of *soxB1-2(RNAi)* recapitulate the *soxB1-2 phenotype*

To determine which genes downstream of *soxB1-2* conferred the seizure-like phenotype, we performed a functional screen for the 86 differentially expressed genes at day 14 for defects in locomotion, rheosensation, and vibration sensation (feeding schemes depicted in Figure 4.13A and B). During the initial screening process, we performed these tests by: 1) visual observation of movement defects, 2) squirting the worms across their dorsal sides and visually observing for lack of rheosensensation response, and 3) by manually tapping the sides of the petri dishes to look for defects in vibration sensation (Figure 4.13). We found 17 genes with striking behavioral defects (Table 4.1), including defects in both rheosensation and vibration sensation and aspects of the seizure-like phenotype. To assign names to genes, we aligned these sequences to a published and fully annotated transcriptome [41]; in cases where a database match was present with an e-value cut-off of e^{-30}, we assigned a name based on the nearest homolog. We named one gene for which RNAi animals had normal movements, but specifically lacked rheosensory and vibration sensory response, *Smed-sargasso* (*sargasso*) after the North Atlantic sea known for its lack of water current.

As proof of concept, we further quantified the movement phenotype of one of the genes that caused seizure-like movements, *sodium/potassium-transporting ATPA-like*, a transmembrane ion pump necessary for regulating the membrane potential of neurons [72]. We observed similar results to loss of *soxB1-2* function in

respect to the significant increase in bending and decrease in overall forward speed of the worms (Figure 4.12). Other aspects of movement phenotypes that we observed involved genes attributed to the neural class, or the neural and epidermal classes, with defects similar to the twisting, corkscrew movements seen with the *soxB1-2* phenotype, which in many cases later progressed to an overall slowing in movement and further signs of defects in epidermal integrity, such as lesions or lysis (Table 4.1). As with *soxB1-2* RNAi, we suspected cilia defects might be a result of knockdown of some downstream genes. Therefore, we performed anti-Acetylated Tubulin labeling on the RNAi animals of downstream genes to assess whether there were also reductions in the abundance of cilia. Indeed, we found that cilia expression was reduced following loss of function of 14 of the screened genes (Figure 4.13C-D).

For genes that did not yield movement defects when knocked down, but rather a loss of sensory stimuli responses, we performed semi-automated behavioral testing post-RNAi and observed significant reductions in the response to rheosensory and vibration stimulation (Figure 4.13E-F). Additionally, during the course of our screen, we noted that some groups stopped eating prematurely in the feeding schedule; these genes were expressed in the auricles, which are thought to be involved in chemosensation [51, 55] as well as the mouth of the pharynx, which is also thought to have chemosensation function [51]. We quantified the chemosensory defects of *pkd2-1, putative protein-37835, echinoderm microtubule associated protein like-1* (*eml1*), and *pkd2L-1* by recording the time these worms

spent in a zone with food, compared to the same zone, without food and normalized these results to those of control animals. We observed a significant reduction in time spent in the zone with food compared to the zone without food for most of these genes (Figure 4.13G), indicating that a subset of genes downstream of *soxB1-2* function have roles in chemosensation and rheosensation. Altogether indicating that *soxB1-2* regulates the transcription of genes necessary for the function of sensory neurons in planarians.

DISCUSSION

A putative ectodermal progenitor population is marked by *soxB1-2* expression

SoxB1 gene function has been implicated in both vertebrates and invertebrates in ectoderm formation, with evidence for both activating and repressive transcription regulatory functions. For instance, in frog embryos, the *SoxB1* gene, *Sox3,* promotes ectodermal fate by repression of *nr5* [62] and in sea urchin embryos, the SoxB1 protein, SpSoxB1, is essential for promoting the transcription of SpAN in the non-vegetal domain [67]. After the early blastula stage, the only cells with nuclear SpSoxB1 are the ectodermal cells, which further supports a role of SpSoxB1 as a major regulator of the asymmetric transcription of SpAN that leads to the specification of the ectoderm in the early embryo [67]. These findings suggest a conserved role for *soxB1* genes in ectoderm formation. Our pseudotime analysis findings suggest that an ectodermal progenitor population expresses *soxB1-2* and that this progenitor population is fated to differentiate into epidermis or neural cells (Figure 4.14A). However, loss of *soxB1-2* function does not cause a total loss of regeneration of neural structures or the epidermis, but rather seems more restricted to particular subset of these populations. This could mean that although *soxB1-2* is expressed in an ectodermal progenitor, it is not essential for specification and differentiation of this population. Alternatively, this population may represent one subset of an ectodermal progenitor in planarians and perhaps there are other ectodermal progenitor populations as well. Future scRNA-seq experiments using emerging technologies that facilitate sequencing of greater cell numbers should

expand the number of *soxB1-2*-expressing progenitor cells available for analysis, which could help to delineate the progression of *soxB1-2*$^{+}$ cells or resolve whether multiple ectodermal progenitor populations arise from pluripotent neoblasts.

SoxB1 genes are implicated in neurectoderm specification [73] and have maintained roles during the specification and maintenance of the nervous system [64, 74-76]. Also, studies have found that *SoxB1* genes play roles in the specification of ciliated sensory structures. For example, the cuttlefish gene *Sof-SoxB1* is broadly expressed in the ectoderm during early development and later becomes restricted to the developing nervous system and the ciliated sensory epithelium [77]. *soxB1* genes are expressed in the neurogenic ciliary bands of acorn worm larvae [78] and the ciliated stigmatal cells of *Ciona intestinalis* [79]. Taken together, these studies indicate a conservation of roles for *SoxB1* genes in ciliated cells, especially ciliated sensory cells. Our findings demonstrate that *Smed-soxB1-2* remains expressed during the ectodermal differentiation process in both the ciliated epidermis as well as ciliated sensory neurons (Figure 4.14A).

The function of the *SoxB1* paralog, *soxB1-1,* in *S. mediterranea*, has been previously investigated*. soxB1-1* is expressed in a subset of neoblasts and anterior photoreceptor neurons [31, 32]. *soxB1-1* loss-of-function leads to depletion of a population of anterior photoreceptor neurons [31]. This function and expression is consistent with a conserved role of *SoxB1* genes in eye formation [66, 80] and during neurogenesis. In *Schmidtea polychroa*, the sister species to *S. mediterranea*, the ortholog to *Smed-soxB1-2, Spol-soxB1-2,* is expressed in both progenitor cells and

differentiated neurons near the head periphery of the embryo during organogenesis, a stage after the appearance of newborn neurons when the very early embryonic nervous system begins to form a pattern in the developing embryo [33, 81]. Later, during embryogenesis when the organs are finishing the maturation process, just prior to hatching, this gene is expressed in the lateral margins of the head and the body [33], which resembles the WISH expression pattern we observed in adult *S. mediterranea* (Figure 4.1). This conservation of expression during embryogenesis reflects the possibility that the function of *SoxB1-2* during differentiation might be conserved during embryonic and adult neurogenesis. However, an analysis of *soxB1-2* expression at the single cell level and examination of the functional consequences of *soxB1-2* inhibition during embryogenesis will be helpful to confirm that this is indeed the case.

Genes associated with epilepsy in humans are found downstream of *SoxB1-2* regulation

Mutations in the *SoxB1* genes *Sox1* and *Sox2* are associated with EDs in humans (GWAS ID: HGVST522). Haploinsufficiency of either of these genes in humans leads to widespread deleterious effects of the nervous system, including eye deformities and hypopituitarism [82-84]. In mice, loss of *Sox1* leads to epileptic seizures [12, 13], possibly due to the role of *Sox1* in specification of ventral striatum neurons [13] and maturation of telencephalic precursors in the developing brain [85]. Idiopathic epilepsies with a monogenic or polygenic inheritance are thought to cause up to 47% of all EDs in humans, with only approximately 2% of these

having a monogenic link [86]. Therefore, the genetics underlying epilepsy remains a complex issue. In the case of monogenic epilepsies, the most common genes linked with these disorders are ion channel subunits [87]. We used a dataset of 499 genes associated with epilepsy in humans [6] to determine if there was any overlap with the genes that have reduced expression in our day 14 downregulated list; indeed, 36% of the genes (which stay downregulated through day 24 following RNAi) are related to genes associated with human EDs. For example, inhibition of the downregulated gene *trpc-like* that is expressed in a subset of *soxB1-2*$^{+}$ neurons, leads to slow twisting movements that resemble the seizure phenotype. *trpc-like* shows similarity to the epilepsy-associated gene *ankyrin-3* (e-value $2e^{-96}$). Transient Receptor Potential-Canonical Channels (TRPC) are Ca^{2+}-permeable cation channels containing ankyrin repeats [88].

Ankyrin-3 is known for clustering Ca^{2+} and Na^{+} channels in the axons of neurons [89], indicating that mutations to these genes might disrupt normal Ca^{2+} signaling that is necessary for neuronal function. *Atpa-like* gene inhibition caused snake-like movements that resembled the seizure-phenotype. This gene very closely resembles *Na^{+}/K^{+}-transporting ATPase subunit alpha-2 precursor* (e-value 0), which is another gene associated with epilepsy [6]. The function of this gene is necessary for forming ion gradients, which affects establishment of membrane potential and Ca^{2+} movement across the membrane [90]. These actions are necessary for controlling the electrical excitability of neurons as well as other cell types. scRNA-seq data confirms the expression of this channel in *SoxB1-2+* epidermal cells and not

neuronal cells, however, the lack of confirmed neuronal expression is likely due to the limited number of neurons in the current scRNA-seq datasets; there are only 9 *SoxB1-2+* neurons currently available for analysis. Given the conservation of this gene with its mammalian counterpart, we speculate that it is expressed in a subset of neuronal cells as well.

Two GABA receptor genes that were downregulated following *SoxB1-2* knockdown led to defects in sensory function. Although these did not recapitulate aspects of the seizure phenotype in planarians, the expression of these genes in neuronal cells and reduction in mechanosensory function following their knockdown implicates these genes in planarian neuronal physiology. *gabrg3-L-1* shows similarity to human *$GABA_A$ Receptor Beta 1 Subunit* (*GABRB1,* e-value $6e^{-12}$) and *gabrg3L-2* shows sequence similarity to *$GABA_A$ Receptor Beta 3 Subunit* (*GABRB3,* e-value $6e^{-10}$). These genes are part of the $GABA_A$ receptor, the ionotropic receptor for the main inhibitory neurotransmitter of the central nervous system [91]. Mutations in this receptor are highly implicated in human EDs [92, 93] and even heterozygous disruption of *gabrb3* in mice produces increased epileptiform EEG activity and elevated seizure susceptibility [94]. While these ED-associated gene were expressed in *SoxB1-2+* cells, it will be interesting to confirm the direct transcriptional regulation of these genes by *SoxB1-2*, first by confirming binding of SOXB1-2 to target genes by ChIP-seq.

Pkd genes, cilia, and epilepsy

Many of the genes downregulated following *soxB1-2* RNAi have conserved roles in specification or function of cilia. We observed cilia loss at sensory structures following *soxB1-2* inhibition as well as following knockdown of several downstream genes (Figure 4.13). One gene with reduced expression in our day 14 downregulated list, *foxJ1-4*, is a gene with well-known roles in motile ciliogenesis [95]. *foxJ1-4* was previously implicated in causing cilia loss in planarians, as well ultimately causing edema, likely due to loss of protonephridia function [95]. *foxJ1-4* is expressed in both neuronal and epidermal *soxB1-2*$^{+}$ cells. Prior to inching and edema phenotypes associated with dysfunction of the ventral epidermis and protonephridia, respectively, we observed twisting and curling movements of the *foxJ1-4(RNAi)* worms, indicating a recapitulation of the seizure phenotype. This might indicate a role of cilia in the seizure phenotype.

Furthermore, we observed twisting movements alongside the typical inching movements associated with epidermal cilia dysfunction with RNAi of *C2D2A-like*, which, like *foxJ1-4,* is expressed in both neuronal and epidermal *SoxB1-2+* cells. C2D2A dysfunction was recently identified as a genetic link in Meckel Syndrome, which is an embryonic lethal disorder [96], with findings that C2D2A functions in neuronal primary ciliogenesis as well as ciliogenesis in other tissues and has putative roles in Ca^{2+} signaling [96]. Meckel Syndrome represents one of many ciliopathy diseases that show overlap between neuronal and kidney dysfunction.

Another gene family with overlapping roles in kidney disease and neuronal dysfunction are polycystic kidney disease genes (*pkd* genes). We found that neural function was perturbed following knockdown of three *pkd* genes that were downregulated following *soxB1-2* RNAi. Two of these genes, *pkd1L-2* and *pkd2L1* were expressed in ciliated sensory neurons and their inhibition lead to defects in rheo- and vibration sensations. Knockdown of an addition *pkd* gene, *pkd2-4,* caused jerky movements along with an inching defect. All three of these genes were expressed in *soxB1-2*$^{+}$ neurons. *Pkd1* and *-2* genes encode Polycystin-1 and -2 proteins respectively. Mutations in both of these genes are linked to polycystic kidney disease. These genes are expressed in the primary cilia of the kidney epithelium and loss-of-function mutations stop the normal Ca^{2+} influx that occurs following fluid-flow sensation by the primary cilia. This loss of mechanosensation is thought to stop the normal tissue morphogenesis that is regulated by mechanosensory function [97]. More recently, loss of Polycystin-L (PCL, Ca^{2+} permeable cation channel protein closely related to Polycystin 2 that is encoded by *pkd2-like 1* in mice) function was shown to cause increased neuronal hyperexcitability and susceptibility to seizures via drug inducement [34]. This protein is expressed in the primary cilia of neuronal cells in the brain and loss of its function leads to decreased cyclic AMP production (which is known to inhibit neuronal excitability [98]). PCL interacts with the β2-adrenergic receptor (B2AR) and is required for its localization to the primary cilia in neurons [34]. B2AR functions in cAMP production [99]. Although this represents a very new field of

research, the work of Yao and colleagues [34] suggests a role for primary cilia in EDs and our findings indicate a conservation of function of neuronal primary cilia, Ca^{2+} signaling, and their association with EDs in planarians. This conservation might be further linked by exploration of cAMP levels in planarians following perturbation of cilia genes.

Rheosensation and Vibration Sensation in Planarians

Multiple genes downstream of *SoxB1-2* labeled putative sensory populations. We found that 7 of 9 *SoxB1-2+* neurons expressed *rootletin,* a gene necessary for the assembly of the ciliary rootlet structure, and thus necessary for overall ciliary structure and function [100]. In particular, we noticed gene expression patterns similar to the pattern of the dorsal ciliated stripe [24, 52, 59]. Other putative rheosensory cells have been described in the planarian species *Mesostoma* and *Bothromesostoma* as cells distributed along the body sides [101]. These putative sensory cells penetrate the epidermis, where sensory bristles extended to the external environment [24]. The dorsal ciliated stripe was proposed to function in rheosensation and experiments showing the movement responses to rheosensory stimulus (rheotaxis) have been studied in multiple planarian species [51, 53, 54]. However, the link between gene expression in the dorsal ciliated stripe or other rheosensory cells (such as the lateral rheoreceptive cells described in *Borthromesostoma*) and behaviors has not been formally demonstrated in planarians. Through our behavioral screens, we identified multiple genes that were expressed along the dorsal ciliated stripe, and along two peripheral stripes that we

termed the dorsal peripheral stripe and the ventral peripheral stripe (Figure 4.14B). Following inhibition of *pkd1L-2, sargasso, gabrg3L-1, pkd2L-1,* and *gabrg3L-2,* planarians had a significant reduction in the reaction to water flowing across their dorsal side and to tapping vibrations of their dishes. The gene with the most discrete pattern of expression from this list, *pkd1L-2,* was co-expressed with other genes that caused the rheo- and vibration sensory defects, and all were expressed in the dorsal ciliated stripe and peripheral stripes, indicating that these genes function in rheoreception within cells of these anatomical locations. We identified additional genes with various putative neurosensory patterns throughout the planarian body, including some genes that caused a significant reduction in chemosensation. Furthermore, all of these genes were downregulated following *soxB1-2* RNAi, indicating a role for *soxB1-2* in the specification and maintenance of sensory neurons in planarians.

CONCLUSION

We determined that the *soxB1* gene, *soxB1-2* is expressed in a putative ectodermal lineage-restricted progenitor population and its expression is necessary for further commitment to a subset of ectodermal fates, in particular, ciliated epidermal cells and sensory neurons. Loss of *soxB1-2* function or of a subset of its positively-regulated downstream genes leads to seizure-like behaviors and loss of sensory modalities, including rheosensation, vibration sensation, and chemosensation. Many of the genes downstream of *SoxB1-2* are associated with EDs in humans. In addition, we identified new candidate genes which function in primary cilia and Ca^{2+} signaling, representing potential new candidates to study the functional roles of these genes in EDs, and indicating that these RNAi experiments may present an opportunity to use planarians as a model in which to screen future anti-seizure compounds.

Chapter 4, in full, is in preparation for submission. Kelly G. Ross, Alyssa M. Molinaro, Celeste Romero, Brian Dockter, Katrina L. Cable, Karla Gonzalez, Siqi Zhang, Priscila Rodriguez, Eva-Maria Collins, and Ricardo M. Zayas, 2017. The dissertation author was the primary investigator and author of this paper.

FIGURES

Figure 4.1: soxB1-2 loss of function causes a complex neuronal malfunction phenotype.
(A) Experimental design for images and movement analysis shown in (B-D,H"intact"). Worms were fed 2 times every week for 3 weeks and imaged between 1 week and 1 week + 4 days following the 6th feed.
(B) Seizure-phenotype of *soxB1-2(RNAi)* worms. Control animals are visualized gliding away from light in a generally straight fashion with their ventral surface on the substrate while *soxB1-2(RNAi)* worms stretch out their body, turn onto their sides and exhibit C-shape bending movements (left image), curling of the tail (middle image), and corkscrew movements (right image). Scale bars, 1 mm.
(C-D) *soxB1-2(RNAi)* worms bend more and are slower than control worms when under white light. (C) Bending of animals represented as degrees of bending difference from a straight animal (straight animal angle = 0 degrees). Numbers are normalized to the length of the worm. (D) The speed of worm movement is represented as mm/sec speed normalized to the length of the worm. All data represented as mean with standard deviation whiskers shown for two separate test groups of 10-11 worms. Statistical significance assessed using Student's t tests of each individual experimental group compared to the combined results from both control groups (****$p < 0.0001$).
(E) *soxB1-2* is expressed in putative sensory-neuron rich areas. WISH labeling of *soxB1-2* observed from both the dorsal and ventral sides demonstrates abundant labeling in the head periphery (black arrowheads), the dorsal ciliated stripe (yellow arrows), and the mouth of the pharynx (black arrow). Scale bars, 200 μm.
(F) *soxB1-2* is predominantly expressed within epidermal lineage cells and ciliated neurons. Violin plot of *soxB1-2* expression in major cell type groups of the planarian (assessed from single cell sequencing data). Each black dot represents gene expression within 1 cell.
(G) Experimental design for images, measurements, and behavioral tests shown in (H"14 DPA"-K). Worms were fed 2 times every week for 3 weeks, their heads were amputated 1 day following the last feed, and trunks were allowed to regenerate for 12-14 days before fixation or behavioral testing.
(H-I) *soxB1-2(RNAi)* worms have smaller brains than control worms. Brain lobes (white arrowheads) of intact and regenerating *soxB1-2(RNAi)* worms were visibly smaller than those in control worms. Scale bars, 100 μm. (I) Brain size was quantified using either immunolabeling with anti-Synapsin labeling (seen in (H)) or *chat* WISH and brain area (mm^2) was normalized to the body perimeter (mm) of the animal. Statistical significance assessed using Student's t tests between matching experimental and control groups. $n \geq 10$ worms (*$p < 0.05$, ***$p < 0.001$).
(J) *soxB1-2(RNAi)* causes loss of cilia at the dorsal ciliated stripe and head periphery. Control animals labeled with anti-Acetylated Tubulin display a visible stripe of cilia along the dorsal surface (white arrowhead) and thick cilia labeling at the head periphery (white arrows) while *soxB1-2(RNAi)* animals lacked a visible dorsal ciliated stripe and had visibly thinner cilia labeling at the head periphery. Scale bars, 200 μm.
(K-M) *soxB1-2(RNAi)* worms have reduced reaction to water flow and vibration. (K) Experimental design for behavioral analysis shown in (L-M). Worms were fed twice in one week and assessed 14-19 days following the last feed. (L) When squirted with water on their dorsal surface *soxB1-2* worms had reduced contraction amplitude. (M) The reaction of *soxB1-2(RNAi)* worms was reduced compared to control worms when the dish was tapped to create vibrations in the water. This test was repeated 3 times for each specimen. Amplitude of contraction is the shortest length of worms following stimulus / length of gliding animal. Statistical significance was assessed using Student's t test between matching experimental and control groups. $n \geq 18$ worms (**$p < 0.01$, ***$p < 0.001$). F, Feed; D, Day; DPA, days post-amputation; Ac-Tub, Acetylated Tubulin.

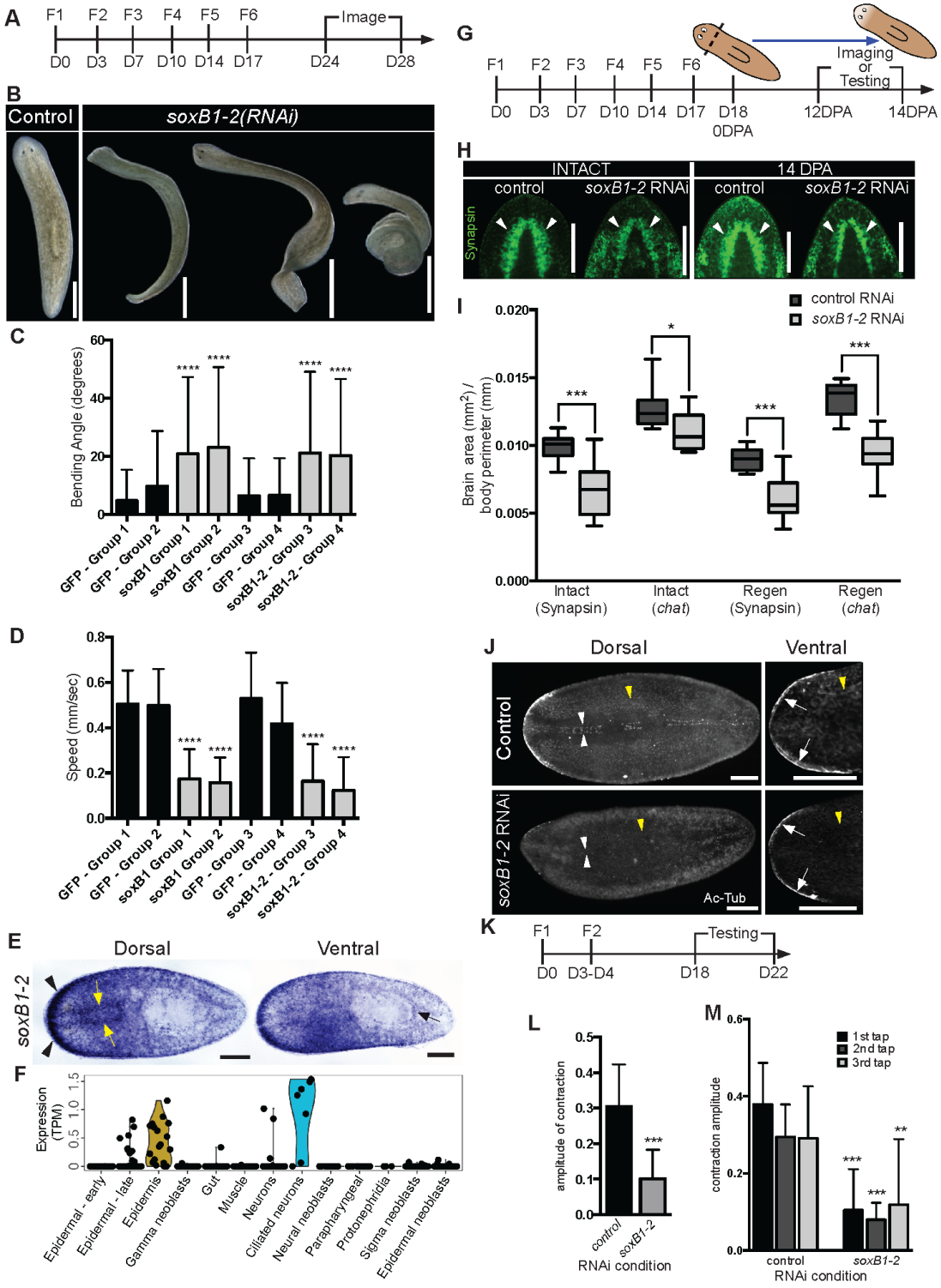
A
F1 F2 F3 F4 F5 F6 Image
D0 D3 D7 D10 D14 D17 D24 D28
B
Control
soxB1-2(RNAi)
C
Bending Angle (degrees)
GFP - Group 1
GFP - Group 2
soxB1 Group 1
soxB1 Group 2
GFP - Group 3
GFP - Group 4
soxB1-2 - Group 3
soxB1-2 - Group 4
D
Speed (mm/sec)
E
Dorsal
Ventral
soxB1-2
F
Expression (TPM)
Epidermal - early
Epidermal - late
Epidermis
Gamma neoblasts
Gut
Muscle
Neurons
Ciliated neurons
Neural neoblasts
Parapharyngeal
Protonephridia
Sigma neoblasts
Epidermal neoblasts
G
F1 F2 F3 F4 F5 F6
Imaging or Testing
D0 D3 D7 D10 D14 D17 D18
0DPA
12DPA
14DPA
H
INTACT
14 DPA
control
soxB1-2 RNAi
Synapsin
I
control RNAi
soxB1-2 RNAi
Brain area (mm2) / body perimeter (mm)
Intact (Synapsin)
Intact (chat)
Regen (Synapsin)
Regen (chat)
J
Dorsal
Ventral
Control
soxB1-2 RNAi
Ac-Tub
K
F1 F2 Testing
D0 D3-D4 D18 D22
L
amplitude of contraction
control
soxB1-2
RNAi condition
M
1st tap
2nd tap
3rd tap
contraction amplitude
control
soxB1-2
RNAi condition

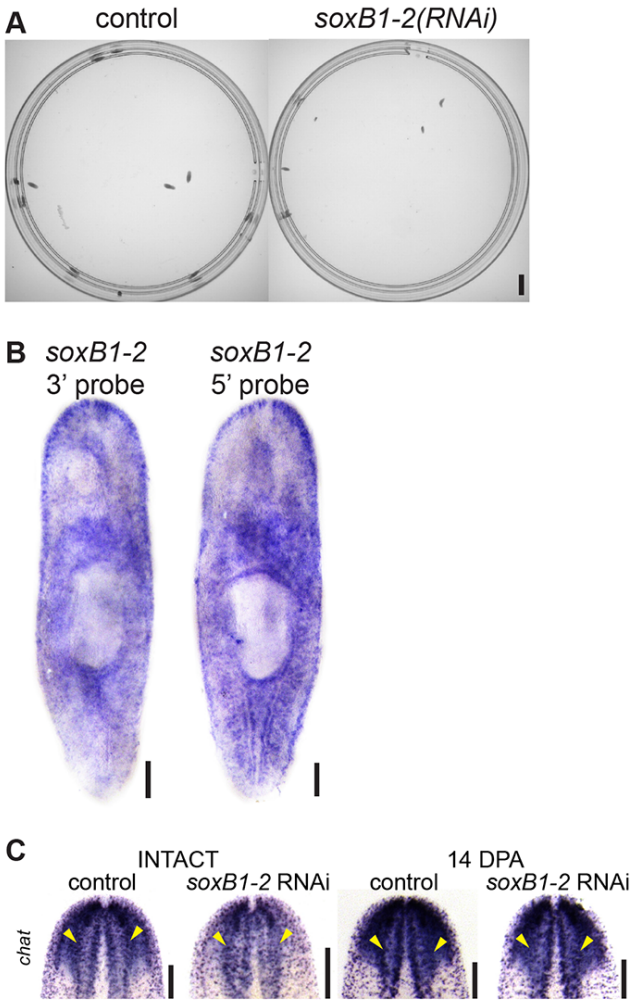

Figure 4.2: Supporting information to Figure 4.1.
(A) *soxB1-2(RNAi)* animals, like control animals, exhibit very little movement, including seizure-like movements when assayed for 10 minutes of activity under infrared light (not detected by planarian photoreceptors). (10 minutes of activity collected at 5 frames per second and flattened into a minimum intensity projection). Scale bar, 1 cm.
(B) Two different versions of the *SoxB1-2* riboprobes had similar expression patterns to the original probe (which was designed in the HMG box region of the gene), including expression in the head periphery, the mouth, and the epidermis. The 3' probe is downstream of the original probe and the 5' probe is upstream of the original probe. Scale bars, 200 µm.
(C) *soxB1-2(RNAi)* worms have smaller brains than control worms. Brain lobes (yellow arrowheads) of intact and regenerating *soxB1-2(RNAi)* worms are visibly smaller than those in control worms when visualized with *chat* riboprobe. Scale bars, 100 µm.

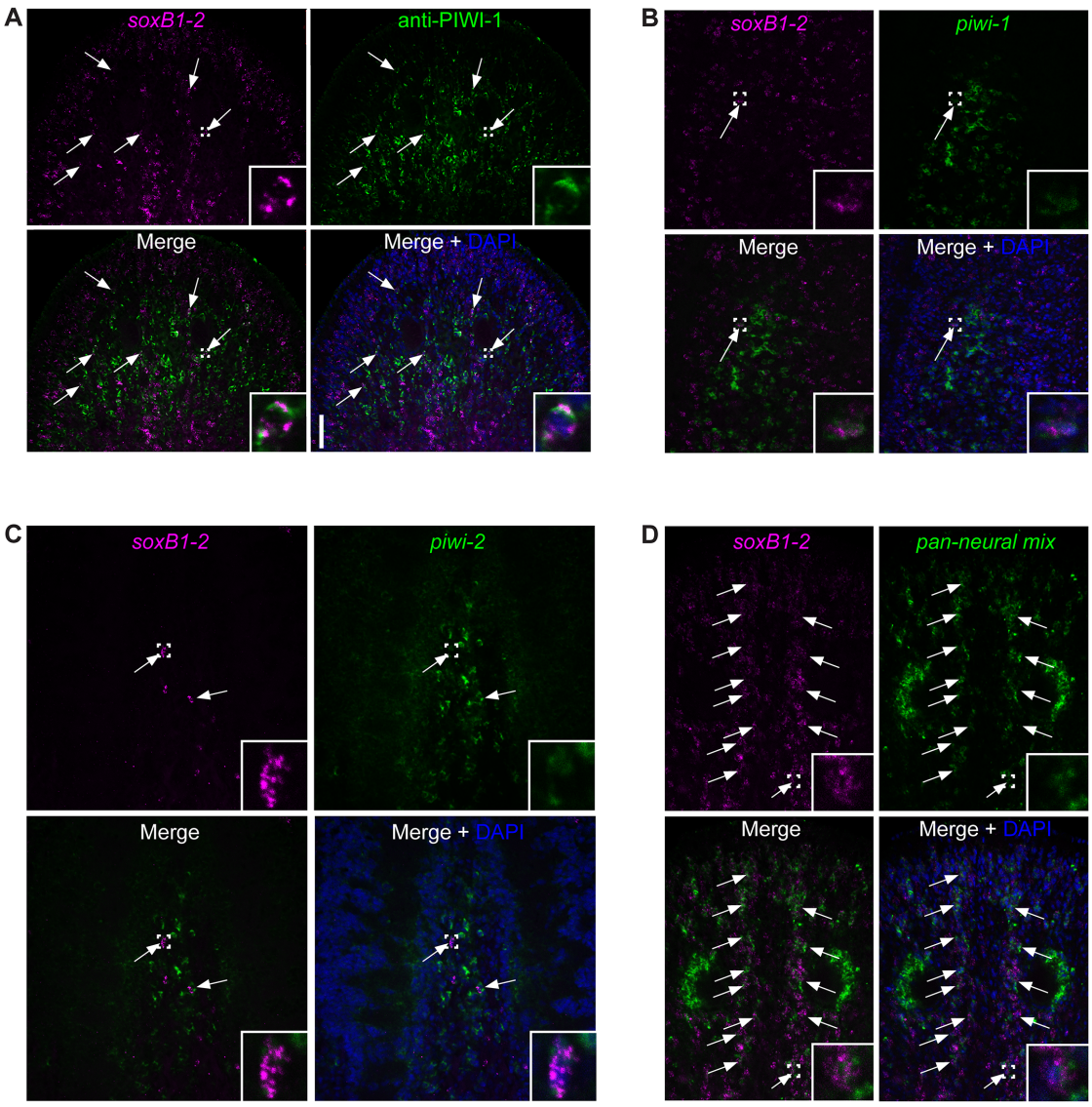

Figure 4.3: *soxB1-2* is expressed in a subset of stem, progenitor, and neural cells.
(A-C) Rare stem/progenitor cells expressed *soxB1-2.* (A) *soxB1-2+* (magenta), PIWI-1+ (green, a marker of stem and progenitor cells) double positive cells were found in the planarian. Shown in the dorsal head region of the planarian. (B) *soxB1-2+* (magenta), *piwi-1* (green, a marker of stem cells) are rare, but can be found in the planarian. Shown in the area anterior to the pharynx. (C) *soxB1-2* (magenta) co-labels a small subset of *piwi-2+* cells (green, a marker of neural progenitor cells and a subset of differentiated neurons) in the area between the brain lobes, known to be rich in neural progenitor cells.
(D) *soxB1-2+* cells in the dorsal ciliated stripe area are positive for a neural marker mix consisting of *synapsin* and *synaptotagmin.* In all images, examples of co-labeled cells are highlighted with white arrows and the white dashed box indicates regions displayed in the higher magnification insets. DAPI is displayed in blue. Scale bars, 50 μm.

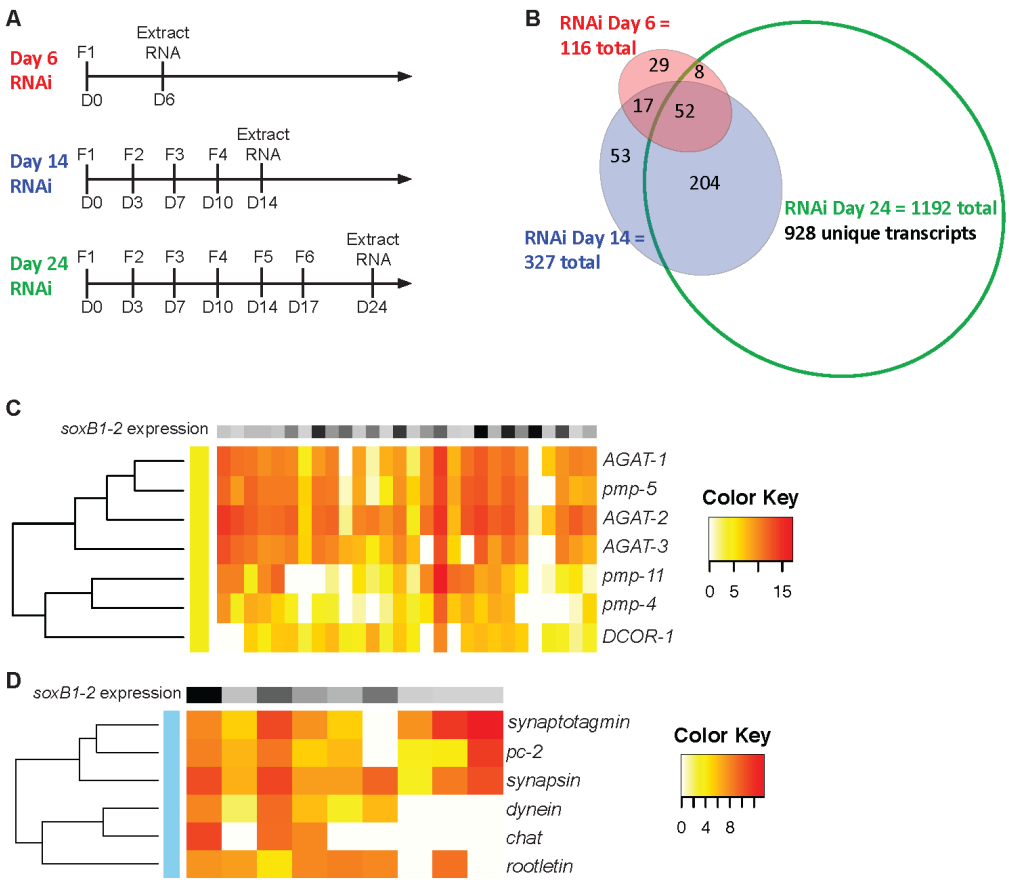

Figure 4.4: Determination of *soxB1-2*-transcriptionally regulated genes by RNA-seq
(A) Experimental set-up for RNAi feedings of *soxB1-2* in day 6, 14, and 24 samples.
(B) Venn diagram displaying the number of genes downregulated following RNAi feedings outlined in (A). The majority of genes downregulated in the day 6 and day 14 samples are also downregulated at day 24.
(C-D) *soxB1-2+* cells are part of epidermal or neural lineages. (C) *soxB1-2+* cells that clustered within the epidermal class express known markers for the epidermal lineage. (D) *soxB1-2+* cells that clustered within the neural class express known markers for the neural lineage. Additionally, 7/9 of these cells express rootletin (a marker of ciliated cells). The color keys indicate the log2 normalized gene expression of each transcript.

Figure 4.5: Supporting information to Figure 4.4.
(A) Reduction in *soxB1-2* expression is stably reduced by day 6 following the first RNAi feeding. Expression of *soxB1-2* was assayed by qPCR, (data is normalized to expression of *soxB1-2* in control animals at the same timepoint which is represented by the red line at 1).
(B) Reduction of *cav-1* is reduced at day 6 following the first RNAi feeding (data is normalized to expression of *cav-1* in control animals at the same timepoint, which is represented by the red line at 1). Data in (A) and (B) is represented as the mean of three biological and technical triplicates, whiskers are the standard deviations.
(C) *soxB1-2+* cells from single cell sequencing data cluster into neural and epidermal classes, highlighting the expression of *soxB1-2*-regulated genes in either the epidermal or neural lineages. Heatmap of gene expression for genes that are downregulated following *soxB1-2(RNAi)* expressed in *soxB1-2+* cells (*soxB1-2* expression in greyscale at the top of the heatmap). Dendrogram based on variable expression of the transcripts displayed on the right of the map. The green bar highlights expression of genes downregulated in the *soxB1-2(RNAi)* group at day 14 post RNAi. The blue bar indicates expression of known neural lineage genes and the yellow bar indicates expression of known epidermal lineage genes. The color key indicates the log2 normalized gene expression of each transcript.

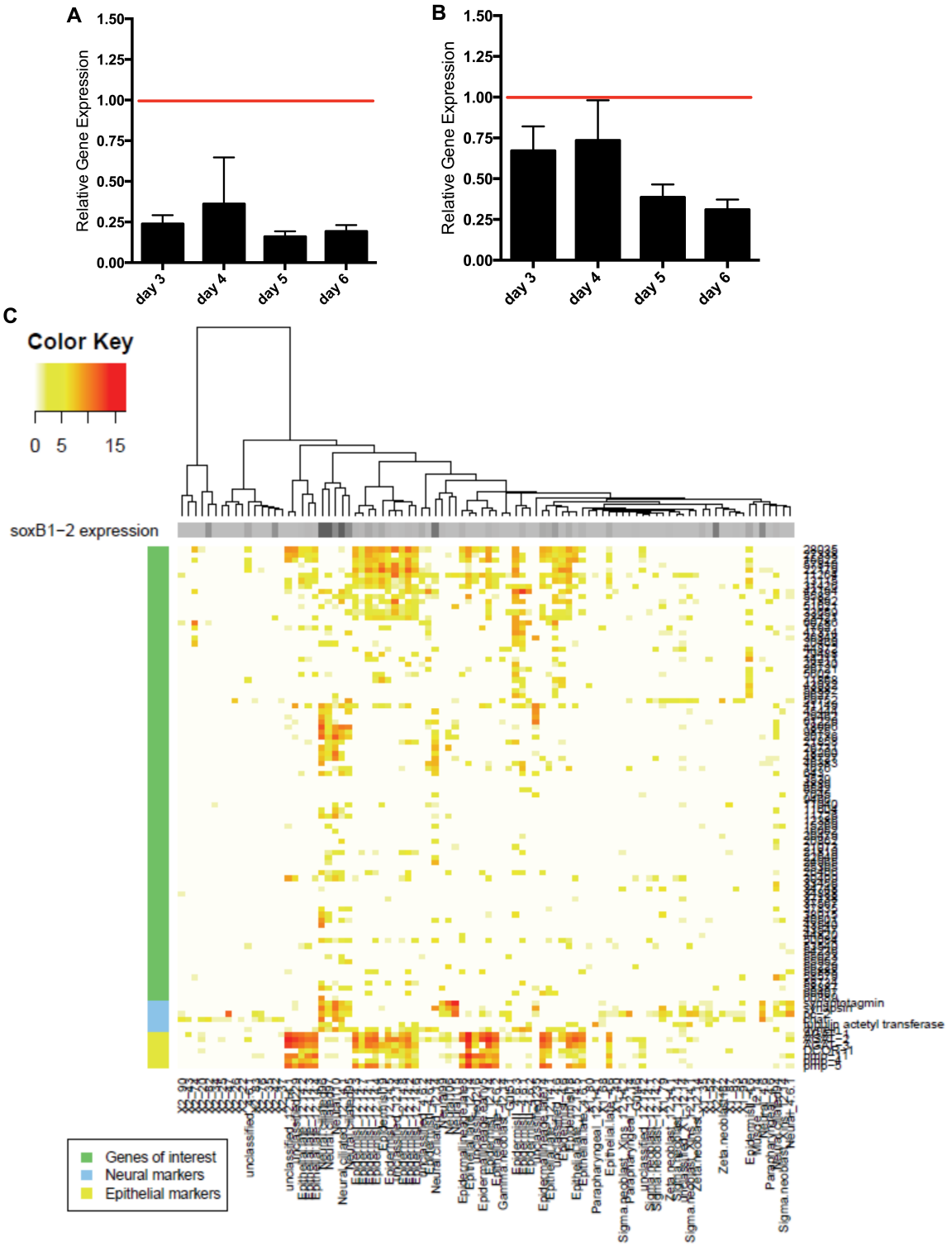
A
Relative Gene Expression
1.50
1.25
1.00
0.75
0.50
0.25
0.00
day 3
day 4
day 5
day 6
B
Relative Gene Expression
1.50
1.25
1.00
0.75
0.50
0.25
0.00
day 3
day 4
day 5
day 6
C
Color Key
0 5 15
soxB1−2 expression
Genes of interest
Neural markers
Epithelial markers

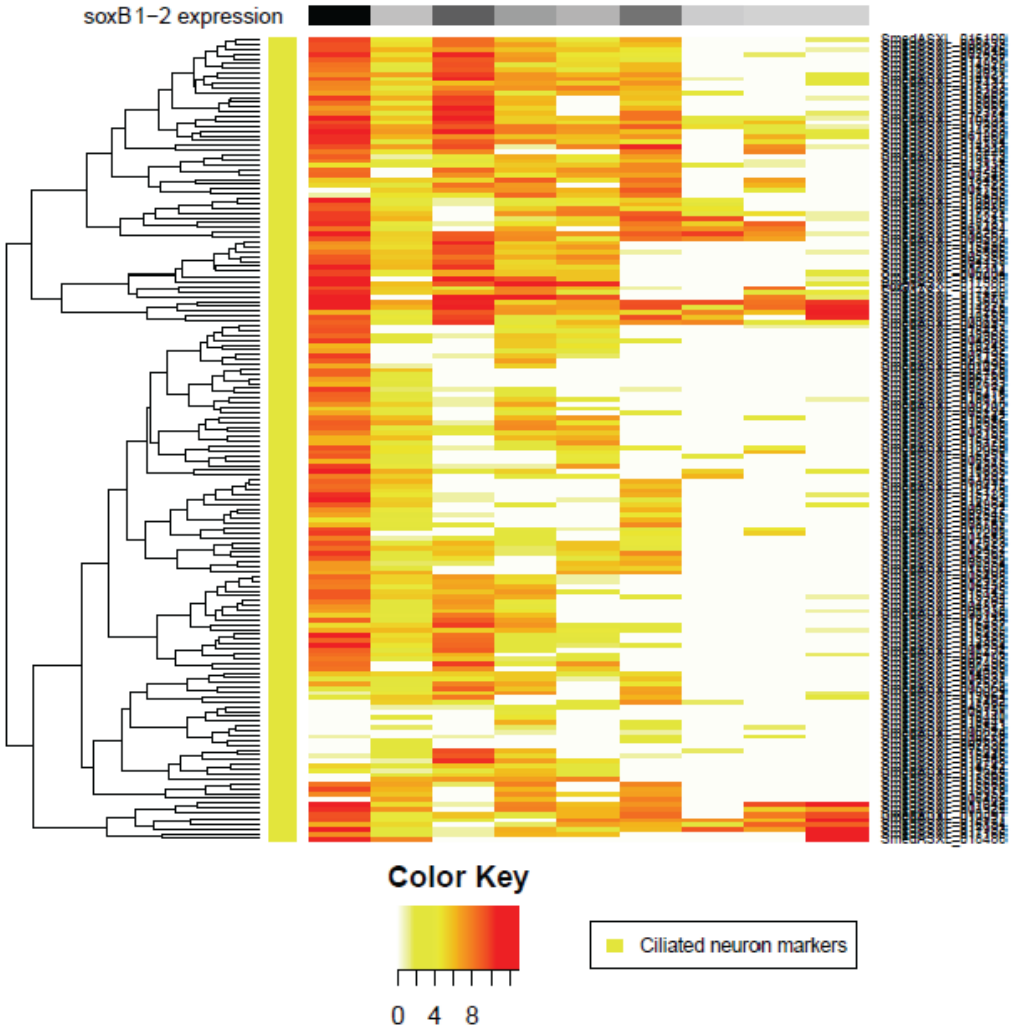

Figure 4.6: *soxB1-2+* neural cells express markers of ciliated neurons. *soxB1-2*-expressing cells that were determined to be neurons based on clustering and expression of known neural markers also express genes that were determined to be enriched in the ciliated neuron class in a previous published single cell sequencing dataset (Wurtzel et al 2015). Ciliated neural genes are listed on the right side of the map. The color key indicates the log2 normalized gene expression of each transcript.

Figure 4.7: *soxB1-2+* cells cluster into three trajectories of cells by PCA analysis.
(A) All *soxB1-2+* cells were first clustered into 9 different groups by hierarchical clustering and these groups were color-coded.
(B) PCA analysis was performed on the *soxB1-2+* cells showing what appeared to be three lineage trajectories stemming from a common population. The left plot displays each point, color-coded from the hierarchical clustering results. The plot on the right displays *soxB1-2* expression. All cells express *soxB1-2.*
(C) By plotting known neural markers on the PCA plot, the cell lineage on the top was determined to be neural.
(D) Plotting of the known stem cell marker *piwi-1* on the PCA plot demonstrates an enrichment of stem cell gene expression at the vertex of all three lineage trajectories.
(E) By plotting known epidermal lineage markers on the PCA plot, the cell lineage on the bottom of the PCA plot was determined to be epidermal.
(F) Genes that are broadly expressed in other known tissue lineages were plotted on the PCA plot to determine the identity of the left lineage trajectory. The cells in this arm were not enriched for the expression of any of these genes. In all PCA plots, the increasing diameter of each single datapoint correlates with an increase in expression of the gene indicated in the plot title. PCA, principle component analysis; PC1, principle component 1; PC2, principle component 2.

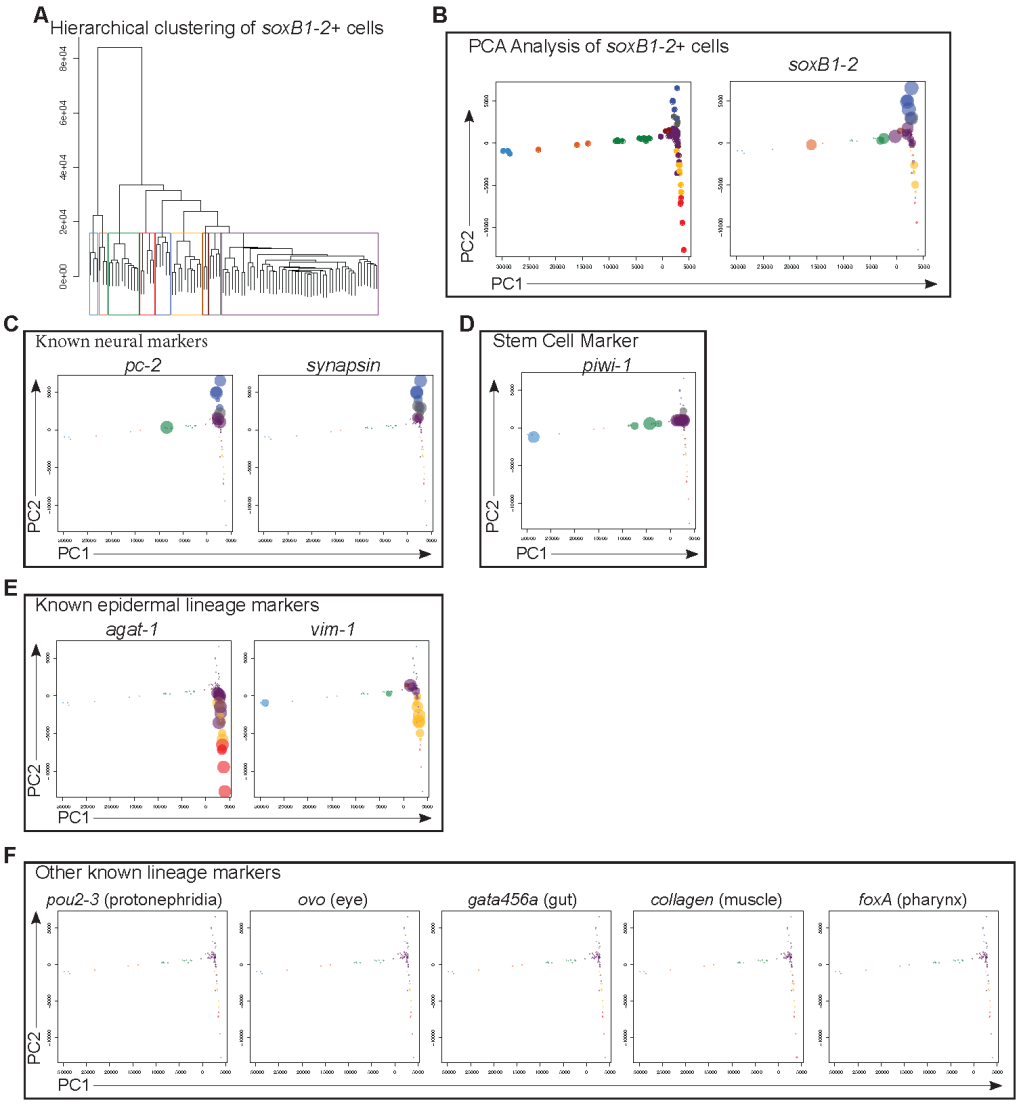
A
Hierarchical clustering of soxB1-2+ cells
B
PCA Analysis of soxB1-2+ cells
soxB1-2
PC2
PC1
C
Known neural markers
pc-2
synapsin
PC2
PC1
D
Stem Cell Marker
piwi-1
PC2
PC1
E
Known epidermal lineage markers
agat-1
vim-1
PC2
PC1
F
Other known lineage markers
pou2-3 (protonephridia)
ovo (eye)
gata456a (gut)
collagen (muscle)
foxA (pharynx)
PC2
PC1

Figure 4.8: Pseudotime analysis predicts differentiation into neural or epidermal lineages from a common ectodermal progenitor population.
(A) PCA analysis of *soxB1-2+* cells associated with neural, epidermal, and stem/progenitor classes displays two lineage trajectories from a common progenitor population. Upper left plot displays the cells, sorted by class. *soxB1-2* expression is plotted on the PCA plot. Known stem/neural progenitor markers, neural lineage markers, and epidermal lineage markers were plotted on the PCA plots to determine the lineages of the branches on the PCA plots to determine the classes indicated in the bottom right plot.. In all PCA plots, the increasing diameter of each single datapoint correlates with an increase in expression of the gene indicated in the plot title.
(B) The PCA results were ordered using waterfall analysis to determine the progression of differentiation. Arrows indicate the order of differentiation along pseudotime.
(C-E) The expression patterns of known markers support the lineage prediction. (C) Known stem and neural progenitor markers *piwi-1* and *piwi-2* are most highly expressed at the vertex of the two lineages, the ectodermal progenitor population. Known neural progenitor markers *ptprd-9* and *ski-1* are highly expressed during differentiation along pseudotime in the neural lineage (D) neural marker genes *synapsin* and *pc-2* increase in pseudotime down the neural lineage. (E) known epidermal lineage markers *pmp-5* and *AGAT-1* increase in pseudotime down the epidermal lineage.
(F-G) Genes indicated to the neural, epidermal, or neural and epidermal *soxB1-2* classes that are downregulated following *soxB1-2* RNAi increase are expressed during the pseudotime lineage trajectories of their respective classes. Red line, local polynomial regression fit; shaded region, 95 % confidence interval. PCA, principle component analysis; PC1, principle component 1; PC2, principle component 2.

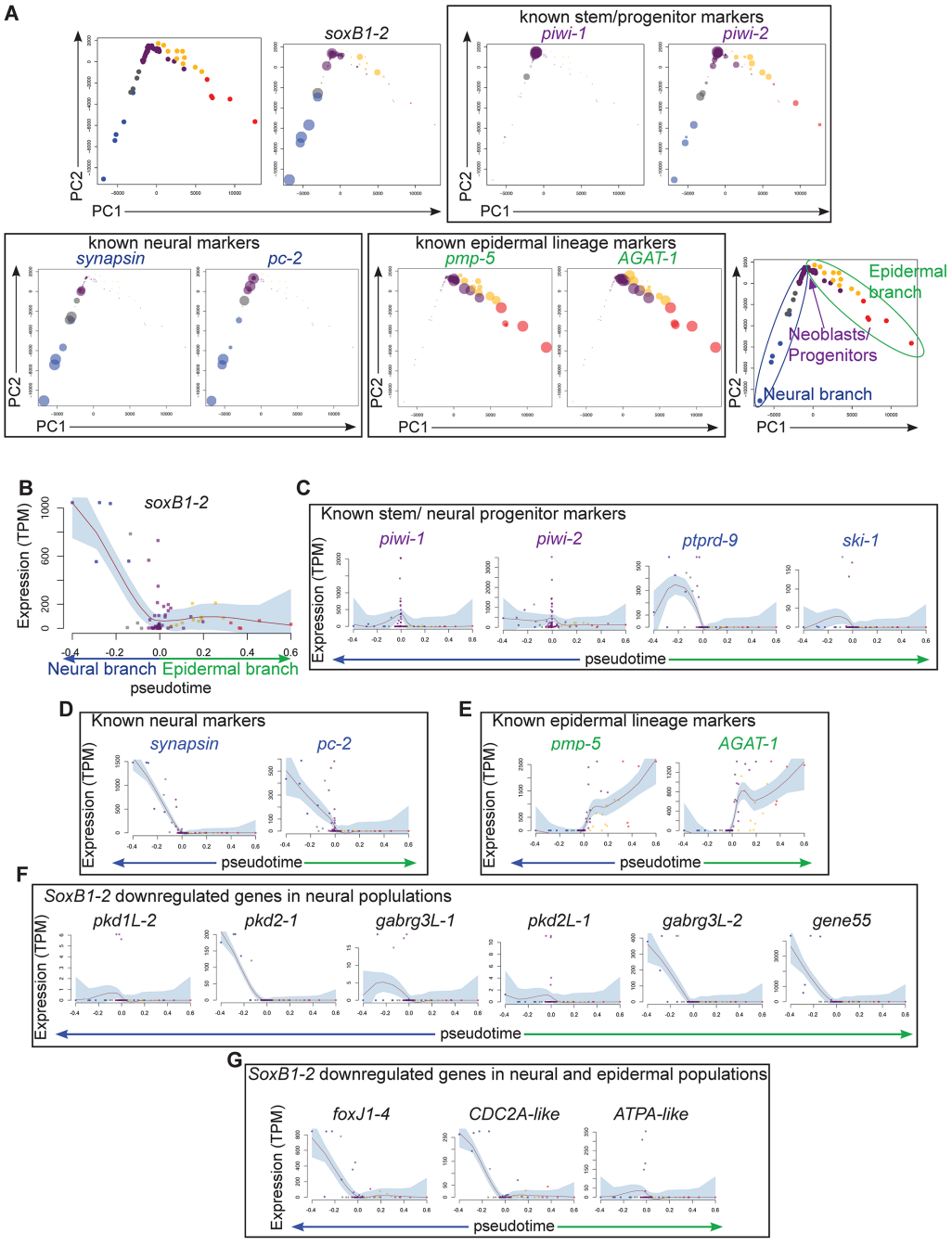
A
soxB1-2
known stem/progenitor markers
piwi-1
piwi-2
known neural markers
synapsin
pc-2
known epidermal lineage markers
pmp-5
AGAT-1
Epidermal branch
Neoblasts/ Progenitors
Neural branch
PC1
PC2
B
soxB1-2
Expression (TPM)
Neural branch Epidermal branch
pseudotime
C
Known stem/ neural progenitor markers
piwi-1
piwi-2
ptprd-9
ski-1
D
Known neural markers
synapsin
pc-2
E
Known epidermal lineage markers
pmp-5
AGAT-1
F
SoxB1-2 downregulated genes in neural poplulations
pkd1L-2
pkd2-1
gabrg3L-1
pkd2L-1
gabrg3L-2
gene55
G
SoxB1-2 downregulated genes in neural and epidermal populations
foxJ1-4
CDC2A-like
ATPA-like

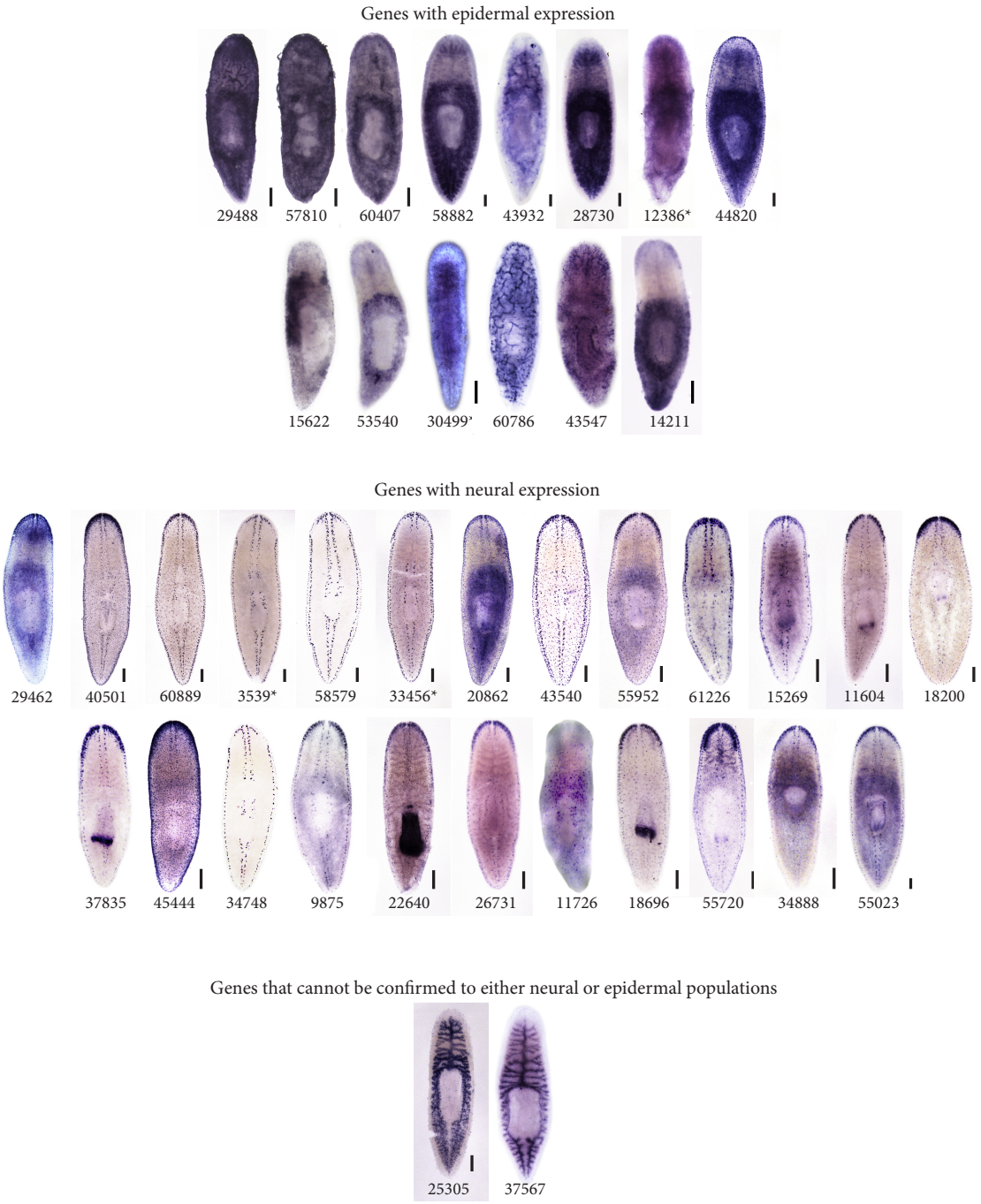

Figure 4.9: Supporting information to Figure 4.11.
Genes of interest were determined from the day 14 down-regulated list based on GO terms or previous inclusion in a list of genes enriched in the ciliated neuron class (Wurtzel et al 2015) and expression patterns determined by WISH. These genes were then sorted for epidermal expression and/or neural expression based on expression of these genes in *soxB1-2+* neural or epidermal cells per clustering from single cell sequencing data, demonstrated in Figure 4.5. Genes are labeled by transcript ID number. Genes that were expressed in neural or epidermal tissues based on expression patterns, but not attributed to these classes based on single cell sequencing data are indicated with an asterisk.

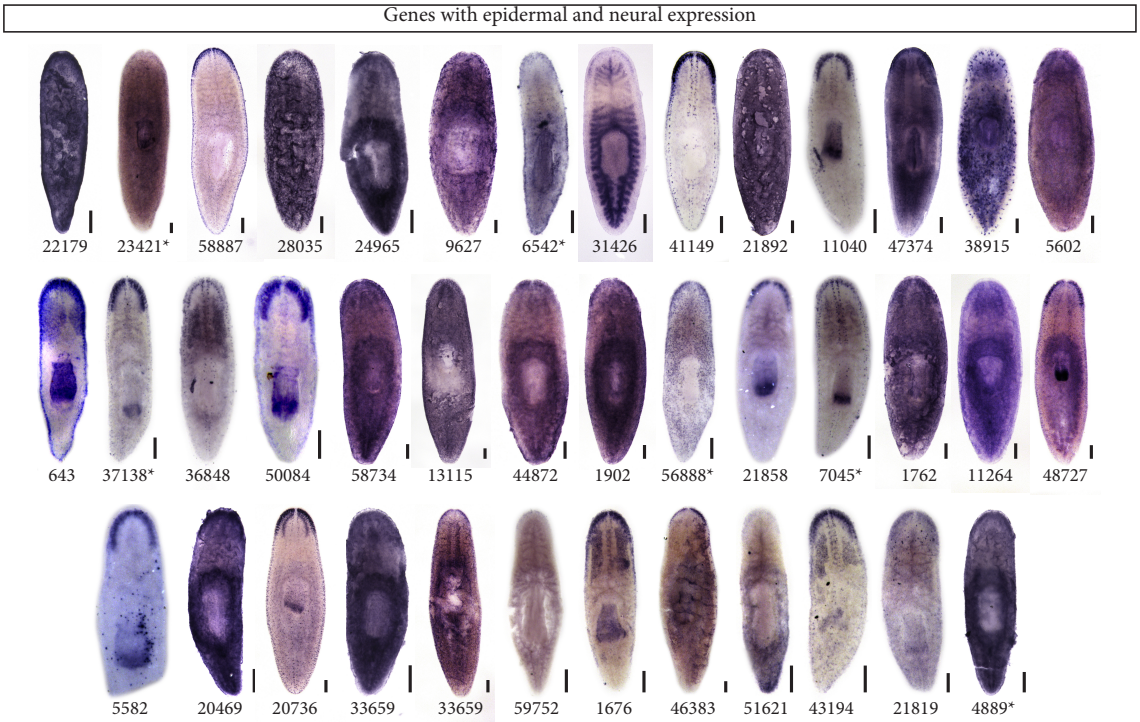

Figure 4.10: Supporting information to Figure 4.11.
Genes of interest were determined from the day 14 down-regulated list based on GO terms or previous inclusion in a list of genes enriched in the ciliated neuron class (Wurtzel et al 2015) and expression patterns determined by WISH. These genes were then sorted for epidermal expression and/or neural expression based on expression of these genes in *soxB1-2+* neural or epidermal cells per clustering from single cell sequencing data, demonstrated in Figure 4.5. Genes are labeled by transcript ID number. Genes that were expressed in neural and epidermal tissues based on expression patterns, but not attributed to these classes based on single cell sequencing data are indicated with an asterisk.

Figure 4.11: The expression patterns of genes downstream of SoxB1-2 reveal epidermal patterns and unique putative sensory populations.
(A-C) Genes of interest from the downregulated at day 14 post-*SoxB1-2(RNAi)* list were sorted into epidermal (A), neural (B), and both epidermal and neural classes (C) based on hierarchical clustering from the single cell sequencing data. Genes that were expressed in neural or epidermal tissues based on expression patterns, but not attributed to these classes based on single cell sequencing data are indicated with an asterisk.
(D) dFISH labeling of the *soxB1-2* downstream gene *pkd2L-1* (green) highlights expression in three putative sensory populations: the dorsal ciliated stripe (red arrows), the dorsal peripheral stripe (white arrows), which is located dorsally to the dorsal-ventral boundary (labeled with *intermediate filament-beta, if-b*, magenta) and the ventral peripheral stripe (yellow arrowheads), which is located ventrally to the dorsal-ventral boundary. Higher magnification inset location is indicated with the dashed white boxes.
(E) Co-expression of the *soxB1-2* downstream gene *pkd1L-2* with *soxB1-2* in the dorsal ciliated stripe and associated peripheral head population was determined by dFISH labeling. Examples of co-labeled cells are highlighted with white arrows and area of the higher magnification inset is indicated with dashed white box.
(F-J) Determination of a putative sensory neuron class. Co-expression of *pkd1L-2* (green) with other genes downstream of *soxB1-2.* (F) *pkd1L-2+* cells are also positive for *sargasso* (magenta, co-labeled cells highlighted with white arrows). There are additional *sargasso+* cells that do not express *pkd1L-2* (yellow arrowheads). (G) *pkd1L-2* cells also express *gabrg3L-1* (magenta, co-labeled cells highlighted with white arrows). (H-I) Like co-labeling with *sargasso*, *pkd1L-2+* cells express gabrg3L-2 (magenta, co-labeled cell examples highlighted with white arrows), although there are *gabr3L-2+* cells that do not express *pkd1L-2* in the dorsal ciliated stripe region and dorsal head periphery in (H) and especially in the more ventral peripheral head region (I) (indicated by yellow arowheads). (J) *hmcn-1-L+* cells (magenta) represent a putative sensory cell type that does not express *pkd1L-2* (*hmcn-1-L+* cells highlighted with yellow arrowheads and *pkd1L-2+* cells marked with white arrowheads). For all co-labeling experiments, n ≥ 3 animals were observed to have consistent labeling patterns.

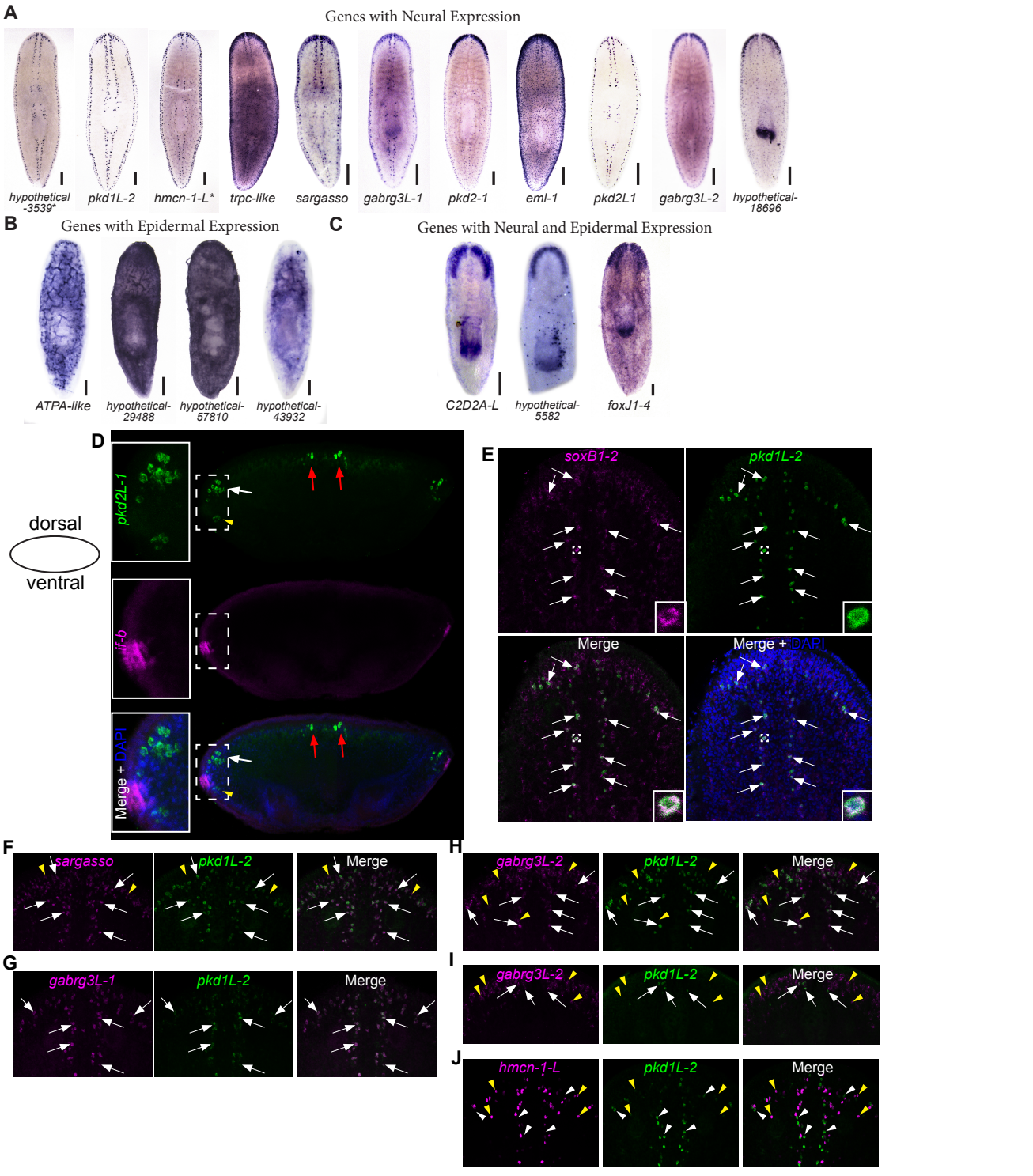
A
Genes with Neural Expression
hypothetical -3539*
pkd1L-2
hmcn-1-L*
trpc-like
sargasso
gabrg3L-1
pkd2-1
eml-1
pkd2L1
gabrg3L-2
hypothetical-18696
B
Genes with Epidermal Expression
ATPA-like
hypothetical-29488
hypothetical-57810
hypothetical-43932
C
Genes with Neural and Epidermal Expression
C2D2A-L
hypothetical-5582
foxJ1-4
D
dorsal
ventral
pkd2L-1
if-b
Merge + DAPI
E
soxB1-2
pkd1L-2
Merge
Merge + DAPI
F
sargasso
pkd1L-2
Merge
G
gabrg3L-1
pkd1L-2
Merge
H
gabrg3L-2
pkd1L-2
Merge
I
gabrg3L-2
pkd1L-2
Merge
J
hmcn-1-L
pkd1L-2
Merge

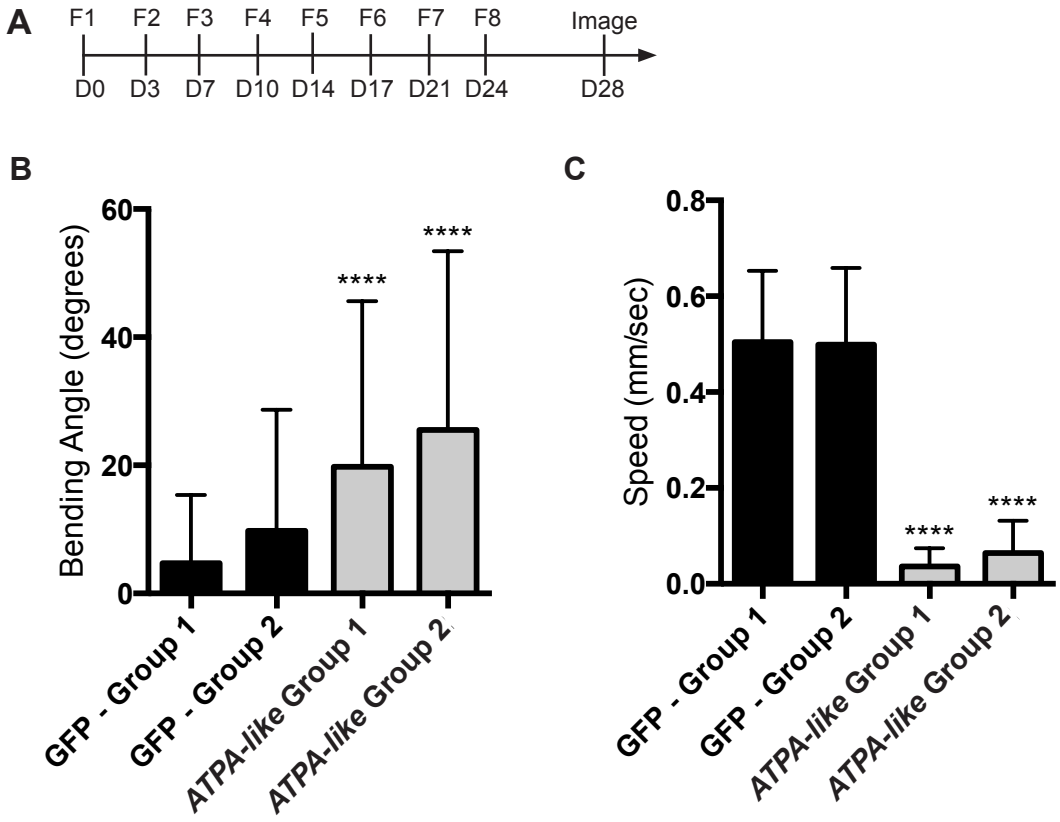

Figure 4.12: Example of a gene downstream of *soxB1-2* that causes seizure-like behaviors with loss of function.
(A) Experimental design for data displayed in (B-C). Worms were fed 8X over 4 weeks and imaged at day 28 following the first feed. F, feed; D, days post-first feed. (B-C) *ATPA-like(RNAi)* worms bend more and are slower than control worms when under white light. (B) Bending of animals represented as degrees of bending difference from a straight animal. Numbers are normalized to the length of the worm. (C) The speed of worm movement is represented as mm/sec speed normalized to the length of the worm. All data represented as mean with standard deviation indicated by the whiskers for two separate test groups of 10-11 worms. Statistical significance assessed using Student's t tests of each individual experimental group compared to the combined results from both control groups (****$p < 0.0001$).

Figure 4.13: Multiple genes downstream of *soxB1-2* transcriptional regulation cause loss of cilia at sensory neuron-rich areas, reduced rheosensation , vibration sensation, and chemosensation.
(A-B) Experimental design for data and images in (C-G). (A) Worms for all genes except for *gabrg3L-2* water flow and vibration sensation experiments, were fed RNAi 8X over 4 weeks, amputated 3 days following the last feed just posterior to the head, and imaged or tested 12-14 days following head amputation. (B) *gabrg3L-2* worms used for water flow sensation and vibration sensation experiments were fed 8X over 4 weeks and assayed between 40 and 42 days following the first RNAi feed. F, RNAi feed; D, days post-first RNAi feed; DPA, days post-amputation. (C-D) *trpc-like, foxJ1-4, C2D2A-like, putative protein-18696, ATPA-like,* and *nervana 3-like* RNAi cause a visible reduction in cilia labeling along the dorsal surface of the worm (white arrowheads) and a reduction of labeling in the auricle region of the worm (yellow arrowheads). Scale bars 200 μm. The number of worms displaying this phenotype are quantified in (D).
(E-F) *pkd1L-2, sargasso-1, gabrg3L-1, pkd2L-1, and gabrg3L-2* RNAi worms have reduced reaction to rheosensory and vibration stimuli. (E) When squirted with water on their dorsal surface these worms had reduced contraction amplitude. (F) The reaction of these worms was reduced compared to control worms when the dish was tapped to create vibrations in the water. This test was repeated 3 times for each specimen. Amplitude of contraction, shortest length of worms following stimulus / length of gliding animal. (G) Knockdown of *pkd2-1, putative protein-37835, eml1,* and *pkd2L-1* cause a reduction in chemosensation. Experimental worms spent a shorter amount of time in the zone of the dish with food compared to when there was no food present. Data is normalized to the time control animals spent in the zone with and without food (represented with the red line). Statistical significance was assessed using Student's t test within groups with or without food. $n \geq 18$ worms (*$p < 0.05$, **$p < 0.01$, ***$p < 0.001$).

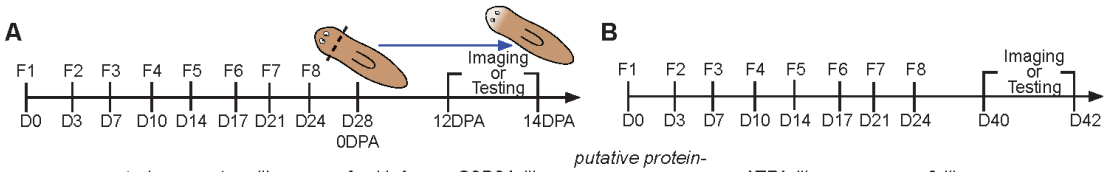

C

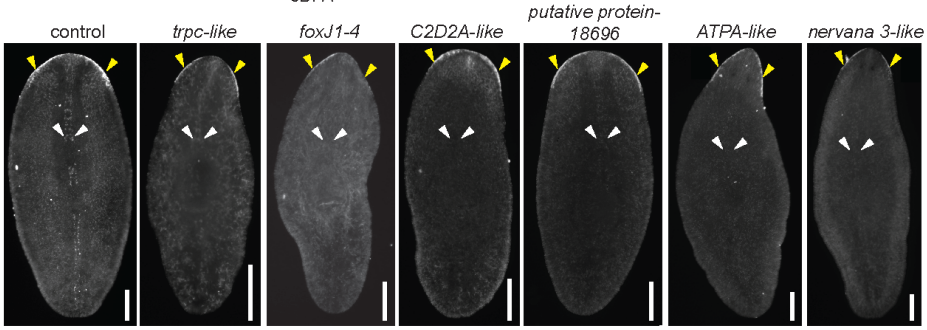

D

Gene	Dorsal Ciliated Stripe Appearance: Resembles Control	Fainter Than Control	Not visible	Auricle Region: Smaller than Control
pkd1L-2		X (6/6)		X
trpc-like		X (6/6)		X
sargasso		X (6/9)		X
gabrg3L-1	X (6/6)			X
Smed-pkd2-1		X (3/3)		X
hypothetical protein-21073	X (4/4)			X
eml-1		X (4/4)		X
pkd2L1	X (4/4)			X
gabrg3L-2	X (9/10)	(1/10)		X
C2D2A-like			X (2/2)	X
hypothetical protein-18696			X (9/9)	
foxJ1-4			X (4/4)	X
ATPA-like		(1/9)	X (8/9)	X
nervana-3-like			X (6/6)	

E

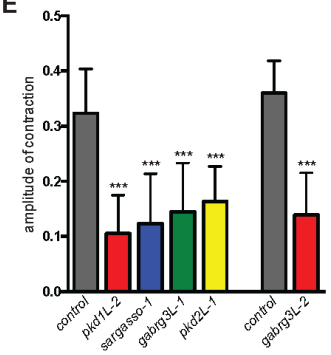

F

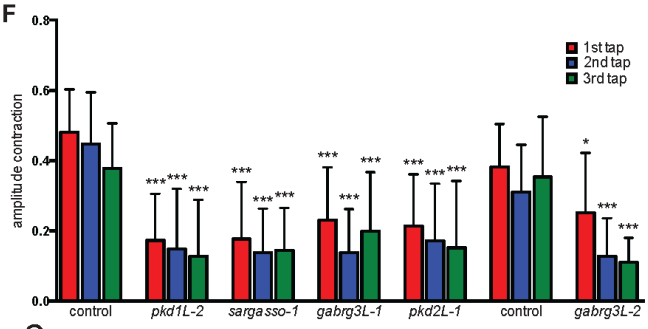

G

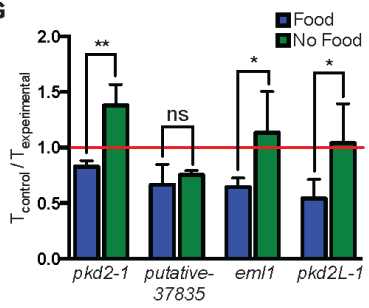

Figure 4.14: *soxB1-2* labels an ectodermal progenitor population and is necessary for the differentiation and maintenance of 3 anatomical populations of rheosensory neurons.
(A) Hypothesis of the role of *soxB1-2* in the differentiation of a population of ectodermal progenitor cells. *soxB1-2* is first expressed in an ectodermal progenitor population that expresses the stem cell marker *piwi-1,* then these cells differentiate through an epidermal fate or neurectodermal fate (expressing markers of neural progenitors) and finally into mature epidermis or ciliated sensory neurons, with ciliated sensory neurons having the highest levels of *soxB1-2* expression.
(B) 3 anatomical populations of rheosensory neurons were identified, the dorsal ciliated stripe (red), dorsal peripheral stripe (blue), and ventral peripheral stripe (purple). Loss or dysfunction of this population (by loss of function of *soxB1-2* or some of its downstream genes) leads to loss of rheosensation. On the left is a cartoon view of these populations from the dorsal side of the worm. On the right is a cartoon view of these populations from a lateral cross section with the dorsal side shown to the top of the image.

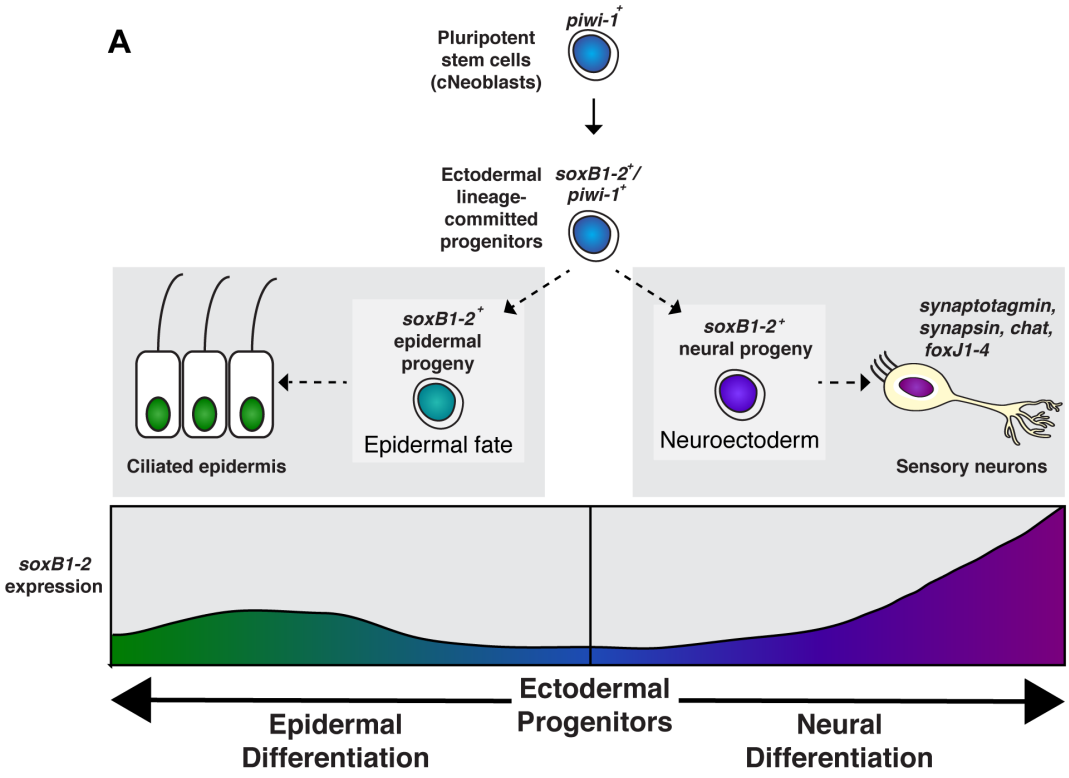
A
Pluripotent stem cells (cNeoblasts)
piwi-1+
Ectodermal lineage-committed progenitors
soxB1-2+/ piwi-1+
soxB1-2+ epidermal progeny
Epidermal fate
Ciliated epidermis
soxB1-2+ neural progeny
Neuroectoderm
synaptotagmin, synapsin, chat, foxJ1-4
Sensory neurons
soxB1-2 expression
Epidermal Differentiation
Ectodermal Progenitors
Neural Differentiation

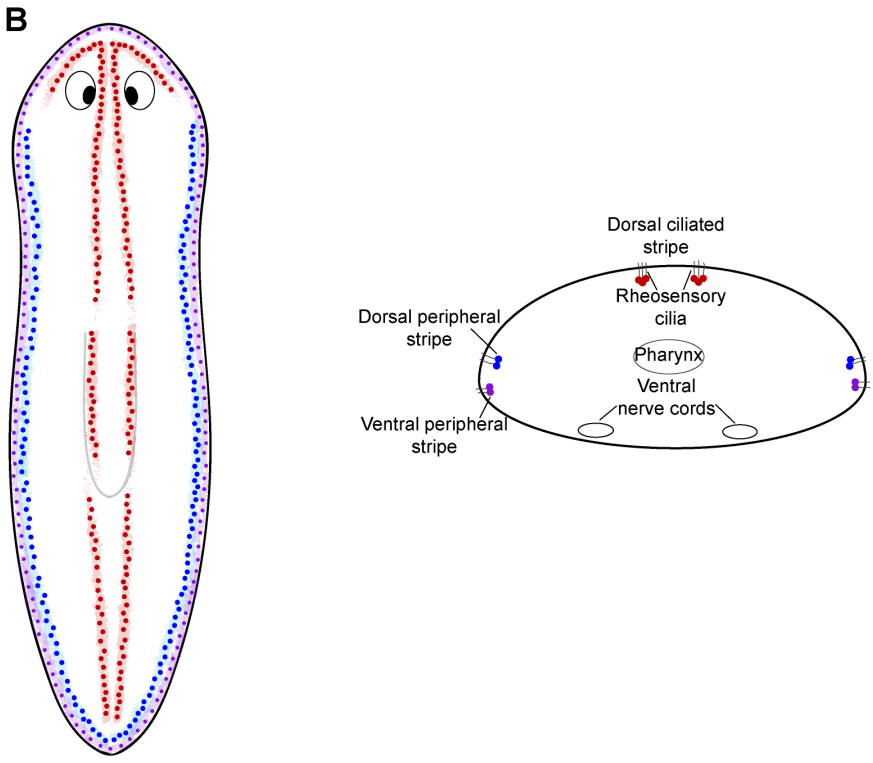
B
Dorsal ciliated stripe
Rheosensory cilia
Dorsal peripheral stripe
Pharynx
Ventral nerve cords
Ventral peripheral stripe

TABLES

Table 4.1: Genes downregulated at day 14 of *soxB1-2* RNAi that display movement or sensory phenotypes.

Gene Name	Expression Category	Movement Phenotype	Reduced Feeding Observed	Rheosensory Defect (# worms with defect / total)	Vibriation Sensation Defect (# worms with defect / total)
pkd1L-2*	Neural	none	none	21/34	22/34
trpc-like	Neural	D26 post-feed: snakelike (10/15), 10DPA: 10/11 immobile	*	*	*
sargasso-1	Neural	none	none	32/32	28/32
gabrg3L-1	Neural	none	none	29/33	29/33
pkd2-1*	Neural	none	yes	0/34	0/34
putative protein-37835	Neural	none	yes	0/31	0/31
eml-1	Neural	none	yes	0/30	1/30
pkd2L1*	Neural	none	yes	12/31	16/31
abcb1-like	Neural and Epidermal	D26 post-feed: intermitent slow movements (6/6)	none	0/6	0/6
gabrg3L-2	Neural	none	none	15/31	15/31
pkd2-4	Neural	10DPA: slow inching, jerky movements (6/6)	*	0/6	0/6
C2D2A-like	Neural and Epidermal	D26 post-feed: inching, twisting or immobile (6/6), 10DPA: lysed (3/6), edemic (3/6) and immobile or inching (3/6)	*	*	*
hypothetical protein-18696	Neural	D26: slow with variable inching movements (31/31)	*	0/31	0/31
foxJ1-4*	Neural and Epidermal	D26 post-feed: slowly twisting (3/6), immobile or inching (3/6)	*	*	*
hypothetical protein-5582	Neural and Epidermal	D26 post-feed: twisting movements (8/16), immobile (2/16), slow with slight inching movements (10/16)	*	0/6	0/6
ATPA-like	Epidermal	D26 post-feed: snakelike movements (15/15)	none	10/10	10/10
nervana 3-like	Neural and Epidermal	D28 post-feed: inching with variable twisting movements(7/7), 10DPA: lysed (3/7), did not regenerate head (1/7), immobile (3/7)	*	*	*

Notes:
1. * denotes that we were unable to perform the these assessments due to the severe movement defects of the worms.

REFERENCES

1. **Epilepsy Across the Spectrum: Promoting Health and Understanding**. Washington, DC: The National Academies Press; 2012.

2. Sisodiya SM, Mefford HC: **Genetic contribution to common epilepsies**. *Current opinion in neurology* 2011, **24**(2):140-145.

3. Kandratavicius L, Balista PA, Lopes-Aguiar C, Ruggiero RN, Umeoka EH, Garcia-Cairasco N, Bueno-Junior LS, Leite JP: **Animal models of epilepsy: use and limitations**. *Neuropsychiatric disease and treatment* 2014, **10**:1693-1705.

4. Ottman R: **Analysis of Genetically Complex Epilepsies**. *Epilepsia* 2005, **46**:7-14.

5. **Genetic determinants of common epilepsies: a meta-analysis of genome-wide association studies**. *The Lancet Neurology* 2014, **13**(9):893-903.

6. Ran X, Li J, Shao Q, Chen H, Lin Z, Sun ZS, Wu J: **EpilepsyGene: a genetic resource for genes and mutations related to epilepsy**. *Nucleic Acids Res* 2015, **43**(Database issue):D893-899.

7. Frankel WN: **Genetics of complex neurological disease: challenges and opportunities for modeling epilepsy in mice and rats**. *Trends in Genetics* 2009, **25**(8):361-367.

8. Colmers WF, El Bahh B: **Neuropeptide Y and Epilepsy**. *Epilepsy currents / American Epilepsy Society* 2003, **3**(2):53-58.

9. Takahashi K, Yamanaka S: **Induction of pluripotent stem cells from mouse embryonic and adult fibroblast cultures by defined factors**. *Cell* 2006, **126**(4):663-676.

10. Ahmed S, Gan HT, Lam CS, Poonepalli A, Ramasamy S, Tay Y, Tham M, Yu YH: **Transcription factors and neural stem cell self-renewal, growth and differentiation**. *Cell adhesion & migration* 2009, **3**(4):412-424.

11. Cowles MW, Brown DD, Nisperos SV, Stanley BN, Pearson BJ, Zayas RM: **Genome-wide analysis of the bHLH gene family in planarians identifies factors required for adult neurogenesis and neuronal regeneration**. *Development* 2013, **140**(23):4691-4702.

12. Malas S, Postlethwaite M, Ekonomou A, Whalley B, Nishiguchi S, Wood H, Meldrum B, Constanti A, Episkopou V: **Sox1-deficient mice suffer from epilepsy associated with abnormal ventral forebrain development and olfactory cortex hyperexcitability**. *Neuroscience* 2003, **119**(2):421-432.

13. Ekonomou A, Kazanis I, Malas S, Wood H, Alifragis P, Denaxa M, Karagogeos D, Constanti A, Lovell-Badge R, Episkopou V: **Neuronal migration and ventral subtype identity in the telencephalon depend on SOX1**. *PLoS Biol* 2005, **3**(6):e186.

14. Kamachi Y, Uchikawa M, Collignon J, Lovell-Badge R, Kondoh H: **Involvement of Sox1, 2 and 3 in the early and subsequent molecular events of lens induction**. *Development* 1998, **125**(13):2521-2532.

15. Meulemans D, Bronner-Fraser M: **The amphioxus SoxB family: implications for the evolution of vertebrate placodes**. *International journal of biological sciences* 2007, **3**(6):356-364.

16. Cimadamore F, Fishwick K, Giusto E, Gnedeva K, Cattarossi G, Miller A, Pluchino S, Brill LM, Bronner-Fraser M, Terskikh AV: **Human ESC-derived neural crest model reveals a key role for SOX2 in sensory neurogenesis**. *Cell stem cell* 2011, **8**(5):538-551.

17. Fortunato S, Adamski M, Bergum B, Guder C, Jordal S, Leininger S, Zwafink C, Rapp HT, Adamska M: **Genome-wide analysis of the sox family in the calcareous sponge Sycon ciliatum: multiple genes with unique expression patterns**. *Evodevo* 2012, **3**(1):14.

18. Jager M, Queinnec E, Chiori R, Le Guyader H, Manuel M: **Insights into the early evolution of SOX genes from expression analyses in a ctenophore**. *Journal of experimental zoology Part B, Molecular and developmental evolution* 2008, **310**(8):650-667.

19. Schnitzler CE, Simmons DK, Pang K, Martindale MQ, Baxevanis AD: **Expression of multiple Sox genes through embryonic development in the ctenophore Mnemiopsis leidyi is spatially restricted to zones of cell proliferation**. *Evodevo* 2014, **5**:15.

20. Fritzsch B, Beisel KW, Hansen LA: **The molecular basis of neurosensory cell formation in ear development: a blueprint for hair cell and sensory neuron regeneration?** *BioEssays : news and reviews in molecular, cellular and developmental biology* 2006, **28**(12):1181-1193.

21. Koster RW, Kuhnlein RP, Wittbrodt J: **Ectopic Sox3 activity elicits sensory placode formation**. *Mechanisms of development* 2000, **95**(1-2):175-187.

22. Okamoto K, Takeuchi K, Agata K: **Neural projections in planarian brain revealed by fluorescent dye tracing**. *Zoolog Sci* 2005, **22**(5):535-546.

23. Baguñà J, Ballester R: **The nervous system in planarians: Peripheral and gastrodermal plexuses, pharynx innervation, and the relationship between central nervous system structure and the acoelomate organization**. *Journal of Morphology* 1978, **155**(2):237-252.

24. Hyman LH: **The invertebrates, Vol. II. Platyhelminths and rhyncocoela.** *New York: McGraw-Hill* 1951b.

25. Labbé RM, Irimia M, Currie KW, Lin A, Zhu SJ, Brown DDR, Ross EJ, Voisin V, Bader GD, Blencowe BJ *et al*: **A Comparative Transcriptomic Analysis Reveals Conserved Features of Stem Cell Pluripotency in Planarians and Mammals**. *Stem cells* 2012, **30**(8):1734-1745.

26. Önal P, Grün D, Adamidi C, Rybak A, Solana J, Mastrobuoni G, Wang Y, Rahn H-P, Chen W, Kempa S *et al*: **Gene expression of pluripotency determinants is conserved between mammalian and planarian stem cells**. *The EMBO journal* 2012, **31**(12):2755-2769.

27. Ramakrishnan L, Desaer C: **Carbamazepine inhibits distinct chemoconvulsant-induced seizure-like activity in Dugesia tigrina**. *Pharmacology, biochemistry, and behavior* 2011, **99**(4):665-670.

28. van Wolfswinkel JC, Wagner DE, Reddien PW: **Single-cell analysis reveals functionally distinct classes within the planarian stem cell compartment**. *Cell stem cell* 2014, **15**(3):326-339.

29. Wagner DE, Wang IE, Reddien PW: **Clonogenic neoblasts are pluripotent adult stem cells that underlie planarian regeneration**. *Science* 2011, **332**(6031):811-816.

30. Eisenhoffer GT, Kang H, Sánchez Alvarado A: **Molecular analysis of stem cells and their descendants during cell turnover and regeneration in the planarian Schmidtea mediterranea**. *Cell stem cell* 2008, **3**(3):327-339.

31. Lapan SW, Reddien PW: **Transcriptome analysis of the planarian eye identifies ovo as a specific regulator of eye regeneration**. *Cell Rep* 2012, **2**(2):294-307.

32. Scimone ML, Kravarik KM, Lapan SW, Reddien PW: **Neoblast specialization in regeneration of the planarian Schmidtea mediterranea**. *Stem cell reports* 2014, **3**(2):339-352.

33. Monjo F, Romero R: **Embryonic development of the nervous system in the planarian Schmidtea polychroa**. *Dev Biol* 2015, **397**(2):305-319.

34. Yao G, Luo C, Harvey M, Wu M, Schreiber TH, Du Y, Basora N, Su X, Contreras D, Zhou J: **Disruption of polycystin-L causes hippocampal and thalamocortical hyperexcitability**. *Human molecular genetics* 2016, **25**(3):448-458.

35. Cebrià F, Newmark PA: **Planarian homologs of netrin and netrin receptor are required for proper regeneration of the central nervous system and the maintenance of nervous system architecture**. *Development* 2005, **132**(16):3691-3703.

36. King RS, Newmark PA: **In situ hybridization protocol for enhanced detection of gene expression in the planarian Schmidtea mediterranea**. *BMC Dev Biol* 2013, **13**:8.

37. Cowles MW, Omuro KC, Stanley BN, Quintanilla CG, Zayas RM: **COE loss-of-function analysis reveals a genetic program underlying maintenance and regeneration of the nervous system in planarians**. *PLoS Genet* 2014, **10**(10):e1004746.

38. Ross KG, Omuro KC, Taylor MR, Munday RK, Hubert A, King RS, Zayas RM: **Novel monoclonal antibodies to study tissue regeneration in planarians**. *BMC Dev Biol* 2015, **15**(1):2.

39. Gurley KA, Rink JC, Sánchez Alvarado A: **Beta-catenin defines head versus tail identity during planarian regeneration and homeostasis**. *Science* 2008, **319**(5861):323-327.

40. Robb SM, Gotting K, Ross E, Sanchez Alvarado A: **SmedGD 2.0: The Schmidtea mediterranea genome database**. *Genesis* 2015, **53**(8):535-546.

41. Brandl H, Moon H, Vila-Farre M, Liu SY, Henry I, Rink JC: **PlanMine--a mineable resource of planarian biology and biodiversity**. *Nucleic Acids Res* 2016, **44**(D1):D764-773.

42. Wurtzel O, Cote LE, Poirier A, Satija R, Regev A, Reddien PW: **A Generic and Cell-Type-Specific Wound Response Precedes Regeneration in Planarians**. *Dev Cell* 2015, **35**(5):632-645.

43. Zayas RM, Bold TD, Newmark PA: **Spliced-leader trans-splicing in freshwater planarians**. *Mol Biol Evol* 2005, **22**(10):2048-2054.

44. Collins JJ, 3rd, Hou X, Romanova EV, Lambrus BG, Miller CM, Saberi A, Sweedler JV, Newmark PA: **Genome-wide analyses reveal a role for peptide hormones in planarian germline development**. *PLoS Biol* 2010, **8**(10):e1000509.

45. Liu SY, Selck C, Friedrich B, Lutz R, Vila-Farre M, Dahl A, Brandl H, Lakshmanaperumal N, Henry I, Rink JC: **Reactivating head regrowth in a regeneration-deficient planarian species**. *Nature* 2013, **500**(7460):81-84.

46. Aslanidis C, de Jong PJ: **Ligation-independent cloning of PCR products (LIC-PCR)**. *Nucleic Acids Res* 1990, **18**(20):6069-6074.

47. Schneider CA, Rasband WS, Eliceiri KW: **NIH Image to ImageJ: 25 years of image analysis**. *Nature methods* 2012, **9**(7):671-675.

48. Molinaro AM, Pearson BJ: **In silico lineage tracing through single cell transcriptomics identifies a neural stem cell population in planarians**. *Genome Biol* 2016, **17**(1):87.

49. Satija R, Farrell JA, Gennert D, Schier AF, Regev A: **Spatial reconstruction of single-cell gene expression data**. *Nature biotechnology* 2015, **33**(5):495-502.

50. Shin J, Berg DA, Zhu Y, Shin JY, Song J, Bonaguidi MA, Enikolopov G, Nauen DW, Christian KM, Ming GL *et al*: **Single-Cell RNA-Seq with Waterfall Reveals Molecular Cascades underlying Adult Neurogenesis**. *Cell stem cell* 2015, **17**(3):360-372.

51. Fraenkel A, Gunn, D. L.: **The orientation of animals.** *New York: Dover* 1961.

52. MacRae EK: **The fine structure of sensory receptor processes in the auricular epithelium of the planarian, Dugesia tigrina**. *Z Zellforsch Mikrosk Anat* 1967, **82**(4):479-494.

53. Pearl R: **The movements and reactions of fresh-water planarians: a study in animal behavior**. *Quarterly Journal of Microscopical Science* 1903, **46**(4):509-714.

54. Köhler O: **Sinnesphysiologie der Süsserwasserplanarien**. *Z vergl Physiol* 1932, **16**:606–756.

55. Farnesi RM, Tei S: **Dugesia lugubris s.l. auricles: research into the ultrastructure and on the functional efficiency**. *Riv Biol* 1980, **73**(1):65-77.

56. Guo T, Peters AH, Newmark PA: **A Bruno-like gene is required for stem cell maintenance in planarians**. *Dev Cell* 2006, **11**(2):159-169.

57. Reddien PW, Oviedo NJ, Jennings JR, Jenkin JC, Sánchez Alvarado A: **SMEDWI-2 is a PIWI-like protein that regulates planarian stem cells**. *Science* 2005, **310**(5752):1327-1330.

58. Stringer CE: **The Means of Locomotion in Planarians**. *Proc Natl Acad Sci U S A* 1917, **3**(12):691-692.

59. Robb SM, Sánchez Alvarado A: **Identification of immunological reagents for use in the study of freshwater planarians by means of whole-mount immunofluorescence and confocal microscopy**. *Genesis* 2002, **32**(4):293-298.

60. Roberts-Galbraith RH, Brubacher JL, Newmark PA: **A functional genomics screen in planarians reveals regulators of whole-brain regeneration**. *Elife* 2016, **5**.

61. Guth SIE, Wegner M: **Having it both ways: Sox protein function between conservation and innovation**. *Cell Mol Life Sci* 2008, **65**(19):3000-3018.

62. Zhang C, Basta T, Jensen ED, Klymkowsky MW: **The beta-catenin/VegT-regulated early zygotic gene Xnr5 is a direct target of SOX3 regulation**. *Development* 2003, **130**(23):5609-5624.

63. Liu YR, Laghari ZA, Novoa CA, Hughes J, Webster JR, Goodwin PE, Wheatley SP, Scotting PJ: **Sox2 acts as a transcriptional repressor in neural stem cells**. *BMC neuroscience* 2014, **15**:95.

64. Bylund M, Andersson E, Novitch BG, Muhr J: **Vertebrate neurogenesis is counteracted by Sox1-3 activity**. *Nature neuroscience* 2003, **6**(11):1162-1168.

65. Graham V, Khudyakov J, Ellis P, Pevny L: **SOX2 functions to maintain neural progenitor identity**. *Neuron* 2003, **39**(5):749-765.

66. Kamachi Y, Uchikawa M, Tanouchi A, Sekido R, Kondoh H: **Pax6 and SOX2 form a co-DNA-binding partner complex that regulates initiation of lens development**. *Genes & development* 2001, **15**(10):1272-1286.

67. Kenny AP, Kozlowski D, Oleksyn DW, Angerer LM, Angerer RC: **SpSoxB1, a maternally encoded transcription factor asymmetrically distributed among early sea urchin blastomeres**. *Development* 1999, **126**(23):5473-5483.

68. Kenny AP, Oleksyn DW, Newman LA, Angerer RC, Angerer LM: **Tight regulation of SpSoxB factors is required for patterning and morphogenesis in sea urchin embryos**. *Dev Biol* 2003, **261**(2):412-425.

69. Ruppert EE, Smith PR: **The functional organization of filtration nephridia**. *Biological Reviews* 1988, **63**(2):231-258.

70. Rink JC, Vu HT, Sánchez Alvarado A: **The maintenance and regeneration of the planarian excretory system are regulated by EGFR signaling**. *Development* 2011, **138**(17):3769-3780.

71. Scimone ML, Srivastava M, Bell GW, Reddien PW: **A regulatory program for excretory system regeneration in planarians**. *Development* 2011, **138**(20):4387-4398.

72. Dobretsov M, Stimers JR: **Neuronal function and alpha3 isoform of the Na/K-ATPase**. *Frontiers in bioscience : a journal and virtual library* 2005, **10**:2373-2396.

73. Saudemont A, Haillot E, Mekpoh F, Bessodes N, Quirin M, Lapraz F, Duboc V, Rottinger E, Range R, Oisel A *et al*: **Ancestral regulatory circuits governing ectoderm patterning downstream of Nodal and BMP2/4 revealed by gene regulatory network analysis in an echinoderm**. *PLoS Genet* 2010, **6**(12):e1001259.

74. Kiefer JC: **Back to basics: Sox genes**. *Dev Dyn* 2007, **236**(8):2356-2366.

75. Phochanukul N, Russell S: **No backbone but lots of Sox: Invertebrate Sox genes**. *The international journal of biochemistry & cell biology* 2010, **42**(3):453-464.

76. Miyagi S, Kato H, Okuda A: **Role of SoxB1 transcription factors in development**. *Cellular and molecular life sciences : CMLS* 2009, **66**(23):3675-3684.

77. Focareta L, Cole AG: **Analyses of Sox-B and Sox-E Family Genes in the Cephalopod Sepia officinalis: Revealing the Conserved and the Unusual**. *PLoS One* 2016, **11**(6):e0157821.

78. Taguchi S, Tagawa K, Humphreys T, Satoh N: **Group B sox genes that contribute to specification of the vertebrate brain are expressed in the apical organ and ciliary bands of hemichordate larvae**. *Zoolog Sci* 2002, **19**(1):57-66.

79. Shimazaki A, Sakai A, Ogasawara M: **Gene expression profiles in Ciona intestinalis stigmatal cells: insight into formation of the ascidian branchial fissures**. *Dev Dyn* 2006, **235**(2):562-569.

80. Kondoh H, Uchikawa M, Kamachi Y: **Interplay of Pax6 and SOX2 in lens development as a paradigm of genetic switch mechanisms for cell differentiation**. *Int J Dev Biol* 2004, **48**(8-9):819-827.

81. Martín-Durán JM, Monjo F, Romero R: **Planarian embryology in the era of comparative developmental biology**. *Int J Dev Biol* 2012, **56**(1-3):39-48.

82. Bardakjian TM, Schneider A: **The genetics of anophthalmia and microphthalmia**. *Current opinion in ophthalmology* 2011, **22**(5):309-313.

83. Laumonnier F, Ronce N, Hamel BC, Thomas P, Lespinasse J, Raynaud M, Paringaux C, Van Bokhoven H, Kalscheuer V, Fryns JP *et al*: **Transcription factor SOX3 is involved in X-linked mental retardation with growth hormone deficiency**. *American journal of human genetics* 2002, **71**(6):1450-1455.

84. Messaed C, Rouleau GA: **Molecular mechanisms underlying polyalanine diseases**. *Neurobiology of disease* 2009, **34**(3):397-405.

85. Chew LJ, Gallo V: **The Yin and Yang of Sox proteins: Activation and repression in development and disease**. *Journal of neuroscience research* 2009, **87**(15):3277-3287.

86. Weber YG, Lerche H: **Genetic mechanisms in idiopathic epilepsies**. *Developmental medicine and child neurology* 2008, **50**(9):648-654.

87. Nicita F, De Liso P, Danti FR, Papetti L, Ursitti F, Castronovo A, Allemand F, Gennaro E, Zara F, Striano P *et al*: **The genetics of monogenic idiopathic epilepsies and epileptic encephalopathies**. *Seizure* 2012, **21**(1):3-11.

88. Vazquez G, Wedel BJ, Aziz O, Trebak M, Putney JW, Jr.: **The mammalian TRPC cation channels**. *Biochimica et biophysica acta* 2004, **1742**(1-3):21-36.

89. Pan Z, Kao T, Horvath Z, Lemos J, Sul JY, Cranstoun SD, Bennett V, Scherer SS, Cooper EC: **A common ankyrin-G-based mechanism retains KCNQ and NaV channels at electrically active domains of the axon**. *The Journal of neuroscience : the official journal of the Society for Neuroscience* 2006, **26**(10):2599-2613.

90. Lingrel JB, Orlowski J, Shull MM, Price EM: **Molecular genetics of Na,K-ATPase**. *Progress in nucleic acid research and molecular biology* 1990, **38**:37-89.

91. Jembrek MJ, Vlainic J: **GABA Receptors: Pharmacological Potential and Pitfalls**. *Current pharmaceutical design* 2015, **21**(34):4943-4959.

92. Moller RS, Wuttke TV, Helbig I, Marini C, Johannesen KM, Brilstra EH, Vaher U, Borggraefe I, Talvik I, Talvik T *et al*: **Mutations in GABRB3: From febrile seizures to epileptic encephalopathies**. *Neurology* 2017, **88**(5):483-492.

93. Janve VS, Hernandez CC, Verdier KM, Hu N, Macdonald RL: **Epileptic encephalopathy de novo GABRB mutations impair GABAA receptor function**. *Annals of neurology* 2016.

94. Tanaka M, DeLorey TM, Delgado-Escueta A, Olsen RW: **GABRB3, Epilepsy, and Neurodevelopment**. In: *Jasper's Basic Mechanisms of the Epilepsies.*

Edited by Noebels JL, Avoli M, Rogawski MA, Olsen RW, Delgado-Escueta AV. Bethesda (MD): National Center for Biotechnology Information (US) Michael A Rogawski, Antonio V Delgado-Escueta, Jeffrey L Noebels, Massimo Avoli and Richard W Olsen.; 2012.

95. Vij S, Rink JC, Ho HK, Babu D, Eitel M, Narasimhan V, Tiku V, Westbrook J, Schierwater B, Roy S: **Evolutionarily ancient association of the FoxJ1 transcription factor with the motile ciliogenic program**. *PLoS Genet* 2012, **8**(11):e1003019.

96. Tallila J, Jakkula E, Peltonen L, Salonen R, Kestila M: **Identification of CC2D2A as a Meckel syndrome gene adds an important piece to the ciliopathy puzzle**. *American journal of human genetics* 2008, **82**(6):1361-1367.

97. Nauli SM, Alenghat FJ, Luo Y, Williams E, Vassilev P, Li X, Elia AE, Lu W, Brown EM, Quinn SJ *et al*: **Polycystins 1 and 2 mediate mechanosensation in the primary cilium of kidney cells**. *Nature genetics* 2003, **33**(2):129-137.

98. Gross RA, Ferrendelli JA: **Effects of reserpine, propranolol, and aminophylline on seizure activity and CNS cyclic nucleotides**. *Annals of neurology* 1979, **6**(4):296-301.

99. Weinshenker D, Szot P, Miller NS, Palmiter RD: **Alpha(1) and beta(2) adrenoreceptor agonists inhibit pentylenetetrazole-induced seizures in mice lacking norepinephrine**. *The Journal of pharmacology and experimental therapeutics* 2001, **298**(3):1042-1048.

100. Yang J, Liu X, Yue G, Adamian M, Bulgakov O, Li T: **Rootletin, a novel coiled-coil protein, is a structural component of the ciliary rootlet**. *The Journal of cell biology* 2002, **159**(3):431-440.

101. Müller HG: **Untersuchungen über spezifische Organe niederer Sinne bei rhabdocoelen Turbellarien**. *Z vergl Physiol* 1936, **23**:253–292.

CONCLUSION OF THE DISSERTATION

Planarians flatworms have an amazing ability to regenerate and maintain a molecularly complex nervous system from a population of adult pluripotent stem cells. In Chapter 1, I provided a comprehensive review of the anatomy of the planarian nervous system and demonstrated the molecular complexity and conservation of the planarian nervous system with vertebrates. This chapter also addressed our current knowledge about how planarian neurogenesis proceeds in both the adult and during embryonic development. In Chapter 2, I described work in which we created seven monoclonal antibodies that label muscle fibers, axonal projections of the peripheral nervous system, two populations of intestinal cells, ciliated cells, and a subset of neoblast progeny. These reagents have aided in visualizing protein expression for analyses following RNAi experiments. In Chapter 3, I expanded on the need for improved methods of protein visualization in planarian tissues by providing a step-by-step methodology chapter on how to perform immunohistochemistry in whole planarians.

In Chapter 4, I used the planarian model system to study *SoxB1* gene function in neurogenesis and found that inhibition of *Smed-soxB1-2* led to a loss of sensory neuron regeneration and function that was accompanied by a striking seizure-like behavioral phenotype. This result suggested to us that *soxB1-2* function is conserved with vertebrate *SoxB1* genes. Additionally, we found that *soxB1-2* expression marks an ectodermal progenitor population in planarians. We performed RNA-seq on *soxB1-2(RNAi)* planarians and functionally assessed 86 putative target genes. This

revealed 17 genes that, when knocked down using RNAi, displayed phenotypes that represented aspects of the *soxB1-2* phenotype; 16 of these genes were expressed in neurons. While several of these genes recapitulated aspects of the seizure-like phenotype, inhibition of an additional set of genes caused a reduction in rheosensation and vibration sensation in planarians. Further expression analysis of the genes that caused sensory defects led to the identification of a rheosensory neuronal population in planarians. Some of the genes found downstream of *soxB1-2* were associated with ED genetics, while others represented genes conserved with humans, but genes not currently associated with EDs. We also found downregulation of multiple polycystic kidney disease (*pkd*) genes and other genes involved in Ca^{2+} signaling that have been linked to primary cilia function. This represents an exciting new field of epilepsy research because it was recently demonstrated that dysfunction of Polycystin-L on the primary cilia of neurons causes an increased susceptibility to drug-induced seizures. Thus, we have identified new potential targets underlying EDs and the compilation of work in this dissertation will aid in establishing planarians as a genetic model system in which to study the molecular basis of EDs.